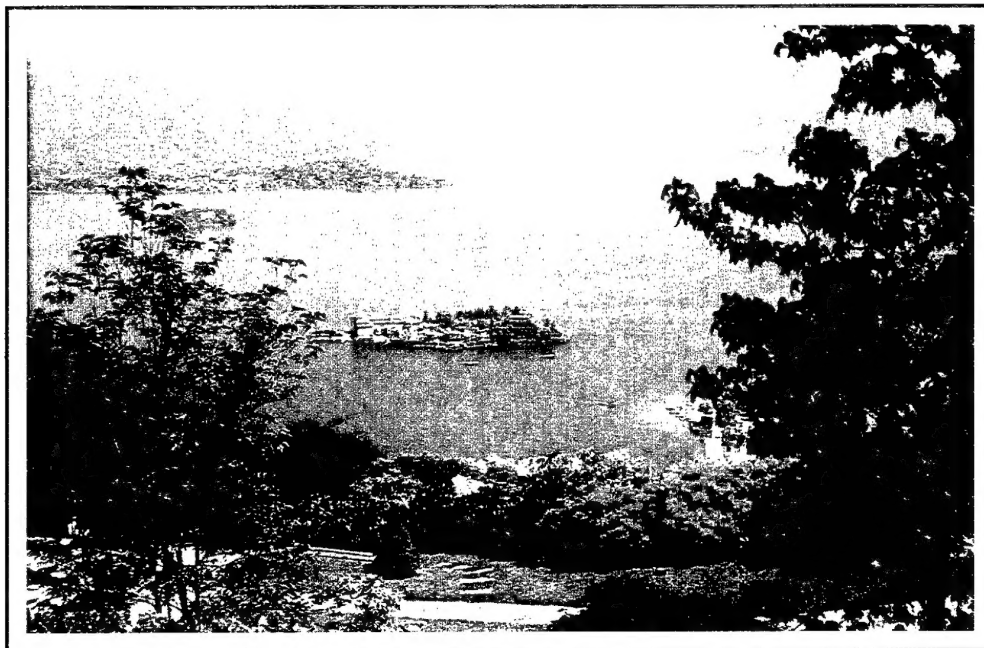# THE FIFTH INTERNATIONAL SYMPOSIUM ON SPECIAL TOPICS IN CHEMICAL PROPULSION

Combustion of Energetic Materials

18 - 22 June 2000
Stresa (Lake Maggiore), Italy

Symposium Organizers:

Professor Kenneth K. Kuo
The Pennsylvania State University

Professor Luigi T. De Luca
Politecnico di Milano

Co-Sponsored by:

The Pennsylvania State University, USA;
Politecnico di Milano, Italy;
U.S. Army Research Laboratory, USA;
U.S. Office of Naval Research, USA;
Societé National des Poudres et Explosifs (SNPE), France;
National Tsing Hua University, Taiwan, ROC;
University of Maryland, USA;
European Office of Aerospace Research and Development, Air Force Office of Scientific Research, United States Air Force Research Laboratory;
United States Army Research Development and Standardization Group (UK);
United States Office of Naval Research, Europe.

REPORT DOCUMENTATION PAGE

Form Approved OMB No. 0704-0188

1. AGENCY USE ONLY (Leave blank)	2. REPORT DATE 6 July 2000	3. REPORT TYPE AND DATES COVERED Conference Proceedings

4. TITLE AND SUBTITLE

5th-ISICP Combustion of Energetic Materials

5. FUNDING NUMBERS

F61775-00-WF056

6. AUTHOR(S)

Conference Committee

7. PERFORMING ORGANIZATION NAME(S) AND ADDRESS(ES)

Politecnico di Milano
Piazza Leonardo Da Vinci 32
Milan 20133
Italy

8. PERFORMING ORGANIZATION REPORT NUMBER

N/A

9. SPONSORING/MONITORING AGENCY NAME(S) AND ADDRESS(ES)

EOARD
PSC 802 BOX 14
FPO 09499-0200

10. SPONSORING/MONITORING AGENCY REPORT NUMBER

CSP 00-5056

11. SUPPLEMENTARY NOTES

12a. DISTRIBUTION/AVAILABILITY STATEMENT

Approved for public release; distribution is unlimited.

12b. DISTRIBUTION CODE

A

13. ABSTRACT (Maximum 200 words)

The Final Proceedings for 5th-ISICP Combustion of Energetic Materials, 19 June 2000 - 22 June 2000

This is an interdisciplinary conference. Topics include: Measurement techniques of thermophysical and ballistic properties of energetic materials (in particular, solid rocket propellant explosives); how to handle data especially in the presence of sensible errors and noise; and to which extent the obtained data depend on the specific data reduction technique implemented.

14. SUBJECT TERMS

EOARD, Combustion, Rocket Engines, Solid Fuels

15. NUMBER OF PAGES

397

16. PRICE CODE

N/A

17. SECURITY CLASSIFICATION OF REPORT	18. SECURITY CLASSIFICATION OF THIS PAGE	19. SECURITY CLASSIFICATION OF ABSTRACT	20. LIMITATION OF ABSTRACT
UNCLASSIFIED	UNCLASSIFIED	UNCLASSIFIED	UL

NSN 7540-01-280-5500

Standard Form 298 (Rev. 2-89)
Prescribed by ANSI Std. 239-18
298-102

Combustion of Energetic Materials

Fifth International Symposium on Special Topics in Chemical Propulsion (5-ISICP)

Stresa (Lake Maggiore), Italy
18-22 June 2000

AQ F01-07-1428

SYMPOSIUM COMMITTEES

Symposium Co-Chairs:

Prof. Kenneth K. Kuo
140 Research Bldg. E., Bigler Rd.
Pennsylvania State University
University Park, PA 16802-2320, U.S.A.
Phone: (1-814) 863-6270
Fax: (1-814) 863-3203
E-mail: kkkper@engr.psu.edu

Prof. Luigi T. De Luca
Politecnico di Milano
32 Piazza Leonardo da Vinci
20133 Milano, MI, Italy
Phone: (39) 02-2399-3912
Fax: (39) 02-2399-3940
E-mail: fivbd@tin.it

Areas of Interest of Committee Members

(a) Reaction Kinetics of Energetic Materials (Solid, Liquid, Hybrid, and Gel Propellants)
(b) Environmental Considerations in Combustion of Energetic Materials
(c) Commercial Applications of Energetic Materials (Airbags, Gas Generators, etc.)
(d) Recycling of Energetic Materials
(e) Safety and Hazards Considerations in Space Launchers and Energetic Materials
(f) Ignition and Combustion of Propellants for Space and Rocket Propulsion
(g) Pyrolysis and Combustion Processes of New Ingredients
(h) Theoretical Modeling and Numerical Simulation of Combustion Processes of Energetic Materials
(i) Combustion Diagnostic Techniques
(j) Thermal Insulation and High-Temperature

International Advisory Committee

Prof. Ronald W. Armstrong USA)[a,e,h]
Dr. Igor G. Assovskiy (Russia)[f,h]
Dr. Volker Aust (Germany)[i]
Prof. Valery A. Babuk (Russia)[f]
Dr. Ezra Bar-Ziv (Israel)[a,i,f]
Prof. Merrill W. Beckstead (USA)[f,g,h]
Dr. Michael Berman (USA)[a]
Dr. Fred S. Blomshield (USA)[f,e]
Mr. Thomas L. Boggs (USA)[e,f]
Prof. Roland Borghi (France)[h,f]
Prof. Derek Bradley (UK)[e,h,i]
Prof. Melvyn C. Branch (USA)[a,i]
Prof. K.N.C. Bray (UK)[h,a]
Prof. Thomas B. Brill (USA)[a,i]

Dr. J.B. Canterberry (USA)[b,e,f]
Mr. Franck Cauty (France)[i,j,f]
Dr. S.K. (Jim) Chan (Canada)[e,e]
Prof. S.H. Chan (USA)[h]
Prof. Paul H.H. Chiu (Taiwan, ROC)[a,f,g,h]
Dr. Chester F. Clark (USA)
Dr. Josephine Covino (USA)[e]
Prof. Fred E.C. Culick (USA)[h,f,a]
Dr. Alain Davenas (France)[b,c,d,e]
Prof. Luigi T. De Luca (Italy)[f,g,h]
Dr. David R. Dillehay (USA)[b,g]
Mr. Gerard Doriath (France)[g,a]
Prof. Lei Du (China)[e,g]
Prof. Boris Ermolaev (Russia)[c,e,h]

Prof. Gerald M. Faeth (USA)[g,f,i]
Prof. Chang-Gen Feng (China)[f]
Dr. Robert A. Fifer (USA)[b,a]
Prof. Yurii V. Frolov (Russia)[h]
Prof. Wei Biao Fu (China)[g,f]
Prof. Luciano Galfetti (Italy)[f,h,j]
Prof. Alon Gany (Israel)[e,f,g,h]
Dr. W. L. Grosshandler (USA)[e]
Dr. J. F. Guéry (France)[h,f,e]
Prof. Ronald K. Hanson (USA)[i]
Prof. Manuel V. Heitor (Portugal)[a,f,g]
Prof. T. Hirano (Japan)[b]
Dr. Guy Lengellé (France)[f,g,h]
Prof. M.C. Lin (USA)[g]
Dr. Joel Lipkin (USA)[b,c,d]
Dr. Alexander N. Lukin (Russia)[e,f,h]
Dr. David M. Mann (USA)[f]
Dr. Ingo May (USA)[a,b,i]
Dr. Carl F. Melius (USA)[a,b]
Prof. Alexander G. Merzhanov (Russia)[c,a,g]
Dr. Richard Miller (USA)[g,h]
Dr. Alexander R. Mitchell (USA)[c,d]
Dr. Mark Morgan (USA)[d]
Dr. Tam Nguyen (Australia)[i,g,f,a,b]
Prof. Takashi Niioka (Japan)[f,h]
Prof. Boris V. Novozhilov (Russia)[f,h]
Dr. Elaine S. Oran (USA)[h]
Dr. Timothy Parr (USA)[i,g]
Dr. Roland Pein (Germany)[a,f,g]
Dr. Arie Peretz (Israel)[b,c,f]
Dr. Rose Pesce-Rodriguez (USA)[b,a]
Dr. Mohan K. Razdan (USA)[b,h,I]
Mr. Jean-Paul Reynaud (France)[f]

Dr. Juan De Dios Rivera (Chile)[b,f,h]
Prof. Oleg Ya Romanov (Russia)[h,i]
Dr. H.F.R. Schoeyer (Netherlands)[g,f,h]
Dr. Hiltmar Schubert (Germany)[b,c,d,e,f]
Mr. Gil Carlos Schuller (Spain)[f,g]
Dr. Robert W. Shaw (USA)[a]
Dr. Hyun Dong Shin (Korea)[f]
Dr. Haridwar Singh (India)[a,c,d,f,g]
Prof. William A. Sirignano (USA)[h]
Dr. D. Sutton (UK)[c]
Mr. Hiroshi Tamura (Japan)[f]Prof. Klaus Thoma (Germany)[c,e,h,i]
Prof. Cai Timin (China)[f,i,j]
Dr. Allen J. Tulis (USA)[f,a,c]
Mr. Nico H.A. Van Ham (Netherlands)[f]
Prof. Pierre Van Tiggelen (Belgium)[a,g,i]
Dr. John A. Vanderhoff (USA)[i]
Dr. Fred Volk (Germany)[a,c]
Prof. Hüseyin Vural (Turkey)[f,h]
Prof. H.G. Wagner (Germany)[a,i,e]
Prof. J.H. Whitelaw (UK)[i,b]
Prof. Forman A. Williams (USA)[h,f,g]
Mr. Stig Wretling (Sweden)[f]
Prof. Xinping Wu (China)[c,f,i]
Prof. Jing-Tang Yang (Taiwan, ROC)[f,h]
Prof. Dingyou Ye (China)[f,i]
Dr. Richard Yetter (USA)[a,i,h]
Dr. Ken Yu (USA)[i]
Dr. Claudio Zanotti (Italy)[f,i,j]
Prof. V.E. Zarko (Russia)[b,f,i]
Prof. Anatoli A. Zenin (Russia)[i,e,f]
Prof. Ben T. Zinn (USA)[f,h]
Prof. Andrey N. Zolotko (Ukraine)[i,h,b]

This program doesn't reflect changes comunicated after 19 may 2000

CONTENTS

POSTER SESSIONS   *Session Co-Chairs: Prof. L. Galfetti and Mr. E. Boyer*

INVITED PLENARY PAPERS

ROOM AZZURRA Area 2b
COMMERCIAL APPLICATIONS OF ENERGETIC MATERIALS
Session Chair: Dr. A. Davenas

ROOM AZZURRA Area 3
COMBUSTION PERFORMANCE OF HYBRID AND SOLID ROCKET MOTORS
Session Co-Chairs: Dr. A. Peretz and Prof. C. Buongiorno

<u>ROOM AZZURRA</u> Area 4a
ENERGETIC MATERIALS COMBUSTION FOR ROCKET PROPULSION
Session Chair: Dr. R. Pein

ROOM AZZURRA Area 5a
COMBUSTION ANOMALIES OF ENERGETIC MATERIALS
Session Chair: Mr. T. Boggs

ROOM AZZURRA Area 5b
COMBUSTION ANOMALIES OF ENERGETIC MATERIALS
Session Co-Chairs: Dr. R.H.W. Waesche and Dr. G. Lengellé

Solid Propellants Convective Ignition and Flame Spreading   121
    by L. Galfetti and G. Colombo

OVERALL SCHEDULE: ROOM AZZURRA (A) + ROOM AZALEA (B)

	Sunday 18 June	Monday 19 June	Tuesday 20 June	Wednesday 21 June	Thursday 22 June
08:00 - 08:15		Open Symposium (B)			
08:15 – 09:00		Invited Paper S1 (B)	Invited Paper S2 (B)	Invited Paper S4 (B)	Invited Paper S10 (B)
09:00 – 10:15		Technical Session 1 S1 (B) or S7a (A) 3+3 papers	Technical Session 5 S3 (B) or S8 (A) 3+3 papers	Technical Session 9 S4a (B) or S10a (A) 3+3 papers	Technical Session 13 S5a (B) or S10c (A) 3+3 papers
10:15 – 10:45		Coffee	Coffee	Coffee	Coffee
10:45 – 12:25		Technical Session 2 S1 (B) or S7a (A) 3+3 papers	Technical Session 6 S3 (B) or S8 (A) 4+4 papers	Technical Session 10 S4b (B) or S10b (A) 4+4 papers	Technical Session 14 S5b (B) or S10c (A) 4+4 papers
12:25 – 14:00		Lunch	Lunch	Lunch	
14:00 – 15:15		Invited Paper S3 (B) — Technical Session 3 S2a (B) or S7b (A) 3+3 papers		Invited Paper S9 (B) — Technical Session 11 S6 (B) or S9 (A) 2+2 paper	Bus tour to Fiat Research Center (Turin) or Fiat Avio (Orbassano) 12:30-19:30
15:45 – 16:10		Coffee	Coffee	Coffee	
16:10 – 17:25	On-Site Registration 15:30 – 18:30	Technical Session 4 S2b (B) or S7c (A) 4+4 papers		Technical Session 12 S6 (B) or S9 (A) 4+4 papers	
17:25 – 17:50		End of Session	End of Session	End of Session	
18:00					
19:00					
20:00					
21:00					

SCHEDULE ROOM AZALEA (B)

	Sunday 18 June	Monday 19 June	Tuesday 20 June	Wednesday 21 June	Thursday 22 June
08:00 – 08:15		Open Symposium			
08:15 – 09:00		1 Behrens, INV	2 Kondrikov, INV	4 Natan, INV	10 Novozhilov, INV
09:00 – 09:25		7a Ramaswamy	8 Oran Khokhlov	10a Blomshield	10c Culick Seywert
09:25 – 09:50		7a Son et al.	8 Caro et al.	10a Beckstead et al.	10c Kumar Lakshmisha
09:50 – 10:15		7a Kato et al.	8 Yunusak Uçer	10a Lubarsky et al.	10c Romanov
10:15 – 10:45		Coffee	Coffee	Coffee	Coffee
10:45 – 11:10		7a Korobeinichev et al	8 Orlandi Fabignon	10b Novozhilov et al.	10c Verri DeLuca
11:10 – 11:35		7a Chan et al.	8 Colasurdo et al.	10b Zenin Finjakov	10c Hessler et al.
11:35 – 12:00		7a Sinditskii et al.	8 Dupays	10b Finlinson et al.	10c Assovskiy Rashkovsky
12:00 – 12:25			8 Ebrahimi Merkle	10b Knyazeva	10c Waesche
12:25 – 14:00		Lunch	Lunch	Lunch	Bus tour to Fiat Research Center (Turin) or Fiat Avio (Orbassano) 12:30-19:30
14:00 – 14:25		3 Fabrizi, INV		9 Coghe, INV	
14:25 – 14:50		7b Hori et al.			
14:50 – 15:15		7b Louwers et al.		9 Zarko et al.	
15:15 – 15:45		7b Sanghavi et al.		9 Cozzi et al.	
15:45 – 16:10		Coffee	Coffee	Coffee	
16:10 – 16:35	On-Site Registration	7c Atwood et al.		9 Altman et al.	
16:35 – 17:00	Registration	7c Weiser et al.		9 Thumann Ciezki	
17:00 – 17:25	15: 30 – 18:30	7c Heiser		9 Zhao et al.	
17:25 – 17:50		7c Kuo Boyer		9 Piotrowski et al.	
18:00		End of Session	End of Session	End of Session	
19:00	Welcome Reception 19:00 – 21:00				
20:00					
21:00					

SCHEDULE ROOM AZZURRA (A)

	Sunday 18 June	Monday 19 June	Tuesday 20 June	Wednesday 21 June	Thursday 22 June
08:00 – 08:15					
08:15 – 09:00		Open Symposium (B) / 1 Behrens, INV (B)	2 Kondrikov, INV (B)	4 Natan, INV (B)	10 Novozhilov, INV (B)
09:00 – 09:25		1 Brill et al.	3 Maisonneuve et al.	4a Tepper Kaledin	5a Berghout et al.
09:25 – 09:50		1 Chakraborthy Lin	3 Russo et al.	4a Mordosky et al.	5a Cai et al.
09:50 – 10:15		1 De Croix	3 Risha et al.	4a Baschung et al.	5a Du et al.
10:15 – 10:45		Coffee	Coffee	Coffee	Coffee
10:45 – 11:10		1 Pein Anders	3 Lukin	4b Rashkovsky	5b Krishnan Rajesh
11:10 – 11:35		1 Chin et al.	3 Le Breton et al.	4b Brewster et al.	5b Fuimori et al.
11:35 – 12:00		1 Lipkin et al.	3 Liu et al.	4b Bozic Blagojevic	5b Pelosi Gany
12:00 – 12:25			3 Char Yeh	4b Wang Wang	5b Galfetti Colombo
12:25 – 14:00		Lunch	Lunch	Lunch	
14:00 – 14:25		3 Fabrizi, INV (B)		9 Coghe, INV (B)	Bus tour to Fiat Research Center (Turin) or Fiat Avio (Orbassano) 12:30-19:30
14:25 – 14:50		2a Machacek et al.		6 Rosenband Gany	
14:50 – 15:15		2a Mitchell		6 Mench et al.	
15:15 – 15:45		2a Shevelev et al.	Coffee	Coffee	
15:45 – 16:10		Coffee		6 Kalontarov et al.	
16:10 – 16:35	On-Site Registration	2b Iwama et al.		6 Glotov et al.	
16:35 – 17:00		2b Chastenet Mobuchon		6 Wang et al.	
17:00 – 17:25	15:30 - 18:30	2b Klemens et al.		6 Babuk et al.	
17:25 – 17:50		2b Engelen et al.		End of Session	
18:00		End of Session	End of Session		
19:00	Welcome Reception				
20:00					
21:00	19:00 - 21:00				

Time		
08:00	**Symposium Opening**	*Prof. K.K. Kuo and Prof. L.T. De Luca*
08:15	**5-ISICP-008-1-IV-RB PLENARY PAPER**	*Session Chair: Prof. K.K. Kuo*

Chemical and Physical Processes that Control the Thermal Decomposition of RDX and HMX

R. Behrens, S. Maharrey, S. Mack, J. Wood (Presented by Dr. R. Behrens)

	Room Azzurra Area 1: Reaction Kinetics of Energetic Materials	**Room Azalea Area 7a: Pyrolysis and Combustion Processes of New Ingredients and Applications**
	Session Co-Chairs: Prof. R. Yetter and Prof. B.N. Kondrikov	*Session Co-Chairs: Dr. J. Goldwasser and Prof. A. Iwama*
09:00	**5-ISICP-003-1-OP-TBB** **Pyrolysis Studies of the Burning Mechanisms of High-Nitrogen Compounds** T. B. Brill, R. W. Beal, H. Ramanathan	**5-ISICP-001-7-OP-ALR** **Energetic Material Combustion Studies on Propellant Formulations and its Components** A.L. Ramaswamy
09:25	**5-ISICP-007-1-OP-MCL** **Formation and Decomposition of CH_2N and CH_2NO in the Combustion of RDX and HMX Studied by Quantum Chemical and Statistical Theory Calculations** D. Chakraborty, M.C. Lin	**5-ISICP-010-7-OP-SS** **Burn Rate Measurements of HMX, TATB, DHT, DAAF and BTATz** S.F. Son, H.L. Berghout, C.A. Bolme, D.E. Chavez, D. Naud, M.A. Hiskey
09:50	**5-ISICP-014-9-OP-MED** **Dynamic Observations of Polymorph Changes in Explosives using Second Harmonic Generation** M.E. DeCroix, B.W. Asay, S.F. Son, B.F. Henson	**5-ISICP-025-6-OP-KK** **Sensitivity Properties and Burning Rate Characteristics of High Energy Density Materials and the Propellants Containing These Materials** K. Kato, K. Kobayashi, S. Miyazaki, S. Matsuura
10:15	**COFFEE**	
10:45	**5-ISICP-002-1-OP-RP** **Investigation of Fuel-rich Boron Combustion in a Pressurized Combustion Bomb** R. Pein, S. Anders	**5-ISICP-005-7-OP-OPK** **Structure of Ammonium Dinitramide Flame at 40 atm** O.P. Korobeinichev, A.A. Paletsky, A.G. Tereschenko, T.A. Bol'shova
11:10	**5-ISICP-001-1-OP-JAW** **The Use of Kinetic Data in the Service Life Testing of HTPB Rocket Propellant** A. Chin, J. A. Wilson, D. Ellison, S. Backer	**5-ISICP-006-7-OP-MLC** **Properties of ADN Propellants** M.L. Chan, R. Reed, A. Turner, A. Atwood, P. Curran
11:35	**5-ISICP-001-2-OP-JL** **Contained Low Pressure Combustion of NIKE and Improved HAWK Rocket Motors:** **Experimental Techniques and Emissions Measurements** J. Lipkin, C. Shaddix, S. Allendorf, R. Peabody, C. Velsko, B. Watkins, S. Williams, A. Moeller, W. Bellow, J. Carson, W. Gray, J. Stephens, S. Kwak	**5-ISICP-013-7-OP-VPS** **Combustion Peculiarities of ADN and ADN-Based Mixtures** V.P. Sinditskii, A.E. Fogelzang, V.Y.Egorshev, A.I. Levshenkov, V.V. Serushkin, V.I. Kolesov
12:00	Meeting Announcements	
12:25	**LUNCH**	

Monday Afternoon, 19 June 2000

14:00 5-ISICP-009-3-IV-AF PLENARY PAPER *Session Chair: Prof. C. Buongiorno*
FiatAvio Activities for Launchers and a Strategy for European Industry
Ing. A. Fabrizi

Time	Room Azzurra	Room Azalea
	Room Azzurra Area 2a: Recycling of Energetic Materials *Session Chair: Dr. A. Mitchell*	**Room Azalea Area 7b:** Pyrolysis and Combustion Processes of New Ingredients and Applications *Session Chair: Dr. C. Clark*
14:25	**5-ISICP-003-4-OP-AKT** Reuse of Demilitarized and/or Excess Energetic Materials as Ingredients in Commercial Explosives O. Machacek, G. Eck, K. Tallent	**5-ISICP-011-7-OP-KH** Burning Rate & PDL Characteristics of a GAP/AP Propellant System K. Hori, M. Kohno, A. Volpi, C. Zanotti, K. Kato, S. Miyazaki
14:50	**5-ISICP-004-4-OP-ARM** Recent Advances in the Chemical Conversion of Energetic Materials A.R. Mitchell, M.D. Coburn, R.D. Schmidt, P.F. Pagoria, G.S. Lee	**5-ISICP-008-9-OP-GS** Diffusion Flame Structure of HNF Sandwiches J. Louwers, G.M.H.J.L. Gadiot, G.G.M. Stoffels, D.J.E.M. Roekaerts
15:15	**5-ISICP-005-4-OP-SAS** Conversion of Demilitarized TNT to Higher Value Products S.A Shevelev, V.A. Tartakovsky, A.L. Rusanov	**5-ISICP-003-7-OP-SNA** Combustion and Thermal Behavior of Ballistically Modified Eva and Estane Based RDX Propellants R.R. Sanghavi, S.N. Asthana, J.S. Karir, Haridwar Singh
15:45	**COFFEE**	
	Room Azzurra Area 2b: Commercial Applications of Energetic Materials *Session Chair: Dr. A. Davenas*	**Room Azalea Area 7c:** Pyrolysis and Combustion Processes of Gun Propellants and Ingredients *Session Chair: Mr. A. Horst*
16:10	**5-ISICP-003-3-OP-AI** Explosively Generated Supercritical Water for Deploying Airbags A. Iwama, T. Tamura, D. Yu	**5-ISICP-005-5-OP-AIA** Combustion Studies of Nitramine Containing Energetic Materials A. I. Atwood, D. T. Bui, P. O. Curran, C. F. Price
16:35	**5-ISICP-004-3-OP-JCC** Prediction of Airbag Inflator Performance J. C. Chastenet, A. Mobuchon	**5-ISICP-017-9-OP-VW** Burning Phenomena of the Doublebase Gun Propellant JA2 V. Weiser, S. Kelzenberg, T. Fischer, A. Baier, G. Langer, N. Eisenreich, W. Eckl
17:00	**5-ISICP-005-3-OP-RK** Energetic Materials as Gas Generators in Explosions Suppression Systems R. Klemens, M. Gieras, B. Szatan, P. Wolański, J. Nowaczewski, A. Maranda, J. Paszula	**5-ISICP-011-8-OP-RH** Theoretical Analysis of Modern ETC-Concepts R. Heiser
17:25	**5-ISICP-001-3-OP-KE** Characterization of the Combustion Behavior of Gas-generating Pyrotechnics Using Propellant Technology Methods K. Engelen, M.H. Lefebvre, J. De Ruyck	**5-ISICP-008-8-OP-JEB** Model Formulation of Laser Initiation of Explosives Contained in a Shell K.K. Kuo, E. Boyer

Tuesday Morning, 20 June 2000

08:15	PLENARY PAPER 5-ISICP-006-1-IV-BNK	Session Chair: Dr. R. Behrens

Extraction of Kinetic Information from Burning and Ignition Experiments
Prof. B.N. Kondrikov

	Room Azzurra Area 3: Combustion Performance of Hybrid and Solid Rocket Motors Session Co-Chairs: Dr. A. Peretz and Prof. C. Buongiorno	**Room Azzalea Area 8: Theoretical Modeling and Numerical Simulation of Combustion Processes** Session Chair: Dr. E.S. Oran
09:00	**5-ISICP-012-6-OP-YM** Hybrid Propulsion for Small Satellites: Logic of Design and Tests Y. Maisonneuve, J. C. Godon, R. Lecourt, G. Lengelle, N. Pillet	**5-ISICP-016-8-OP-ESO** First Principles Simulations of Gas-Phase DDT and the Effects of Hot-Spot Formation E. S. Oran, A. M. Khokhlov
09:25	**5-ISICP-008-6-OP-ARS** Re-Ignition in a GOX/HTPB Hybrid Rocket A. Russo Sorge, M. Roma, F. Liccardo, G. Torella	**5-ISICP-014-8-OP-JDR** Aerothermochemical Model for the Interior Ballistics of Solid Propellant Rocket Motors R. Caro, J. Pérez, J. de Dios Rivera
09:50	**5-ISICP-015-6-OP-GAR** Surface Heat Release of HTPB-based Fuels in Oxygen Rich Environments G.A. Risha, G.C. Harting, K.K. Kuo, A. Peretz, D.E. Koch, H.S. Jones, J.P. Arves	**5-ISICP-007-8-OP-MY** Numerical Simulation of Combustion Processes in Rocket Motors M. Yumusak, A.T. Uçer
10:15	COFFEE	
10:45	**5-ISICP-034-6-OP-ANL** The Advanced Technology of Prevention of the Anomalous Combustion Regimes Development in the Submarine Ballistic Rocket Large-Sized SPRM A.N. Lukin	**5-ISICP-009-8-OP-OO** Numerical Simulation of the Vaporization / Combustion of a Single Aluminum Particle in Air O. Orlandi, Y. Fabignon
11:10	**5-ISICP-004-6-OP-PLB** Experimental and Numerical Study of Casting Process Effects on Small Scale Solid Rocket Motor Ballistic Behavior P. Le Breton, D. Ribéreau, C. Marraud, P. Lamarque	**5-ISICP-021-8-OP-GC** Numerical Analysis of Grain Burnback in Solid Propellants G. Colasurdo, L. Casalino, D. Pastrone
11:35	**5-ISICP-009-6-OP-QYL** Effects of Altitude on Microwave Attenuation of Solid Rocket Exhaust Plumes Q.Y. Liu, P. Zhang, D.M. An	**5-ISICP-005-8-OP-JP** Mass Transfer Effects on Sound Propagation in a Droplet-Gas Mixture J. Dupays
12:00	**5-ISICP-018-6-OP-JMC** Plume Temperature Distribution Measurements of a Spin-Stabilized Rocket J.M. Char, J.H. Yeh	**5-ISICP-025-8-OP-HBE** A Numerical Simulation of the Pulse Detonation Engine with Hydrogen Fuels H.B. Ebrahimi, C.L. Merkle
12:25	LUNCH	

14:00-17:50	POSTER SESSIONS	Session Co-Chairs: Prof. L. Galfetti and Mr. E. Boyer
		Tuesday Afternoon, 20 June 2000

Area 1 — Reaction Kinetics

1	2	3	4	5
5-ISICP-004-7-OP-BMK Cyclodextrin Polymer Nitrate B.M. Kosowski	5-ISICP-012-7-OP-VVN Thermal Decomposition of 1,3,3-Trinitroazetidine in Gas and Liquid Phase V.V. Nedelko, B.L. Korsounskii, N.V. Chukanov, T.S. Larikova, N.N. Makhova, I.V. Ovchinnikov	5-ISICP-022-8-OP-FV None Equilibrium Reactions in Combustion and Detonation Processes F. Volk		5-ISICP-005-1-PP-JDM Combustion Experiments on TNT and Tritonal in Closed Chambers with Either an Air or Nitrogen Atmosphere J.W. Forbes, J. Chandler, B. Cunningham, L. Green, J. Reaugh, A. Kuhl, J.D. Molitoris

Area 2 — Environmental, Commercial, Recycling & Safety

1	2	3	4	5
5-ISICP-006-3-OP-HRB FTIR Absorption Spectroscopy of Environmentally Friendly Airbag Gas Generant H.R. Blomquist, S.T. Thynell, C.F. Mallery	5-ISICP-007-3-PP-CMW Nitramine Propellant Formulations for Airbag Inflators C. M. Walsh	5-ISICP-004-2-PP-SGB Combustion Properties Relevant to Cofiring of Solid Rocket Motor Washout Material S.G. Buckley, R. Moehrle, J. Lipkin, G. Mower, and L.L. Baxter	5-ISICP-002-2-OP-JRS Aerosol Emission Measurements of Rocket Motors from Contained Open Burn Events J.R. Stephens	5-ISICP-009-7-OP-CLY Combustion Synthesis of SiO_2 in Premixed Flames C.L. Yeh, E. Cho and H.K. Ma
5-ISICP-001-4-OP-AV Methods for Recovery of Ingredients from Solid-Propellant Rocket Motors A. Vorozhtsov, A Salko, S. Bondarchuk	5-ISICP-006-4-OP-ALR Chemical Conversion of 2,4,6-Trinitrotoluene (TNT) to New High Performance Polymers A.L. Rusanov, L.G. Komarova, M.P. Prigozhina, V.A. Tartakovsky, S.A. Shevelev, M.D. Dutov	5-ISICP-003-5-OP-BMK Development of Passivated Pyrophoric Metal Powders (Hafnium and Zirconium) With Reduced Electrostatic Discharge (ESD) Sensitivity B.M. Kosowski	5-ISICP-004-5-OP-BNK Deflagration Regimes and Safety Areas of Nitrobenzene and Proparhyl Alcohol G.D. Kozak, B.N. Kondrikov	

Area 3 — Hybrid & Solid Rocket Motors

1	2	3	4	5
5-ISICP-012-9-OP-IGA Bomb Testing and Similarity of Propulsion Systems I.G. Assovskiy	5-ISICP-045-6-OP-CM Burning Rate Data Reduction of Ariane Boosters Small-Scale Test Motors L.T. DeLuca, A. DeNigris, C. Morandi, F. Pace, A. Ratti, M. Servieri, A. Annovazzi, E. Tosti, R.O. Hessler, R.L. Glick	5-ISICP-024-9-OP-ROH Motor Variability Effects on Burning Rates Measured in Subscale Rocket Motors R.O. Hessler, R.L. Glick, C. Morandi, L.T. DeLuca, A. Annovazzi, E. Tosti	5-ISICP-029-6-PP-GJV Ballistic and Combustion Properties of High-Pressure Exponent Hydrocarbon-Based Fuel-Rich Propellants G.J. van Zyl	5-ISICP-033-6-OP-JLC Rocket Testing at EMRTC J.L.M. Cortez, J. Forster, A. Perryman, J. Rusek
5-ISICP-008-3-PP-BG Study of Multi-Perforated Combustion Paste Propellant Rocket Motor B. Gao, D.Y. Ye, S.X. Jia	5-ISICP-021-6-OP-AG Parametric Investigation on Similarity and Scale Effects in Hybrid Motors R.D. Swami, A. Gany			

POSTER SESSIONS (continued)   Session Co-Chairs: Prof. L. Galfetti and Mr. E. Boyer

Tuesday Afternoon (14:00-17:50), 20 June 2000

Area					
Area 4 _Energetic Materials_ _Ignition & Combustion_	5-ISICP-020-6-OP-VVA **Active Electric-Discharge Control of Slow-Combustion-to-Detonation Transition** V.V. Afanasyev, S.V. Ilyin, N.I. Kidin, N.A. Tarasov, A.V. Lapin, A.K. Kuzmin 5-ISICP-007-4-PP-MS **The Nimic Energetic Materials Compendium (EMC)** M. Fisher, M. Sharp	5-ISICP-013-6-OP-VVA **Combustion of Propellant Grain, Forcing by Heat-Conducting Elements with Memory Effect** V.A. Arkchipov 5-ISICP-022-6-OP-CZ **CO_2 Laser Applications in the Combustion of Energetic Materials** C. Zanotti, P. Giuliani	5-ISICP-038-6-OP-SR **Acoustic Emission of Underwater Burning Solid Rocket Propellants** S. Rampichini, D. Ruspa, L.T. DeLuca	5-ISICP-026-6-OP-BNK **Solid Propellant Ignition by Co_2 Laser Radiation** B.N. Kondrikov, L.T. DeLuca	5-ISICP-030-6-OP-GAR **Laser Ignition Characterization of N-5 Double-Base Solid Propellant** G.A. Risha, K.K. Kuo, D.E. Koch, J.R. Harvel
Area 5 _Defects &_ _Flowfield_	5-ISICP-008-5-PP-RWA **Influence of Microcracking on Pressure-Dependent Energetic Crystal Combustion** R.W. Armstrong, C.F. Clark, W.L. Elban	5-ISICP-043-6-OP-GH **Experimental Research of Typical Defects Propagation Process in Solid Rocket Motor** G. He, T. Cai, P. Liu	5-ISICP-014-6-OP-OVM **Aerodynamics and Combustion in the Countercurrent Type Vortex Combustion Chamber** V.A. Arkchipov, O.V. Matvienko	5-ISICP-019-6-OP-AG **Parametric Investigation of Supersonic Combustion of Solid Fuels** I. Feldman, A. Gany	5-ISICP-032-6-OP-JMC **Supersonic Combustion Phenomena under different Combustion Chamber Design** Jir-Ming Char, Wen-Jay Liou
Area 6 _Metal_ _Combustion_	5-ISICP-001-5-OP-MMM **Combustion and Flame Spreading of Aluminum Tubing in High Pressure Oxygen** M.M. Mench, K.K. Kuo, J. Haas	5-ISICP-029-8-PP-AU **Ignition and Combustion of Boron Particles in Fluorinated Environments: Experiment and Theory** A. Ulas, K.K. Kuo, C. Gotzmer			
Area 7 _New Ingredients_	5-ISICP-008-7-OP-CB **Reforming and Pyrolysis of Liquid Hydrocarbons and Partially Oxidised Fuels For Hypersonic Propulsion** C. Bruno, M. Filippi	5-ISICP-007-6-OP-GCH **Burning Rate Characterization of OXSOL Liquid Oxidizer** G.C. Harting, J.W. Mordosky, B.Q. Zhang, T.T. Cook, K.K. Kuo	5-ISICP-014-7-OP-VYE **Mechanism of Modifying the Burning Rate of Compositions Containing Nitro- and Nitrato Groups by High-Energy Polynitrogen Compounds** V.P. Sinditskii, V.Y. Egorshev, V.I. Kolesov, M.V. Berezin, A.E. Fogelzang	5-ISICP-015-7-OP-VVS **Flame Structure of Hydrazinium Nitroformate** V.P. Sinditskii, V.V. Serushkin, and S.A. Filatov	5-ISICP-003-2-PP-AVDH **HNF/HTPB Based Composite Propellants** A.E.D.M. van der Heijden, H.L.J. Keizers, W.H.M. Veltmans

Area 8 Modeling & Numerical Simulation	**5-ISICP-028-8-PP-RL** Application of a Eulerian-Lagrangian Two-Phase Flow Solver on a LPP Reactive Flow O. Boisneau, R. Lecourt	**5-ISICP-027-8-PP-MDG** Numerical Simulation of Solid Motor Ignition Transient M. Di Giacinto	**5-ISICP-030-8-PP-AA** Zero-Dimensional Unsteady Internal Ballistics Modeling A. Annovazzi, A. Tamburini	**5-ISICP-023-8-PP-LG** Numerical Modeling of Solid Rocket Motors L. Galfetti	**5-ISICP-018-8-OP-AGK** The Features of the Reaction Initiation for the Singular Crystals in the Thermomechanical Ignition Models A.G. Knyazeva
	5-ISICP-026-8-OP-NS Navier-Stokes Solution for Solid Fuel Regression Rate in 2-D Hybrid Rocket Motor N. Serin, Y. Göğüş	**5-ISICP-024-8-OP-HYW** Prediction of Hybrid Fuel Regression Rates in Turbulent Boundary Layer Combustion H.Y. Wang, J.M. Most, G. Lengellé	**5-ISICP-004-8-PP-AKM** The Analysis of Gun Pressure Instability A.K. Macpherson, A.J. Bracuti, D.S. Chu, P.A. Macpherson	**5-ISICP-002-8-OP-VVS** Shock-Wave Calculation Model for Detonation of Multicomponent Energy Carrier Containing Combustible Phase V.N. Okhitin, V.V. Selivanov, A.V. Zibarov	**5-ISICP-003-8-OP-TSP** Basic Scheme for Computer Simulation of Decomposition Reactions for Energetic Compounds T.S. Pivina, A.A. Porollo, T.V. Petukhova, V.P. Ivshin
Area 9 Combustion Diagnostics	**5-ISICP-021-9-OP-YMT** Diagnostic Methods for the Combustion of Energetic Materials Y.M. Timnat	**5-ISICP-006-9-OP-VSA** Interferometric Techniques and Automatic Data Processing in Propellants Combustion Research V.S. Abrukov, I.V. Andreev, I.G. Kocsheev	**5-ISICP-002-9-OP-UB** Imaging of Mixing and Combustion Processes in a Supersonic Combustion Ramjet Chamber U. Brummund, F. Scheel	**5-ISICP-007-9-OP-VW** Spectroscopic Flame Diagnostics by Analyzing NIR Water Bands W. Eckl, V. Weiser, N. Eisenreich	**5-ISICP-004-9-OP-YLS** Quantitative Measurement of Flame Generated Particulate Oxide by Interferometry Technique Yu.L. Shoshin, I.S. Altman
	5-ISICP-011-9-OP-FC Spontaneous Radiation Heat Feedback Measurements in Radial Burning Propellant Samples F. Cozzi, G.S. Tussiwand, A.L. Ramaswamy	**5-ISICP-016-9-OP-KJF** Propellant Characterization & Evaluation Using Low and High Energy Laser Diagnostics K.J. Fleming, W.J. Andrzejewski, V.M. Loyola, T.A. Broyles	**5-ISICP-010-9-OP-SVI** On a Method for Measuring Non-Stationary Burning Velocity in Condensed Systems Based on Interferometric Measurements S.V. Ilyin, O.S. Danilov	**5-ISICP-009-9-PP-URC** Nonsteady Solid Propellant Regression Rate Measurements by a Plane Capacitor Method U. Carretta, R. Dondé, C. Guarnieri	

	Tuesday Afternoon (14:00-17:50), 20 June 2000				
Area 10 **Propellant & Motor Stability** **Ablation**	**5-ISICP-041-6-OP-FSB** T-Burner Response Analysis Using the SPP/SSP Code F.S. Blomshield, D.E. Coats, S.S. Dunn, J.C. French	**5-ISICP-004-10-PP-FEC** Some Effects of Pressure Coupling and Velocity Coupling on the Global Dynamics of Combustion Chambers F.E.C. Culick, G. Isella	**5-ISICP-027-6-OP-FC** Radiation-Driven Burning of Energetic Solid Materials With Phase Transition F. Cozzi, L.T. DeLuca, B.V. Novozhilov	**5-ISICP-016-6-OP-VNM** On Stability of the Combustion of Ammonium Perchlorate V.N. Marshakov, G.V. Melik- Gaykazov, A.G. Istratov	**5-ISICP-046-6-OP-IAF** Surface Spin Combustion in Gas-Solid System I.A. Filimonov, N.I. Kidin, A.S. Mukasyan
	5-ISICP-001-10-PP-FC Degradation of a Thermal Insulator Under Vibration and Acceleration A. Eythrib, F. Cauty, G. Colombo, A. Menalli, L. Galfetti	**5-ISICP-002-10-PP-CZ** Thermal Protection Wall-Effect on the Combustion of Solid Propellant at Subatmospheric Pressure C. Zanotti, P. Giuliani, M. Turco, M. Kohno	**5-ISICP-003-10-OP-LG** Macrokinetic Characterization of Ablative Materials A.A. Zenin, L. Galfetti, A. Menalli	**5-ISICP-012-8-OP-RSB** Analysis of Vorticity Effects in Oscillatory Flow Fields of Simulated Solid Propellant Rocket Motors R. S. Brown	

Wednesday Morning, 21 June 2000

08:15	PLENARY PAPER 5-ISICP-036-6-IV-BN	Session Chair: Prof. Y.M. Timnat

PLENARY PAPER 5-ISICP-036-6-IV-BN
The Status of Gel Propellants in Year 2000
B. Natan, S. Rahimi (Presented by Dr. B. Natan)

	Room Azzurra Area 4a: Energetic Materials Combustion for Rocket Propulsion	Room Azzurra Area 10a: Propellant and Motor Stability
	Session Chair: Dr. R. Pein	Session Co-Chairs: Prof. F.E.C. Culick and Prof. S. Krishnan.
09:00	**5-ISICP-002-3-OP-FT** Formulation and Combustion of Gelled Liquid Propellants with Alex™ Particles F. Tepper, L. A. Kaledin	**5-ISICP-040-6-OP-FSB** Summary of Multi-Disciplinary University Research Initiative in Solid Propellant Combustion Instability F.S. Blomshield
09:25	**5-ISICP-005-6-OP-JWM** Combustion of Gelled RP-1 Propellant with Alex™ Particles J.W. Mordosky, B.Q. Zhang, G.C. Harting, T.T. Cook, K.K. Kuo, F. Tepper, L. A. Kaledin	**5-ISICP-022-9-OP-MB** Examples of Unsteady Combustion in Non-Metallized Propellants M.W. Beckstead, K.V. Meredith, F.S. Blomshield
09:50	**5-ISICP-002-7-OP-BB** Combustion Phenomena of a Solid Propellant Based on Aluminium Powder B. Baschung, D. Grune, H. H. Licht, M. Samirant	**5-ISICP-024-6-OP-BTZ** Active Damping of Combustion Instabilities With Oscillatory Liquid Fuel Sprays E. Lubarsky, Y. Neumeier, B.T. Zinn
10:15	COFFEE	
	Room Azzurra Area 4b: Energetic Materials Combustion for Rocket Propulsion	Room Azzurra Area 10b: Propellant and Motor Stability
	Session Co-Chairs: Dr. R.L. Glick and Dr. F. Blomshield	Session Co-Chairs: Prof. F.E.C. Culick and Prof. S. Krishnan
10:45	**5-ISICP-017-8-OP-SAR** Nonsteady Combustion of Composite Solid Propellants S. A. Rashkovsky	**5-ISICP-010-8-OP-BVN** Limit Cycles for Solid Propellant Burning Rate at Constant Pressure B.V. Novozhilov, F. Cozzi, L.T. DeLuca
11:10	**5-ISICP-004-1-OP-MQB** Combustion of Heterogeneous Solid Propellants M. Q. Brewster, G. M. Knott, B. T. Chorpening	**5-ISICP-028-6-OP-AAZ** Characteristic Features of Burning Rate Response Functions of Solid Propellants: A Review A.A. Zenin, S.V. Finjakov
11:35	**5-ISICP-003-6-OP-VSB** Burning Rate Modifiers Effects on a Modified Polyvinyl Chloride-Based Propellants V.S. Bozic, Dj.Dj. Blagojevic	**5-ISICP-023-6-OP-JCF** HMX T-Burner Pressure Coupled Response at 200, 500, and 1000 psi J.C. Finlinson, R. Stalnaker, F.S. Blomshield
12:00	**5-ISICP-018-9-OP-NFW** Study on the Action Temperature of Catalysts to Solid Propellant Burning Rate Using Embedded Thermocouple N.F. Wang, L. Wang	**5-ISICP-015-8-OP-AGK** The Stationary Modes of the Reaction Front and Their Stability for Solid Media with Regard to Chemically Induced Internal Stresses and Strains A. G. Knyazeva
12:25	LUNCH	

Wednesday Afternoon/Evening, 21 June 2000

14:00	PLENARY PAPER 5-ISICP-023-9-IV-AC _Session Chair: Prof. L.T. De Luca_

Elastic Laser Scattering as a Diagnostic Tool in Reacting Two–phase Systems
Prof. A. Coghe

	Room Azzurra Area 6: Metal Combustion _Session Co-Chairs: Prof. M. Beckstead and Prof. A. Gany_	**Room Azalea Area 9: Combustion Diagnostic Techniques** _Session Co-Chairs: Prof. A Coghe and Prof. V.E. Zarko_
14:50	**5-ISICP-007-7-OP-VR** **Testing of Metal Powders Behavior in a Hot Stage Microscope** V. Rosenband, A. Gany	**5-ISICP-001-9-OP-VEZ** **Critical Assessment of the Microwave Method for Measuring Steady-State and Transient Regression Rates of Solids** V.E. Zarko, V.V. Perov, V.N. Simonenko
15:15	**5-ISICP-002-5-OP-MMM** **Flame Spreading and Violent Energy Release (VER) Processes of Aluminum Tubing in LOX/GOX Environments** M.M. Mench, K.K. Kuo, J.H. Sturges, P. Houghton, J.G. Hansel	**5-ISICP-015-9-OP-FC** **Laser Recoil Experiments** F. Cozzi, L. Asa, S. Palozzo, R.O. Hessler
15:45	COFFEE	
16:10	**5-ISICP-011-6-OP-LK** **Initiation and Combustion of Al/NH$_4$ClO$_4$/Viton Ignition Mixture** L. Kalontarov, Y. Borkowski	**5-ISICP-005-9-OP-ISA** **Determination of the Temperature of Condensed Particles Within the Flame by Their Radiation** I.S. Altman, D. Lee, Yu.L. Shoshin, J.D. Chung, M. Choi
16:35	**5-ISICP-020-9-OP-VEZ** **Evolution and Motion of Aluminum Agglomerates in Combustion Products of Model Solid Propellant** O.G. Glotov, V.V. Karasev, V.E. Zarko, T.D. Fedotova, M.W. Beckstead	**5-ISICP-013-9-OP-HKC** **Comparison of PIV and Colour-Schlieren Measurements of the Combustion Process of Boron Particle Containing Solid Fuels Slabs in a Rearward Facing Step Combustor** A. Thumann, H.K.Ciezki
17:00	**5-ISICP-003-9-OP-LW** **Experimental Observations on Disruptive Burning of Coated Aluminum Particles** L. Wang, H.Q. Liu, M.H. Liu, N.F. Wang	**5-ISICP-026-9-OP-WZ** **Quick Spectroscopic Diagnostics for the Flame Temperature** W. Zhao, S. Zhu, K. Tian, D. Liu
17:25	**5-ISICP-001-6-OP-VAB** **Experimental Study of Evolution of Condensed Combustion Products in Gas Phase of Burning Solid Rocket Propellant** V.A. Babuk, V.A. Vasilyev, P.A. Naslednikov	**5-ISICP-025-9-OP-BZ** **Process Tomography (PT) as Diagnostic Tool for Combustion Phenomenon** T. Piotrowski, A. Plaskowski, B. Zygmunt
20:00	Symposium Gala Dinner and Summerfield Memorial Awards	

Thursday Morning, 22 June 2000

08:15 PLENARY PAPER 5-ISICP-001-8-IV-BVN   Session Chair: Prof. B.N. Kondrikov
Nonlinear Combustion in Solid-Propellant Rocket Motors
Prof. B.V. Novozhilov

Time	Room Azzurra Area 5a: Combustion Anomalies of Energetic Materials — Session Chair: Mr. T. Boggs	Room Azalea Area 10c: Propellant and Motor Stability — Session Co-Chairs: Dr. B. Natan and Prof. B.T. Zinn
09:00	**5-ISICP-007-5-OP-HLB** Convective Burning in Gaps of PBX 9501 H.L. Berghout, S.F. Son, B.W Asay	**5-ISICP-020-8-OP-FECC** Some Influences of Noise on Combustion Instabilities and Combustor Dynamics F.E.C. Culick, C. Seywert
09:25	**5-ISICP-019-8-OP-TC** Investigation of Combustion Flow Field in Composite Propellant Cracks T. Cai, W.P. Zhang, G. He	**5-ISICP-031-6-OP-KNL** A Computational Study of the L* Instability with a Nonlinear Frequency Response K.R. Anil Kumar, K.N. Lakshmisha
09:50	**5-ISICP-042-6-OP-GH** Research on Convective Burning and Propagation Mode in Solid Propellant Grain Cracks L. Du, G. He, T. Cai, P. Liu	**5-ISICP-010-6-OP-OR** Low-Frequency Stability of Solid Propellant Combustion in Rocket Motors O. Romanov
10:15	COFFEE	
	Room Azzurra Area 5b: Combustion Anomalies of Energetic Materials Session Co-Chairs: Dr. R.H.W. Waesche and Dr. G. Lengellé	**Room Azalea Area 10c: Propellant and Motor Stability** Session Co-Chairs: Dr. B. Natan and Prof. B. T. Zinn
10:45	**5-ISICP-002-6-OP-SK** Experimental Investigation of Erosive Burning of Composite Propellants Under Supersonic Cross Flow Velocity S. Krishnan, K. K. Rajesh	**5-ISICP-044-6-OP-MV** Intrinsic Burning Stability of Solid Propellants with Variable Thermal Properties M. Verri, L.T. DeLuca
11:10	**5-ISICP-035-6-OP-TN** Improvement of Flameholding Characteristics by Incident Shock Waves in Supersonic Flow T. Fuimori, M. Murayama, J. Sato, H. Kobayashi, S. Hasegawa, T. Niioka	**5-ISICP-019-9-OP-ROH** Frequency Response of a Model Subscale Rocket Motor R.O. Hessler, R.L. Glick, R. Bertelé, D. Cedro, G. Fiorentino, L.T. DeLuca
11:35	**5-ISICP-017-6-OP-AG** Analysis and Testing of Fuel Regression Rate Control in Solid Fuel Ramjets D. Pelosi-Pinhas, A. Gany	**5-ISICP-013-8-OP-IGA** Charge Design and Non-Acoustic Instability of Solid Rocket Motors I.G. Assovskiy, S.A. Rashkovskiy
12:00	**5-ISICP-037-6-OP-LG** Solid Propellants Convective Ignition and Flame Spreading L. Galfetti, G. Colombo	**5-ISICP-039-6-OP-RHWW** Space Shuttle Booster Internal Flows and Slag Expulsion R.H. Woodward Waesche
12:25	LUNCH	
12:30	Bus Tour To Fiat Research Center (Orbassano, near Turin) or Fiat Avio (Turin)	
19:30	End of Symposium	

ABSTRACTS OF
INVITED PLENARY PAPERS

ROOM AZALEA

Chemical and Physical Processes that Control the Thermal Decomposition of RDX and HMX[†]

R. Behrens, S. Maharrey, S. Mack[#], and J. Wood[+]
Sandia National Laboratories[*]
Combustion Research Facility
P.O. Box 969
Livermore, California, USA
E-mail: rbehren@sandi.gov

RDX and HMX are two cyclic nitramines that are used extensively as ingredients in both propellants and explosives. Understanding the reactive processes that control the decomposition and reaction of these materials over a wide range of time scales is important for assessing their behaviors under the various conditions encountered during their life cycle. These conditions range from normal storage conditions to combustion of the propellant or explosive, and include environments encountered in various accident scenarios. The time scales of interest range from changes that occur over years ($\sim 10^9$ sec) for aging to changes that occur in $\sim 10^{-9}$ sec for detonations. Our work focuses on reaction processes that control the decomposition of RDX and HMX at intermediate time scales (10^{-2} to 10^5 sec). These results are useful for assessing the changes that occur in propellants or explosives that are exposed to fires and for providing insight into the reaction processes that may occur in the condensed phase on the surface of burning propellants.

Simultaneous thermogravimetric modulated beam mass spectrometry (STMBMS), optical microscopy, and scanning electron microscopy (SEM) have been used to examine the chemical and physical processes that control the thermal decomposition of RDX and HMX in the solid and liquid phases. The results show that a set of complex processes, involving several different parallel reaction pathways, control their decomposition. The relative importance of the different pathways depends on the phase of the reactant and the extent of confinement of the gaseous decomposition products with the remaining reactant.

The decomposition of RDX (mp $\sim 202°C$) has been examined over a temperature range from 160°C to 220°C. In the solid phase, the nucleation and growth of a non-volatile residue (NVR) among the RDX particles control the rate of reaction. The nucleation of the NVR appears to be preceded by the "sintering" of the RDX particles to form agglomerates. Once the NVR nucleates, its growth is controlled by the transport of RDX to its surface where a portion of the RDX molecule is incorporated into the NVR while the other portion is released as gaseous products. The main gaseous products evolved by this interaction are H_2O, CO/N_2, CH_2O, NO, and N_2O. Concomitantly, more complex gaseous products evolve from the decomposition of the NVR while it continues to grow via reactions with RDX. These products include: formamide, N-methylformamide, N,N-dimethylformamide,

dimethylnitrosamine and C_3H_9N (a form of amine). The maximum rate of reaction occurs just prior to depletion of the RDX, similar to the behavior observed in the growth of polymers.

In the liquid phase, the four reaction pathways observed in our previous work[1,2] continue to be observed. However, now the STMBMS experiments can be varied over a more extensive set of experimental conditions. This allows the non-linear "autocatalytic" channel to be examined more closely. Under low confinement conditions of the gaseous decomposition products, the first-order RDX decomposition reaction that forms oxy-s-triazine as one of the primary products still accounts for a major fraction of the decomposition. However, under higher confinement conditions the non-linear reaction process involving the nucleation and growth of the NVR and it reaction with the RDX becomes more dominant. This reaction pathway leads to the formation of CH_2O and N_2O as the major products of decomposition. Under the highest confinement conditions of our experiments this non-linear reaction channel appears to be pseudo-first-order during the first stages of the decomposition.

The decomposition of HMX (mp ~270°C) in the solid phase has been examined over the temperature range from 175°C to 260°C. The identities of the decomposition products (both major and minor products) are identical to those observed in the decomposition of RDX that occurs via interactions with the NVR. However, the decomposition of HMX is further complicated by the fact that the reactions between HMX and the NVR now occur in microscopic bubbles formed within grains of HMX. Platelet-shaped grains are formed within HMX particles as the HMX undergoes the $\beta \to \delta$ phase transition. During the first 30% of decomposition, reaction occurs at sites within these grains, leading to the creation of bubbles containing gaseous products. The size of the bubbles appears to be limited by the thickness of the HMX grain (~ 0.3 to 2 μm), with the gaseous products being released from the bubble as it intersects the grain boundary. The size and number density of the bubbles created in the decomposition process are determined from SEMs of the NVR created in each bubble as it nucleates and grows. Thus, there is ~ 1 gas bubble, containing a reactive gas mixture (N_2O and CH_2O), in every 10 μm^3 of HMX. The creation of these bubbles within HMX may have significant implications for the safety of propellants and explosives involved in slow cookoff situations associated with fires.

Mathematical models characterizing these processes are currently being developed and parameters for the models are being determined from the STMBMS and SEM data.

[1]R. Behrens and S. Bulusu, "Thermal-Decomposition Of Energetic Materials .3. Temporal Behaviors Of the Rates Of Formation Of the Gaseous Pyrolysis Products From Condensed-Phase Decomposition Of 1,3,5-Trinitrohexahydro-S-Triazine," Journal Of Physical Chemistry **96** (#22), 8877-8891 (1992).

[2]R. Behrens and S. Bulusu, "Thermal-Decomposition Of Energetic Materials .4. Deuterium-Isotope Effects and Isotopic Scrambling (H/D; C-13/O-18; N-14/N-15) In Condensed-Phase Decomposition Of 1,3,5-Trinitrohexahydro-S-Triazine," Journal Of Physical Chemistry **96** (#22), 8891-8897 (1992).

5-ISICP-009-3-IV-AF

FIAT Avio Activities for Launchers and a Strategy for European Industry

A. Fabrizi
Responsabile Unità Business Spazio FIAT Avio
Fiat Avio – Comprensorio BPD
Colleferro, RM, Italy
Tel: +39-06-9728-5345
Fax: +39-06-9728-5626
E-mail: Fiat.Spazio@mclink.it

A short introduction is done about Fiat Avio space activities focusing on launchers. The view of the market position, commercial launchers, market growth, and market shares between small and medium-heavy launchers is presented. Then Fiat Avio strategy is depicted. This consists mainly in being ready to cover the non-geo market that cannot be neglected by the European industry. This strategy foresees the preparation of technologies and "building blocks" to minimize lead time of new launchers and the development of small launchers to serve European early needs and to test system approach and building blocks. Main characteristics of building blocks and relevant small and medium launchers performances are presented. The conclusion focuses on the proposed program, that is a revision of the "Vega" program proposed last year, but including higher technology content, higher performances and better synergies with Ariane, as well as on the strategy that enables all European industry to be presented also on the non-geo market.

THIS PAGE HAS BEEN DELIBERATELY LEFT BLANK

Extraction of Kinetic Information from Burning and Ignition Experiments

B.N. Kondrikov
Mendeleev University of Chemical Technology
Moscow 125047, Russia
Tel: (095)496-6818
Fax: (095)200-4204
E-mail: bkondr@orc.ru

A comprehensive analysis of kinetics and overall mechanisms of chemical reactions of a series of solid propellants and propellant ingredients (mostly of the classes of O-, C-, and N-nitrocompounds) is carried out. Results of an investigation of NM, AN, ADN, HAN and aliphatic azides are also included for comparison. Chemical reactions responsible for propagation of steady state burning, ignition, and self-ignition (including initiation of explosion by shock or weak impact and friction) are examined. In every particular case thorough inspection of the relevant data and specific methods of extraction of kinetic parameters is implemented. Careful comparison of the kinetic constants derived from the abundant information obtained through the investigation of the slow thermal decomposition of the corresponding substances is performed. General features of the main chemical transformations are manifested. The results presented in about two hundred original publications are reviewed, many of which are in general use, but have never been considered together, while others have actually been forgotten. Some of the data are practically unknown within the international scientific community.

The main result of the study is the clarification of high pressure, including high dynamic pressure and influence on kinetic parameters of the substances under consideration. It is demonstrated that within the limits of accuracy of the kinetic data taken from the measurements at a high pressure, and having regard to the level of reliability of the corresponding methods of data processing, the monomolecular reaction of thermal decomposition of the substances considered is scarcely affected by the high pressure. Several exceptions, including Nitromethane and Trinitrotoluene kinetics, are discussed and possible mechanisms of the pressure influence are proposed.

Generalization of the data in the field of the usual kinetic measurements performed at low pressures (about one atmosphere) and low temperatures (about four to seven hundred degrees Kelvin) is especially interesting. It is well known that the data from different scientists sometimes differ drastically in their positions at the Arrhenius plot. It is proposed that this scatter is by no means a characteristic feature of the substances (or investigators) considered. At the same time, some of the nitrocompounds studied are extremely unstable in this sense. It has been proven that, in general, this is not a result of an instrumental mistake or a wrong general approach (although these sometimes do take place), but is connected with specificity of a chemical nature of the compound.

For all of the substances studied, the most reliable figures of kinetic constants are recommended for the use in the broad region of temperatures (from about four to ten hundred K) and pressures of up to several GPa, which presumably is good enough for application of the data in a variety of the propulsion technology.

THIS PAGE HAS BEEN DELIBERATELY LEFT BLANK

The Status of Gel Propellants in Year 2000

B. Natan and S. Rahimi
Faculty of Aerospace Engineering
Technion - Israel Institute of Technology
Haifa 32000, Israel
Tel: 972-4-829-2395
Fax: 972-4-823-1848
E-mail: aerbeny@aerodyne.technion.ac.il

Gel propellants have been studied for several decades for various kinds of applications. The motivation for the use of these propellants lies mainly to their safety and their energy density due to addition of metal particles.

Slurry fuels are considered as the first generation of metal particle containing liquid fuels. Significant research has been conducted on slurries since the early 1950's and there is an overlapping between slurries and gels. However, since the slurries lack the basic ingredients that make gels behave the way they do, suspension of particles within the liquid is not quite successful.

What are gels? Gels are liquids whose rheological properties have been altered by the addition of certain gelling agents (gellants) and as a result, their behavior resembles the behavior of solids. The definition of a gel is not straightforward. As D. Jordan Lloyd said in her survey on the problem of gel structure in 1926, "The colloidal condition, the gel, is one which is easier to recognize than to define."

From the propulsion aspect, gels can be used in guns and also in tactical and strategic missiles. Theoretical evaluations exhibit significant benefits of gels over conventional liquid propellants. In addition, the viscoelastic/viscoplastic properties reduce spill in cases of accidental leakage, hence increasing safety. From the fluid mechanics point of view, gels behave as time-dependent, non-Newtonian fluids. In general, gel propellants exhibit shear-thinning (viscosity decreases with increasing applied shear stress), thixotropic (viscosity decreases in time at constant applied shear stress) behavior.

The early studies on gels dealt with gelled liquids, especially HAN/TEAN combinations for gun purposes. For missile applications, the studies concentrated in the last two decades on Hydrazine-IRFNA and JP-5 or RP1 with and without aluminum particles burning with oxygen or hydrogen peroxide.

Research was done on several areas concerning gels:

- Concept feasibility: theoretical predictions and applications.
- Rheological characterization: definition of the gel type, measurement of the rheological
- properties, identification of the parameters that affect their behavior.
- Combustion behavior characterization: measurement of gel fuel droplet burning rates,
- theoretical modeling (in particular characterization of secondary atomization of aluminized slurry/gel fuel droplets), combustion of gel fuels in small motors, ignition.

- Atomization: investigation of non-Newtonian fluid atomization characteristics, feeding systems.
- Flow behavior: flow of shear-thinning fluids in pipes and injectors, thixotropic effect.
- Processing: preparation of gel propellants, gellants, compatibility of the ingredients.
- Applications: experimental rocket motors for various purposes.
- Patents of gel propellant/gellant compositions.

The full paper is a review that deals with all these aspects of gel propellants.

Elastic Laser Scattering as a Diagnostic Tool in Reacting Two-phase Systems

A. Coghe
Dip. Energetica, Politecnico di Milano
Via La Masa 34 – 20156 Milano, Italy
Tel: +39 02 2399 8537
Fax: +39 02 2399 8566
E-mail: aldo.coghe@polimi.it

In combustion environments, optical diagnostic methods are preferable because they are non-interfering; although problems of beam access can be serious in practical cases. The potentially more attractive techniques are based on the interaction of laser light and matter (light scattering), and are very suitable in reacting systems because they are capable of in situ detection of temperature, molecular species and physical properties (velocity, size and concentration) of small particles (solid or liquid). Moreover, very high space and time resolution may be achieved, depending on the light source, detection mode and photosensor type. Regarding accuracy, it is difficult to compare optical techniques in a general way, but the near-impossibility of probing inside high temperature reacting flows makes necessary their use, and acceptable, even a loss of accuracy.

Light scattering processes are known as elastic when the incident energy is conserved. That means no absorption takes place, and the light frequency does not change. There are also non-elastic scattering processes, typically Raman and fluorescence, involving molecules, and depending on their physico-chemical characteristics (energy and nature); they are thus usable to detect molecular species. Elastic scattering is only function of the number, size and optical properties (refractive index and shape) of particles, and is normally used to measure particle concentration, velocity or size. Elastic scattering from molecules (Rayleigh scattering) depends also on the type of molecules, through their cross-section, and may be used to measure species concentration, and thus density and temperature. However, the efficiency of molecular scattering is very low compared to that of particles whose typical size ranges from one to hundreds of microns. In real combustion systems, the presence of micro-particles, naturally occurring or generated by the combustion process (soot or other particulate), is almost unavoidable, and thus molecular scattering can be hardly applied. Absorption phenomena concern a relatively large number of photon-particle interactions and related techniques dominate in the measurement of concentrations of non emitting species. A significant limitation is that they are "path" methods which integrate along the line of sight, whereas scattering methods give point information.

A wide range of optical instruments has been developed in the past to measure particle size, velocity and other physical properties, like particle concentration and mass flux, all based on sampling the elastic scattering pattern at different angles relative to the incident laser beam or combining measurement of amplitude, frequency and phase shift of the scattered light at fixed angles. While several specific texts and review papers provide general introduction to the laser-Doppler anemometry (LDV) and particle-sizing methods, only specialist descriptions on specific applications can be found in the literature about their last developments and that of other techniques (planar Mie scattering visualisation and particle image velocimetry, PIV). A large fraction of reported

applications are mainly concerning with spherical particles in isothermal conditions and spray combustion. This review will address applications in reacting particle laden flows and extension to non-spherical particles. It is an attempt at presenting the various existing or proposed techniques, and discussing the performance criteria of interest in basic and applied configurations.

Special attention will be directed to compare overall accuracy, and to the interpretation of the measurement of a given property, after careful elimination of the other properties affecting the data. Many problems, for example, have been identified which can reduce the reliability of velocity and size measurements in particle laden reacting flows. Turbulent refractive index fluctuations, due to temperature and composition gradients, may induce beam steering of the laser beams, and thus distortion of interference fringe pattern. Temperature gradients cause density gradients, and thus LDV measurements would be biased in favor of the fluid velocity in the region of high particle concentration (conditioned sampling). Chemical reactions may also modify the volumetric particle concentration and could produce a selective effect, depending on the particle properties. Poor signal-to-noise ratio, relatively small amplitude, and high flame luminosity, are other limiting features of light scattering measurements in combusting flows.

The two-phase flows combustion process depends, among other physics-chemical phenomena, on fluid and particle dynamics. Moreover, since momentum-to-drag ratios determine the capability of particles to follow the gas flow streamlines, and particle spatial distribution may influence heat release and flame distribution, it is clear that simultaneous measurements of particle size and velocity are of fundamental importance. Because in two-phase flows different size classes might have different velocities, it is also very important to have both data simultaneously for each individual particle. Recent advances in the LDV/PDA instrumentation make the technique suitable, not only for laboratory use, but also for in-situ simultaneous detection of particle size, velocity and concentration in large-scale, complex environments, although the applicability is presently limited to spherical particles. It should be remembered that studies conducted to characterise two-phase flows prior to 1986 were not based on "in-situ" measurements of particle size and velocity, but on averaged information deduced from line-of-sight measurements of particle size distribution (diffraction technique), independently from velocity measurements.

The PDA technique will be discussed in some detail because it has been used in many applications: atomisation of real fluids, molten metals as well as the sprays of solid particles, and supposed they are spherical. Atomised molten metals solidify with a spherical particle shape and hence the PDA technique can be correctly applied, if a scattering angle is selected in order to have comparable sensitivity for both signals from reflection (melt particles) and first-order refraction (liquefied droplets). However, difficulty may arouse in presence of high particle number density that limits light transmissivity and reduces the detectability of smaller particles. Other difficulties in obtaining accurate and repeatable particle velocity and size data are associated with the finite amplitude range of the instruments, due to the amplitude discrimination of the electronic units. This implies that only a finite range of particle sizes contributes to the velocity (or size) information. The amplitude range of the instrument should be carefully matched to the available size range of particles in the flow.

Finally it should be kept in mind, in selecting the measurement method, the relationship between the Lagrangian reference framework, as obtained by motion picture, and the Eulerian reference, as obtained by local point measurements. A spatial distribution is obtained when particles in a given

22

volume of space are instantaneously sampled, as in most high-speed photographic methods; a temporal distribution is generated by particles passing through a sampling control volume during a given interval of time, and each particle is individually counted. If all of the particles travel at the same velocity, the spatial and temporal distributions are identical. Otherwise the spatial distribution may be transformed into the temporal one by multiplying the number of particles of a given velocity by that velocity.

THIS PAGE HAS BEEN DELIBERATELY LEFT BLANK

5-ISICP-001-8-IV-BVN

Nonlinear Combustion in Solid-Propellant Rocket Motors

B.V. Novozhilov
Institute of Chemical Physics, Russian Academy of Science
4, Kosygina Street
Moscow, 117977 Russia
Tel: 007-095-432-8575
Fax: 007-095-137-6130
E-mail: boris@center.chph.ras.ru

In the recent past, increased attention has been paid to nonlinear acoustics in the problem of non-steady motions in combustion chambers. It has been also understood that nonlinear combustion may be of importance to obtain possible limit cycles and triggering phenomena. There are few papers considering nonlinear combustion modeling that are based mainly on the idea associated with velocity coupling. The purpose of this paper is to consider combustion-acoustic problems in solid-propellant rocket motors in the framework of nonlinear acoustics and nonlinear propellant burning rate response to varying pressure.

As an example, a combustion chamber having a rigid head-end and an aft-end nozzle is considered. The port and lateral burning surface areas are assumed to be constant. To reduce a number of governing parameters, the simplest propellant model is used. It may be characterized by the first derivatives of the propellant burning rate, surface temperature, and burning temperature with respect to pressure and the ambient temperature.

The first two longitudinal acoustic modes are considered with the second-order acoustics and combustion non-linearity. An approximate method used in the derivation of the amplitude equations follows the analytical framework introduced by Culick.

To write boundary conditions for an acoustic field at the propellant surface, the idea of nonlinear gas velocity response functions to oscillatory pressure is used. They have been calculated within the framework of the ZN theory and described:
  a) self-interaction of the first harmonic to give the second-order corrections to the second mode of the burning rate and gas velocity,
  b) interaction of the first and second modes to give the second-order corrections to the first mode.

As a result, a set of the governing differential equations is obtained that contains two real equations for the modulus and phase shift of the first mode and a complex equation for the complex amplitude of the second mode. These equations are analyzed to obtain the possible limit cycles and to study their stability. Numerical calculations are performed to find the amplitude-time history that may include triggering phenomena.

It has been shown when both acoustic non-linearity and non-linearity of solid propellant burning rate response to oscillatory pressure are considered new qualitative effects arise as compared to the case when only acoustic non-linearity is accounted for.

The most important of these effects are:

1. Formation of limit cycles occurs not only when one of the modes is linearly unstable, but also in the case of both linearly stable modes.

2. It is possible the formation of two different frequency shifted limit cycles (stable or unstable) are at the same fundamental frequency. In this case, the final result of the amplitude-time history is strongly dependent on the initial conditions.

3. If a limit cycle exists in the region of both linearly stable modes, triggering phenomena arise. Some sets of the initial conditions lead to the amplitudes monotonically decreasing to zero. For large initial disturbances, unstable pressure and burning rate fluctuations may result in "triggering" (or nonlinear instability). Such phenomena could not be predicted by the analysis with only acoustic non-linearity.

ABSTRACTS OF PAPERS
TO BE PRESENTED IN

ROOM AZZURRA

AREA 1:

REACTION KINETICS OF ENERGETIC MATERIALS

SESSION CO-CHAIRS:

PROF. RICHARD YETTER
AND
PROF. BORIS KONDRIKOV

Pyrolysis Studies of the Burning Mechanisms of High-Nitrogen Compounds

T.B. Brill, H. Ramanathan, R.W. Beal
Department of Chemistry
University of Delaware
Newark, DE 19716 USA
Tel: (302) 831-6079, Fax: (302) 831-6335
E-mail: brill@udel.edu

The chemical origin of the burning rate differences of 5-amino-1H-tetrazole (5-ATZ) and its hydrohalide (HCl, HBr, HI) salts were revealed by flash pyrolysis at 350°C, 400°C and 450°C by T-jump/FTIR spectroscopy. Comparison of the products indicated that two global decomposition channels exist. The first channel is dissociation of the salt to form HX and 5-ATZ followed by decomposition of neutral 5-ATZ. The second channel involves decomposition of the $[5\text{-ATZH}]^+$ ion directly. The ratio of these two channels depends on the compound. The 5-ATZ channel is favored over the $[5\text{-ATZH}]^+$ channel in the order HCl > HBr > HI, which is the trend of the pK_a values of these acids. This information enables both the ordering of the burning rates as a function of pressure as well as the trend in the pressure dependence to be rationalized. Similar studies on the azo and hydraza-bridged amino- and nitrofurazans reveal that the hydraza linkage converts to the azo linkage early in the decomposition sequence and before the remainder of the compound decomposes. This leads to the prediction that the azo and hydraza-bridged compounds may have similar burning rates.

27

THIS PAGE HAS BEEN DELIBERATELY LEFT BLANK

Formation and Decomposition of CH_2N and CH_2NO in the Combustion of RDX and HMX Studied by Quantum Chemical and Statistical Theory Calculations

D. Chakraborty and M.C. Lin
Department of Chemistry
Emory University
1515 Pierce Drive
Atlanta, GA 30322, U. S. A.
E-mail: chemmcl@emory.edu

CH_2N and CH_2NO are two key free radicals which play a pivotal role in the combustion of RDX and HMX near the burning surface. The H atom and OH radical produced by their decomposition are the most important chain-carriers in the combustion of these cyclic nitramine systems.

Both CH_2N and CH_2NO radicals can be formed directly from the fragmentation of methylene nitramine, CH_2NNO_2, the building block of RDX an HMX:

$$CH_2NNO_2 \rightarrow CH_2N + NO_2 \qquad\qquad (1)$$
$$ \rightarrow CH_2NONO \rightarrow CH_2NO + NO. \qquad\qquad (2)$$

In addition, the bimolecular reaction of CH_2N and NO_2 thus formed, can also generate CH_2NO, together with other molecular products, such as HCN and CH_2O, according to the following mechanism:

$$CH_2N + NO_2 \rightarrow CH_2NONO^{\#} \rightarrow CH_2NO + NO \qquad\qquad (3)$$
$$ \rightarrow CH_2NNO_2^{\#} \rightarrow HCN + HONO \qquad\qquad (4)$$
$$\phantom{CH_2N + NO_2 \rightarrow CH_2NNO_2^{\#}} \rightarrow CH_2O + N_2O, \qquad\qquad (5)$$
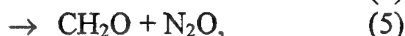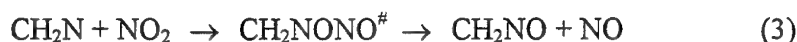
where "#" stands for internal excitation.

The unimolecular decomposition of CH_2N and CH_2NO formed in these reactions, which dominate the early stages of RDX and HMX combustion, produces H and OH by the following unimolecular processes:

$$CH_2N \rightarrow H + HCN \qquad\qquad (6)$$
$$CH_2NO \rightarrow H + HCNO \qquad\qquad (7)$$
$$ \rightarrow HCNOH \rightarrow HCN + OH. \qquad\qquad (8)$$
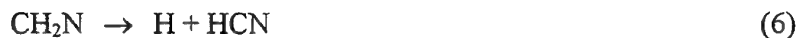
The kinetics and mechanisms for the formation and decomposition of CH_2N and CH_2NO, described above, are not known, and they cannot be easily determined experimentally because of the absence of reliable direct diagnostic methods for these nonfluorescing radicals. In view of such a short-coming, and the critical importance of the reactions for kinetic modeling of RDX and HMX combustion processes, we have recently carried out a series of high-level molecular orbital and statistical-theory calculations to predict their thermal rate constants over a wide range of temperature and pressures.

In our ab initio molecular orbital calculations, the geometries of all molecular and transition-state species involved in the reactions, have been computed with the hybrid density functional theory (B3LYP) using the 6-311G(d,p) basis set. Their energies were calculated with the modified Gaussian-2 method (G2M) developed at Emory University [A.M. Mebel, K. Morokuma and M.C. Lin, J. Chem. Phys. 103, 7414, (1995)]. The method was designed to approximate the restricted coupled cluster calculation with single, double and triple substitutions, RCCSD(T), with the 6-311G(3df,2p) basis set using a series of single-point energy calculations for electron correlation and basis set expansion.

The computed energies for all molecular species and transition states were employed to calculate the T, P-dependent rate constants for the 8 reactions given above with the Rice-Ramperger-Kassel-Marcus (RRKM) theory over the 300-2000 K range at 1-200 atm pressure. These results will be presented in detail at the conference.

Dynamic Observations of Polymorph Changes in Explosives using Second Harmonic Generation[*]

M.E. DeCroix, B.W. Asay, S.F. Son, and B.F. Henson
Los Alamos National Laboratory
MS C920
Los Alamos, NM 87545 USA
Phone: (505) 667-9683; Fax: (505) 667-0500; mdecroix@lanl.gov

For over 30 years, the dynamic β to δ phase transition in HMX has been implicated in the thermal decomposition of the explosive. In recent work at LANL, measurements of the phase transition in HMX were made *in situ* using second harmonic generation (SHG). The kinetics of the polymorph change were found to closely match commonly accepted thermal decomposition parameters and the phase change was identified as the initial step in the ODTX kinetics. For TATB and PBX 9502, a crystalline structure change upon heating causes an increase in the SHG signal from the explosive. The kinetics of this structural change were closely matched commonly accepted thermal decomposition parameters.

In this work, we use nonlinear second harmonic generation (SHG) to observe a polymorph or structure change in explosives prior to ignition. Rapid heating with a CO_2 laser ignites the explosives. This study used 1 cm diameter pressed pellets of the explosives HMX (octahydro-1,3,5,7-tetranitro-1,3,5,7-tetrazocine,$C_4H_8N_8O_8$), PBX 9501 (95% HMX, 2.5% Estane, 2.5% BDNPA/BDNPF), TATB (1,3,5-triamino-2,4,6-trinitrobenzene, $C_6H_6N_6O_6$), and PBX 9502 (95% TATB, 5% Kel-F). In the previous work, the CO_2 power densities of the past measurements had to be low, due to limitations of the laser turn-on time. Also, the temporal resolution of these past measurements was coarse, ~30 ms. In this work, the CO_2 laser beam was released with a mechanical shutter, so higher power densities and higher heating rates could be studied. The SHG probe could be moved temporally relative to the shutter opening with a 5 ms resolution, which increased the temporal resolution for the SHG measurements. Also, the SHG signal was measured using a photo multiplier tube and micro-thermocouples were used to measure the surface temperature of each pellet during the entire heating process. The first order rate law the measured surface temperatures were used to calculate times for the phase transition or structural change. An approximate nucleation and growth rate law, using the measured surface temperatures, was used to calculate times for the phase transition or structural change. These calculated transition times compare well with the SHG measurements.

THIS PAGE HAS BEEN DELIBERATELY LEFT BLANK

Investigation of Fuel-rich Boron Combustion in a Pressurized Combustion Bomb

R. Pein and S. Anders
DLR – German Aerospace Center, 74239 Hardthausen Germany
Tel: 49-6298-28-324
Fax: 49-6298-28-175
Roland.Pein@dlr.de

The objective of this work is to investigate the combustion of fuel-rich propellants as used for gas generators in ducted rockets. This work was inspired by the lack of data concerning the combustion process in ducted rocket primary combustion chambers.

The experimental facility consisted of a combustion bomb very similar to that described by Glotov et al.[1]. The pressure inside this modified apparatus could be varied between 1 and 100 bar. Two different types of propellants were used, a HTPB-based, boron-containing, and a GAP-based, boron-containing fuel-rich propellant. A small piece (about 1 g) of propellant is placed into a propellant holder which is fastened on top of the inner tube. The propellant is ignited by a glowing wire which is heated electrically. The gaseous and particulate combustion products flow downward in the inner tube. They are quenched at the exit of this tube by cold nitrogen flowing between the inner and the outer tube. The solid combustion products are collected on a filter on the bottom of the bomb and subjected to chemical analysis. This was done using a Mettler automatic titration controller 1200 including a Titronic 110 burette for the boric acid titrations, and a Perkin Elmer Plasma 400 ICP atomic emission spectrometer for the determination of B. The dependence of unconverted boron, boron oxide, boron carbide, and total boron content from combustion pressure was measured. For comparison the equilibrium composition of the solid combustion products was computed in dependence of combustion pressure.

The results for the HTPB-based propellant show a decrease of total boron content with increasing pressure which is probably due to a more efficient conversion to the reaction products (Fig.1). At low pressure the conversion of the boron is poor, the experimental values are somewhat above equilibrium. The boron oxide content of the combustion products decreases with increasing pressure and shows larger deviations from equilibrium at low pressure (Fig.1). There is a strong increase of B_4C content with pressure, there are large deviations from equilibrium at low pressure and at higher pressures B_4C concentration approaches the equilibrium value. There is a decrease in content of unconverted boron versus pressure. The results from the thermodynamic calculations give no unconverted boron, the conversion is complete. The GAP-based propellant shows a different behavior. Here the boron oxide content of the combustion products increases with pressure and the boron carbide content decreases.

From the results it can be concluded that boron carbide can be a prevailing species in the exhaust of a ducted rocket primary combustion chamber. This should be taken more into account as input for analytical and numerical model calculations for ducted rocket secondary combustion chambers, because very often it is assumed in these computations that mainly heated, unreacted elementary boron enters the secondary combustor. Thus , not only boron combustion but also boron carbide combustion as well as some amount of preconversion has to be considered.

1. O. G. Glotov and V. Ya. Zyrianov, "The effect of pressure on characteristics of condensed combustion products of aluminized solid propellant", archivum combustionis, Vol.11 (1991) No. 3-4, 252-262
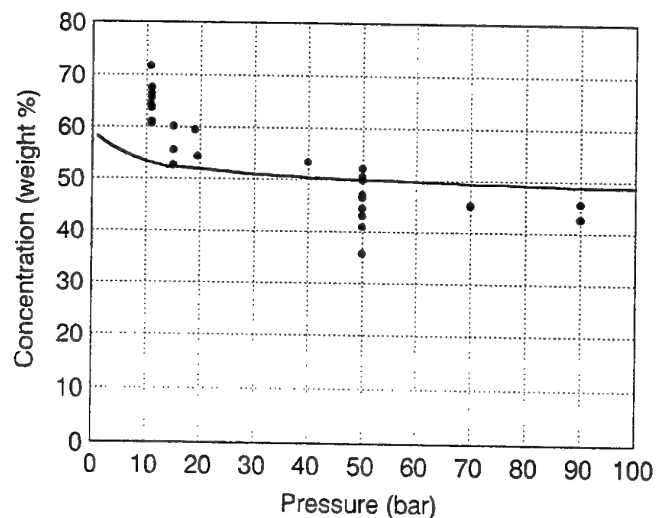
Fig. 1   Total boron content of the combustion products versus combustion pressure (HTPB-based Propellant, solid line corresponds to equilibrium computations)
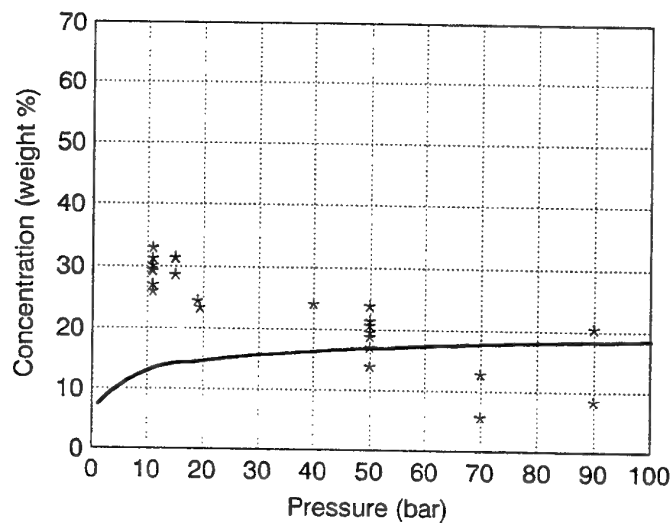
Fig. 2 B_2O_3 content of the combustion products versus combustion pressure (HTPB-based Propellant, solid line corresponds to equilibrium computations)

The Use of Kinetic Data in the Service Life Testing of HTPB Rocket Propellant

A. Chin, J.A. Wilson, D. Ellison, S. Backer
Navy Surface Warfare Center - Crane
300 Highway 361, Crane, IN 47552
Tel: (812) 854-1021
Fax: (812) 854-2890
wilson_jim@crane.navy.mil

The Service Life assessment of Naval rocket propellant has changed little in the last 40 years. The primary thrust of the Navy evaluation program has been to static fire a small number of motors every few years and based on the test results, extend the service life if warranted. This process has a number of short falls of which the lack of long-range predictability is the most serious. Because of the small number of motors tested, the built-in variability of individual rocket motors and the fact that the environmental history of the motors is unknown, it is unlikely that un-serviceability will be detected much before the actual end of motor's service life. This places a great deal of stress on the Weapon manager and ultimately on the Fleet. Obviously, some method of long-range service life predictability is essential to both the Fleet and Weapon managers.

This paper will outline a project undertaken by NSWC Crane in support of a US Air Force. The goal of this program was to establish if a specific HTPB based rocket motor would be serviceable for at least twenty year beyond the current stockpile age. In order to accomplish this task NSWC Crane was faced with the development of a new approach to rocket motor service life work. Based on the success of the NSWC Crane gun ammunition service life program, Crane engineers quickly developed a rocket motor plan based on accurate kinetic testing and data analysis.

One of the major barriers in using the same basic process for rocket propellant and gun propellant is the fact that the activation energy of rocket propellant is only a fraction of the activation energy normally produced by most gun propellants. The standard micro-watt level Heat Flow Calorimeter (HFC) does not have the sensitivity required to measure the propellant activation energy at the lower (60°C to 70°C) temperature range. The ability to accomplish this task was made possible by the availability of HFCs with nano-watt detection capability.

The basic evaluation process used in the subject evaluation included 7 primary elements; (1) dissection of 1 rocket motor per motor type, (2) kinetic testing of propellant samples, (3) calculation of the accelerated aging plan based on the kinetic data and Arrhenius equation, (4) small scale mechanical properties testing of propellant samples [aged and un-aged], (5) accelerated aging of the full rocket motors, (6) transportation vibration testing and (7) static firing of the motors.

The wide spread use of the evolved processes discussed in this paper can have a dramatic effect on acquisition strategies, logistics storage and movement, and future demil requirements.

THIS PAGE HAS BEEN DELIBERATELY LEFT BLANK

Contained Low Pressure Combustion of NIKE and Improved HAWK Rocket Motors: Experimental Techniques and Emissions Measurements*

J. Lipkin, C. Shaddix, S. Allendorf
Sandia National Laboratories,
Livermore, CA 94551-0969 USA
Telephone: 1-925-294-2417; Fax: 1-925-294-1217; E-mail: jlipkin@sandia.gov

R. Peabody
Sandia National Laboratories, Albuquerque, NM, USA

C. Velsko and B. Watkins
Lawrence Livermore Laboratory, Livermore, CA, USA

S. Williams, A. Moeller and W. Bellow
Bechtel Nevada, N. Las Vegas, NV, USA

J. Carson and W. Gray
Radian International LLC, Research Triangle Park, NC, USA

J. Stephens
Los Alamos National Laboratory, Los Alamos, NM, USA

S. Kwak
US Army Defense Ammunition Center, McAlester, OK, USA

Three rocket motor propellant burn tests were recently carried out in an excavated cavern located in a tunnel complex on the US Department of Energy's Nevada Test Site, Mercury, NV, USA. The NIKE rocket motor containing double base propellant was used in two tests (two and four motors, respectively), and a third test used two Improved HAWK rocket motors containing composite propellant.

In each of these tests, relatively small quantities of explosive were used to initiate non-propulsive propellant burns. The initiation procedure closely followed that used in the US Department of Defense rocket motor demilitarization process commonly called "crack-and-burn". In this procedure, linear shaped charges and explosive cutting tape are used to split each rocket motor case longitudinally and partially around its circumference. The total time required for the propellant to burn out in these tests was typically 20-30 s.

The cavern, known as the X-tunnel Test Chamber, encloses a volume of 4644 m³ (164,000 ft³)[1] that is sealed with a reinforced steel and concrete barrier. This barrier was designed to provide containment of the propellant combustion products as well as protection from possible high-velocity explosive fragments and pressure transients.

The NIKE and Improved HAWK rocket motors were selected for these tests because they contain propellant types that are representative of the two most common formulations found

---

[1] The approximate dimensions of the X-tunnel Test Chamber are: 30.5 m (100 ft) long, 15.2 m (50 ft) wide, and 10.7 m (35 ft) high.

in the US demilitarization inventory, i.e., double base and composite, respectively. Each NIKE M88 rocket motor contains 341 kg (750 pounds) of double base type propellant, and each Improved HAWK dual thrust motor contains 294 kg (647 pounds) of composite type propellant. Test parameters are summarized in Table 1.

Table 1. Contained rocket motor burn tests

Test Name	Test Type[1]	Number of Motors	N.E.W.[2] (kilograms)	Inert Weight (kilograms)
SUNSPOT	B1	2	682[3]	404
THUNDERBIRD	B1	4	1364[3]	808
DAZZLER	B2	2	588[4]	223

1 - B1 = Burn of NIKE rocket motors; B2 = Burn of Improved HAWK rocket motors

2 - Net Explosive Weight (excluding initiating explosive charges)
3 - NC/NG (double base) Propellant
4 - Composite Propellant

In addition to measuring the relatively rapid pressure and temperature transients in the test chamber, the gas species and aerosols produced by combustion of the propellants were monitored and sampled over several hours after initiation of a test. A number of toxic gases, chemicals and US Resource Recovery Act listed hazardous metals were identified as combustion effluents. These included, for example: CO_2, CO, NOx, HCN, HCl, Pb, Cr, products of incomplete combustion (including volatile organic chemicals, semi-volatile organic chemicals, dioxins, and furans), residual energetic material, and aerosols.

Time averaged concentrations of many of these species were measured by using appropriate US Environmental Protection Agency standardized methods. In addition, a few species (bulk gases, NOx, CO, and aerosols) were measured on a time-resolved basis using both standard instrumentation and specially developed techniques. These measurement methods and the data obtained from this unique series of tests are summarized and reported in this paper.

AREA 2a:

RECYCLING OF ENERGETIC MATERIALS

SESSION CHAIR:

DR. ALEX MITCHELL

Reuse of Demilitarized and/or Excess Energetic Materials as Ingredients in Commercial Explosives

O. Machacek, G. Eck, K. Tallent
Universal Tech Corporation
5925 Forest Lane, Suite 500
Dallas, Texas 75230
Tel: (972) 490-9906, Fax: (972) 490-9908
E-mail: utecOldm@airmail.net
Send also to utecrd@terraworld.net

This paper outlines the extensive work which has been accomplished by Universal Tech Corporation (UTeC) in the area of recycling energetic materials that have been derived from either demilitarization efforts or manufacturing excess. The following information is broken into two sections: Rocket Motor Propellants and Conventional Ammunition Propellants/Explosives.

Rocket Motor Propellants

UTeC received its initial exposure to the recycling of rocket motor propellants through a contact with CSD in early 1992. CSD and UTeC entered a joint venture investigating the development of a commercial explosive formulation containing a Class 1.3 composite propellant from the Minuteman III Stage III Rocket Motor. This propellant was a typical Ammonium Perchlorate (AP)/Aluminum (AL)/Rubber Binder type propellant. During 1992, UTeC was successful in developing a large diameter packaged commercial explosive product containing up to 30% of the downsized composite propellant.

As a result of UTeC's successes, UTeC, in cooperation with CSD, designed a facility dedicated to the processing of demilled or excess rocket motor propellants and their subsequent use as an energetic ingredient in a commercial explosive product. This facility (located near Columbus, Kansas) known as the PRUF Plant, houses a propellant shredder as well as the final product mixing and packaging equipment. The PRUF Plant was constructed in 1995 and was partially re-engineered in 1997.

In this process, approximately 1,500 pounds of propellant (propellant is usually a block configuration weighing no more than 40 pounds each) is placed onto a belt conveyor. The propellant is then remotely dumped into the awaiting solution filled shredder. The shredder downsizes the propellant into approximately 1-inch irregularly shaped pieces. The shredded propellant is continuously taken away from the shredder by an auger system and is finally collected in a hopper. This process is repeated until approximately 3,500 pounds of shredded propellant has been collected. The shredded propellant is then mixed with other ingredients to form a watergel slurry. The slurry is then packaged in 4-inch to 6-inch diameter shot bags.

To date, the PRUF Plant has processed approximately 1.8 million pounds of Class 1.3 composite propellant, which equates to approximately 7.8 million pounds of finished product. The current production rate is approximately 4,500 pounds of propellant processed per day, which equates to approximately 19,500 pounds of finished blasting agent per day.

Conventional Ammunition Propellant/Explosives

This category includes single, double and triple base smokeless powders. These smokeless powders were used in tank field artillery, air defense and other tactical ammunition pieces typical of Army ground weapons and Navy ship-borne artillery weapons. Reuse work of propellants of this type grew out of the fact that huge quantities are available, and the fact that open burning/open detonation OB/OD is becoming less favorable.

UTeC as well as several other companies, including Orica/Energetic Solutions and Dyno Nobel have produced explosive products containing propellants of this type. UTeC has developed a successful product containing up to 60% of either single or triple base smokeless powders. The product uses the propellant grains, in their original form, and a high-density oxidizer solution. The solution is mixed with a gelling system and then poured around the propellant grains in the charge container. After a short time, the gel thickens and completely crosslinks. This product has a high density, high velocity of detonation and high energy as well as being resistant to "dead-pressing". The current production rate of this product, which is made and manufactured by SEC, is approximately 3 million pounds per year.

In the area of demilitarized explosives, UTeC has developed a watergel slurry explosive product, which contains Ammonium Picrate, or Explosive D. At this time, neither UTeC nor SEC is producing or marketing the Ammonium Picrate slurry.

Recent Advances in the Chemical Conversion of Energetic Materials

A. R. Mitchell, M. D. Coburn, R.D. Schmidt, P. F. Pagoria, G. S. Lee
Lawrence Livermore National Laboratory
Energetic Materials Center, MS L-282, P.O. Box 808
Livermore, CA 94550 USA
Tel: 925-422-7994
Fax: 925-424-3281
E-mail: mitchell4@llnl.gov

The demilitarization of nuclear and conventional munitions in Russia and the West is producing millions of pounds of surplus energetic materials. Historically, energetic materials (high explosives, propellants, and pyrotechnics) have been disposed of by open burning/open detonation (OB/OD). The use of OB/OD is becoming unacceptable due to public concerns and increasingly stringent environmental regulations. Clearly, there is a great need to develop environmentally sound and cost-effective alternatives to OB/OD.

Since the early 1990's, Lawrence Livermore National Laboratory (LLNL) has been a world leader in exploratory research on the resource recovery and reuse (R^3) of surplus energetic materials. We have investigated the use of recycled high explosives as raw materials for producing a variety of higher value products. In this paper we examine chemical conversion activities from a global perspective, with an emphasis on work from LLNL.

THIS PAGE HAS BEEN DELIBERATELY LEFT BLANK

Conversion of Demilitarized TNT to Higher Value Products*

S.A Shevelev, V.A. Tartakovsky
N.D.Zelinsky Institute of Organic Chemistry, Russian Academy of Sciences,
117913, Leninsky prospekt 47, Moscow, Russia
Telephone: +7 (095) 135 63 40; Fax: +7 (095) 135 53 28
E-mail: shevelev@cacr.ioc.ac.ru

A.L.Rusanov
A.N.Nesmeyanov Institute of Organo-Element Compounds, Russian Academy of Sciences,
117813, 28 Vavilov Str., Moscow, Russia
Telephone: +7 (095) 135 61 66; Fax: +7 (095) 135 50 85
E-mail: alrus@ineos.ac.ru

The goal of our research is to develop the scientific methodology needed for the chemical conversion of surplus TNT (2,4,6-trinitrotoluene) into higher value products. Although the military use of TNT is well-documented, the production of civilian products from TNT is virtually unknown. We now describe some of our results using TNT as a multipurpose raw material for the chemical synthesis of a variety of materials.

Specifically, we have developed more ecologically acceptable conversions of TNT into 2,4,6-triaminotoluene (TAT), 2,4,6-trihydroxytoluene and 2,4,6-triisocyanatotoluene (TICT). In addition, we have studied both the regioselective reductions and regioselective nucleophilic displacements of nitro groups in TNT. We have also converted TNT into a variety of heterocyclic compounds. In summary, our investigations demonstrate that TNT is a versatile building block for the synthesis of new materials ranging from polymers to heterocyclic compounds displaying pharmacological and agrochemical activities.

THIS PAGE HAS BEEN DELIBERATELY LEFT BLANK

AREA 2b:

COMMERCIAL APPLICATIONS
OF ENERGETIC MATERIALS

SESSION CHAIR:

DR. ALAIN DAVENAS

Explosively Generated Supercritical Water for Deploying Airbags

A. Iwama
The Institute of Space and Astronautical Science (ISAS),
3-1-1 Yoshinodai Sagamihara Kanagawa Pref. 229-8510, Japan
Tel: +81-(0)42-759-8283; Fax: +81-(0)42-759-8461
E-mail: hori@pub.isas.ac.jp

T. Tamura and D. Yu
Nippon Kohki Company, Nishigo-mura, Nishishirakawa-gun, Fukushima
Pref.   961-8021, Japan

The installation of inflators on cars is going so quickly and widely that a huge discrepancy exists between the mass production and the environment awareness. Abatement of pollutant gases such as carbon monoxide, nitrogen oxides, cyan, and hydrogen chloride cannot get to a level to stand even in new generation inflators. This report presents a novel inflator to achieve a clean gas emission and a high efficiency gasification ratio over 91wt% owing to supercritical water when inflator-mounted cars are fired at operation and disposal.

Supercritical Water as a Gas Generant
Water would dissolve non-polar substances at the conditions exceeding the supercritical point (22.1MPa, 647.35K), and can assist a rapid molecule cleavage against the high bonding energy. Combustion gases of projectile propellant or explosive make it possible to produce supercritical water when the combustion products is impinged at a hypersonic velocity into water from starter nozzles. Even below the freezing point of water, the supercritical conditions can be get to the specified maximum region within an allowable delay time.

Heavy Wall Inflators for Passenger Seat
A combustor having dual combustion chambers was made tentatively for obtaining fundamental performance as an inflator. A dual chamber type inflator incorporates two single combustors symmetrically. A current trend of new inflator development is going from monotonical airbag inflation aspect to a step-like one with a delay timer. However, no radical alternation is made concerning the requirements: the waiting time (70ms) from event occurrence to the maximum pressure, and the maximum pressure (40MPa). The total volume of both the single and dual combustor is 380 ml, and an equal gas generant quantity is partitioned to the dual chambers. Every main combustion chamber loading water, oxygen gas and liquid hydrocarbon begins to run by means of starter ignition for which conventional igniter and debris of an explosive or composite propellant including nitramines is and generates clean gases free from toxic gases and hazard particulates.

Sixty weight percent H_2O_2 water solution, 60~70ml, without stabilizer, was contained in closed cartridges that are placed respectively in the assembled dual combustion chambers, and then has been decomposed as far as possible by maintaining the H_2O_2 water solution loading inflator at 330 K, 12~48h. An example is discussed of the main gas generant candidate converted from 60ml of H_2O_2 60wt% solution to water and oxygen gas that occupies a void space in the cartridges, and n-hexane. The starters are composed of nitramine-based propellant and igniter. The explosive or propellant of a similar composition and amount is loaded in both the first and second starter.

An example of the pressure-time traces in combustion chamber and 60l tank to pass the criteria imposed on the passenger side inflator will be shown.

Conclusion
Supercritcal water was produced by means of composite propellants including explosive ingredients, owing to which the inflater shall play a stable performance between 230~360 K. Therefore, such a gas generant system could contribute to new inflator design. The combustion gas exhausted to the environment through the inflator and airbag vent holes on accident operation and disposal, is not injurious directly to human body, and the gas temperature blowing into airbag is variable between 500~800K, which depends on hardware configuration, starter composition, gas generant composition and these quantity. Frozen water at the initial ambient condition would have a little effect on the inflator performance because of overwhelmingly high energy starters. It is a remarkable issue to employ forced or spontaneous decomposition products of H_2O_2 stored in cartridge as the main gas generant. The generated oxygen is effectively consumed to enhance the inflator performance and to adjust the gas temperature, achieving an excellent solubility with liquid hydrocarbons that is a property inherent to supercritical water.

Prediction of Airbag Inflator Performance

J.C. Chastenet, A. Mobuchon
SNPE Propulsion, Centre de Recherche du Bouchet
Rue Lavoisier, 91710 Vert-le-Petit, France
Tel: 33-1-64-99-11-74, Fax: 33-1-64-99-15-62
E-mail: jc.chastenet@propulsion.snpe.com

Airbag operating involves a great number of highly dependent components where the pyrotechnical charge used in an inflator as a gas generator is only one of the components. Moreover, specifications of these systems are more and more drastic in terms of performance, toxicity, lifetime, etc. Research and development of new gas generator compositions need to take into account all these aspects very early in the studies.

This paper describes the methodology performed by SNPE Propulsion for this purpose. This methodology is based on:

* thermodynamic prediction of theoretical performance,
* global modeling by means of a lumped parameter model,
* experimental demonstrator test,
* complete CFD simulation,
* prototype test.

For all of these steps, except the last, which is not under direct SNPE responsibility in the frame of an airbag industrial organization involving SNPE, examples of applications are given.

Thermodynamic prediction is a classical technical area. This point is only illustrated and identified limitations are given.

The lumped parameter model is described in regard to all of its possibilities: combustion of propellant grain or in bulk, multi-species with chemical interactions (overall reactions, chemical equilibrium or full chemical kinetics), real gas effects, thermal losses, hole erosion, and so on. This model is used for different purposes: prediction by direct simulation, experimental interpretation, determination of parameters impossible to measure, sensibilities studies.

The experimental devices used to validate new composition performances are illustrated. Typical demonstrator tests in a constant volume tank allow specific phenomena identification and their introduction in the lumped parameter model.

Special analyses are done on possible interactions between pyrotechnical composition combustion and other components of the system: igniter composition, filter in combustion chamber, expansion of high-pressurised gas in hybrid generator, etc.

If necessary for a better understanding of the system operations, full CFD simulations are performed with a model ordinarily used for rocket motor studies.

THIS PAGE HAS BEEN DELIBERATELY LEFT BLANK

Energetic Materials as Gas Generators in Explosions Suppression Systems

R. Klemens, M. Gieras, B. Szatan, P. Wolanski
Warsaw University of Technology
Institute of Heat Engineering
ul.Nowowiejska 25
00-665 Warsaw, Poland
Tel: 00-48-22-8-250-241
Fax: 00-48-22-8 -250-565
E-Mail: klemrud@itc.pw.edu.pl


J. Nowaczewski, A. Maranda, J. Paszula

Military University of Technology
Warsaw, Poland

The aim of the research was making use of energetic materials as gas generators for membranes perforation, and also for dispersing extinguishing material in active explosion suppression systems. Water was used as the extinguishing material. The results obtained for the water were compared with those obtained for typical extinguishing powders. Two kinds of energetic materials were used for the research as neutral gas generators (pyrotechnic and powder materials).

The pyrotechnic mixtures contained sodium azide (NaN_3) and potassium perchlorate ($KClO_2$). In the course of combustion, the pyrotechnic mixtures generates a nontoxic gas, the main components of which is nitrogen. Depending on the additional components applied, there can appear in the gaseous products small amounts of oxygen, hydrogen and water steam.

The decomposition reaction follows the following course:

$$8NaN_3 + KClO_4 \rightarrow 12N_2 + 4Na_2O + KCl$$
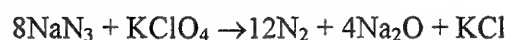
As can be seen, besides the gaseous combustion products, there also appear solid products in the form of potassium chloride (KCl) and sodium monoxide (Na_2O). From 1g of the mixture about 0.4 dm^3 gaseous and about 0.5 g solid products are obtained. Linear combustion velocity of the mixture depends upon: charge density, fineness of components, mode of combustion reaction initiation, and on applied components. The above velocity is in the range of a few to some scores of centimeters per second. The pyrotechnic mixture was prepared in the form of granulate of the size 0.5÷3 mm. The granulate was used for preparing charges of the mass equal to 30÷50 g, which were then placed in cardboard tubes covered with a paraffin layer. The electric igniters were used to initiate combustion of the pyrotechnic mixture. The charges were placed inside a steel container of 2 dm^3 volume, that contained about 1 dm^3 of explosion suppressing material (water or suppressing powder). The outlet of the container was closed by an aluminum membrane 1-2 mm thick with initial cross-shaped incisions 0.2 mm deep on its surface. In case of using the water, one charge was only used and placed over the water surface. While using extinguishing powders, two smaller charges had to be applied; one of them was placed directly on the membrane surface and the other one over the powder surface. When only one charge was placed over the suppressing powder surface, it often

happened that the membrane was not perforated because of compaction of the suppressing powder. The effectiveness of the worked out device was then tested using it for suppressing the explosion of corn starch-air mixture. Research carried out in an explosion chamber of 1.25 m^3 volume proved that in the case of suppressing powder dispersion, the pyrotechnic charges acted too slowly in order to efficiently suppress the developing explosion. While in the case of water dispersion, the action is fast enough to enable efficient explosion suppression. In the second part of the research, powder charges were used. The advantage of the powders, especially the smokeless ones, over the pyrotechnic mixtures, is that only gaseous products are produced in the course of combustion, while their burning velocity increases exponentially along with the pressure increase. For the purpose of research, fine and porous nitrocellulose powders were selected because of their high burning velocity. The powder P-100 had the highest burning velocity, and therefore it was used for the research. As it was in the case of pyrotechnic charges, the powder charge was divided into two parts while the suppressing powders were dispersed. The main charge of 35-40 g mass was placed over the powder surface while the auxiliary charge of 2÷5 g mass was located directly on the membrane surface. When water was used as the suppressing material, it was enough to use only one charge placed over the water surface. In all the mentioned above cases, the main charge (pyrotechnic or powder one) located over the surface of the suppressing material was placed inside the steel combustion chamber having perforated walls. It prevented a loss of some amount of the charge in case the cardboard tubes burst too early. The research carried out in the explosion chamber proved that in the case of using powder charges, the rate of dispersion of the extinguishing powder or water is high enough to suppress efficiently the developing explosion.

Characterization of the Combustion Behavior of Gas-generating Pyrotechnics Using Propellant Technology Methods

K. Engelen, M.H. Lefebvre
Royal Military Academy, Department of Chemistry
30 Av. Renaissance, 1000 Brussels, Belgium
Tel: 32-2-7376351
Fax: 32-2-7376353
E-Mail: Karen.Engelen@cgmc.rma.ac.be

J. De Ruyck
Vrije Universiteit Brussel, Department of Mechanical Engineering
1040 Brussels, Belgium

Depending on the application, gas-generating pyrotechnics have to fulfill a series of requirements such as combustion temperature, gas composition, and yield of gas. Sodium azide (NaN_3) is often used as a gas-generating agent in gas generators, because it delivers a gas-mixture that predominantly consists of harmless nitrogen and because its combustion temperature is relatively low. Unfortunately, this chemical is highly toxic. Moreover, it has to be mixed with an oxidizer to achieve proper combustion, which results in a low yield of gas. Double base propellant (DB), which has traditionally been used in the rocket-industry, could be suggested as an alternative. DB does not need an oxidizer to achieve combustion and yields significantly more gas. Unfortunately, its delivered gas-mixture contains toxic and reactive gases, such as carbon monoxide and hydrogen-gas, and it has a relatively high combustion temperature. Consequently, DB cannot be selected as a proper alternative in many applications. In previous work [1, 2] we developed composite-type gas-generating materials fueled with double base propellant (DB), azodicarbonamide (ADCA), nitroguanidine (NQ), or guanidine nitrate (GN) and oxidized with potassium nitrate (KNO_3) or potassium perchlorate ($KClO_4$). A conventional NaN_3-based material ($NaN_3/KNO_3/MgCO_3$) and a classical double base propellant were chosen as benchmarks.

One area of current interest in the development of gas-generating pyrotechnics is their combustion behavior. In this work we examined and compared the burning characteristics of the previously proposed gas-generating materials using investigation and calculation methods, which are typical for propellant technology. Solid propellant combustion properties at constant volume conditions are traditionally investigated by performing closed vessel tests. The pressure inside the vessel is measured as a function of combustion time using a suitable pressure gauge. Quantities that can typically be calculated from the pressure history are the burning rate, the dynamic vivacity, and the absolute vivacity.

In this work the loading density is chosen so that the maximum pressure is as close as possible to 130-150 bar, which is the region of interest for this study. The burning rate and the dynamic and absolute vivacity are calculated from the recorded pressure history using equations based on NATO-standards. Figures 1 and 2 show the burning rate and the absolute vivacity of the successfully ignited pyrotechnic compositions, respectively. These curves are a fit out of five tests per investigated composition. The reproducibility of the burning rate and of the vivacity is good despite the fact that the chosen loading densities are low. The good reproducibility is thanks to the specific ignition method that we used. The tested pyrotechnics

are ignited with a stoichiometric CH_4/O_2-mixture to assure homogeneous ignition in order not to deteriorate the form function of the grains. From the recorded pressure histories we also obtained valuable information concerning the ease of ignition and the ignition delay.
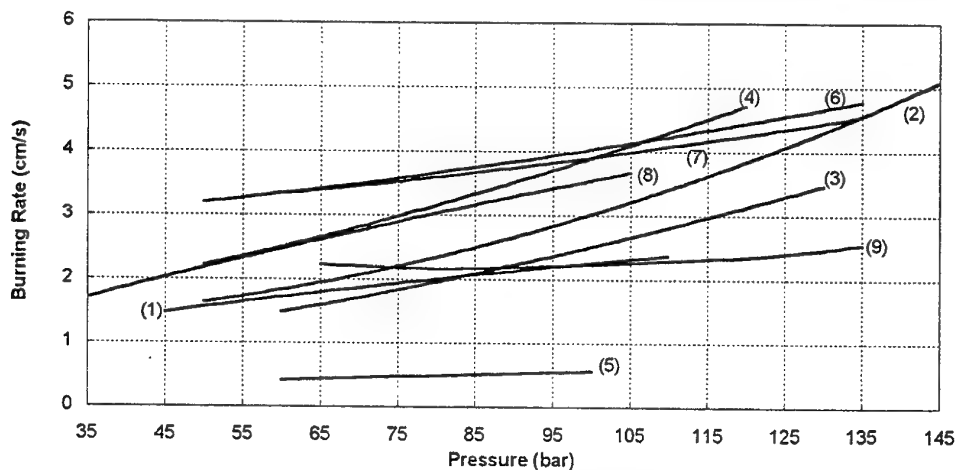
Fig. 1: Burning rate versus pressure: (1) $NaN_3/KNO_3/MgCO_3$, (2) DB, (3) DB/KNO_3, (4) $DB/KClO_4$, (5) NQ, (6) NQ/KNO_3, (7) $NQ/KClO_4$, (8) $ADCA/KClO_4$ and (9) $GN/KClO_4$.
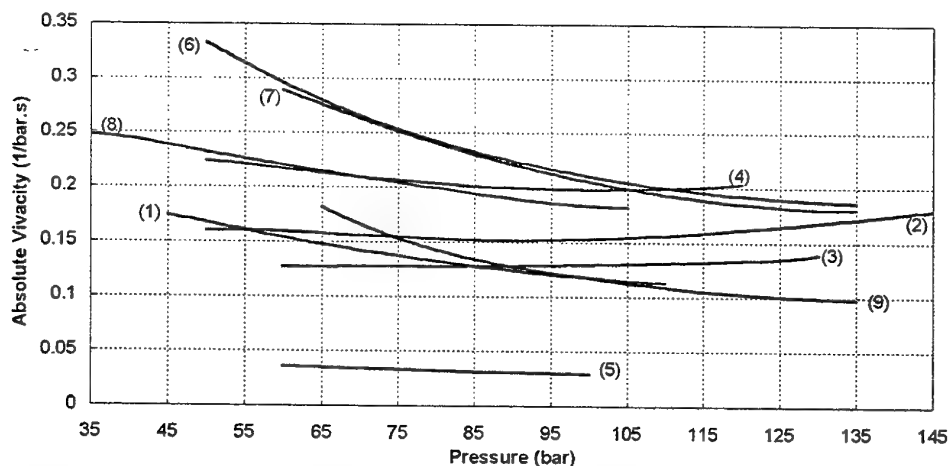
Fig. 2: Absolute vivacity versus pressure: (1) $NaN_3/KNO_3/MgCO_3$, (2) DB, (3) DB/KNO_3, (4) $DB/KClO_4$, (5) NQ, (6) NQ/KNO_3, (7) $NQ/KClO_4$, (8) $ADCA/KClO_4$ and (9) $GN/KClO_4$.

References

[1] K. Engelen and M.H. Lefebvre, "Chemical Formulation of Solid Propellant for Specific Gas Generators", 24'th International Pyrotechnics Seminar, pp. 203-216, 1998.

[2] K. Engelen, L. Vanneste, M.H. Lefebvre and J. De Ruyck, "Pyrotechnic Propellant for Nitrogen Gas Generator", Bulletin des Sociétés Chimiques Belges, Vol. 106, pp. 349-354, 1997.

AREA 3:

COMBUSTION PERFORMANCE OF HYBRID AND SOLID ROCKET MOTORS

SESSION CO CHAIRS:

DR. ARIE PERETZ
AND
PROF. CARLO BUONGIORNO

Hybrid Propulsion for Small Satellites: Logic of Design and Tests

Y. Maisonneuve, J.C. Godon, R. Lecourt
Office National d'Etudes et de Recherches Aérospatiales, Centre du Fauga-Mauzac 31410
Mauzac, France
Tel: 05-61-56-63-95
Fax: 05-61-56-63-87
E-mail: maison@onera.fr

G. Lengelle
Office National d'Etudes et de Recherches Aérospatiales, BP 72, F - 92322
Châtillon Cedex, France

N. Pillet
Centre National d'Etudes Spatiales, Centre de Toulouse, F - 31401 Toulouse
Cedex 4, France

In spite of a few demonstration models, the concept of hybrid propulsion has not at present been developed. Yet this type of propulsion has many specific advantages (cheapness, safety, ease of use, performance) which gives new emphasis for specific applications (such as micro-satellites and small launchers).

Recently ONERA with their own resources and with the financial support of CNES carried out work done on the possibility of developing hybrid propulsion systems. The objective has been to offer an alternative to propulsion by hydrazine for the positioning and control of micro-satellites or small interplanetary probes, which require high velocity impulse. In contrast to liquid propellant or solid propellant rockets, it is not possible to directly control the mixture ratio in hybrid propulsion. The operation of the motor is a result of the coupling of the reactive flow and of the behavior of the pyrolysis of solid fuel. The performance is not defined only by the choice of the fuel grain and the oxidizer, but directly dependent on its conception and in particular on the evolution of its internal geometry.

This document presents a study of a design code of hybrid propulsion PE/H_2O_2 (87%) systems, for 100-500 kg micro-satellites class, as well as its operating characteristics. The simplified hypotheses used at the moment do not allow for a perfect optimization. Developments will follow and keep the same logic but with less restrictive hypotheses and more realistic calculations. At the same time, an experimental study has been started with the aim of better understanding the operating range of hybrid propulsion motor and to enable us to better understand the rate of polyethylene pyrolysis for the design study.
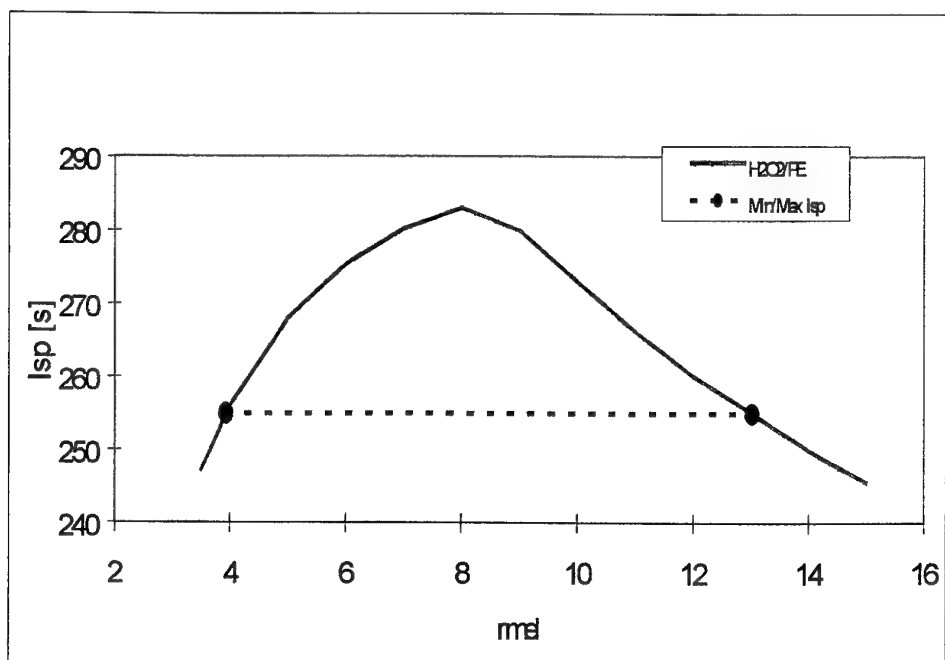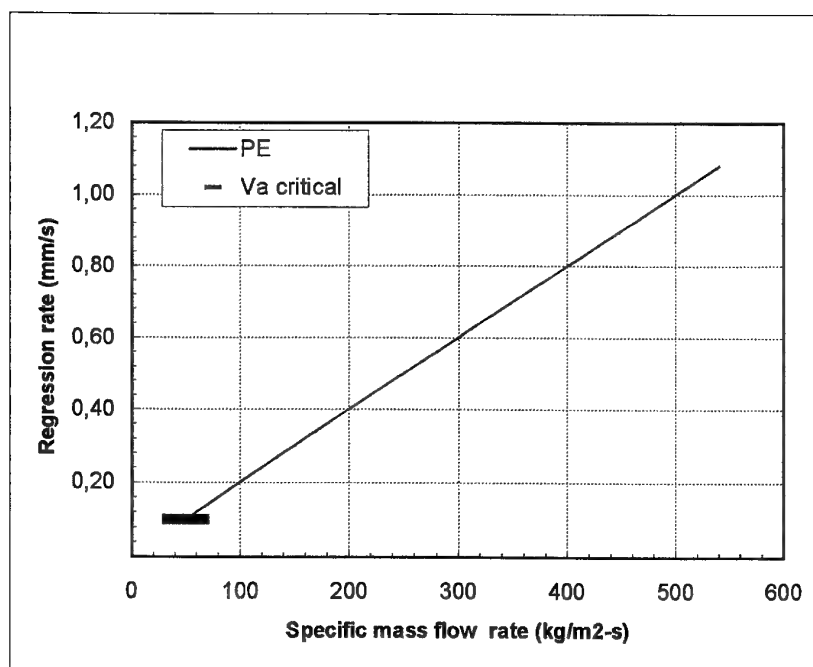
Re-Ignition in a GOX/HTPB Hybrid Rocket

A. Russo Sorge, M. Roma, F. Liccardo
Department of Space Science and Engineering "L.G. Napolitano"
University of Naples "Federico II", P.le Tecchio, 33 Naples, 80125 Italy
Tel: 39-081-7682355 Fax: 39-081-5932044
E-mail: russosor@unina.it

G. Torella
Italian Air Force Military Academy, Pozzuoli (NA), Italy

Experimental tests have been carried out on a hybrid rocket with GOX/HTPB as propellants and a hypergolic ignition system using Nitric Acid and Furfural alcohol in order to verify:
1. The re-ignition capability of such kind of rocket
2. The regression rate behavior in the following working phases

In fact, one of the main advantages of hybrid rockets is the re-ignition capability during the mission. That is possible because combustion can be stopped and restarted again through the liquid injection.

There are several possibilities to obtain re-ignition in a hybrid rocket.

If oxygen is the oxidizer, hypergolic liquids must be used for ignitions. Obviously, this is not very convenient in terms of weight. However, the ignition system needs a very small amount of hypergolic liquids. If H_2O_2 is used as oxidizer instead, combustion restarts with its simple injection because it decomposes by a catalytic bed assuring a high reaction heat and therefore a temperature high enough to initiate combustion. The carbon residue, always present on the fuel surface at the end of the combustion, could make it difficult to restart combustion. Moreover, during the following phases geometric and physical characteristics of the fuel change. Therefore the regression rate can be affected by this and its behavior will differ from what might have been determined by the conditions of the first ignition. We know that the regression rate represents a parameter of fundamental importance in hybrid, as in solid propellants. In the former, the complexity of phenomena involved and the tested dependence of the regression rate both on thermo-fluid-dynamic parameters and on geometric parameters, makes the formulation of a satisfactory analytical model of combustion phenomena extremely complex.

An accurate determination of the aforesaid effects makes it possible to improve the notoriously low value of $\dot{r}$ (one of the major drawbacks of hybrid propulsion), and to make $\dot{r}$ uniform along the grain surface, eliminating the excessive fuel residue at the end of the test. On the other hand, it allows for accurate control of the hot gas flow for different input conditions (oxidizer flow rate and temperature, chamber pressure, etc.). However, numerous experimental measurements of regression rate on a bench motor are needed. In fact, in hybrids, even more than in solid rockets, it is very important to reproduce real operation conditions, not only as far as pressure values are concerned but, above all, as regards oxidizer flow and modes of injection, physical and chemical fuel conditions at the ignition time.

Many tests have been carried out measuring the fuel diameter at the end of each ignition; then the chamber temperature is the same at each restarting. Other tests are in progress, using a measurement system based on an ultrasonic transducer placed on the fuel surface, in order to

obtain more precise indications on the regression rate behavior after more and more ignitions. By using this method we can stop and restart the combustion without a large break between two ignitions and then we can evaluate how the chamber temperature affects the re-ignition capability and the regression rate. Results will be reported in the paper.

Surface Heat Release of HTPB-based Fuels in Oxygen Rich Environments

G.A. Risha, G.C. Harting, K.K. Kuo, A. Peretz, D.E. Koch
140 Research Building East
The Pennsylvania State University
University Park, PA 16802
Tel: (814) 863-2264
Fax: (814) 863-3203
E-mail: gch104@psu.edu

H.S. Jones and J.P. Arves
Lockheed Martin Michoud Space Systems
New Orleans, LA 70189

An experimental study was conducted to determine the dependence of the regression rate of two solid-fuel formulations (cured HTPB and JIRAD fuel) on operating conditions near the head-end of a hybrid motor. Cylindrical fuel samples were burned in a windowed combustor at pressures ranging from 0.79 to 3.55 MPa. The burning was sustained by a diffusion flame created over the fuel surface by an impinging oxidizer jet. The gaseous oxidizer, delivered at an initial temperature between 220 and 298 K, was a mixture of oxygen and nitrogen with the oxygen mass fraction ranging from 0.21 to 1.00. For both fuels, the regression rate increased with oxidizer mass flow rate, oxygen mass fraction, and oxidizer temperature, but decreased with pressure. Measured regression rates, surface temperatures, and operating parameters were used to validate a simple power-law regression rate correlation for each fuel. An analytical model was also developed to consider the effects of species diffusion, heterogeneous surface reactions, and fluid-dynamic/heat transfer processes. The heats of decomposition of these solid fuels were determined from a fast thermolysis study using a gas chromatograph/mass spectrometer equipped with a pyrolyzer. The model indicated that more energy was available at the surface than that required for decomposition of the solid fuels alone. This excess energy implies that heterogeneous reactions at the solid fuel surface can potentially play an important role in the combustion of solid fuels in an oxidizing environment. Additionally, the amount of surface heat release was found to decrease with increasing solid fuel regression rate which suggests that higher blowing rates reduce the amount of oxygen available for reaction at the surface.
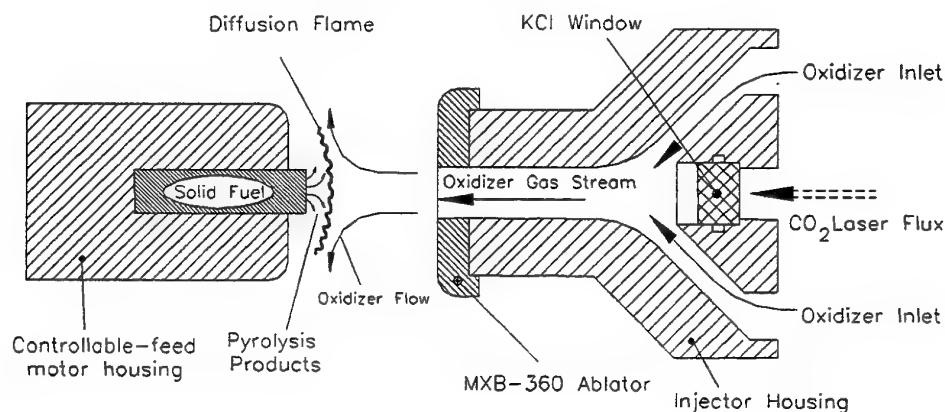
Schematic diagram of the oxidizer injector and sample configuration

THIS PAGE HAS BEEN DELIBERATELY LEFT BLANK

The Advanced Technology of Prevention of the Anomalous Combustion Regimes Development in the Submarine Ballistic Rocket Large-Sized SPRM

A.N. Lukin

Physics-Chemical Mechanics Department, Institute of Applied Mechanics,
Ural Branch of the Russian Academy of Sciences,
Bldg. 222, Gorky Str., Izhevsk, Udmurt Republic, 426000, Russia
Tel: +7 (3412) 75 2731
Fax: +7 (3412) 43 1713
E-Mail: lukin@lam.ipm.udm.ru

Characteristic property of the modern submarine ballistic rockets (SBR) [1] are first of all, the control system accuracy, the high dynamic complexity and dynamic loads, and a large influence of impact and vibrational loads accompanying the solid propellant rocket motor (SPRM) start on the rocket functionability. Moreover, the tendency of development of modern SBR large-sized SPRM is characterized by increased propellant mass (the intrachamber loading coefficient $\geq$ 0.95) and small relative lengthening.

Improvement of modern SBR top stages (large-sized SPRM characteristics and reduction of terms and material expenses on their improvement and manufacturing) depend largely on achieved results in understanding the regularities of a course and possible accuracy of the anomalous physics-chemical processes, which can arise during the operational period.

In this connection, the important direction of the SBR top stages SPRM improvement is investigation of methods of optimal organization of the intrachamber processes development of the SPRM initial stage operation with the purpose of reduction of impact and vibrational actions on the rocket and its systems.

The main peculiarity of the structural diagrams of SBR top stages propulsion systems is that the firmly fastened internal channel charge has a partially non-fastening and unarmored end-face surfaces in the vicinity of the front bottom. In these conditions the end-face combustion surface can make up to 50 % and more of the whole combustion surface. The engine case has a "cocoon" type design and is manufactured from the organic plastic materials. For such conditions, the thickness of the nonflowing clearance between the SPRM case front bottom internal surface and the charge end-face surface can increase in 20 - 100 times at the operating pressures in the combustion chamber (5 - 10) MPa.

Operation of such engine can occur in abnormal mode. In a number of cases, listed peculiarity of the considered SPRM can cause the increased sensitivity of the SPRM initial stage operation to various kinds of the non-estimated actions. "Non-estimated actions" are implied not only deviations of working parameters from the separate units and elements of the SPRM, but also possible design errors, violations of technological process modes and aging of the materials, both in the design of SPRM, and the charge. The intraballistic parameters in the initial stage of the large-sized SPRM operation in many respects are determined by the physics-chemical processes proceeding in the pyrotechnic ignition system (IS) and subsequent heat effect of the IS charge combustion products (CP) on the motor main charge. In the considered situation, the reason of an anomalous mode of ignition and combustion in the SPRM combustion chamber beginning can serve the non-estimated action from the

pyrotechnic IS. Such non-calculated effect results in non-monotonicity of the working processes course during the propellant charge ignition. In the course of filling the intrachamber volume with CP coming from the IS and from the already ignited part of the charge, joint elastic deformations of the propellant charge and the organic plastic engine case may occur. However, the elongated deaf end-face clearance has no time to be expanded to the necessary size. In the result, close to the interface of the end-face clearance with the boot, which fastens the charge end-face with the rocket engine bottom, the powerful local dynamic loads may arise, caused by the gradually increased compression wave propagation phenomenon. Development of the above-mentioned phenomenon results in the boot breaking off from the engine case and from the charge.

The numerical study of the physics-chemical processes subsequent to the boot breaking off is conducted. The gas dynamics equations are solved numerically by Yu. M. Davydov's "large particles method" [2]. For the complex check-up of the developed mathematical model of the physics-chemical processes, the numerical calculation results have been compared with the fire stand tests results.

Calculation results show, in particular, the appearance of strong rarefaction waves, resulting in either extinction of the propellant charge (complete or temporary) or transition to a mode of the unsteady burning [3].

Realization of the described above, or similar, anomalous mode ignition, (which is accompanied by intensive shock waves rise in the large-sized SPRM combustion chamber) shows they are extremely dangerous for the modern SBR and especially for SBR top stages [1]. The general-arrangement diagrams of mentioned rockets are characterized by extreme possible use of the whole volume, which contain in the envelope of the rocket case. The beginning of the "non-estimated" vibrational and impact loads in the engine chamber can call the anomalous resonant effects in the whole system which result in damage of its various units and elements. For example, the devices of onboard control system - gyrostabilizer, astrooptical navigational device.

Executed calculations demonstrate that the described above ignition in an abnormal mode appearance in the SPRM can be prevented. The appropriate technology for prevention of the solid propellant charge anomalous ignition regimes was developed. This technology provides monotony of the SPRM operation during the start period by means of the CP selection, coming from the IS, both in space orientation and in time. In this conditions the $(\partial P / \partial t)$ maximum values are reduced, the flame propagation velocity along the end-face clearance increases in some times, the time straggling of the propellant surface located in the end-face cavity connecting to combustion have decreased, and the boot breaking off probability is essentially reduced.

For practical realization of new ignition technology, two special SPRM IS design schemes were elaborated. The first design scheme has mobile elements of design. The second SPRM IS design scheme has larger reliability, as does not contain any mobile elements of design.

References

1. Velitchko, I.I. (ed.), "The Ballistic Rockets of the Submarines of Russia. The Selected Articles," *The State Rockets Center "The Academician V.P.Makeev's Constructor Bureau"*, Miass, 1994, 279 p. (in Russian).

2. Davydov, Yu.M., "Large Particles Method," *Encyclopaedia of Mathematics, Vol. 5, Kluwer Academic Publishers:* Dordrecht / Boston / London, 1990, pp. 358 - 360.

3. Price, E.W., "L^* - Instability," *Nonsteady Burning and Combustion Stability of Solid Propellants, Chapter 9, AIAA Volume 143, Progress in Astronautics and Aeronautics, AIAA*, New York, 1992, pp. 325-359.

THIS PAGE HAS BEEN DELIBERATELY LEFT BLANK

Experimental and Numerical Study of Casting Process Effects on Small Scale Solid Rocket Motor Ballistic Behavior

P. Le Breton , D. Ribéreau, C. Marraud, P. Lamarque
SNPE

B.P. 57, 33166 Saint Medard en Jalles, Cedex, France
Tel: 33(0) 5-56-70-52-41
Fax: 33(0) 5-56-70-52-92
E-mail: p.lebreton@propulsion.snpe.com

It is now well admitted that the ballistic response of solid rocket motors depends on the process used to manufacture it. Usually, the empirical parameters necessary to predict the performance of a motor (hump effect and scale factor), linked to the manufacturing process, are deduced from the exploitation of previous firing tests. The objective of our studies is to explain physical phenomena linked to those empirical parameters.

One step in these studies has been to manufacture, with the same propellant, six small scale grains using three casting processes and to study the influence of the manufacturing process on the ballistic behavior. Three of those grains have been fired. The exploitation of firing tests results gave the hump effect for each casting process, and the scale factor between two casting processes. The last three grains have been cut in several samples for local measurements of burning rate (strand-burner and ultrasound measurements) and density. Nuclear Magnetic Resonance (NMR) imaging visualizations have also been done. The main results of experimental analysis are the profile of the radial burning rate on the web coherent with the hump effect, the strong ratio between radial and axial burning rates on each point of the web, and the visualization of propellant stratification by NMR imaging due to the casting method.

The experimental results have then been compared to a numerical simulation performed using a new code developed at SNPE to compute surface burn-back with varying burning rate. In this mathematical model, the propellant should not be homogeneous like it is constant burning rate simulations. The nature and the form of the heterogeneities are linked to the casting method. They may be deduced from a casting simulation performed at SNPE with the MONTREAL® code or from NMR imaging. The burning rate at one point of the combustion area depends on the local angle between the combustion front and a physical parameter characteristic of the propellant flow organization.

Experimental and numerical results are in very good agreement. This means that the simulation gives results very closed to experimental results in term of hump effect, scale factor between two casting processes, local burning rate profiles, and local anisotropy of propellant. Our conclusion is that our model is able to predict the global behavior of a grain motor when the stratification can be deduced from casting simulations or NMR imaging visualizations.

THIS PAGE HAS BEEN DELIBERATELY LEFT BLANK

Effects of Altitude on Microwave Attenuation of Solid Rocket Exhaust Plumes

Qingyun Liu, Ping Zhang
Department of Flight Vehicle Engineering
Beijing Institute of Technology
P.O. Box 327
Beijing 100081 P. R. China
Tel: 0086-010-68914186, Fax: 0086-010-68911040
E-mail: liuqy@public2.east.net.cn

Dongmei An
Basic Division, Beijing Inst. of Machinery
P. O. Box 2865
Beijing 100085 P. R. China

Introduction

The microwave attenuation of signal transmitting through rocket exhaust plume is dependent on the rocket motor; including formulation of propellant and configuration of motor, microwave frequency, as well as environment in which the missiles or rockets fly, such as the ambient temperature, pressure, both of which are flight altitude dependent. The effects of altitude on the microwave attenuation of solid rocket exhaust plume are investigated in this paper. The IACH[1,2] program developed in Beijing Institute of Technology, which incorporate the effects of finite-rate chemical kinetics, turbulent eddy viscosity and electron-conductive model was used to calculate the signal attenuation of the exhaust plume corresponding to altitude of 5, 10, 15, 20km, assuming the Mach number of the freestream is 0.9. Also the predicted results are analyzed. The increase of altitude will lead to the decrease in temperature level due to the reduced rates of mixing and combustion, both of which are pressure dependent. As altitude increasing, the value of the electron number density along centerline of plume decays slowly downstream of the peak position and therefore higher flight altitude will produce a longer plume.

Approach

The signal attenuation phenomenon is known to be caused by the interaction of the microwave signal with free electrons present in the hot rocket exhaust plume. It is assumed that the interaction between ions, neutral atoms or molecules and the electromagnetic wave can be negligible due to their heavy qualities of about 50000 times of that of electron. MEXWELL equations are solved to calculate the microwave attenuation of rocket plume using electron-conductive model. The free electron number density n_e, the electron-neutral collision frequency υ_e and the microwave frequency ω determine the microwave attenuation of the plume. The attenuation per unit length α is computed using the following equation

$$\alpha = 46.07 \times 10^{-6} \frac{n_e}{\upsilon_e \left[1 + (\omega/\upsilon_e)^2\right]} \tag{1}$$

The exhaust plume is not a uniform medium, electron density and collision frequency varies with both radial and axial position in the plume, and since the temperature and exhaust

composition varies with position. The IACH program can be run successfully for calculating the axial and radial distribution of the physical, chemical and electromagnetic parameters of the plume considering the effects of finite-rate chemical-kinetics, turbulent eddy viscosity and electron-conductive model. The total microwave attenuation A is integrated through the path in the plume and finally determined by

$$A = -8.686 \int_a^b \alpha \, dZ \quad (\text{dB}) \tag{2}$$

where a and b are the start and end point of plume path respectively.

1 Governing Equations

The parabolized axisymmetric Navier-Stokes equations are listed below:

Global Continuity

$$\frac{\partial(\rho u)}{\partial x} + \frac{1}{r}\frac{\partial(\rho v r)}{\partial r} = 0 \tag{3}$$

Conservation of Momentum

$$\rho u \frac{\partial u}{\partial x} + \rho v \frac{\partial u}{\partial r} = -\frac{\partial p}{\partial x} + \frac{1}{r}\frac{\partial}{\partial r}(\mu r \frac{\partial u}{\partial r}) \tag{4}$$

Conservation of Energy

$$\rho c_p \left[u\frac{\partial T}{\partial x} + v\frac{\partial T}{\partial r} \right] = u\frac{\partial P}{\partial x} + \mu(\frac{\partial u}{\partial r})^2 + \frac{1}{r}\frac{\partial}{\partial r}\left[\mu r \frac{c_p}{\Pr}\frac{\partial T}{\partial r} \right] +$$
$$\mu \frac{\text{Le}}{\Pr}\frac{\partial T}{\partial r}\sum_{i=1}^{n} c_{pi}\frac{\partial F_i}{\partial r} - \sum_{i=1}^{n}\dot{\omega}_i h_i \tag{5}$$

Conservation of Species

$$\rho u \frac{\partial F_i}{\partial x} + \rho v \frac{\partial F_i}{\partial r} = \frac{1}{r}\frac{\partial}{\partial r}(\frac{\text{L}_e}{\Pr}\mu r \frac{\partial F_i}{\partial r}) + \dot{\omega}_i \tag{6}$$

State

$$\rho = \frac{pW}{RT} \tag{7}$$

2 Implicit/Explicit Schemes

In this paper Eqs.(3~6) are solved using a forward marching technique. Explicit difference schemes are used for the momentum and energy equations, implicit difference schemes are used in the solution of the species conservation equations to eliminate the stiffness. This mixed explicit/implicit scheme ensure the stability of the approach, and allows integration step sizes to be increased by orders of magnitude without sacrificing accuracy. The Donaldson/Gray[3] turbulence model and Sutherland's law are used to calculate the viscosity for turbulent and laminar flow.

3 Finite-Rate Chemical Kinetic Model

For two-way unit reaction $A + B + \cdots\cdots \Leftrightarrow C + D + \cdots\cdots$, The net product rate is written below:

$$\dot{\omega} = K_f[A][B]\cdots\cdots - K_b[C][D]\cdots\cdots \tag{8}$$

Where K_f and K_b are the forward and reverse rate coefficients, respectively. The reverse rate coefficient is derived from $K_b = K_f/K_c$, where K_c is the equilibrium constant of the reaction expressed with mole concentration. A list of chemical reactions and their rate

coefficients K_f and equilibrium constants K_c for calculations of flame structures are given in [4]. The thermodynamic properties (specific heat c_p, enthalpy, h, entropy s) of each species is expressed as a seventh-order polynomial in temperature, and their coefficients are given in [5].

Inputs

The propellant formulation is shown in table 1. The chamber pressure is 70atm. The nozzle radius at the exit plane(Re) is 5mm. The microwave frequency is 10GHz. The impurity level of alkali metal (potassium) is assumed to be from 0ppm to 50ppm. A comprehensive computer program NASA-CEC-71 is used to calculate the parameters in chamber and at the nozzle exit plane. The nozzle exit condition is shown in table2. The external conditions is shown in table 3. Reaction mechanism for nonequilibrium afterburing exhaust plume is shown in table 4.

Table 1 The Propellant Formulation

RDX	Al	NH_4ClO_4	HTPB	K_Z	$2F_e^{\#}$	Potassium
39.4%	6%	40.6%	8.9%	4.1%	1%	0~50ppm

Table 2 Parameters at the nozzle exit plane

Pressure (atm)	1.0		
Tempreture (K)	1282		
Speed (m/s)	2438		
Composition	Mole fraction Potassium0ppm	Composition	Mole fraction Potassium50ppm
AL2O3(S)	2.5398E-02	AL2O3	2.5398E-02
CO	2.6631E-01	CO	2.6631E-01
CO2	5.9442E-02	CO2	5.9436E-02
CL	9.4540E-08	CL	9.4577E-08
CL-	5.2060E-08	CL-	5.2100E-08
E-	6.1650E-13	E-	6.1770E-13
FECL2	2.8603E-03	FECL2	2.8602E-03
H	4.4502E-07	H	4.4540E-07
HCL	7.3195E-02	HCL	7.3165E-02
H2	2.9969E-01	H2	2.9969E-01
H2O	1.1223E-01	H2O	1.1224E-01
N2	1.6086E-01	K	7.8170E-11
O	2.8780E-15	K+	1.0000E-15
OH	1.9830E-09	KCL	2.9209E-05
O2	5.3420E-16	N2	1.6086E-01
		O	2.8840E-15
		OH	1.9850E-09
		O2	5.3520E-16

Table 3 Ambient conditions

Altitude	Temperature (K)	Sonic speed (m/s)	Pressure (Pa)
5km	255.7	320.5	0.54048E5
10km	223.3	299.5	0.26500E5
15km	216.7	295.1	0.12112E5
20km	216.7	295.1	5.5293E3

Table 4 Reaction mechanisms for nonequilibrium afterburning exhaust plume

$$k_f = AT^{-B} \exp(C/RT)$$

Reaction							A	B	C
O	+ O	+ M	=	O2	+	M	0.100E-28	1.0	0.0
H	+ H	+ M	=	H2	+	M	0.100E-28	1.0	0.0
O	+ H	+ M	=	OH	+	M	0.100E-28	1.0	0.0
H	+ OH	+ M	=	H2O	+	M	0.100E-27	1.0	0.0
CO	+ O	+ M	=	CO2	+	M	0.500E-28	1.0	-4000.0
OH	+ OH		=	H2O	+	O	0.100E-10	0.0	-1000.0
OH	+ H2		=	H2O	+	H	0.400E-10	0.0	-5500.0
O	+ H2		=	OH	+	H	0.300E-10	0.0	-8200.0
H	+ O2		=	OH	+	O	0.300E-09	0.0	-16500.0
CO	+ OH		=	CO2	+	H	0.500E-12	0.0	-600.0
H	+ HCL		=	CL	+	H2	0.880E-10	0.0	-4622.0
HCL	+ OH		=	H2O	+	CL	0.720E-11	0.0	-3250.0
OH	+ CL		=	HCL	+	O	0.300E-10	0.0	-5000.0
H	+ CL	+ M	=	HCL	+	M	0.300E-28	1.0	0.0
K+	+ E-	+ M	=	K	+	M	0.200E-21	1.5	0.0
K+	+ CL-		=	K	+	CL	0.100E-07	0.5	0.0
KCL	+ H		=	K	+	HCL	0.300E-10	0.0	4072.0
CL	+ E-	+ M	=	CL-	+	M	0.300E-29	0.0	0.0
H	+ CL-		=	HCL	+	E-	0.170E-11	0.0	-6210.0

Results and Discussion

A series of calculations were made corresponding to altitude of 5, 10, 15, 20km, assuming the flying Mach number is 0.9. Figure 1 shows the temperature along centerline of the exhaust plume for each attitude. It indicates that the temperature along the centerline of exhaust plume decreases with increasing altitude due to the reduced rates of mixing and combustion, both of which are pressure dependent.

The influence of altitude on electron number density distributions can be seen from Fig.2 and Fig.4. Although the contributions of alkali metal impurities to the total energy of propellant can be negligible, they are the main contributors of free electrons because of their low ionization potentials. Therefore, the effects of altitude on the characteristics of signal attenuation of plume differ for different concentration of alkali metal levels. Lower maximum electron number density along the centerline of exhaust plume are reached as altitude increases in the case of absence of alkali metal impurity, whereas higher ones are achieved at higher altitude for the formulation containing 50ppm potassium impurity, which found in

typical composite propellants. Further study should be done for this divergence. From Fig.2 and Fig. 4, we can also see that the electron number density levels decay slowly downstream of the peak position, and therefore a higher flight altitude will produce a longer plume, due to the reduction in recombination and attachment rates resulted from the low ambient pressure.

Calculated attenuations of signal transmitting vertically through exhaust plume are shown in Fig. 3 and Fig.5 for both formulations of propellants. The significance of alkali metal impurity to microwave attenuation is enforced by the values of attenuation at same altitude, as discussed in early papers[6,7,8]. The maximum signal attenuation maintains the ascending trend with the increasing altitude from 5km to 15km, then transforms to descent up to 20km. This points out the strong dependence of microwave attenuation on flight altitude, and it is insufficient to estimate the in-flight attenuation from attenuation measured under sea-level conditions. Further emphases should be given on the complex effects of altitude (pressure) on the coupled mixing and afterburning.

Reference

[1] Jisong Cui, Studies of computer program for rocket exhaust plume flowfields characteristics predictions with chemical reactions: [dissertation] Beijing: Beijing Institute of Technology, 1988

[2] Qingyun Liu, Theoretical Prediction and Experimental Investigation on Microwave Attenuation Characteristics of Solid Propellant Exhaust Plumes: [dissertation] Beijing: Beijing Institute of Technology, 1992

[3] R. R. Mikatarian, etal, A Fast Computer Program for Non-equilibrium Rocket Plume Predictions AD751984, 1972

[4] D. E. Jensen and G. A. Jones, Reaction Rate Coefficients for Flame Calculations COMBUSTION AND FLAME 32, 1-34,1978

[5] S. Gordon and B. J. McBride Computer Program for Calculation of Complex Chemical Equilibrium Compositions, Rocket Performance, Incident and Reflected Shocks, and Chapman-Jouguet Detonations NASA SP-273 Interim Revision N78-17724, March 1976

[6] Wood W A, DeMORE J E Microwave attenuation characteristics of solid propellant rocket exhaust products AIAA 65-183, 1965

[7] Smoot L D, Underwood D L, Schroeder R G Prediction of microwave attenuation characteristics of rocket exhausts AIAA 65-181, 1965

[8] Ping Zhang and Qingyun Liu Prediction of Microwave Signal Attenuation by An Anti-Tank Missile's Exhaust Plume ACTA ARMAMENTARII, Vol.18, No.4, pp321-325, 1997
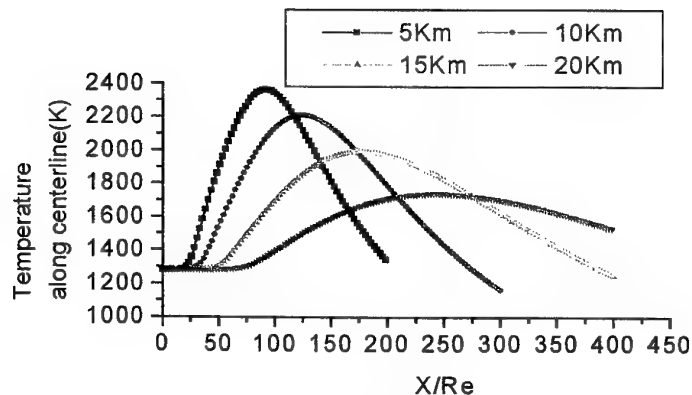
Fig. 1 Temperature along centerline of exhaust plume at different altitude
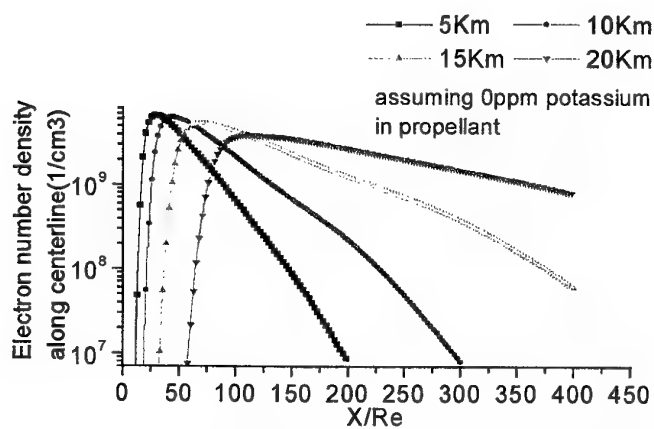

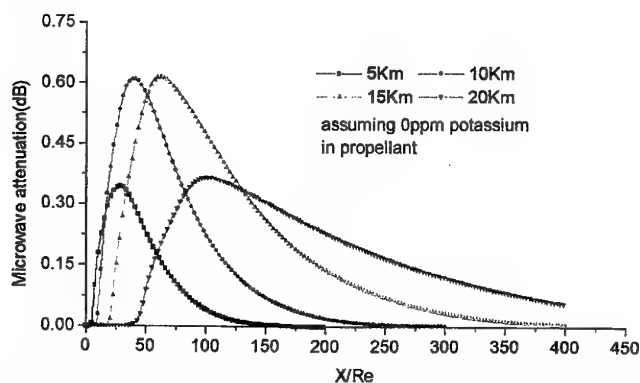Fig. 2 Electron number density along centerline of exhaust plume at different altitude

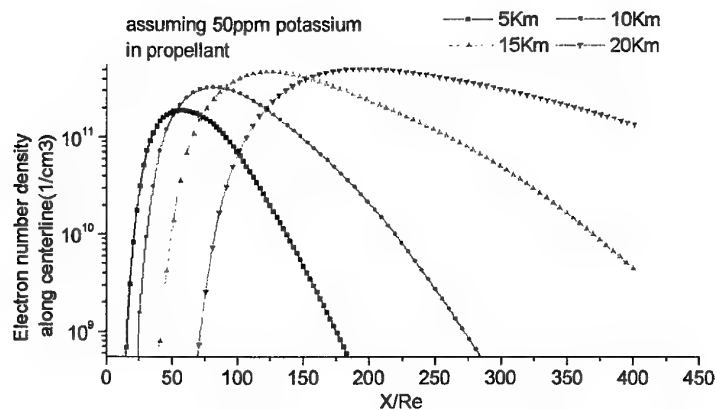Fig.3 Attenuation of signal transmitting vertically through exhaust plume

Fig. 4 Electron number density along centerline of exhaust plume at different altitude
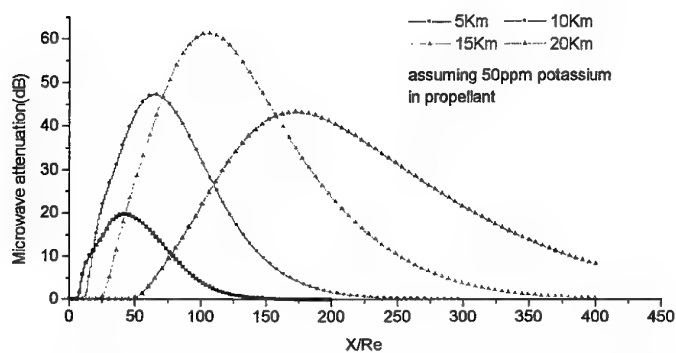

Fig.5 Attenuation of signal transmitting vertically through exhaust plume

THIS PAGE HAS BEEN DELIBERATELY LEFT BLANK

Plume Temperature Distribution Measurements of a Spin-Stabilized Rocket

Jir-Ming Char
The Chinese Air Force Aeronautical Technology School
P.O. Box 90395, Kang-Shan, Taiwan
Tel: (0) 07-6254189
Fax: (0) 06-2358894
Email: char@cc.cafa.edu.tw
Jun-Hsien Yeh
Cheng-Shiu Institute of Technology
Department of Industry and Management
Kaohsiung, Taiwan, R.O.C.
Email: sparkyeh@tpts5.seed.net.tw

Rocket plume temperature distribution plays an important role on the heat transfer analysis of carrier. Thus, a non-intrusive IR scanner is used in this paper to analyze the influence of spin motion induced by nutation instability on plume centerline temperature measurements of spinning solid-propellant rockets. A solid-propellant rocket motor test stand is employed in the present study, as shown in Fig. 1. The test stand contains a gimbals arrangement, two servomotors, a gearbox, a spin disk, and a linkage which are manufactured by stainless steel to avoid corrosion caused by the rocket plume. Since a special filter is built into the IR scanner, only 4.3 μm wavelengths can pass the filter, so the emissivity of a rocket plume that contains metal particles at this band must be determined first.

Two values of emissivity are used in this study. One is 0.138 and another is 0.125. Both are derived from equation (1). Where ε_g is 0.107 as obtained by Professor Kuo's experiment and ε_s is 0.033 obtained by optically thick theory and the table of Bauer and Plass. Another ε_s value is 0.25 obtained by Morizum's method.

$$\varepsilon = \varepsilon_g + \varepsilon_s - \varepsilon_g \times \varepsilon_s \tag{1}$$

Where ε is flame emissivity, subscript g indicates gas, and s indicates soot particles.

Figure 2 shows that the average error of temperature measurement is below 3.5% even with a 10% error of estimated emittance value. Thus, the single value of 0.138 is used as the emittance to analyze the rocket plume temperature distributions.

Figures 3 and 4 show the influence of spin rate on rocket plume temperature distributions. The data displayed in Fig. 3 is the rocket plume temperature distribution at various burning time under no-spin condition. At the early burning stage, the rocket plume contains a high-percentage of flammable gas and is cooled by the vortex of ambient air, which is induced by the transient plume jet of the rocket. Hence, the plume at the nozzle exit has a low temperature during the early burning stage. After a short period, high-temperature particles apparently are ejected and emit high-intensity IR that causes the increase of plume temperature at the nozzle exit. Because the metal particles cause high temperatures to exist at the nozzle exit, the temperature distribution curve presents the retroflex phenomena. This is due to the plume jet induced cooling effect from the mixing of high-temperature particles with the cold air vortex. For this reason, the plume temperature decreases abruptly while combustion gas is ejected from the nozzle and then increases when the secondary combustion

of the plume occurs. Figure 4 shows no retroflex phenomena due to the spin motion at the spin rate of 600rpm.
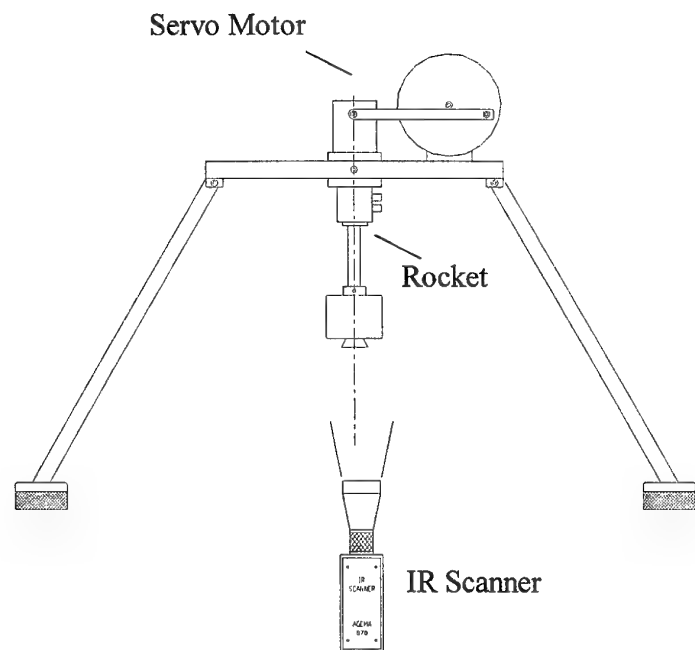

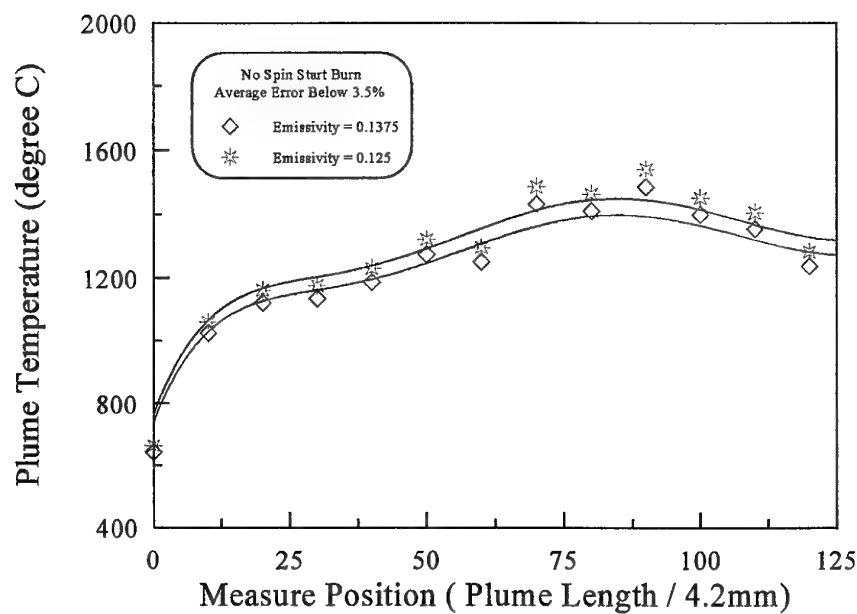Fig. 1. Spinning rocket test stand

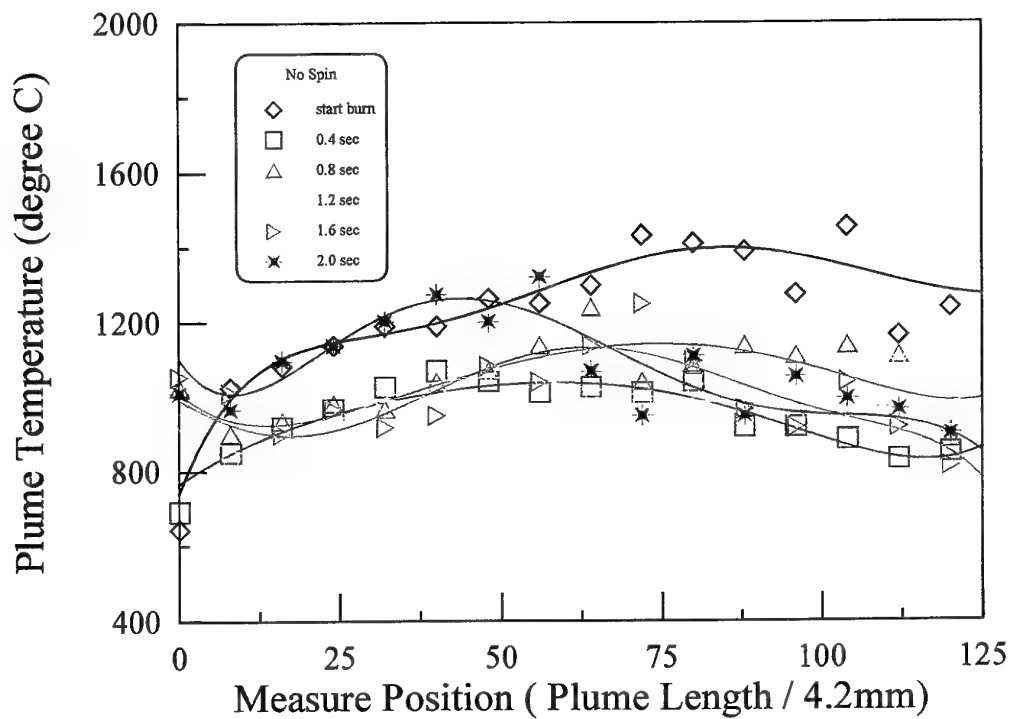Fig. 2 Effect of emissivity on plume temperature

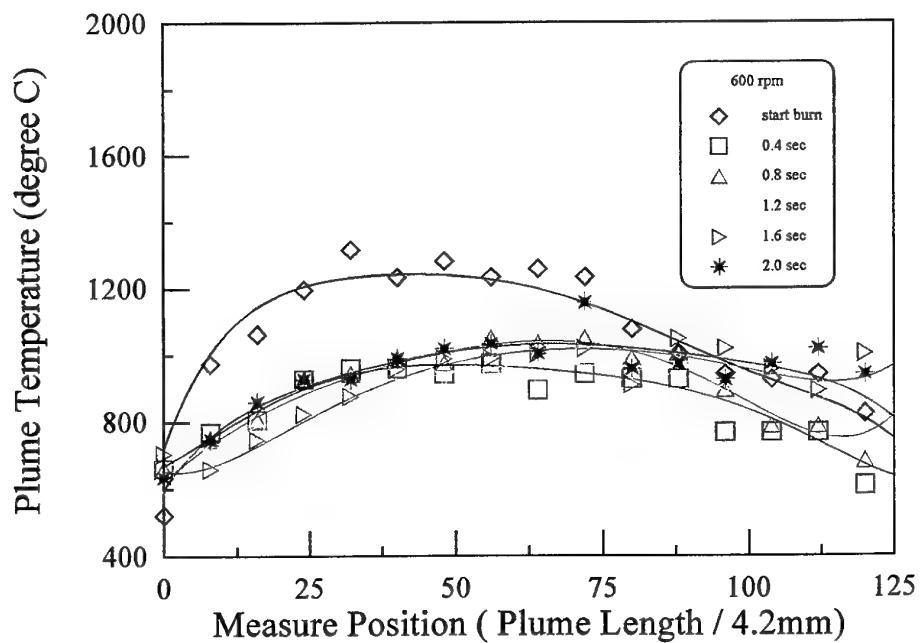Fig. 3 Temperature distribution of rocket plume at no spin condition

Fig. 4 Temperature distribution of rocket plume at 600 rpm

THIS PAGE HAS BEEN DELIBERATELY LEFT BLANK

AREA 4:

ENERGETIC MATERIALS COMBUSTION FOR ROCKET PROPULSION

SESSION CHAIR:

DR. ROLAND PEIN

Formulation and Combustion of Gelled Liquid Propellants with Alex™ Particles

F. Tepper and L.A. Kaledin
Argonide Corporation
Sanford, FL 32771
Tel: (407) 322-2500
Fax: 407-322-1144
http://www.argonide.com
E-mail: fred@argonide.com

Aluminum is a highly energetic metal that can react with a wide variety of oxidizers to produce propellants with high specific impulse. When added to a liquid fuel aluminum substantially increases theoretical density Isp of hydrocarbon as well as alcohol fuels, potentially reducing the size of tankage and overall system weight. However, aluminum tends to agglomerate in burning liquid hydrocarbon droplets delaying combustion within the engine, reducing delivered performance. We believed that very rapid oxidation of Alex™ nanosize aluminum could mitigate the agglomeration and could lead to an increase in delivered specific impulse.

The study consists of five elements – code computations for aluminum/liquid fuel mixtures with liquid oxygen, formulation of Alex™ gels in RP-1 kerosene and alcohols, study of their rheology and dynamic stability, determination of ignition delay and small rocket engine tests that are the subject of another paper at this conference. The study includes consideration of the use of Alex™ in alcohols and diols as potential monopropellants.

Gels were formulated of 5, 30 and 55 weight percent Alex™ in RP-1 (kerosene) using a combination of wetting and gelling agents. The viscosity of such gels was measured as a function of aluminum content, temperature and shear rate. We found that their viscosity at high shear rates was within the capability of existing pumping systems. The rheology of such gels was found to be non-Newtonian, so called Yield Pseudoplastic. At loadings greater than 30 weight percent Alex™ no foreign gellant is necessary to achieve dynamic stability as measured by centrifuging the gels at 1300 rpm for one hour. In contrast, micron size aluminum gels required 5% fumed silica as a gellant to achieve dynamic stability, as did the gels containing 5% Alex™.

Figure 1 is a schematic of a bomb that is being used to measure ignition delay of Alex™/RP-1 gels as compared to RP-1 gels without any aluminum. We squirt the gels into the bomb that had been pre-heated to a defined temperature and with an oxidizing gas of defined pressure. There is an internal transducer that measures pressure rise, our principal data output. We measure the time from very first indication of a rise until rapid ramp up of pressure. The pressure rise as a result of ignition is about 3-4 times original pressure (using oxygen), and the device has a design peak pressure of about 3000 psia. Data on ignition delay of Alex™/RP-1 versus RP-1 gels in pressurized oxygen at 400-600 C are compared.
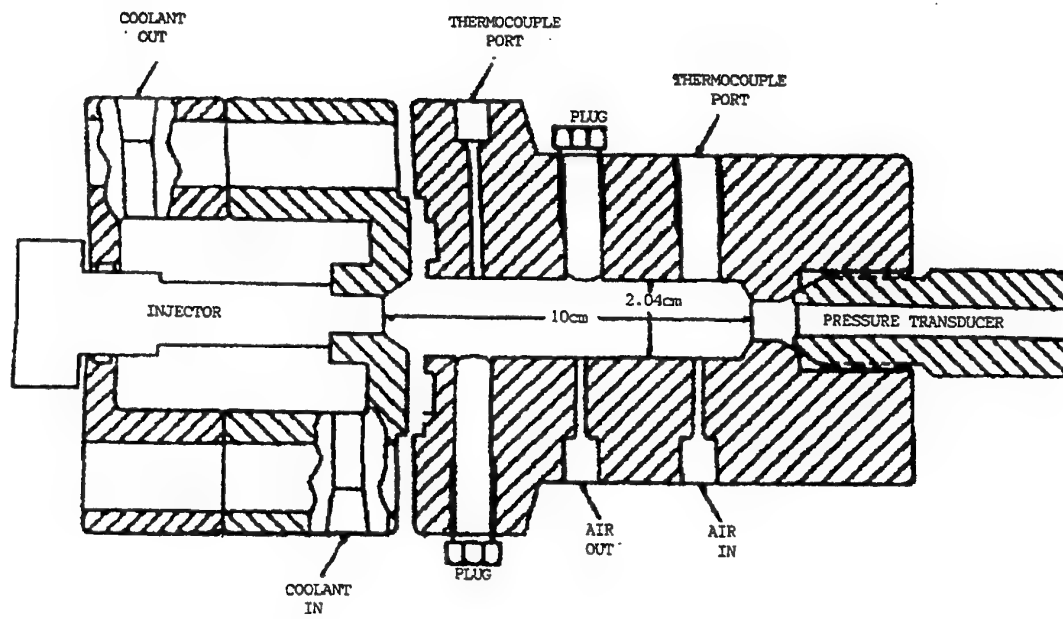
Figure 1 – Device for Measuring Ignition Delay of Gels

Combustion of Gelled RP-1 Propellant with Alex™ Particles

J.W. Mordosky, B.Q. Zhang, G.C. Harting, T.T. Cook, and K.K. Kuo
140 Research Building East
The Pennsylvania State University
University Park, PA 16802
Tel: (814) 863-2264, Fax: (814) 863-3203
E-mail: jwm136@psu.edu

F. Tepper and L.A. Kaledin
Argonide Corporation
Sanford, FL 32771

Combustion tests of gelled RP-1 propellant with Alex particles were performed in an experimental rocket engine. The addition of aluminum particles to gelled RP-1 propellant has the potential to cause a significant increase in the heat release over RP-1 alone due to the high volumetric energy release of aluminum. Previous studies of gelled RP-1 propellant with conventional aluminum powders have yielded very low combustion efficiencies. This may have been the result of incomplete combustion due to the aluminum particles being too large. Alex particles are formed by exploding an aluminum wire, and their diameters are on the order of 90 nanometers. The use of these nano-sized particles can, theoretically, lead to more complete combustion. More complete combustion can, in turn, lead to performance increases such as higher flame temperature, increased specific impulse, and greater c^* combustion efficiency. The rocket engine consists of a cylindrical chamber with a converging diverging nozzle. The propellants are introduced through a coaxial injector and gaseous oxygen is used to atomize the gel (Fig. 1). The engine operating conditions are as follows: chamber pressures ranging from 100-1000 psig, gel propellant mass flow rates ranging from 1-10 g/s, gaseous oxygen mass flow rates ranging from 5-20 g/s, and O/F ratios ranging from 1-4. The percentage of Alex particles in the gelled RP-1 propellant ranged from 0-55% by weight. In the lower percentage loadings, the RP-1 was gelled by adding fumed silica and a surfactant was used in the gel propellants with higher Alex loadings. The c^* combustion efficiency was found to range from 0.7-0.95. Preliminary results shown in Table 1 and Fig.2 seem to indicate that the addition of Alex particles to gelled RP-1 propellant increases the c^* combustion efficiency over gelled RP-1 propellant alone.

Table 1 Comparison of two engine tests #4 (with Alex) and #8 (without Alex)

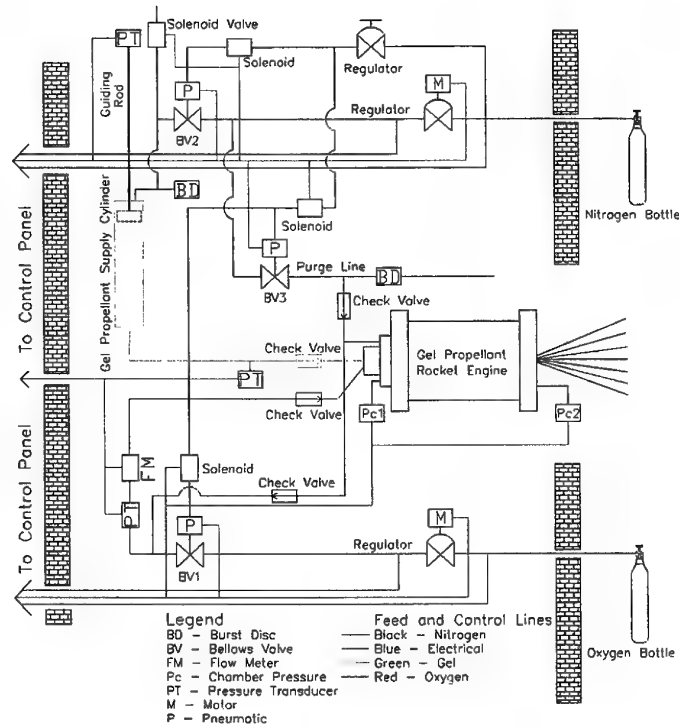| Test Number	#4	#8
Weight % Alex	5	0
Oxygen Mass Flow Rate	8.5	10.3
Gel Mass Flow Rate (g/s)	5.52	5.35
O/F Ratio	1.54	1.93
Chamber Pressure (psig)	189.5	190
c^* efficiency	0.937	0.817

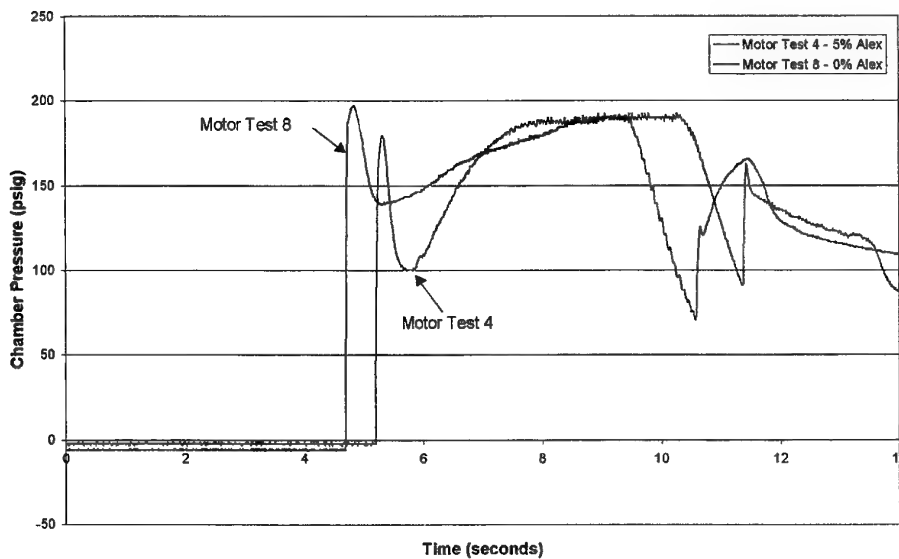Fig. 1 Schematic diagram of feed and control lines for gel propellant rocket engine

Fig. 2 Comparison of pressure-time traces for two similar engine tests

Combustion Phenomena of a Solid Propellant Based on Aluminium Powder

B. Baschung, D. Grune, H.H. Licht, M. Samirant
A. French-German Research Institute of Saint Louis
5, Rue du Général Cassagnou - BP34 - 68301 Saint Louis – France
E-mail: baschung@isl.tm.fr

This paper presents the combustion behavior of a new solid propellant formulation with 15% ultrafine aluminium powder. This aluminium powder produced in Russia is called ALEX. Its grain size is around 50 to 200 nm. To evaluate the propellant burning results, a second comparable solid propellant was produced: it also contains 15% aluminium (called YX) but its grain size is in the order of 10 to 100 μm. Both aluminium powders are compatible with the propellant formulation. REM examinations show that the shape of ALEX is spheric while YX has the shape of flakes.

The combustion experiments are performed in a high-pressure closed vessel at loading densities corresponding to pressures up to 280 MPa. These experiments allow to determine the constants of the Abel equation of state (co-volume and force), the dynamic vivacity and the burning rate.

The following results are obtained:
1. Although both propellant grains have the same geometry (flakes), the burning behavior is quite different.
2. Considering the dynamic vivacity, the YX-propellant burns like a conventional flake propellant. On the other hand, the dynamic vivacity of ALEX-propellant increases very fast between 10 and 15% of burnt mass and is also burning like a flake propellant later on; the values of dynamic vivacity with ALEX-propellant are higher by a factor two than the YX-propellant.
3. For a given pressure, the burning rate of the ALEX-propellant is always higher than the one of the YX-propellant. As an example, at 100 MPa the burning rate of ALEX-propellant is in the order of 200 mm/s in contrast to the YX-propellant which only reaches a burning rate of about 90 mm/s.
4. For each propellant, a VIEILLE's burning law is given with a correlation factor of $r^2=0.999$. The burning rate pressure exponent of the ALEX-propellant is with 0.66 very low compared to the YX-propellant for which a high exponent of 0.80 is calculated.

In the outlook it is shown that the ALEX-propellant seems to be useful for applications in the high-pressure rocket propulsion as an igniter or as a booster, and also for projectiles as an additional accelerator.

THIS PAGE HAS BEEN DELIBERATELY LEFT BLANK

AREA 4:

ENERGETIC MATERIALS COMBUSTION FOR ROCKET PROPULSION

SESSION CO-CHAIRS:

DR. ROBERT GLICK
AND
DR. FRED BLOMSHIELD

Nonsteady Combustion of Composite Solid Propellants

S.A. Rashkovsky
Moscow Institute of Heat Technique
Dzerzhinskaja St. 12-24, Dzerzhinskij, Moscow region, 140056, Russia
Tel: (007-095) 550-4647
E-mail: rash@rash.mccme.ru

The modern models of solid propellant nonsteady combustion, like the Flame Modeling (FM method) and Zeldovich-Novozhilov modeling (ZN method), describe only the combustion of homogeneous (double-base) propellants. Unlike double-base propellants, composite solid propellants (CSP) contain disperse components (AP, RDX, HMX) the sizes of which are of order of or exceed the condensed phase thermal layer thickness. Because of this, strictly speaking, the FM method and ZN method are unsuitable for description of CSP nonsteady combustion. These methods may be used for description of nonsteady combustion of CSP containing only fine grained (ultra-dispersed) particles of dispersed components.

A model of CSP nonsteady combustion taking into account a propellant heterogeneous structure is suggested in this work. The model considers the quasi-steady gas flame and reaction zones of condensed phase propellant components while the thermal layers of condensed phase components are considered as nonsteady but chemically inert. This allows formulating the phenomenological model of CSP nonsteady combustion in the framework of ZN method. Unlike the ZN method, the suggested model is a two-temperature one: one temperature describes the thermal condition of the dispersed propellant component (e.g. AP) while the other temperature describes the thermal condition of the propellant binder. Two models of CSP nonsteady combustion are considered in this work. The first model neglects the thermal interaction of solid propellant condensed phase components. The combustion of each propellant component is similar to combustion of monopropellant and their interaction is realized through a secondary diffusion flame in the gas phase. It is shown that the correlation of the component burning rates determines the nonsteady combustion of the whole propellant. The model suggested is used for calculation of the linear frequency response function for sinusoidal pressure fluctuations. It is shown that different modes of CSP nonsteady combustion exist depending on the value of the component burning rate correlation. Thus, under certain conditions, the mutual amplification of the component burning rate fluctuation is possible; this causes the resonance of the whole propellant burning rate. It is shown that a resonance mode of propellant nonsteady combustion is possible, even though each individual component is not prone to resonance combustion under the same conditions. The range of CSP components performances, which cause a resonance mode of combustion under sinusoidal pressure fluctuation, is investigated.

The second model considered in this paper takes into account the thermal interaction of propellant components through the condensed phase. This interaction and its effect on CSP combustion are considered for the first time in this work. It is shown that the thermal interaction of the propellant components through a condensed phase essentially effects on the combustion process and this has to be considered when simulating both steady and nonsteady CSP combustion. It is shown that, in contrast with double-base propellants, during nonsteady combustion of CSP the characteristic time of burning rate changes is proportional to the characteristic time of the dispersed component burning away. Last, the results obtained in

this work are compared with well-established experimental data relevant to CSP nonsteady combustion.

Combustion of Heterogeneous Solid Propellants

M. Q. Brewster, G. M. Knott, B. T. Chorpening
Department of Mechanical and Industrial Engineering
168 Mechanical Engineering Building
1206 West Green Street
University of Illinois
Urbana, IL 61801
Tel: (217) 244-1628
Fax: (217) 244-6534
E-mail: brewster@uiuc.edu

This work is concerned with combustion of heterogeneous propellants, primarily ammonium perchlorate (AP) and hydrocarbon polymer binder. The goal is to develop a mechanistic understanding of the combustion of this mixing- and kinetically-limited system through complementary experimental and computational investigations. A simplified two-dimensional sandwich geometry is used to aid in comparison between experiments and computational simulations. Chemiluminescent emission imaging is used in the experiments. Simplified chemical kinetics are assumed in the computations. The focus is describing energy and generic species mass transfer characteristics and flame structure well enough to be able to simulate macroscopic combustion behavior, particularly burning rate. The role of key non-dimensional quantities is delineated which in turn delineates the effect of key dimensional parameters such as length scales, mixture fractions, and pressure. Both experimental and computational results show that polymer/AP length scales and pressure have similar pronounced effects on flame structure and therefore on heat feedback to the solid. Under almost all conditions a partially premixed, kinetically-limited leading edge flame is observed. Partially premixed, kinetically-limited leading edge flames form near the AP/binder interface over the oxidizer. Here is where the maximum heat flux back to the solid generally occurs. A premixed monopropellant flame forms over the AP and trailing diffusion flames form farther from the surface. Under conditions of large Peclet number the leading edge flame is split into two distinct branches. For small Peclet numbers the leading edge flames merge together. Flame structure domain plots are generated in terms of Peclet number and Damkohler number. The results are used to infer trends about the effects of AP-particle size, AP-mass loading, and pressure on combustion of AP-composite propellants.

THIS PAGE HAS BEEN DELIBERATELY LEFT BLANK

Burning Rate Modifiers Effects on a Modified Polyvinyl Chloride-Based Propellants

V.S. Bozic, and Dj.Dj. Blagojevic
Faculty of Mechanical Engineering, Belgrade University, 27 marta 80,
11000 Belgrade, Yugoslavia
Tel: 381 11 106 322
Fax: 381 11 106 322
E-mail: vladica@infinity.co.yu

Combustion of modified polyvinyl chloride–based propellants and various additives were studied. Several burning rate modifiers were utilised separately in basic propellant formulations. Studies were conducted to determine the effects of the burning rate modifiers on propellant burning rate. Also, the influence of different plasticizers on propellant burning rate is shown.

Five ammonium perchlorate grinds with nominal particle sizes of 20, 60, 100, 200 and 250 microns were used in experimental propellants. The first three grinds were obtained by milling, while the other two were commercially supplied. The particle size of the burning rate modifiers added in the propellant formulations were not measured, and therefore the specific surface of the additives were not determined.

The whole Flexolite class of propellants can be divided into three groups at the base of their energy properties: low-energy, medium-energy and high-energy propellants. A total of 26 propellant formulations were prepared for measurements.

The basic medium-energy formulation is F. The following conclusions can be drawn from the burning rate data: at the pressures of the study, the burning rate of the catalyzed materials was above that of a pure formulation of F.

The influences of copper chromate (CC) and iron oxide (IO) on burning rate of propellant F are shown in Fig. 1 for a 20 microns grind of ammonium perchlorate. As Flexolite propellants do not have rheologic problems with a greater percent of CC, copper chromate was added in amounts of 0.5%, 3% and 5%. Iron oxide was added in an amount of 3%. From Fig. 1 it can be seen that CC is better catalyst that IO for 3%, and that 5% of CC does not have a significant effect on the burning rate in comparison with 3% of CC. As the concentration of the copper chromate was increased, the burning rate exponent also increased.

The influence of Sicomin-Rot K 3130 S on the medium-energy propellants in the Flexolite series for a 20 microns grind of AP is shown in Fig. 2. This catalyst was added at levels of 0.5%, 1%, 3%, 3.5%, 5%, and 5.5%. An addition of 5% in comparison with 3% has significant influence on the burning rate.

A comparison of 3% of all of these catalysts has shown that CC is the most effective single catalyst, while a comparison of 5% of the catalysts has shown that Sicomin-Rot K 3130 S is the most effective single catalyst. We can concluded from above results that CC is the best catalyst if it is added in quantity up to 3%, while if we must increase the burning rate more, we must use Sicomin-Rot K 3130 S. This catalyst is much cheaper than copper chromate.
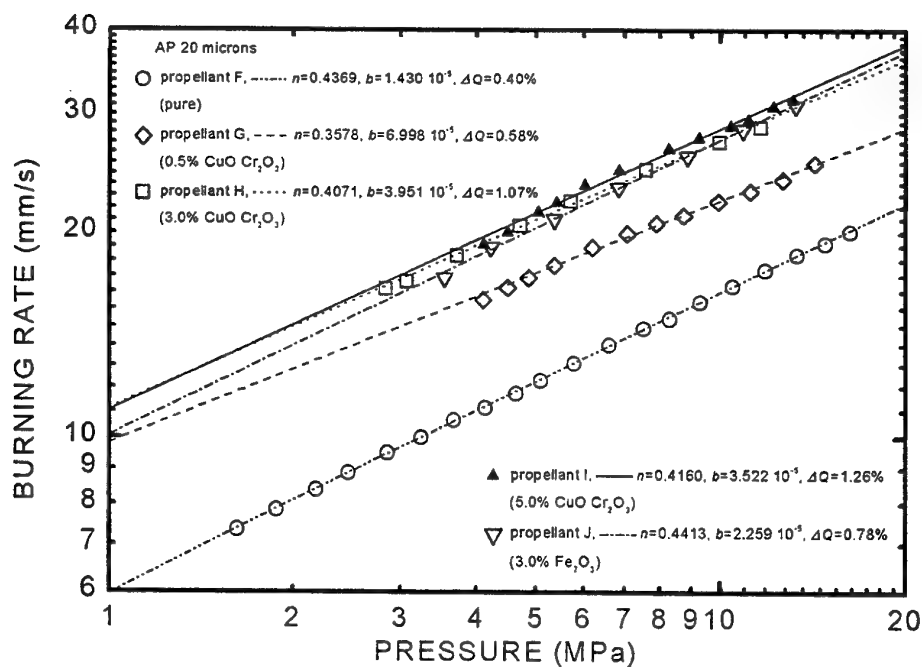
Fig. 1 Influence of Copper Chromate and Iron Oxide on medium-energy propellants (AP 20μ)
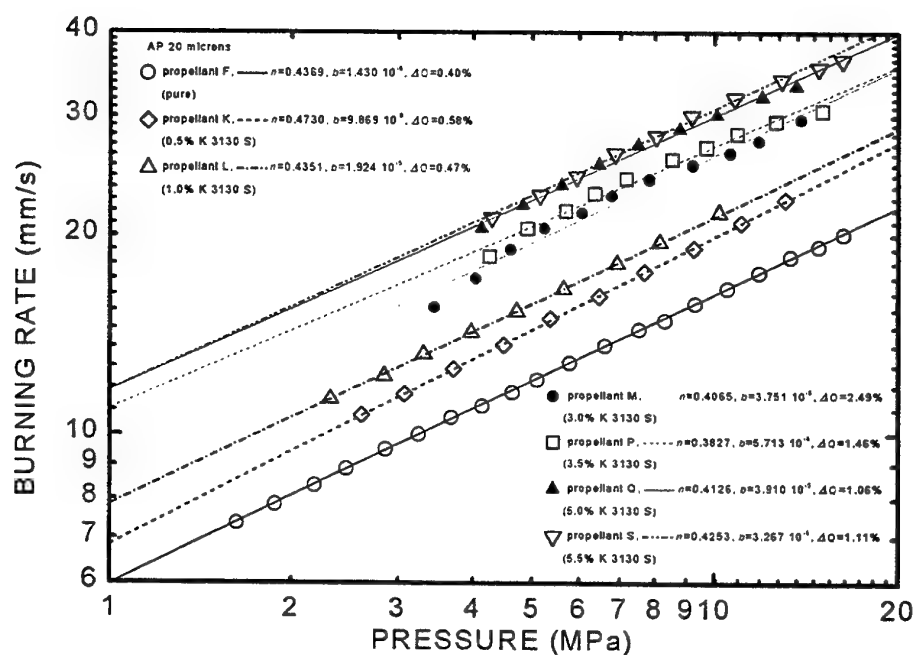

Fig. 2 Influence of catalyst Sicomin-Rot K 3130 S on medium-energy propellants (AP 20 μ)

Study on the Action Temperature of Catalysts to Solid Propellant Burning Rate Using Embedded Thermocouple

Wang Ning Fei
Modern Chemistry Research Institute, Xi'an P. R. China
E-mail: srm802@nwpu.edu.cn

Wang Liang
College of Astronautics, Northwestern Polytechnical University
127 Youyi Rd. W. Xi'an, 710072 P. R. China
Tel: 86-29-8493595
Fax: 86-29-8493406
E-mail: wliang@nwpu.edu.cn

The addition of some catalysts alters the combustion mode of double base and CMDB propellants, which leads to the plateau burning region. The mainly used catalysts are lead salts, copper salts and carbon black. But people know little about how the catalyst acts and what is the action temperature, which is very important for understanding the catalytic mechanism. This paper introduces a method to determine the action temperature of catalysts using embedded thermocouples.

The formulations of the CMDB propellants are listed in Tab.1. The experimental sample was made by extrusion. The Burning rate results are showed in Fig.1.

Tab.1 Formulations of propellant samples

	NC	NG	RDX	Pb salt	Cu salt	C_B	Others
1	34.5	25.2	30	2.5	0.4	0.3	7
2	37.7	25.2	30	0	0	0	7
3	35.2	25.2	30	2.5	0	0	7
4	37.3	25.2	30	0	0.4	0	7
5	37.4	25.2	30	0	0	0.3	7

Using ribbon thermocouples (3.5 microns thick, 50 microns wide) of tungsten/rhenium alloys, which were embedded in the propellant samples, we have got the temperature profiles T-t at different pressures. Through a series of calculation, we can get the heat release in a temperature interval. A typical Q-T curve is shown in Fig.2. Comparing the heat release difference among the different formulations, we can find the different action temperatures of different catalysts. The action temperatures of Cu salt, Pb salt and Pb salt +Cu salt +C_B are respectively about 600K, 500K and 450K.
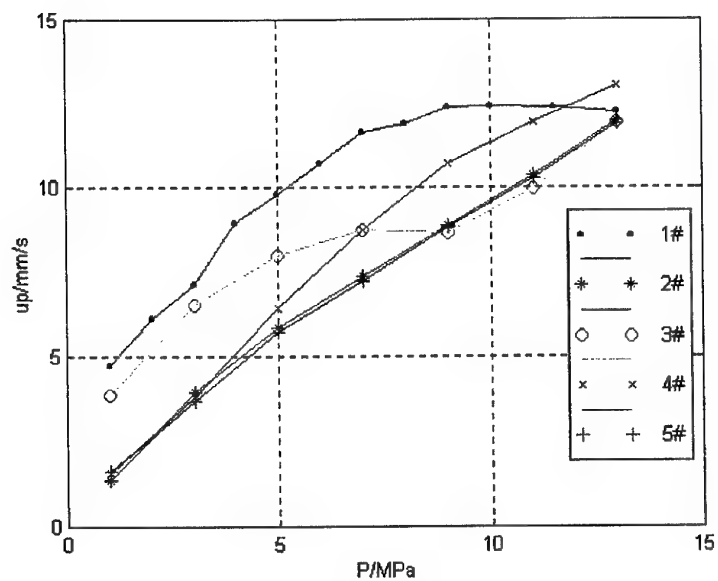
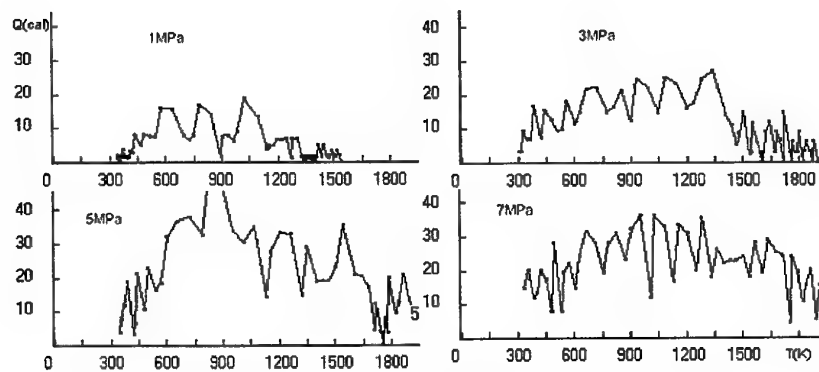Fig.1 The burning rate results of the samples

Fig.2 Q-T curve of sample $1^{\#}$ at 1-7MPa

AREA 6:

METAL COMBUSTION

SESSION CHAIR:

PROF. MERRILL BECKSTEAD
AND
PROF. ALON GANY

Testing of Metal Powders Behavior in a Hot Stage Microscope

A. V. Rosenband, A. Gany

Faculty of Aerospace Engineering, Technion- Israel Institute of Technology

Technion City, 32000 Haifa, Israel

Tel: +972-4-8293492

Fax: +972-4-8231848

E-mail: aervaro@aerodyne.technion.ac.il

Metal powders are used as fuel components in solid propellants because of their high density and high heat release when burned. Some metal powders such as aluminum, boron, titanium, titanium hydride, as well as their mixtures, can be considered as candidate additives to solid rocket propellants. This work has investigated experimentally the microscopic behavior of powders of these metals subjected to heating in inert and oxidative atmospheres. A windowed heated cell with direct access to microscopic observation has been used for this study. Summary of measured ignition temperatures T_{ign} of the investigated metal powders in air is presented in the Table.

Metal powder	$T_{ign}, {}^0C$	Metal powder	$T_{ign}, {}^0C$
Ti	840	Ti/2B	853
TiH_2	830	$TiH_2/2B$	829
B	870	$TiH_2/Al(50/50)$	852
Al	-	$TiH_2/Al(20/80)$	977

Particular attention has been given to the study of aluminum particles behavior because of their widespread use in rocket propellant formulations. It was observed that aluminum particles brought into close contact and maintained under appropriate heating conditions can agglomerate. Agglomeration appears as liquid bridges resulting from molten metal flowing through cracks in the metal oxide layer surrounding each particle, and even as the coalescence of particles into larger size liquid drops. The experiments revealed the following characteristics:

1. In inert atmosphere, aluminum particle agglomeration did not depend on the initial particle sizes and always took place at temperatures somewhat above the melting point of aluminum.

2. Formation of large droplets was observed during fast cooling of aluminum particles preliminary heated to temperature of 1200^0C.

3. The agglomeration process in air seemed to depend on the initial size of aluminum particles. The smaller the particles size, the easier the agglomeration.

4. In oxidative atmosphere, the agglomeration temperature was lower than in inert gas. The higher the oxygen content in the atmosphere, the lower the agglomeration temperature.

5. Agglomeration in air depended on the thickness of initial oxide film around the aluminum particles. Preliminary oxidation of aluminum particles resulted in a noticeable increase of agglomeration temperature.

6. Dilution of aluminum particles by a small amount of finely dispersed particles of another component, for instance, titanium hydride, seemed to prevent agglomeration phenomena.

7. Mixtures of Ti/2B and TiH$_2$/2B did not reveal exothermic reaction when heated in argon up to 1200^{0}C.

Flame Spreading and Violent Energy Release (VER) Processes of Aluminum Tubing in LOX/GOX Environments

M.M. Mench, K.K. Kuo, J.H. Sturges
140 Research Building East
The Pennsylvania State University
University Park, PA, 16802
Tel: (814) 863-6270, Fax: (814) 863-3203
E-mail: mmm124@psu.edu

P. Houghton, J.G. Hansel
Air Products and Chemicals, Inc.
7201 Hamilton Boulevard
Allentown, PA 18195-1501

The unintentional combustion of aluminum heat exchange equipment used in liquid oxygen (LOX) service is an important safety issue. In this study, the promoted ignition, flame spreading, and combustion phenomena of aluminum tubing filled with LOX, surrounded by a shell of gaseous oxygen (GOX), were systematically observed and recorded with over seventy promoted combustion tests. The aluminum 3003 tube samples used were 30.48 cm long and 3.175 mm outer diameter. Two different thicknesses (0.254 and 0.356 mm) of the aluminum tube sample wall were used for comparison testing. Figure 1 shows a schematic of the test chamber and an aluminum tube sample with a pyrotechnic igniter that were used for the experimental testing. Parameters studied and discussed in this paper include the tube- and shell-side pressures, LOX and GOX purities, tube sample wall thickness, and the effect of sample igniter location are discussed. Results from high-speed movie films indicate that under certain operating conditions, a transition from a "normal" (much slower) burning mode to an extremely rapid and violent burning mode occurs. The "Violent Energy Release," or VER burning mode, is characterized by extremely high flame spreading rates (1-2 orders of magnitude higher than the flame propagation rate in a purely GOX environment), a high luminosity flame zone, and a very rapid rate of heat release. Figure 2 shows two consecutive frames of high-speed film approximately 0.3 milliseconds apart in time. The rapid onset of transition to VER and the striking transformation between normal and VER burning modes can be clearly seen. Continued insight into the controlling mechanisms of the VER reaction has been obtained, and a physical description of the transition mechanism is presented. It is believed that the onset of transition to VER is triggered by a high rate of convective mass flux of oxygen to the reaction zone, caused by the density change from liquid to gas phase of oxygen. The high tube-side oxygen flow velocity lowers the diffusion resistance of oxygen to the reaction zone and atomizes the molten aluminum near the reaction region, removing oxide accumulations and exposing fresh aluminum to direct chemical attack. This process results in greatly enhanced homogeneous and heterogeneous reaction rates.
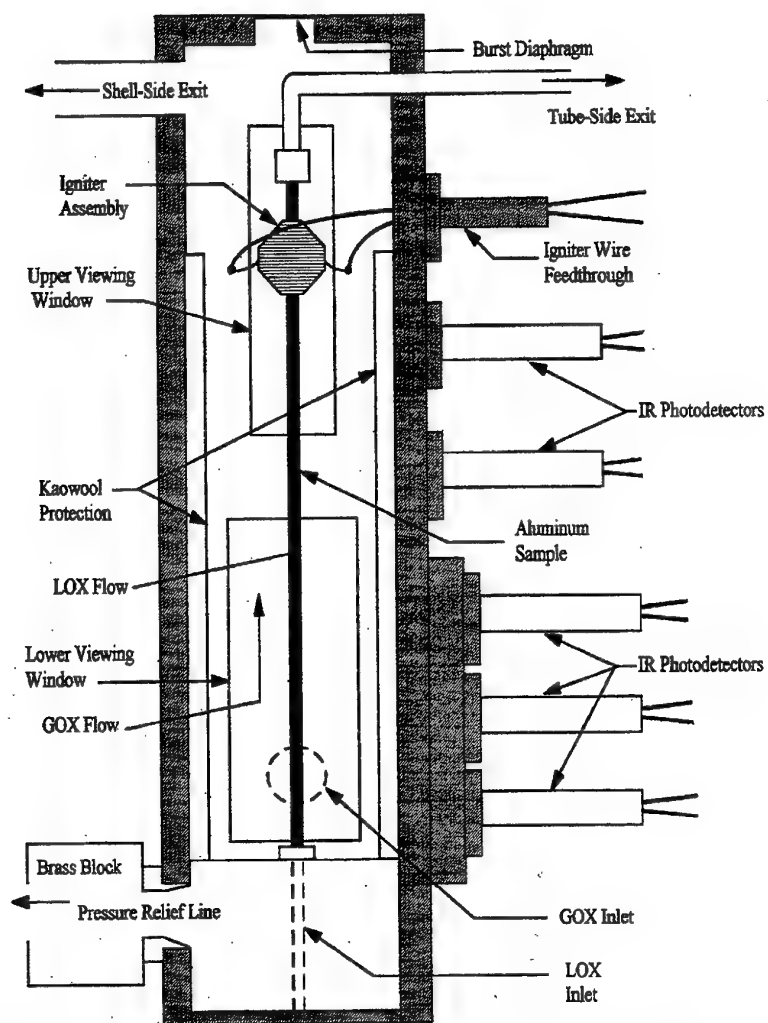
Fig. 1 Schematic of the Aluminum Tube Sample Used for Al/LOX Combustion Tests
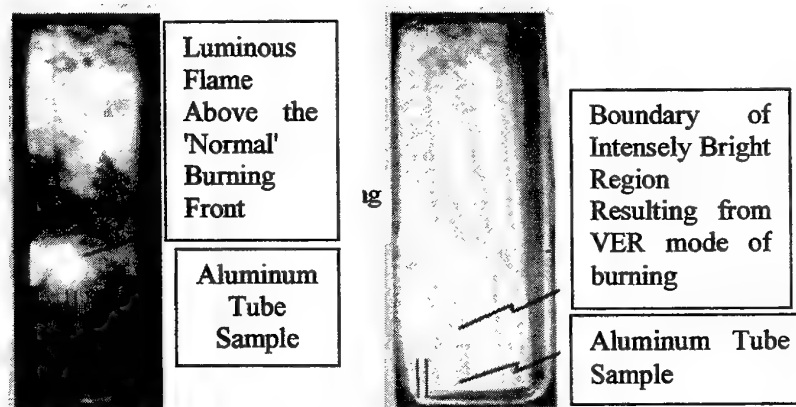

Fig 2 Consecutive Frames of HYCAM Film Immediately Before and After Transition to VER

Initiation and Combustion of Al/NH₄ClO₄/Viton Ignition Mixture

L. Kalontarov, Y. Borkowski
Rocket Systems Division, Israel Military Industries (IMI) Ltd., P.O.B. 1044/66
Ramat Hasharon 47100 Israel
Tel: 972-8-9277270
Fax: 972-8-9277620
E-mail: kalontar@bezeqint.net

Thermal decomposition, ignition, and combustion of Al/NH$_4$ClO$_4$/Viton (39/56/5 weight percent ratios) have been studied by means of thermal gravimetry (TG), differential thermal analysis (DTA) and firing in double bomb. It was found that the decomposition process strongly depends on the heating rate. At low heating rates (less than 120°C/min), the TG curve shows two fields of the weight loss centered at $T_1 \cong 316$°C and $T_2 \cong 374$°C. Above approximately 385°C there was no indication of weight loss, leveling of at 39 % - the exact weight percent of the aluminum in the mixture. DTA thermogram of the composition shows two exotherms approximately at the same temperatures as the above weight losses and two endotherms near 240°C and 660°C. The second endotherm is caused by the aluminum melting. Thus both TG and DTA show that the aluminum does not take part in the mixture decomposition at low heating rates, i.e. the mixture under these conditions does not ignite. The TG and DTA curves for the pure AP have insignificant deviations from the mixture curves. The change of the heating rate (e.g. from 2°C/min to 6°C/min) strongly influences the TG curves. The mixture starts to decompose at lower temperatures than the pure AP. This means that the processes of the weight losses for mixture and pure AP are kinetically different indicative the AP-Viton interactions in the course of the mixture decomposition.

At high heating rates (more than 120°C/min), the TG curve undergoes major changes. Instead of two relatively slow fields of weight loss, there is a very sharp weight loss followed by a bright flash. This indicates the ignition of the mixture. It can be seen that there is a threshold heating rate between non-ignition and ignition. Also, the threshold heating rate depends on the sample mass, tending to decrease as the mass increases. These phenomena have been analyzed in terms of thermal explosion theory. The critical condition for the ignition is fulfilled easier for increased sample mass (i.e. sample size) because of the heat loss decrease. The ignition dependence on the heating rate is more complex. It reflects the complexity and variety of physico-chemical processes taking place in the mixture upon heating. In a pyrotechnic mixture there are a number of reaction pathways and the ignition is only one of them. The dominant pathway is defined by the reaction rate at a given temperature and consequently it depends on the heating rate.

The combustion of the mixture has been studied in double bomb. The double bomb consisted of two chambers (small and large) separated by thin aluminum disk. The different quantities of the mixture charge were initiated in the small chamber and the pressure history was measured in both of them. The experimental peak pressure was compared with theoretical one calculated by ICT Thermodynamic Code. It was found that the dependence of the rate of the pressure increase in the small chamber on the loading density is strongly nonlinear. This

means that there is change of the combustion mechanism probably from conductive to convective burning.

Evolution and Motion of Aluminum Agglomerates in Combustion Products of Model Solid Propellant

O.G. Glotov, V.V. Karasev, V.E. Zarko
Institute of Chemical Kinetics and Combustion
Russian Academy of Sciences
Novosibirsk 630090, Russia
Tel: 7-3832-332292
Fax: 7-3832-342350
E-mail: zarko@ns.kinetics.nsc.ru

T.D. Fedotova
Novosibirsk State University
Novosibirsk 630090, Russia

M.W. Beckstead
Brigham Young University
Provo, Utah 84602, USA

A new approach for studying model of agglomerate evolution has been elaborated. The approach is based on the use of "super heterogeneous" propellants that generate model agglomerates with given size and structure. A "Super heterogeneous" propellant consists of a non-metalized, homogenized matrix filled with a finite number of small metalized insertions. Each insertion converts into an agglomerate in the combustion wave. Uniformity of size and metal content of model agglomerates allows a better treatment of experimental data obtained via sampling techniques. Important features of the approach is that the model agglomerates burn in the flow of combustion products of known composition and velocity field. It is advantageous in comparison with the case of real propellants where the combustion is characterized by a great variety of agglomerate sizes and a less specified velocity field. In the present work, the aluminum content in the inclusions was 42.6 % (that roughly corresponds to the aluminum content in "pocket" volume for real propellant) and the size of the sampled agglomerates was 400-540 μm.

The visualization experiments were performed at atmospheric pressure in order to evaluate the drag coefficient for burning model agglomerates. Natural-luminosity images and trajectory points of burning particles moving in combustion products of non-metalized propellant were obtained using a gated CCD computer camera in conjunction with a chopper wheel. Rotation speed and slot arrangement of the chopper wheel were chosen to expose the CCD camera to the flame at intervals of 3 ms for a duration of 0.5 ms. The treatment of trajectories permitted obtaining the drag resistance coefficient as a function of Reynolds number, Re. For Re values in the range 7-9 the value of K in the expression $C_d=K/Re$, is $K= 45\pm7$.

The experiments on investigation of macro kinetics of the model agglomerates combustion were carried out in the pressure range 1-80 atm. The correlation for aluminum combustion efficiency has been obtained in the form: $\eta = 2.86 \cdot t^{0.28} \cdot P^{-0.20}$, where $\eta = m_{Al} / m_{Al}^0$ - incompleteness of aluminum combustion (in our experiments $\eta = 0.3-0.7$); m_{Al} – mass of unburnt aluminum in sampled agglomerate, m_{Al}^0 – initial mass of aluminum in agglomerate; t

– residence time for agglomerate in flame of super heterogeneous propellant (20 ms $<t<$90 ms), P – pressure (10 atm$<P<$70 atm).

In addition, it was found that the mass fraction of oxide accumulated on the burning agglomerate and increased with aluminum conversion extent. This is described by $\varphi=0.54+0.21\cdot\xi$, where $\varphi = m_{ox}^{ag} / m_{ox}^{exp}$ – mass fraction of oxide accumulated on agglomerate; m_{ox}^{ag} – mass of oxide in sampled agglomerate; m_{ox}^{exp} – expected by calculation mass of oxide forming in course of combustion of aluminum; $\xi = 1-\eta$ - completeness of aluminum combustion.

Due to oxide accumulation the agglomerate mass monotonously increases with completeness of aluminum combustion ξ (or with time): $m/m_0 = 0.46+0.18\cdot\xi$, where m is the mass of sampled agglomerate, m_0 is the initial mass of the inclusion before burning. Note that the agglomerate starts its evolution in the flame from the effective initial mass $m = 0.46\cdot m_0$ that is close to the mass of aluminum in the insertion ($m_{Al}^0 = 0.426\cdot m_0$).

Thus, the approach proposed allowed us to obtain valuable information on agglomerate motion and evolution that can be useful in analysis of data on real polydispersed agglomerate populations. The work should be continued with various propellant formulations and different sizes of agglomerates.

Experimental Observations on Disruptive Burning of Coated Aluminum Particles

L. Wang, H. Liu, M.Liu
College of Astronautics, Northwestern Polytechnical University
127 Youyi Rd W. Xi'an 710072, China
Tel: 86-29-8493406
Fax: 86-29-8491000
E-mail: wliang@nwpu.edu.cn

N. Wang
Xi an Modern Chemistry Research Institute
Xi an 710065, China

To fully liberate energy of Al particles on the order of milliseconds during the operating process of a solid rocket motor, an idea that combustion is intensified with the aid of disruptive burning mechanism is tried. For this reason, let surfaces of Al particles within the composite propellant be coated with a surfactant (OP) of high molecular weight. In the combustion process the surfactant forms an impermeable shell, so that Al particles are rapidly and completely burnt out by means of disruptive burning. CO_2 laser ignition and T-burner experiments demonstrate tentatively the feasibility of the idea. The results of experimental observations are as follows.

1. The laser ignition experiments
(a) From the records of a high-speed video camera we can see that after laser irradiation the particles collapsed by the samples with coated Al particles spread toward all directions. This phenomenon shows disruptive burning process of microexplosion type occurs indeed instead of dispersing of accumulated Al particles. But for pure Al particles there is no phenomenon of disruptive burning.
(b) At the same time radiation signal histories of different samples of particles are measured by means of monochrometer (=514.5nm)-photomultiplier-high speed Fourier transform analytical system. Curves measured indicate the radiation peak value Y (reflecting reaction temperature) of coated Al samples is 80.88mv, and the period x (reflecting ignition delay behavior) reaching the peak value is 0.1875s. Whereas corresponding values of pure Al particles are respectively Y=10.55mv and x=4.1562s.
(c) In addition, after laser ignition experimental samples are diagnosed by use of a scan electron microscope. Regardless of ignition or non-ignition surfaces, from a complete picture of the SEM photo the coated Al particle sample burns more violent than the pure Al particle sample. And as viewed from the local sample, residue size of coated Al particles are much less than those of pure Al particles.

2. The T-burner tests
(a) CMDB propellants in disk form, which have the same basic formulation and size, are tested at a T-burner. One propellant is made of pure Al particles. Another contains coated Al particles. Test results show that if the propellant with coated Al particles is used, residue quantity left on the tube wall of the combustion chamber notably decreases.
(b) The residues mentioned above are then measured by the aid of a malvern particle analyzer. The results indicate large particle (diameter>120 m) percentages of burning residues of the

propellant contained pure Al particles are greater than those of the propellant with coated Al particles.

Experimental Study of Evolution of Condensed Combustion Products in Gas Phase of Burning Solid Rocket Propellant

V.A. Babuk, V.A. Vasilyev, P.A. Naslednikov
Baltic State Technical University
1, First Krasnoarmeyskaya Street, Saint Petersburg, 198005 Russia
Tel: (7-812)-2591138
Fax: (7-812)-3162409
babuk@peterlink.ru

In two-phase flow of solid rocket propellant (SRP) combustion products, condensed combustion products (CCP) suffer a set of physical and chemical transformations, which constitute the CCP evolution process. Process of CCP formation in surface layer of burning propellant and the CCP evolution in gas phase define efficiency of the metal fuel as a component of SRP. The objective of this paper is experimental study of the CCP evolution in the gas phase of burning SRP.

At present time, experimental information about the CCP evolution in gas phase is limited and, sometimes, contradictory. The following statements are considered to be generally accepted.

CCP consist of two main fractions: agglomerates (sizes of the agglomerates may reach hundreds and even thousands of micrometers) and particles of highly dispersed oxide (HDO) of the order of 1 micrometer in diameter.

In two-phase flow, interactions between the gas and condensed phases and interactions between the CCP fractions are possible. These interactions lead to change in properties of the flow.

The investigation method used in this work is as follows. Samples of SRP are burnt in constant volume bomb or constant pressure bomb in the media of inert gas. The main "tool" for obtaining of quantitative information is quench-collection of CCP at various stages of the evolution. All the totality of the CCP particles quenched are collected and then subjected to detailed analysis including determination of the sizes, chemical composition, and structure of the CCP particles. Mass representativeness of the CCP collection is not less than 95%. To obtain information of qualitative character about burning zone, high speed filming is used.

The study involves aluminized SPR on the basis of AP and ADN.

The investigation results are as follows.

HDO particles are solid and spherical. Agglomerates consist of metal and oxide. There may be bubbles in the agglomerates. Results of study of microsections of agglomerates showed that an agglomerate may be considered to be a system consisting of metal drop, oxide drop (oxide "cap"), and bubbles, and being in state close to equilibrium one.

During the CCP evolution, mass of metal in agglomerates is decreasing and mass of HDO particles is increasing monotonously. This behavior is caused by burning of agglomerate metal in gas-phase mode with formation of HDO particles. Burn rate of metal in agglomerate

changes in dependence on agglomerate properties and parameters of environment. For the evolution times studied in the experiments, dispersity of the agglomerates characterized by agglomerate size distribution changes weakly.

Interaction between burning agglomerate and external gas flow leads to formation of specific "tail" with agglomerate burning products, where condensation, leading to HDO particles formation, and coagulation of these particles take place. Parameters of the "tail" depend on parameters of burning agglomerate and characteristics of external flow blowing around the agglomerate. These parameters have influence on HDO particles coming from the "tail" into external flow.

In the evolution, quantity of oxide in agglomerates either remains the same or decreases. The latter (case of oxide removal from agglomerates) is connected with chemical interaction between aluminum and its oxide in agglomerates with formation of gaseous products. The oxide removal is promoted by pressure decrease, environment temperature increase, and decrease in content of oxide in agglomerate. As a result of the interaction between the metal and oxide in agglomerate, formation of bubbles with gaseous products of the reaction in agglomerate, and periodical change in agglomerate size are possible.

HDO particles may deposit from external gas flow on agglomerates. However, in the case when these particles deposit on the surface of metal, that took place in the experiments done, chemical interaction between aluminum drop and oxide particles, which deposited on it, takes place with formation of gaseous products.

HDO particles at the propellant burning surface are formed in combustion of metal particles, which do not take part in agglomeration. These HDO particles can grow during evolution. This opportunity depends on quantity and properties of agglomerates in a flow. Thus, at propellant burning surface, mass-medium diameter of these particles is, as a rule, in the range 0,4 - 0,6 micrometers for propellants used, and at the distance 70mm from the burning surface, this parameter can grow up to 0,6-1,0 micrometers.

Reliability of the data obtained is confirmed by rather big volume of experimental data and also by special investigations of methodical questions (influence of thermal stresses on characteristics of quench-collected particles, influence of coagulation of HDO particles during dispersity analysis on the results of the analysis, etc.).

The investigation results allow us to formulate physical concepts concerning the evolution of all the totality of CCP in two-phase flow and to create information basis for development of mathematical model for this process, providing possibility of prediction of two-phase flow parameters in rocket motor combustion chamber.

AREA 5:

COMBUSTION ANOMALIES OF ENERGETIC MATERIALS

SESSION CHAIR:

MR. THOMAS BOGGS

Convective Burning in Gaps of PBX 9501

H.L. Berghout, S.F. Son, and B.W Asay
Los Alamos National Laboratory
MS C920, DX-2
Los Alamos, NM 87545
Phone: (505)667-9620; Fax: (505)667-0500; Email: berghout@lanl.gov

Impact or thermal ignition of high explosives (HE), results in deformation that can lead to fracture. Fracture, combined with high pressure, dramatically increases the available surface area and potentially changes the mode of combustion. Recent impact and cookoff experiments on PBX 9501, (HMX, octahydro-1,3,5,7-tetranitro-1,3,5,7-tetrazocine, with a binder), have shown complex cracking patterns caused by impact or pressurization. Fast reactive waves have been observed to propagate through the cracks at about 500 m/s. We present experiments that investigate the propagation of fast reactive waves in cracks of PBX 9501, focusing on the reactive wave velocity and on the interplay of pressure and crack size. Experiments at initial pressures of 6.0 MPa reveal monotonic reactive wave propagation velocities around 7 m/s for a 100-μm slot. We observe reactive wave velocities as high as 100 m/s in experiments at initial pressures of 17.2 MPa and various slot widths. Similar experiments at lower pressure exhibit oscillatory reactive wave propagation in the slot with periodic oscillations whose frequencies vary with combustion vessel pressure. This is the first reported observation of oscillatory combustion in cracks of a high explosive material such as PBX 9501. Threshold pressure experiments for combustion propagation into closed-end slots of PBX 9501 find that combustion propagates into 2-mm, 1-mm, 100-μm, 50-μm, and 25-μm slots at approximately 0.1, 0.2, 0.9, 1.6, and 1.8 MPa, respectively. This is the first known study that focuses on the effect of convective burning in voids of PBX 9501.

THIS PAGE HAS BEEN DELIBERATELY LEFT BLANK

Investigation of Combustion Flow Field in Composite Propellant Cracks

Cai Timin Zhang Wenpu He Guoqiang
College of Astronautics, Northwestern Polytechnical University
Xian, China

The existence of cracks and its propagation in composite propellant grain exerts great influence on the performance and reliability of SRM. Significant research work on flame spreading and combustion in propellant cracks and on crack propagation has been done by K. K. Kuo, M. Kumar and C. T. Liu et al. since nineteen eighties. In this paper, two-dimensional combustion flow field in composite propellant cracks was studied by both theoretical calculation and experimental method to provide pressure distribution and flame spreading rate distribution in cracks for further study on crack propagation and its effect on SRM internal ballistics.

In the numerical calculation, finite element method was used to solve 2-D unsteady compressible Navier-Stokes equation system. For each element, linear function was adopt for pressure interpolation, and quadratic function for velocity interpolation. Mid point method was used to solve the discrete equations. During calculation, heat transfer and ignition criterion, erosive burning effect and crack deformation under the pressure loading were coupled. Numerical grid was adjusted by varying the location of boundary nodes to adapt variation of crack geometry. The entire combustion flow process in the crack was calculated from the beginning of ignition by hot gas flow up to the moment that all burning surface has been ignited.

In the experimental study, a crack combustion simulator with transparent window was designed and developed. Two propellant samples inside the simulator constitute a crack, the width and length of crack can be regulated by spacers. Combustion chamber pressure was controlled by a nozzle, and pressurization rate was mainly controlled by the quantity of ignition charge. Pressures in the propellant crack and combustion simulator were measured by pressure transducers and data acquisition system. The state of combustion and flame spreading rate inside the propellant crack were photo-taken and recorded by a high speed motion analyzer. The combustion flow field in the crack of composite propellant was calculated and measured for different width of crack and different pressurization rate. Results of calculation and experiment show good agreement, see Fig. 1, and the following conclusions were obtained:

1. The flame spreading rate in crack increases with increasing of pressurization rate, and increases with decreasing of crack width, see Fig. 2; The pressure at crack tip also increases with increasing of pressurization rate, and increases with decreasing of crack width, see Fig. 3.

2. The relationship between flame front position and ignition time can be depicted with good accuracy by a cubic polynomial, flame spreading rate always becomes maximum near the middle position of crack. The value of flame spreading rate in the crack is about one to three orders higher than that in combustion chamber of SRM. See Fig. 2.

3. In the process of combustion flow in crack, there is a certain moment at which gas starts to flow in two contrary directions, see Fig. 4. In this example, when t=1.5ms, at X/L>0.4, flow towards crack tip; X/L<0.4, flow towards crack inlet.
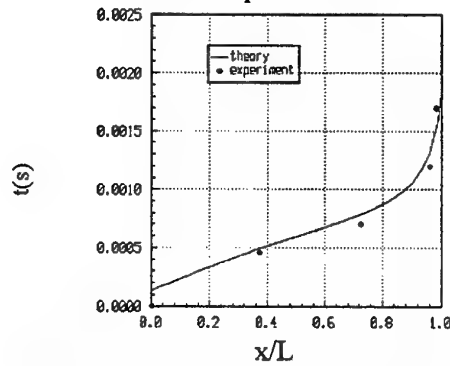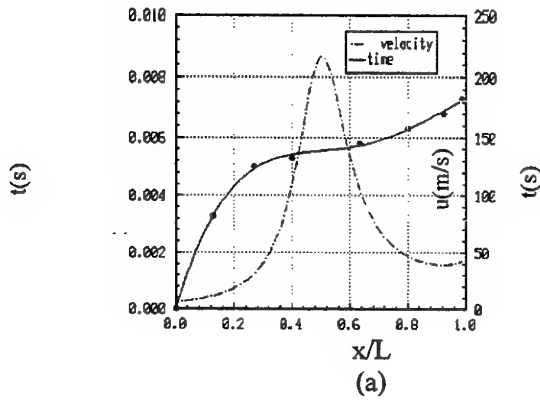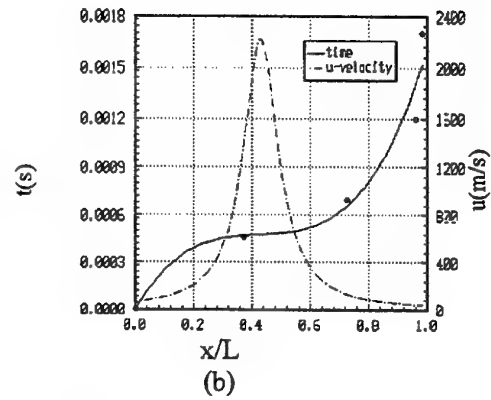
dp/dt=0.5Gpa/s,L=210mm,b=4.0mm
Propellant B

Fig.1 Flame front position variation with the time

L=200mm,b=4mm, dp/dt=500MPa/s

L=200mm,b=3.6mm,dp/dt=200MPa/s

(a)

(b)

dp/dt=130MPa/s

L=200mm,b=2.5mm

L=200mm,b=5mm

(c)

(d)
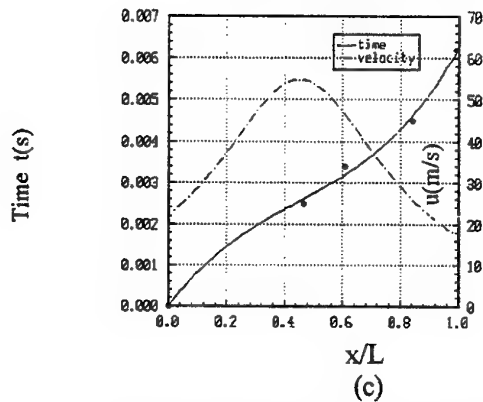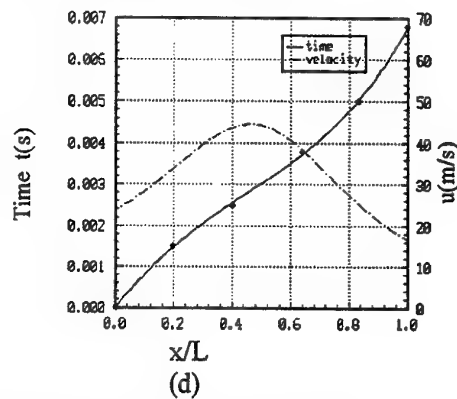
Fig.2 Flame front position variation with the time (by experiment)

106
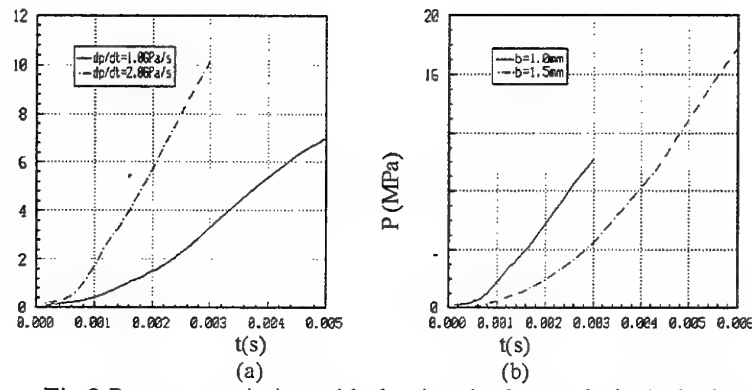
Fig.3 Pressure variation with the time in the crack tip (calculated)
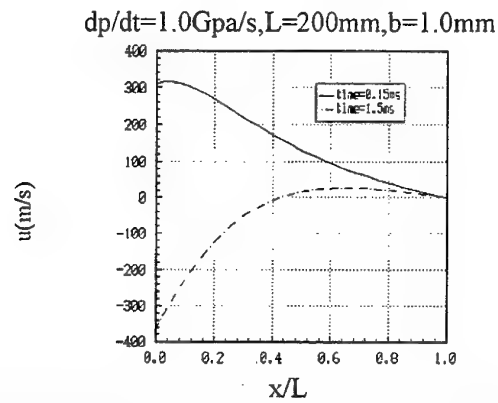
dp/dt=1.0Gpa/s,L=200mm,b=1.0mm

Fig.4 Longitudinal velocity distribution along crack length at various times (calculated)

THIS PAGE HAS BEEN DELIBERATELY LEFT BLANK

Research on Convective Burning and Propagation Mode in Solid Propellant Grain Cracks

L. Du
The 4st Research Academy of CASC
Xi'an, P.R.China, 710025

G. He, T. Cai, P. Liu
College of Astronautics
Northwestern Polytechnical University
127 Youyi Road W. Xi'an, P.R.China,710072)
Tel: 086-29-8493646; Fax: 086-29-8491000
E-mail: gqhe@nwpu.edu.cn

Crack on solid-propellant grain surface can significantly affect the ballistic performance of a solid rocket motor, even cause catastrophic failure. Propagating mechanism and anomalous combustion in solid propellant grain cracks were studied. This paper presents the experimental research results from some recent test motor firings, the numerical analysis results of convective burning flow field in defect cavity, and the Squeezing Propagation Mode (SPM) of a single surface crack in burning solid propellants.

A real-time X-ray radiography system was used to obtain the pictures of destruction process of grain structural during static firing. Several defect propagation modes of solid propellant and its structural destruction conditions were put forward for different cracks and operating conditions. The serious coupling phenomena between ignition and combustion in a crack and grain structure were described. The propagation tendency at the flaw leading-edge and the propagation critical conditions were studied in detail. The results provide some experimental bases and study ways of evaluating combustion safety of solid propellant grain with defects. Some conclusions in the paper were applied to fault diagnosis of some full-scale motor firing test.

In the experimental work for crack propagation, test samples were rapidly pressurized in a combustion environment. The effects of pressurization rate and boundary condition on the development of crack propagation under various operating conditions were studied. Some typical images of crack propagation process were shown in Fig.1 to Fig.3. Chamber pressurization rates were varied from 0.5 to 15.0 GPa/s. Three different kinds of boundary condition were investigated. For different pressurization rates, Squeezing Propagation Mode was observed.

Fig.1 The combustion images of HTPB propellant with crack

Fig.2: The propagation images of HTPB propellant with crack on combustion surface

Fig.3: The propagation images of NEPE propellant with crack in round sample

A numerical analysis was performed to study convective burning flow field in solid propellant crack. The implicit TVD scheme was used to solve the 2-D Navier-Stokes equation with gas injection and erosive burning. The pressure distribution inside the crack was obtained and the relation between the length and depth of crack and the pressure in crack tip was also discussed (see Fig.4 to Fig.5).
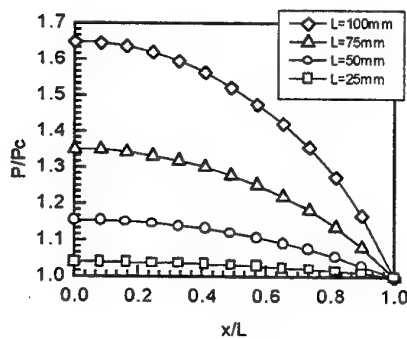

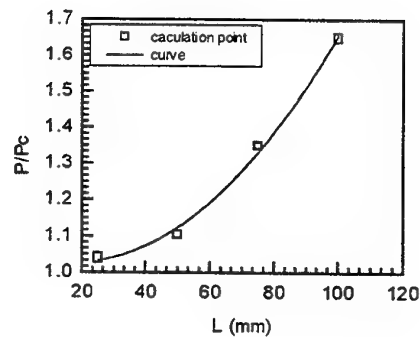Fig.4: Pressure distribution along crack axis with different crack length

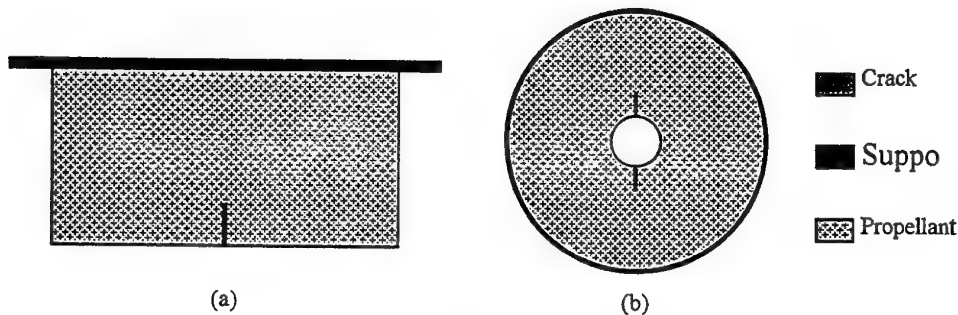Fig.5: Relation between the pressure in tip and the crack length

Fig6: Experimental Grain

110

Associated with the characteristic of stress distribution in the high-loaded solid propellant grain under burning condition, two types of crack on its cavity surface, the transverse surface crack (see Fig.6.a) and the longitudinal surface crack (see Fig.6.b), were taken into account.

Respectively, one brick-shaped experimental grain and the other disc-shaped one are employed for simulating above two types of crack. Through numerical approach by FEM, the Squeezing Propagation Mode (SPM) was concluded to be rational for describing single surface crack propagation of combusting grain (see fig.7). In detail, this model is denoted by an empirical formula, which illustrates the effects on transverse tearing stress of the surface crack tip due to three factors, such as pressure of combusting gases on main burning surface, pressure of gases in the gap of surface crack, and deepness of surface crack. According to this model, the longitudinal surface crack was found easier to propagate than the transverse surface crack.
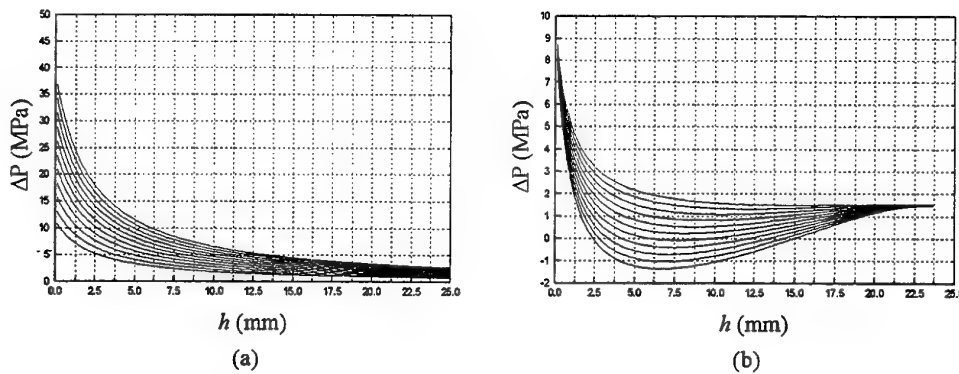
Fig.7 Pressure Difference Needed to Lift up the Transverse Tearing
Stress σ_{cx} to a Given Level 4MPa versus Crack Depth

(a) Case: Associated with brick-shaped experimental grain, and P_B is varied from 1, 2, 3, 4, 5, 6, 7, 8, 9, to 10MPa with respect to these ten curves in the figure from bottom to top.
(b) Case: Associated with disc-shaped experimental grain, and P_B is varied from 1, 2, 3, 4, 5, 6, 7, 8, 9, to10MPa with respect to these ten curves in the figure from top to bottom.

THIS PAGE HAS BEEN DELIBERATELY LEFT BLANK

AREA 5:

COMBUSTION ANOMALIES OF ENERGETIC MATERIALS

SESSION CO-CHAIRS:

DR R.H. WOODWARD WAESCHE
AND
DR. GUY LENGELLÉ

Experimental Investigation of Erosive Burning of Composite Propellants Under Supersonic Cross Flow Velocity

S. Krishnan[*], K.K. Rajesh[†]
Department of Aerospace Engineering
Indian Institute of Technology Madras, Chennai-600 036, India
Tel: 91 44 4458154
Fax: 91 44 2350509 or 2352545
skrish@aero.iitm.ernet.in

The realised erosive burning test facility is shown in Fig. 1. It comprises of a gas generator, a transition duct, and a test chamber. A high pressure and high velocity cross flow of combustion products parallel to the burning propellant surface, needed to simulate actual rocket conditions, is provided by the gas generator by burning an eight pointed neutral star grain. A pyrotechnic igniter is used to ignite the gas generator and is threaded on to the head end plate of the gas generator. The hot combustion products from the gas generator are directed to the test chamber through the transition duct. The transition duct has a circular cross section at entry and a rectangular cross section at the exit and gives two-dimensional flow into the test chamber. The test chamber has in it chamber block, bleed nozzle assembly, test channel, and end nozzle assembly, Fig. 1.
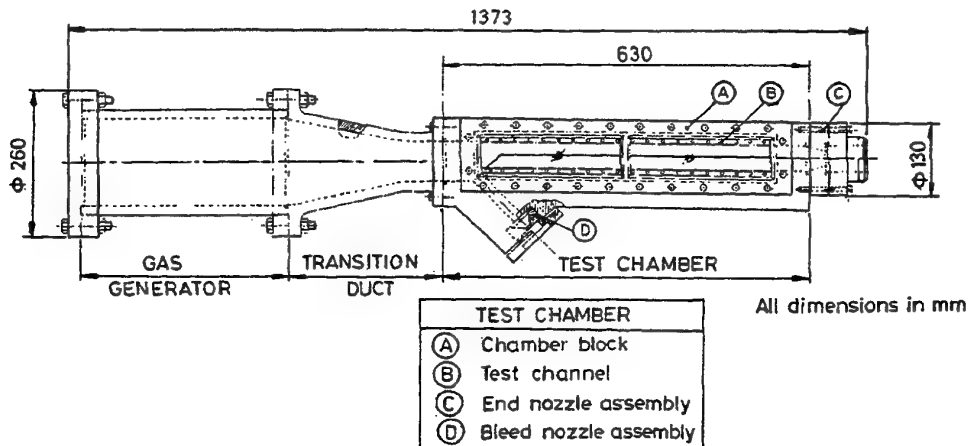

TEST CHAMBER	
Ⓐ	Chamber block
Ⓑ	Test channel
Ⓒ	End nozzle assembly
Ⓓ	Bleed nozzle assembly

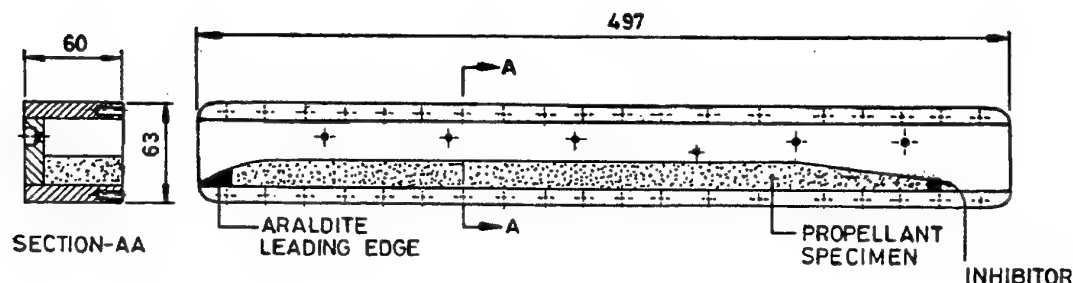Fig. 1   Erosive burning test rig assembly.

Fig. 2   Erosive burning test channel in nozzleless mode.

With a suitable nozzle in the bleed nozzle assembly a small amount of combustion products from gas generator is bled off. The chamber block, a heavy stainless steel casting, can accommodate interchangeable two-dimensional test channels as shown in Fig. 2. To the bottom plate of the test channel a specimen propellant is stuck using an epoxy resin. A tapered leading edge cast out of epoxy is glued to the front portion of the specimen propellant. The bleed flow and the leading edge ensure a smooth development of boundary layer from the beginning of the specimen propellant.

The test rig can be used for the measurement of erosive burning purely under subsonic cross flow condition by having a suitable nozzle in the end nozzle assembly. Under this *nozzled mode* the test channel has a specimen propellant of constant thickness and experiences subsonic cross flow. Under the *nozzleless mode*, the end nozzle assembly is not fitted. The specimen propellant has a constant thickness up to the geometric throat, which is 366 mm away from the leading edge. The supersonic portion has a length of 81mm with a suitable angle of expansion, Fig. 2. Thus the flow changes from subsonic to supersonic cross flow over the specimen propellant. This enables the measurement of erosive burning either under sonic as well as supersonic cross flow Mach number.

The burning of the propellant specimen either under nozzled mode or nozzleless mode is viewed through a window assembly made out of polymethylmethacrylate and the burning rate is measured by a high speed motion picture camera at various pressures and cross flow Mach numbers.

The details of the experimental observations under nozzleless mode of operation for three different composite-propellant formulations with significantly varying normal burning rates [5 mm/s at 5MPa (specimen propellant formulation I), 9 mm/s at 5MPa (specimen propellant formulation II), and 16mm/s at 5MPa (specimen propellant formulation III)] are discussed. From the obtained experimental results typical choked flow conditions that can occur in nozzleless motors are explained. *The choking station movement in a nozzleless mode of operation is experimentally demonstrated.*

The erosive burning data of this study generated under supersonic cross flow Mach numbers up to 1.6 are the first in open domain.
The obtained erosive burning rate data of the propellants under transonic and supersonic cross flow Mach numbers show similar trends as in the case of subsonic cross flow Mach numbers. The erosive burning under supersonic conditions also increases with increase in pressure and

114

supersonic cross flow velocity. Also a slow burning propellant is more sensitive to erosive burning than a fast burning propellant even under transonic and supersonic cross flow Mach numbers. Under low pressures (< 0.3 MPa) the burning rate falls below the normal burning rate even under supersonic cross flow Mach numbers, thus exhibiting the "supersonic negative erosion", Fig. 3. This supersonic negative erosion is significant for faster burning propellants and is argued to be due to the dominant mass transfer effect due to blowing into the boundary layer.
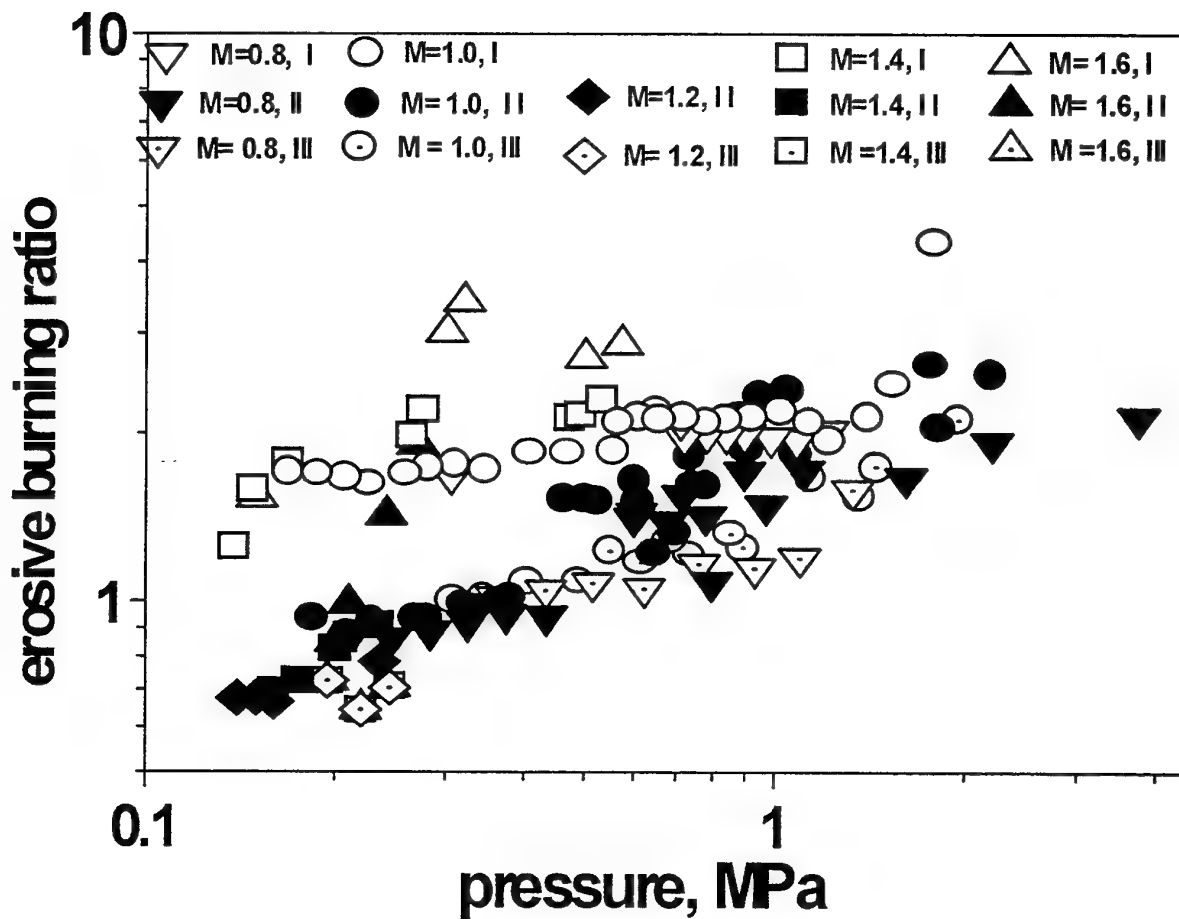

Fig. 3 Erosive burning ratio versus pressure at various cross flow Mach numbers (M = 0.8 to 1.6) of the three formulations (specimen propellant formulations I, II and III).

THIS PAGE HAS BEEN DELIBERATELY LEFT BLANK

Improvement of Flameholding Characteristics
by Incident Shock Waves in Supersonic Flow

T. Fuimori, M.Murayama and J. Sato
Research Institute, Ishikawajima-Harima Heavy Industries Co., Ltd.
Toyosu, Koto-ku, Tokyo 135-0061 JAPAN

H. Kobayashi, S. Hasegawa and T. Niioka
Institute of Fluid Science, Tohoku University
Katahira, Aoba-ku, Sendai 980- 8577 JAPAN
Tel: (81)22-217-5271
Fax: (81)22-217-5323
E-mail: niioka@ifs.tohoku.ae.jp

It is one of the major technological challenges for the development of the supersonic ramjet engine to achieve stable combustion while maintaining moderate pressure loss throughout the entire range of operating conditions. The flame stabilization becomes crucial under low total temperature conditions. Assuming that the scramjet engine starts at a flight Mach number of 4 and an altitude of 25000 m, and the inlet Mach number of the combustor is one-third of the flight Mach number, the inlet temperature is less than 800 K, and pressure in the combustor is about 1 atm. Then, the ignition distance of stoichiometric hydrogen-air mixture is a few meters and over the length of the combustor. This has been proven in both experimental and analytical studies. Some methods for stabilizing flame in supersonic flows have been investigated, including plasma torches, and pre-burning to reduce ignition time in low-temperature flow. Another method is to increase the residence time of gases in the recirculation flow generated by such as a strut base or a backward facing step.

The objective of this study is to investigate the effect of incident shock waves on flameholding behind a fuel injection strut in supersonic flow, and elucidate the structure of the flameholding region. A non-premixed hydrogen flame was established behind a fuel injection strut in Mach 2.5 supersonic airflows with total temperature between 400K and 900 K. The shock waves interacted with the wake behind the fuel injection strut, which improved the flameholding characteristics remarkably by enlarging the recirculation flow and enhancement of mixing. The incident position and the strength of the shock waves control the size of the recirculation flow and flameholding limit. As the strength increases, the upper limit of fuel flow rate for flameholding increases. As the incident points of the shock waves move downstream from the strut base, the upper limit decreases and finally the flame is not stabilized for any flow rate. Instantaneous OH distribution in the flameholding region was observed by laser induced fluorescence. The main reaction occurs near the base at the small fuel flow rate. As the flow rate increases, O-H distribution moves downstream and varies between the front and the middle section of the wake. On the other hand, homogeneous OH distribution is observed around the rear throat region of the wake until the blow-off. This suggests that the upper flameholding limit is largely determined by the stability of flame base in the throat region.
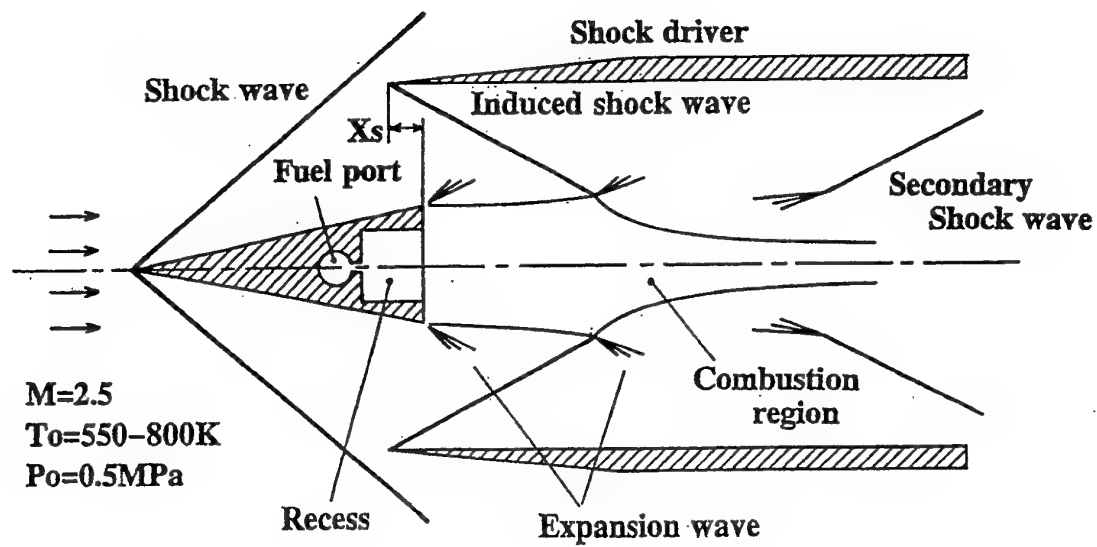
Schematic explanation of the wake combustion region into which Shock waves are introduced.

Analysis and Testing of Fuel Regression Rate Control in Solid Fuel Ramjets

D. Pelosi-Pinhas, A. Gany
Faculty of Aerospace Engineering, Technion - Israel Institute of Technology
Haifa 32000, ISRAEL
Tel: 972-4-8292554
Fax: 972-4-8230956
E-mail: gany@techunix.technion.ac.il

The solid fuel ramjet (SFRJ) is a simple air breathing engine. The combustion chamber contains a solid fuel grain, often of a hollow cylinder shape, where the air flows through the port. Because of their high specific impulse (3-4 times than that of solid rocket motors), SFRJ motors are particularly suitable for long range missile and projectile propulsion. However, the variable flight conditions over a wide operating envelope of altitudes and velocities significantly affect the motor performance. The fuel mass flow rate depends on the chemical and physical properties of the fuel, on the air mass flow rate through the port and on the geometry (mostly the length and the internal diameter) of the fuel grain. Consequently, once the fuel is successfully ignited, there is no way to control the combustion process. An increase in flight velocity and/or a decrease in flight altitude imply a decrease in the fuel/air ratio (and vice versa), causing significant losses in the motor performance and sometimes even total extinction of the flame.

The objective of this work is to investigate the possibility of controlling the solid fuel burning rate in ramjet motors and to determine the effectiveness of such a regulation over a wide range of flight conditions. The method is based on an air division valve, which divides the incoming airflow from the diffuser into two separate flows; a part of the air (the principal airflow) is drawn directly into the combustion chamber through the port of the solid fuel grain, while the other part (the bypass airflow) flows through a bypass to the aft-mixing end of the combustion chamber (see Fig.1).

A theoretical model has been developed, which takes into account the parameters that influence the burning rate of the solid fuel (air mass flow rate, port diameter), and characterizes a general regulation law for the air division valve, permitting, for instance, operation at a desirable fuel to air ratio, over a wide range of flight velocities and altitudes. The model is based on the dependence of the fuel gasification rate on the flow characteristics assuming diffusion flame and forced convection phenomena through the boundary layer. Initial theoretical predictions indicate that burning rate control over a wide range of operating conditions (as an example, climbing from sea level to 15 km with a constant fuel/air ratio) may be feasible through a control of the port to bypass airflow ratio.

An experimental demonstration of the regulation concept is needed in order to examine the theoretical approach. For this purpose an experimental facility has been designed and built. Two basic stages are in progress. The first phase includes some preliminary experiments that do not require the use of the bypass; a variation of the inlet air mass flow rate, the total temperature and the fuel port diameter will enable us to define fuel characteristics, mainly the fuel regression rate. After this first stage, the work can be completed by running the main experiments that will include the air division valve and bypass facilities. Finally, a

comparison between the predicted and the real results is expected, yielding clear conclusions on the feasibility and the effectiveness of the regulation concept.
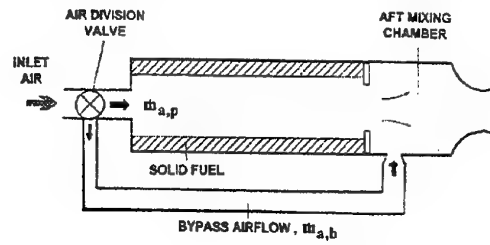

Figure 1. Schematic description of the combustion chamber showing the air-division valve concept.

Solid Propellants Convective Ignition and Flame Spreading

L. Galfetti, G. Colombo
Laboratorio di Termofisica, Dipartimento di Energetica
Politecnico di Milano - Campus Bovisa, 20158 Milan, Italy
Tel: +39-02-2399-8526
Fax: +39-02-2399-8566
E-mail: galfetti@clausius.energ.polimi.it

Ignition and flame spreading mechanisms are essential for the control of the ignition transient in solid propellant rocket motors. The extensive experimental research of the last forty years allows a fairly good control of the overall ignition transient, but a deeper knowledge of the complex phenomena involved is needed, above all, to develop more accurate numerical modelling approaches.

This paper describes experimental measurements of solid propellants ignition transients, including the first flame onset and the following flame front propagation rate. A composite AP/HTPB propellant sample, rectangular shaped to assure a flat plate laboratory geometry, is ignited under the action of a non-reacting convective flux in air atmosphere at ambient pressure. Propellant is heated by a blower, which is provided with an adjustable 2-d nozzle to obtain different temperature and velocity distribution. Heat flux is measured along the sample length by means of a microcalorimeter, made of a copper disk to which a microthermocouple is soldered. Ignition delay times are measured using three different approaches: a video-recording, an acoustic technique and the surface temperature measurement. A photodiode signal is always recorded in all tests. The first approach is based on the use of a Xybion video-camera, of a U-Matic Sony video-recorder, a FOR-A timer and a reference scale. The second one relates to the power spectral density of the acoustic signal, measured by an omnidirectional microphone, coming from the onset of the propellant combustion. The power spectral density vs frequency and vs time is plotted in a spectrogram, which allows to check the time of beginning and the following develo pment of the combustion process. In this last approach, the ignition delay time is evaluated from the slope change of the surface temperature profile due to the first flame appearance. Results obtained, using these techniques, are presented for three different temperature and velocity distributions along the propellant sample; a critical discussion of these techniques is also offered.

The same techniques are used to measure the flame spreading along the propellant surface. Flame spreading is evaluated both with and without the presence the hot air flow responsible for ignition; the obtained results are critically compared.

Conclusions stress the advantages of the acoustic technique to measure ignition delay times and flame spreading phenomena, the results of the ignition delay time in the range of low heating fluxes and the role of the hot jet in sustaining the flame propagation.

THIS PAGE HAS BEEN DELIBERATELY LEFT BLANK

ABSTRACTS OF PAPERS
TO BE PRESENTED IN

ROOM AZALEA

AREA 7:

PYROLYSIS AND COMBUSTION PROCESSES OF NEW INGREDIENTS AND APPLICATIONS

SESSION CO-CHAIRS:

DR. JUDAH GOLDWASSER
AND
PROF. AKIRA IWAMA

Energetic Material Combustion Studies on Propellant Formulations and its Components

A.L. Ramaswamy
Dept. of Electrical Engineering
University of Maryland, College Park, MD 20742
Tel. (301) 405 3671
Fax. (301) 314 9281
albalal@eng.umd.edu

Energetic material combustion studies on propellant formulations and its components as well as other/ future candidate energetic material components such as AP, HMX, RDX, TNAZ, NTO and CL-20 have been performed. The propellant formulations examined contained ADN as the oxidizer (in single crystal and "prill"/ spherical form). The overall performance of the formulation was found to be sensitive to the microstructure of its oxidizer component and can be improved by "tailoring" the microstructural characteristics of the oxidizer components as well as the formulation itself. In fact combustion experiments where the ignition of the propellant is filmed at the highest magnifications inside an ESEM (Environmental Scanning Electron Microscope) show that "hick-ups" or "micro-explosions" of the formulation components are providing local increases in the burn rate which affect the overall performance. Such localized events may form a contribution to the observed instabilities.

The nature of the "micro-explosions" can be understood when the initiation of energetic materials is studied at a fundamental level. This has been performed for single crystals of AP, ADN, HMX, RDX, TNAZ, NTO and CL-20. It is known from the early work of Bowden and Yoffe in the 1940's that in energetic materials an input energy, irrespective of its original form i.e. impact, friction, shock etc. is degraded into heat and concentrated in small regions or "hot spots". Thermal ignition of the energetic material then occurs at the "hot spot". Different physical mechanisms were identified for the degradation/ concentration of the input energy to form a "hot spot".

Evidence has now been obtained for the fact that initiation infact starts at a "reaction site" which is smaller than the critical "hot spot" size. "Reaction sites" form in high densities on crystal facets, expand and coalesce to form the critical "hot spot" site for self-supporting propagation of the reaction. Microscopy studies of "reaction sites" in all the above-mentioned energetic materials has revealed that the sites show a crystallographic shape or structure, but that the shapes and structures vary according to the energetic material and the crystal habit on which they form. For example in AP 2.5 million "reaction sites" were found in an area 1 mm in diameter! The precise position of the molecules in the crystal lattice appears to be controlling the initiation and also subsequent combustion. ESEM and AFM (Atomic Force Microscope) micrographs are included here respectively of ADN and AP crystals, showing the formation of "reaction sites". The latter micrograph (taken by Dr. J. Sharma) shows a single "reaction site" in AP at nm level/ scale!

Such phenomena are thus highly localized and start at the molecular level. The effects of component microstructure on the ignition of the same are being understood and modeled at a fundamental level. This is providing a valuable insight which can help in the manufacture of formulations which are microstructurally "tailored" to provide a more stable and efficient

burning. Collaborations with companies such as Thiokol has already shown/proven, that such microstructural variations can be implemented at the manufacturing level.
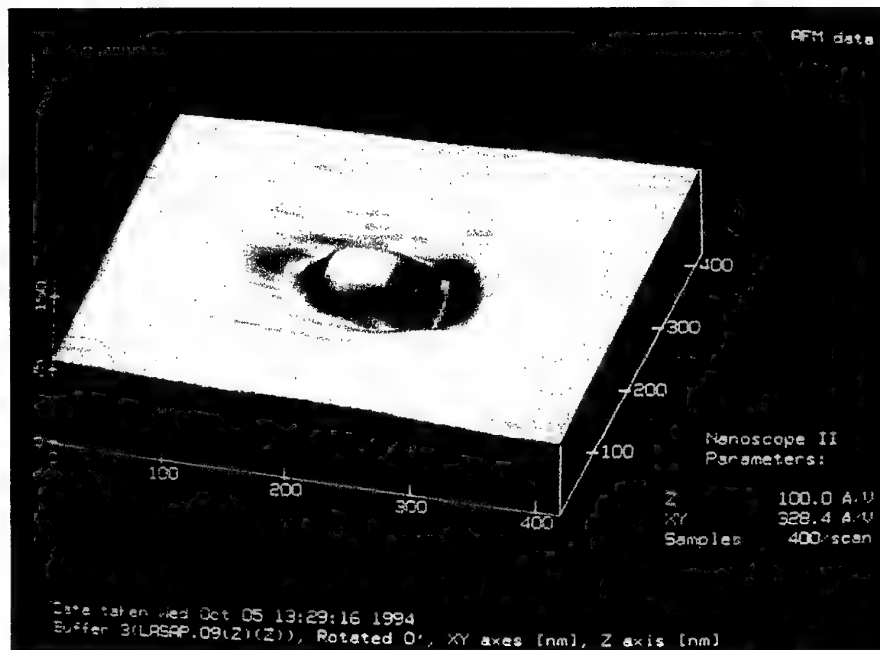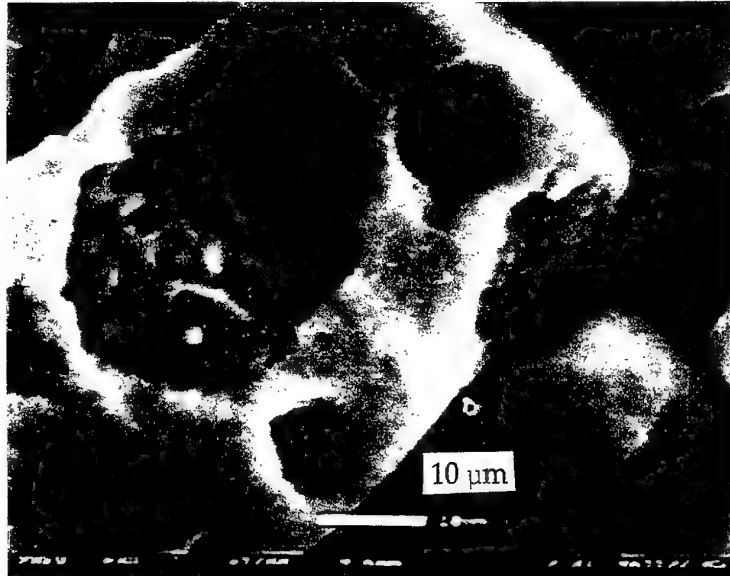
Burn Rate Measurements of HMX, TATB, DHT, DAAF and BTATz

S.F. Son, H.L. Berghout, C.A. Bolme, D.E. Chavez, D. Naud, and M.A. Hiskey
MS C920
Los Alamos National Laboratory
Los Alamos, NM 87545
Telephone: 1-505-665-0380; Fax: 1-505-667-0500; E-mail: son@lanl.gov

In this paper we present new burn rate results for several energetic materials. The burn rates of HMX (octahydro-1,3,5,7-tetranitro-1,3,5,7-tetrazocine), PBX 9501 (HMX and Estane-based binder), TATB (1,3,5-triamino-2,4,6-trinitrobenzene), and PBX 9502 (TATB and KelF binder) are reported and compared with existing data. Burn rate data of these common explosives complement and extend existing data sets. Burn rate data of three novel high-nitrogen materials are presented in this work. Specifically, the high-nitrogen monopropellants considered are 3,6-dihydrazino-s-tetrazine (DHT), 4,4'-diamino-3,3'-azoxyfurazan (DAAF), and 3,6-bis($1H$-1,2,3,4-tetrazol-5-ylamino)-s-tetrazine (BTATz). High-nitrogen compounds may be key to meeting the advanced performance objectives of next-generation solid propellants. High-nitrogen solids offer the possibility of high performance, reduced emissions, and lower plume signature (low temperature and no HCl) than current propellant systems. The theoretical specific impulse is comparable to HMX. In contrast to HMX, however, high-nitrogen materials tend to be insensitive to impact. Because high-nitrogen energetic materials have intrinsically large positive heats of formation and produce low molecular weight reaction products, they are particularly suitable for consideration in high-performance propellant applications. BTATz appears particularly interesting because of its rapid burn rate, low-pressure exponent and high heat of formation. The effect of binder is investigated for all but one of these materials.

THIS PAGE HAS BEEN DELIBERATELY LEFT BLANK

Sensitivity Properties and Burning Rate Characteristics of High Energy Density Materials and the Propellants Containing These Materials

K. Kato and K. Kobayashi
Research & Development Department, Taketoyo-Plant, NOF Corporation
61-1 Kitakomatsudani Taketoyo-cho, Chita-gun
Aichi-ken 470-2398 Japan
Telephone: +81-569-72-1954, Fax: +81-569-73-7376, E-mail: nofrdsr@gld.mmtr.or.jp

S. Miyazaki and S. Matsuura
Research & Development Center, Nissan Motor Co., Ltd.
21-1, Matobashinmachi
kawagoe-City Saitama-ken, 350-1107 Japan

Recently many kinds of High Energetic Density Materials (HEDM) have been developed. Among these materials are Glycidyl Azide Polymer (GAP) as a binder for propellants, and Ammonium Dinitramide (ADN) and Hydrazinium Nitroformate (HNF) as an oxidizer. These materials were made by a new synthetic process in this study and evaluated experimentally.

Thermal decomposition tests, impact sensitivity tests, and friction sensitivity tests were conducted for GAP, ADN and HNF. The impact sensitivity and the frictional sensitivity of GAP are low. The ignition energy of GAP is low. The impact sensitivity of ADN is highly dependent on its shape. The needle type has high impact sensitivity, although the granular type has low impact sensitivity. The friction sensitivity is low for both types of ADN. The impact sensitivity and the frictional sensitivity of HNF are higher than those of ADN.

The burning rates of GAP propellants were measured. It is proved that the burning rate of GAP/Ammonium Perchlorate (AP) propellants are well explained by the Granular Diffusion Flame Theory (Figure 1). As the concentration of AP is increased, the diffusion process becomes slower and chemical reaction process in the gas phase becomes faster. As the particle diameter is small, the diffusion process becomes faster. The burning rate of GAP/Ammonium Nitrate (AN) is not affected by the diameter of the AN particle. When AP is added to the GAP/AN propellant, the diffusion process of the decomposition products of AP becomes a rate-controlling process. The burning rate of GAP/AD N propellants was also measured.
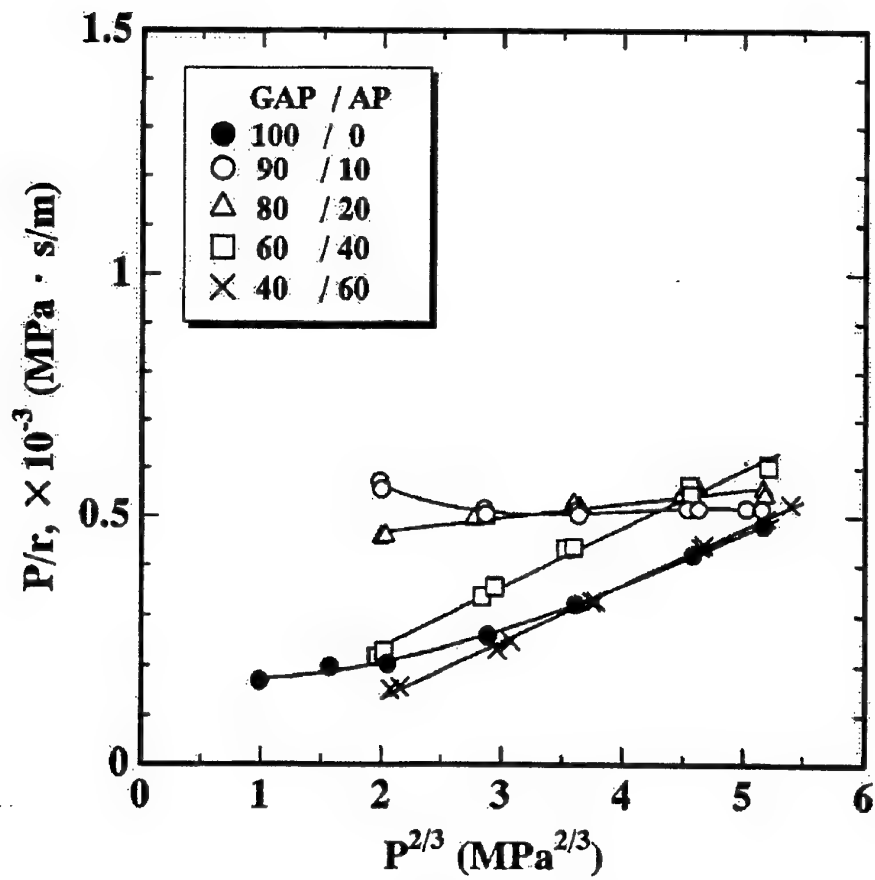
Fig.1 Relation between P/r and $P^{2/3}$ in GDF theory for the different GAP/AP ratio.

Structure of Ammonium Dinitramide Flame at 40 atm

O.P. Korobeinichev, A.A. Paletsky, A.G. Tereschenko, T.A. Bol'shova
Institute of Chemical Kinetics and Combustion Siberian Branch Russian Academy of
Sciences
630090 Novosibirsk, Russia
Telephone: +7(3832) 332852
E-mail: korobein@ns.kinetics.nsc.ru

The study of the propellants flame structure at high pressures close to those in a combustion chamber of a rocket motor is a difficult, but important task. Ammonium dinitramide (ADN) is a new energetic material that can be used as an oxidizer when developing an ecological pure solid propellant. The two zones of ADN flame structure at 1-6 atm was studied in [1]. This work examines the structure of a wide third zone of ammonium dinitramide flame at 40 atm using probing mass-spectrometry, microthermocouples and modeling. The method of probing dynamic mass-spectrometry has been applied earlier to the study of the flame structure of double based propellants at pressures of 15 and 20 atm [2]. Strands 10 mm in diameter and 15 mm high were burnt in argon atmosphere. A probe of stainless steel (with an inlet orifice 180 microns in diameter and internal angle of 40 degrees) was used to withdraw samples from a zone of high pressure and temperature. The intensity profiles (I_i) of mass peaks 30, 28, 44, 32 amu were measured for the main products of ADN combustion when burning surface of a strand moved from a probe starting from 1,2 mm to 16 mm. Using these data and results of calibrations, the concentration profiles of the main combustion products NO, N_2, O_2, N_2O and H_2O were found. The decrease of N_2O concentration and the rise of N_2 and O_2 concentrations is observed within a zone 8-10 mm wide. The concentration of NO in this zone does not undergo significant changes.

Temperature profiles were found using uncovered Pt-PtRh (10%) Π-shaped thermocouples 20 and 50 microns in diameter. The second flame zone, about 1 mm wide, was detected in ADN flame at 40 atm nearby ADN burning surface, within which temperature rises from ~1100 K to 1400 K. A similar zone of temperature rise was detected in [1] within 6-12 mm from ADN burning surface at 6 atm. The temperature rise from 1400 K to 1800 K is observed with further increases of the distance from the ADN burning surface at 40 atm from 1,5 mm to 8 mm.

The obtained experimental data (combustion products composition and temperature) were used as boundary conditions when calculating the structure of the third wide zone of ADN flame at 40 atm using CHEMKIN code, which has been applied before to describe the structure of ADN flame at 6 atm [3]. A mechanism incorporating 170 reactions for 29 species was used for calculations. Experimental and calculation data showed satisfactory agreement. The calculations have shown that the rise of the distance from the burning surface from ~1,5 cm to ~50 cm results in further temperature rise to ~2150 K (the fourth flame zone) due to the decomposition and consumption of NO and accumulation of O_2 and N_2. The calculated values of the temperature and final ADN combustion products composition come close to the thermodynamically equilibrium ones.

Acknowledgment

References

[1]   O.P. Korobeinichev, L.V. Kuibida, A.G. Shmakov, A.A. Paletsky, "Molecular-Beam Mass-Spectrometry to Ammonium Dinitramide Combustion Chemistry Studies", Journal of Propulsion and Power, 1998, vol. 14, No 6, pp. 991-1000.

[2]   O.P. Korobeinichev, L.V. Kuibida, A.A. Paletsky "Study of Solid Propellant Flame Structure By Mass-Spectrometric Sampling" Combustion Science and Technology, 1996, Vols.113-114, pp.557-571.

[3]   O.P. Korobeinichev, A.A. Paletsky, L.V.Kuibida, A.G. Shmakov, T.A. Bolshova "Ammonium Dinitramide Combustion Chemistry Studied by Molecular Beam Mass-Spectrometry and Modeling", In:Proceeding of 21st International Symposium on Space Thechnology and Science. Sonic City, Omiya, Japan,May 24-31,1998. (Editor Kuniori Uesugi),V 1, 1998, p.81-85.

Properties of ADN Propellants[*]

M.L. Chan, R. Reed, A. Turner, A. Atwood, and P. Curran
Naval Air Warfare Center Weapons Division
China Lake, CA 93555-6100
Tel: (760) 939-7265
Fax: (760) 939-7351
E-mail: ChanML@navair.navy.mil

Ammonium dinitramide (ADN) is a very powerful organic oxidizer that can replace ammonium perchlorate (AP) in propellant compositions. Calculations have shown that, when incorporated in propellant formulations, ADN can make those propellants capable of performance equal to or higher than that of the conventional hydroxyl-terminated polybutadiene (HTPB)/AP propellants. ADN propellants will not produce toxic HCl in the exhaust and will greatly minimize the secondary smoke problem that is caused by the nucleation of HCl. Because of their environmentally friendly characteristics and demonstrated low toxicity exhaust products to humans, ADN propellants are highly desirable.

A number of propellant formulations have been researched in recent years and several have been designed to capture the merit of using ADN as a solid oxidizer. Currently, China Lake formulators are working with ADN material produced with a low-cost synthesis route by Bofors, Sweden, in collaboration with scientists at the National Defense Research Establishment of Sweden. This ADN appears to be composed of either plate- or needle-like crystals and exhibits excellent chemical purity when subjected to ion chromatography inspection. The results of this inspection showed it is at least 99% pure, with 0.13% nitrate and 0.03% sulfate as impurities; no nitrite was detected. The trace amount of sulfate ion is probably derived from the synthesis reaction.

Portions of this ADN material have been made into prills by the Chemical Systems Division (CSD) of United Technologies under a Navy sponsored program. The spherical/prilled ADN has an average particle size of 300 μm and is produced from a prilling process developed by CSD investigators that involves molten ADN and mineral oil emulsion technology.

The formulators made two series of minimum-signature propellants. The propellants were formulated with either ADN or ADN/CL-20 mixtures. The binders used were ORP-2A/nitrate ester and PCP/nitrate ester. These have been shown to be excellent binders for propellant materials. Four propellants (PCP/NE/ADN, PCP/NE/ADN/CL-20, ORP-2A/NE/ADN, and ORP-2A/NE/ADN/CL-20) are currently under study. These propellants processed and cured well and, therefore, resulted in void-free samples.

Propellant samples, about 100 grams in size, were prepared for burning rate evaluation in the window bomb apparatus. The results showed that CL-20/ADN propellant can sustain good burning rates at pressures up to 68 MPa and have a burning rate around 1.5-1.77 cm/s at 6.895 MPa. Similar burning rates were also obtained from the ADN propellants.

---

[*] Approved for public release; distribution is unlimited.

High-energy propellant compositions containing ADN were successfully prepared and characterized. The compositions contained ALEX (electro-exploded aluminum of less than 0.1 nm in size), spherical aluminum, and a polyalkylene oxide binder plasticized with nitrate esters. Recrystallized ADN was used (nominal size of 70 µm) because the prills produced more sensitive compositions. In some of the formulations, BAMO/NMMO (BN-7) was used to further enhance energy and burning rates. Burning rates were typically 6.8-7.6 cm/s at 41.3 MPa. At 27.5-41.3 MPa, the pressure exponent decreased to 0.55 but increased over lower pressure ranges.

Other propellant properties such as mechanical, thermal, and processing properties will be optimized and the results will also be included in this paper.

Combustion Peculiarities of ADN and ADN-Based Mixtures

V.P. Sinditskii, A.E. Fogelzang, V.Y.Egorshev, A.I. Levshenkov, V.V. Serushkin, V.I. Kolesov

Mendeleev University of Chemical Technology
9 Miusskaya Square, 125047, Moscow, Russia
Tel: (095)-496-6027, Fax: (095) 496-6027
E-mail: vps@rctu.ru

Nowadays, a continuing interest is drawn to combustion of chlorine-free oxidizers. Being a peculiar representative of this type of energetic materials, Ammonium Dinitramide (ADN) is of particular interest from both theoretical and practical standpoints with respect to ascertainment of its combustion mechanism. This paper presents an analysis of observed combustion features of ADN and its mixtures with paraffin, water, and formamide.

Effects of small amounts of the fuel added to ADN, type of the material enclosing ADN pressed strand, and the strand cross-section size on the burning rate, have been examined to allow the following observations.

1. In spite of the fact that ADN is an oxidizer, combustible surroundings have been found to exert practically no effect on the burning rate of ADN pressed strands. In contrast, even minor amounts of organic admixtures turned out to have a strong effect on ADN burning behavior, extending considerably the pressure of its deflagration limit from 0.2 MPa for purified crystalline ADN to the vacuum area.

2. Within the pressure range of 2-10 MPa, a decrease in the strand cross-section size leads to a decrease in the ADN burning rate, accompanied by a notable burn rate data scatter. A small amount of organic substances added to ADN appeared to suppress the scatter and strongly affecting the burn rate within this pressure interval. Study on combustion of ADN single crystals revealed that they were incapable of sustained burning at all over this pressure interval.

The main reason for the observed combustion behavior is assumed to be a dominant role of condensed-phase decomposition reactions in burning of ADN. The ADN surface temperature is controlled by dissociation of the surface layer, thus determining its dependence on pressure. Since the amount of heat released in the condensed phase is chemically limited, combustion of ADN occurs on the verge of condensed phase energetic potentials, starting from the pressure of 20 MPa to pressures up to 10 MPa, where the gas phase chemistry begins to play a perceptible role in combustion. Because of the condensed-phase location of the primary heat source, burning is attended with significant dispersion of the molten surface layer consisting of initial ADN and Ammonium Nitrate, the condensed decomposition product. Entrainment of the condensed phase to the gas zone reaches its maximum in the pressure region of unstable combustion (2-10 MPa), resulting in an increasing burn rate data scatter. Within this area of pressures, dispersion of the condensed phase backs up the combustion, facilitating removal of the condensed products from the surface and compensating for deficient heat feed back from the gas. Conversely, at the vicinity of low-pressure limit of ADN deflagration, where a fraction of ADN ejected to the gas is considerably larger, dispersion hinders the burning progress through lowering the heat that can be generated in the condensed phase.

Suppression of an excessive dispersion by means of reducing the surface tension of the polar molten layer under the action of apolar admixtures results in decreasing the lower-pressure limit of deflagration, on the one hand, and reduction in both burning rates and their scatter in the pressure interval of 2 to10 MPa, on the other hand.

ADN water and formamide solutions placed in 4-6 mm i.d. glass tubes have shown a transition from laminar to turbulent burning regime characterized by a steep rise of the burning rate first. At pressures above 15 MPa, this turbulent burning regime seems to give way to another more stable combustion regime marked by a week dependence of the burning rate on pressure, as well as good constancy of the burning rate throughout the tube. While the burning rate observed for this "pseudolaminar" regime increases with the combustion temperature, at the laminar combustion regime, any additive to ADN proves to decrease the burning rate irrespective of the physical state of the composition and nature of the additive.

AREA 7:

PYROLYSIS AND COMBUSTION PROCESSES OF NEW INGREDIENTS AND APPLICATIONS

SESSION CHAIR:

DR. CHESTER CLARK

Burning Rate & PDL Characteristics of a GAP/AP Propellant System

K. Hori, M. Kohno
Institute of Space & Astronautical Science, Propellant Section
3-1-1 Yoshinodai Sagamihara Kanagawa, Japan, 229-8510
Tel.: 81-42-759-8283, Fax: 81-42-759-8461
E-mail hori@pub.isas.ac.jp

A. Volpi, C. Zanotti
TEMPE-CNR

K. Kato
Nippon Oil & Fats Co.

S. Miyazaki
Nissan Motor Co.

For the application to a mass flux controllable gas generator, GAP is one of the most suitable high energetic materials because of its high pressure exponent. However, its PDL and low pressure burning rate characteristics have not been well investigated yet despite, for such an application, it is necessary to know them in detail. Moreover a GAP/AP propellant system is considered more feasible because the addition of AP to GAP may be effective to extend the combustible region which in turn boosts the studies on the behavior of a GAP/AP propellant system.

Burning rate under high pressures of a GAP/AP propellant system were obtained with a strand burner. The PDL and low pressure burning rate have been investigated by means of a X-ray device as functions of the AP content, AP particle size and depressurization rate. The X-ray device used in this work is simply composed of a X-ray source, a combustion chamber and one X-ray sensor. The X-ray source, equipped with a closed-circuit cooling system, has a square emission area of 0.6*0.6mm2 and 40 degrees emission angle. The X-ray tube voltage can be varied over the range of 20 to 100kV, while the tube current can be set from 1 to 4mA. The propellant sample is placed on an Aluminum plate below, in which the sensor is positioned in a removable housing and the depressurization rate is controllable. The sensor consists of a plastic scintillator which is connected to a phototube whose sensitive area is reduced to a circle of 3mm diameter. The signal at the output of the sensor is sent to a digital acquisition system controlled by PC.

Precise calibration between sample length and sensor output gives the instantaneous sample length during the burning test, thus, through its time derivative, the instantaneous burning rate. Therefore, it is possible to obtain low pressure burning rate and PDL simultaneously in one burn at a certain depressurization rate. Results of PDL and low pressure burning rate measurements of a GAP/AP propellant system will be presented and the combustion mechanism will be discussed.

THIS PAGE HAS BEEN DELIBERATELY LEFT BLANK

Diffusion Flame Structure of HNF Sandwiches

J. Louwers, G.M.H.J.L. Gadiot
Research Group Rocket Technology, TNO Prins Maurits Laboratory,
P.O. Box 45, 2280 AA Rijswijk, The Netherlands

G.G.M. Stoffels, D.J.E.M. Roekaerts
Thermal and Fluids Sciences, Applied Physics, Delft University of Technology,
Lorentzweg 1, 2628 CJ Delft, The Netherlands
Tel: +15 2782418; Fax: +15 2781204; E-mail: genie@ws.tn.tudelft.nl

Hydrazinium nitroformate ($N_2H_5C(NO_2)_3$, HNF) is a new energetic oxidizer that, combined with an energetic binder such as glycidyl azide polymer ($[C_3H_5N_3O]_n$, GAP) yields enhanced performance compared with conventional ammonium perchlorate (NH_4ClO_4, AP) based solid propellants. In addition, HNF's combustion gases do not contain chlorine.

The combustion of HNF is characterized by a very short flame standoff, high regression rate, high burn rate exponent, and high monopropellant flame temperature in comparison with the combustion of AP. Therefore, it is expected that the combustion characteristics of HNF based propellants are significantly different from those of AP-based propellants.

In this paper we focus on experiments in which we have used Planar Laser-Induced Fluorescence (PLIF) to study the structure of the flame. In addition to neat HNF, sandwiches consisting of HNF and GAP are used. In comparison to propellants, sandwiches have a 2D-structure, which simplifies the experimental difficulties of those encountered in propellants. The observed flame structure is a combination of a HNF flame (premixed flame) and a HNF/GAP flame (diffusion flame).

Small samples of neat HNF or sandwiches are ignited by a CO_2 laser pulse in a high-pressure cell with optical access through sapphire windows. OH or CN molecules are excited by a sheet of laser light crossing the flame in a direction perpendicular to the HNF/GAP surface, while the induced fluorescence is detected by an intensified CCD camera perpendicular to the laser sheet.

OH and CN-PLIF images have been obtained at different pressures for neat HNF and for sandwiches consisting of HNF and GAP. A typical OH-LIF sequence of a HNF/GAP/HNF sandwich at 0.35 MPa is given in Figure 1a. It is found that at higher pressures the area where no OH is seen is smaller and that the boundaries are sharper due to the decreasing diffusion. In Figure 1b, a typical CN-LIF image of a HNF/GAP/HNF sandwich at 0.14 MPa is shown. Just like in the case of OH, the structures become smaller and sharper at higher pressures. The experimental results are compared with results obtained from a numerical model developed at Delft University of Technology.

The main conclusion of this work is that the influence of the diffusion flame is extremely small. This is in agreement with the observation that the burn rate of HNF-based propellants is almost independent of the particle size. This can be seen in Figure 2, where the regression rates of HNF/GAP propellants with coarse HNF (C15, Υ) and fine HNF (S16, ϖ) are given. For comparison, the results for neat HNF and GAP are also shown.
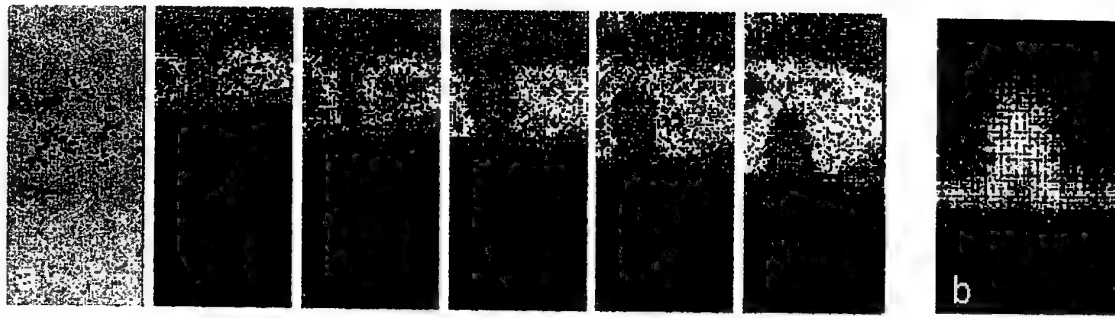
Figure 1: a) Typical OH-LIF sequence of a HNF/GAP/HNF sandwich at 0.35 MPa.
b) CN-LIF image of a HNF/GAP/HNF sandwich at 0.14 MPa

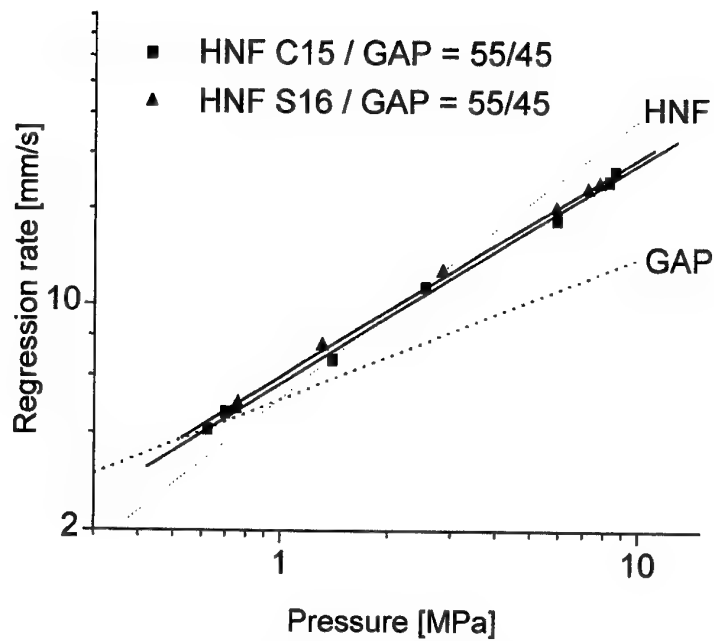Figure 2: Regression rate of HNF/GAP propellants compared to that of neat HNF and GAP. (ϖ, C15 coarse HNF; Υ, S16 fine HNF)

Combustion and Thermal Behavior of Ballistically Modified Eva and Estane Based RDX Propellants

R.R. Sanghavi, S.N. Asthana, J.S. Karir and Haridwar Singh
High Energy Materials Research Laboratory,
Armament Post, Sutarwadi,
Pune - 411 021, India
Telephone: +91 020 5881303 ext. 2211; Fax: +91 020 5881316
E-mail: root@drerdl.ren.nic.in

Thermoplastic elastomers (TPEs) behave emerged as potential binders for modern/advanced propellants and explosive formulations. Unique structure features of TPEs contribute towards desired cohesive strength up to moderately high temperatures and flexibility even at sub-zero temperature. Elastomeric nature of TPEs confers high resistance on propellant systems to hyper-velocity impact, from warhead fragments and charge jets as well as to sympathetic detonation. In view of these advantages, TPEs have scope for application in the field of guns as well as rocket propellants and explosives. Basically thermoplastic elastomers are copolymers of ABA of AB type comprising of the hard segment (A) capable of crystallization or association leading to thermoplastic behavior and the soft segment (B) providing elastomeric characteristic to the polymer.

During this work, commercially available TPEs namely ethylene-vinyl acetate (EVA) and polyurethane-ester-MDI (Estane), were evaluated as binders for nitramine based systems for both gun/rocket applications. AP was added as an additive and GAP was incorporated as an energetic plasticizer. Effect of inclusion of selected ballistic modifiers was also studied. An attempt has been made to evolve a mechanism to explain the trends obtained.

The propellant compositions comprising of 80 % RDX, 16% TPE binder and 4 % plasticizer were prepared by solvent technique. The thermochemical parameters were computed by computer software (Therm) developed at HEMRL. The ballistic parameters were obtained by combusting a propellant sample in a closed vessel (CV) and acoustic strand burner. Thermal studies were carried out at a heating rate of $10°C/min.$ on Differential Thermal Analyzer (DTA) in static air medium and Differential Scanning Calorimetry (DSC) in N_2 atmosphere.

EVA based formulations gave relatively higher force constant (by about 10-50 J/g) as well as flame temperatures (by about 50-100 K) than estane based formulations. GAP based formulations gave superior ballistic than corresponding TA based formulations. Incorporation of 10-20% AP at the cost of RDX resulted in further increase in energetics. Closed vessel evaluation results corroborate the theoretically predicted performance level. The burn rate relationships obtained for these formulations are given below.

$0.14\text{-}0.16 \, P^{0.95\text{-}1.1}$
TA plasticized

$0.16\text{-}0.17 \, P^{0.9\text{-}1.0}$
GAP plasticized

EVA

$0.11\text{-}0.13 \, P^{0.98\text{-}1.15}$
TA plasticized

$0.13\text{-}0.14 \, P^{0.95\text{-}1.05}$
GAP plasticized

Estane

Inclusion of ballistic modifiers, namely ferric oxide, basic lead salicylate-Cu_2O-carbon black combination and sodium borohydride (adsorbed on Al_2O_3) led to decrease (by about 15-25 J/g) in F. However, their addition lead to enhancement of burn rate as brought out by following relationship obtained for Fe_2O_3, BLS/Cu_2O/C-black combination and $NaBH_4$.

$$r = 0.170\text{-}0.183\ P^{\ 0.82\text{-}0.93} \qquad\qquad r = 0.177\text{-}0.191\ P^{\ 0.8\text{-}0.9}$$
$$\text{TA plasticized} \qquad\qquad\qquad \text{GAP plasticized}$$

The best results were obtained with a typical ballistic modifier.

$$r = 0.191\text{-}0.212 P^{0.65\text{-}0.68}$$

A major achievement was realization of pressure index value of the order of 0.65 - 0.68 which is not reported in the high pressure regions. (15-250 MPa).

Acoustic burn rate data also brings out that EVA based formulations have superior combustion characteristic than estane based formulations. 10-20% AP containing formulations with TA plasticized Estane binder did not undergo combustion in the pressure range studied (35.4-10.8 Mpa), while corresponding EVA based formulation gave sustained combustion at 8.8 MPa and GAP plasticized composition gave stable combustion even at 3.4 MPa.

DSC of TPE based formulation did not exhibit the endotherm/exotherm corresponding to binder. The compositions gave an endotherm at about 200-205°C and exotherm about 220-240°C in all the cases. These trends bring out that the thermal decomposition of RDX is a rate determining step. In general, ballistic modifier brought down the decomposition temperature. The effect was more pronounced with the typical ballistic modifier. The trends obtained suggest that the AP plays an important role in catalyzing decomposition of TA based formulations, while ballistic modifiers catalyzed decomposition of GAP / GAP involving reactions to a greater extend in condensed phase / near surface region. An attempt has been made to correlate the thermal decomposition and combustion pattern to pinpoint the site of action of additives.

AREA 7:

PYROLYSIS AND COMBUSTION PROCESSES OF GUN PROPELLANTS AND INGREDIENTS

SESSION CHAIR:

MR. ALBERT HORST

Combustion Studies of Nitramine Containing Energetic Materials

A. I. Atwood, D. T. Bui, P. O. Curran, and C. F. Price
Code 4T4310D, Combustion Research Branch
1 Administration Circle, China Lake, CA 93555
Tel: (760) 939-0203
Fax: (760) 939-2597
E-mail: atwoodai@navair.navy.mil

Nitramines are widely used in both explosive and propellant formulations. RDX and HMX have been widely studied and used extensively as the main ingredients in many formulations due to their capability of producing high energy, high specific impulse and impetus during combustion. While considerable data exist on the combustion of the neat ingredients, less is known about the behavior of these ingredients in a heterogeneous explosive or propellant formulation. Many explosive formulations are simple bimodal formulations and represent excellent models for examining the effects of binder on the neat monopropellant combustion. Comparisons of heterogeneous formulations will be made to the neat monopropellant deflagration data in this paper.

When used as an explosive, nitramines are often mixed with a small amount of binder or desensitizing agent such as Viton or wax. This is done to improve the safety and handling characteristics of the material without compromise to performance. Two of these types of explosives, PBXN-5 and Composition A-4, are described in this paper. The two explosives are used in a wide variety of applications. CompA-4 consists of 97% RDX and 3% of Candelilla Wax: PBXN-5 consists of 95% HMX and 5% Viton A.

While the combustion behavior of an explosive formulation may be of little concern to the explosive formulator, it is of particular importance in understanding combustion related hazards. A recent JANNAF workshop on long duration low amplitude loading hazards identified steady state combustion data on explosives as a critically needed model input parameter.(ref1) Additionally, the accurate modeling of explosive response to a hazard threat such as cook-off or performance changes that may result from thermal exposure requires an understanding of the temperature effects on steady state combustion. The burning rate temperature sensitivity of the nitramine containing materials will also be examined in this paper. The low pressure burning rate temperature sensitivity of PBXN-5 was reduced when compared to that of neat HMX for equivalent experimental conditions. PBXN-5 burning rate temperature sensitivity was nearly constant over the range of pressures tested (0.69-10.34 Mpa).

One means to achieve the increased rocket propellant performance needs of the future is to increase solid rocket motor operating pressures. Increased operating pressures can be achieved with the improved rocket motor case technology that is currently available. While attractive, this mode of performance increase is not without its own practical limitations. Solid rocket propellants often experience an increase in burning rate pressure exponent at elevated pressures. A burning rate pressure exponent near unity may result in a motor explosion. Combustion instability is also an additional problem at elevated pressures. High pressure oscillations were observed in some of the closed bomb firings made with explosive powders and appear to be related to a delayed ignition. Pressurization rates (dp/dt) ranged

from 0.14-1.4 x 10^{12} pa. Burning rate measurements were measured for the materials described in this paper over the pressure rage of 0.69 to 138 Mpa. A combination of high pressure window bomb and closed bomb combustion tests was used to obtain the combustion data. A comparison of explosive to propellant burning rates will also be made.

Reference

1. P. J. Baker. "Workshop Report on Low-Amplitude/Long-Duration Impact and Shock Loading of Energetic Materials" presented at the 18th JANNAF Propulsion systems Hazards Subcommittee Meeting, Cocoa Beach Florida, 18-21 October, 1999.

Burning Phenomena of the Doublebase Gun Propellant JA2

V. Weiser, S. Kelzenberg, T. Fischer, A. Baier, G. Langer, N. Eisenreich, W. Eckl
Fraunhofer-Institut für Chemische Technologie (ICT)
Joseph-von-Fraunhoferstr.-Str. 7
D-76327 Pfinztal 1 (Berghausen), F.R.G.
Tel: 49 (0)721 4640-156; Fax: 49 (0)721 4640-111; E-mail: vw@ict.fhg.de

Energy transfer from the gaseous phase governs ignition and combustion of solid rocket and gun propellants. In addition to conduction and convection, radiation of the flame contributes to the heat feedback which controls the burning rate in dependence of pressure. The dependence on initial temperature is given by physical parameters of the conversion of the solid to the gaseous state.

The experimental investigation concerned the well known gun propellant JA2. Burning rates were measured in dependence of pressure and initial temperature confirming a simplified law for the burning rate. The evaluation yielded the pressure exponent which could be directly assigned to the heat feedback and the temperature of the condensed phase conversion to the gas phase at about 670 K.

The measurements comprised also spectroscopic measurements in the wavelength ranges of 300 nm to 14000 nm which locally resolved along the linear flame zone profile. Their analysis gave profiles of species in the flames including di-atomic flame radicals and tri-atomic molecules of the combustion final products. In addition, gas phase temperatures were derived by application of the Single Line Group model which gave approximately 2700 K closely below the adiabatic flame temperature at 7 MPa. They are compared to temperatures from a continuous broad band assigned to soot particle emission. In summary these data enabled an estimation of the heat feedback of the flame to the burning surface.

THIS PAGE HAS BEEN DELIBERATELY LEFT BLANK

Theoretical Analysis of Modern ETC-Concepts

R. Heiser
Fraunhofer-Institut für Kurzzeitdynamik
Ernst-Mach-Institut, Am Klingelberg 1
D-79588 Efringen-Kirchen, Germany
Phone: +49 (0)7628 905043, Fax: +49 (0)7628 905077
E-mail: heiser@wiwei.emi.fhg.de

This paper deals with the prediction of the performance of modern types of ETC-guns. Such concepts are supposed to be an option for guns with increased performance compared to fielded systems. The advantage, besides the performance, consists of fast and reliable ignition, as well as of the compensation of the temperature sensitivity. Modern concepts are based on high loading density (≥ 1.2 g/cm^3), but only on minimum electric energy that appears to be sufficient for both ignition and control of the main combustion processes.

Conventional interior ballistics codes, such as lumped parameter models or fluid dynamics based models successfully applied to many charge configurations, are used to analyze the main propulsion features of such ETC-concepts. The interesting part is that the computational results of the codes compare fairly well for systems in the whole range of loading densities, as long as the spatial pressure gradient shows a conventional shape. However, there exist ETC-concepts under current investigation with non-conventional pressure gradient. For these cases, the computational results differ significantly. The differences can be explained. The consequences with respect to the performance are amazing.

Another essential issue is coupled to the sensitivity of systems with high loading density. The computational results show how the sensitivity is affected by the charge design.

THIS PAGE HAS BEEN DELIBERATELY LEFT BLANK

Model Formulation of Laser Initiation of Explosives Contained in a Shell

K.K. Kuo and E. Boyer
140 Research Building East
The Pennsylvania State University
University Park, PA 16802
Tel: (814) 863-2264
Fax: (814) 863-3203
E-mail: jeb19@psu.edu

Laser initiation can provide a novel way to remotely destroy unexploded ordnance. The overall setup of a laser penetrating an unexploded shell is shown in Fig. 2. In order to better understand the processes taking place and to provide a predictive capability, a comprehensive theoretical model has been formulated for simulating the physical and chemical processes associated with the laser initiation of explosives contained in a shell. The formulation is based upon various experimental observations and physical principles. When viewed at a closer scale (shown in Fig. 1), it can be seen that many complex processes are taking place, due to interactions of the laser beam, metal shell, and explosive core. Each of the important processes was examined in detail as a submodel; these submodels were then combined to form a complete description of laser drilling and initiation. The overall formulation considers the following major processes: 1) laser heating of the metal shell casing, 2) melt layer formation and expulsion of molten material from the heated zone due to the recoil pressure force generated from metal vaporization, 3) bubble formation and bursting in the melt layer, 4) ejection of liquid droplets from the rupturing bubbles, 5) in-depth heat transfer to the metal and solid explosives, 6) formation of a high-velocity plume jet of metal vapor, 7) turbulence interaction and chemical reaction between the plume jet and ambient air, 8) liquid- and gas-phase chemical reactions of the RDX explosive in producing fragmented chemical species, and 9) runaway ignition of RDX explosive caused by laser energy input and chemical reactions between the decomposed species of RDX. Where possible, experimental data have been incorporated. In the course of model formulation, a literature survey of relevant work on laser drilling and RDX combustion was performed. The model presented here provides the
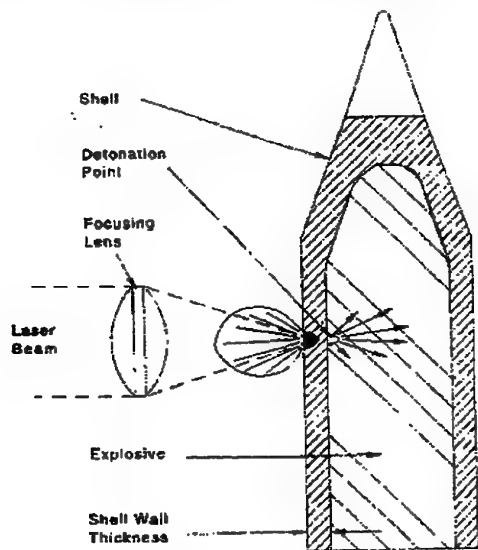

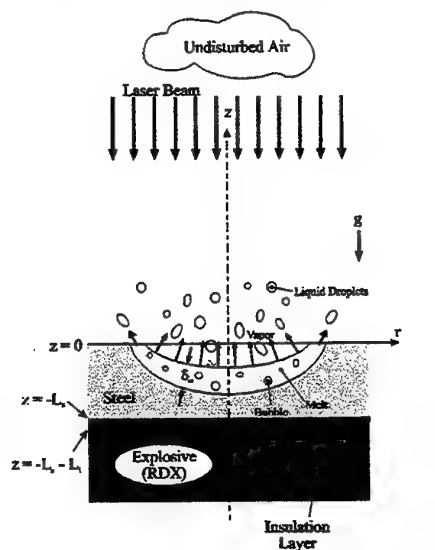Fig. 2. Overall view of laser drilling into shell

Fig. 1. Diagram of laser drilling process.

147

most detailed and complete formulation available.

AREA 8:

THEORETICAL MODELING AND NUMERICAL SIMULATION OF COMBUSTION PROCESSES

SESSION CO-CHAIRS:

DR. ELAINE ORAN
AND
DR. FRED VOLK

First Principles Simulations of Gas-Phase DDT and the Effects of Hot-Spot Formation

E. S. Oran, A. M. Khokhlov
Laboratory for Computational Physics and Fluid Dynamics
Naval Research Laboratory, Code 6404
Washington, DC 20375, USA
Tel: 202-767-2960; Fax: 202-767-6260
E-mail: oran@lcp.nrl.navy.mil

Gas-phase Deflagration-to-Detonation Transition (DDT) is the unsteady process by which a generally turbulent flame, or deflagration, becomes a powerful supersonic reaction wave, a detonation. DDT is extremely complex, and involves deflagrations, shocks and shock reflections, boundary layers, and all of their interactions with each other. DDT not only has important practical consequences, but it is also one of the major unsolved problems in combustion and detonation theory. For example, DDT is most likely the mechanism by which the propellants on the USS Iowa exploded, spreading partially reacted and hot material to the ship magazine, which subsequently ignited. In the design of engines for high-speed flight, DDT must occur repeatedly and in the minimum distance possible, or, in some cases, not at all. DDT occurs in small gas-filled channels in granular energetic materials. Knowing whether DDT occurs in thermonuclear supernovae is important in astrophysics and cosmology for understanding the element abundance and determining the age, size, and curvature of the universe. Because of the unsteady nature of DDT and the wide range of spatial and temporal scales involved, both experimental diagnostics of DDT are difficult to obtain and computations of the process are difficult to perform.

Here we report the results of two- and three-dimensional numerical simulations of DDT in channels containing acetylene-air and ethylene-air mixtures. The geometry and mixtures are the same as those for which experiments are currently being performed, so the results may be qualitatively, and to some extent quantitatively, to experiments [1]. The simulations solve the reactive Navier-Stokes equations including a self-consistent description of the chemical reactions, molecular diffusion, viscosity, and thermal conduction. The model reproduces the laminar flame and detonation properties of the mixtures initially at room temperature and in the pressure range 0.1—1 atm. The simulations were done using adaptive mesh refinement at a level that resolved the laminar flame and all of the chemical and physical processes associated with flame development, propagation, and interaction with shocks.

In the computations shown here, a turbulent flame is created through the interaction of a shock and an initially laminar flame. This interaction results in a Richtmyer-Meshkov instability that greatly changes the surface area of the flame by driving unreacted material into reacted material, or vice versa [2]. The flame becomes more turbulent after repeated interactions with reflected shocks. Besides generating turbulence in the flame brush, these interactions substantially increase the rate of burning. This turbulent system generates fluctuations that create local hot spots in unreacted material. Then, under the right conditions, the hot spots can eventually give rise to a DDT event that quickly consumes all of the unburned material.

Depending on the Mach number of the initial shock, three situations arise [3]. The weakest shock (M = 1.4) creates a turbulent flame brush, but there is no DDT, at least within the

timeframe of the computation. For a slightly stronger shock (M = 1.5), DDT arises in unreacted, but preheated and compressed material, outside of the flame brush. For the strongest shock (M = 1.6), DDT occurs in a pocket of unreacted material that has been entrained in the flame brush.

We have shown that for all of the cases in which there is a DDT event, the transition to detonation occurs by the Zeldovich gradient mechanism [4]. This means that for detonation to occur, there must be a gradient in chemical induction time, and the region of the gradient must be large enough. The critical length of this gradient is a function of the pressure, temperature, and the type of gas mixture. In the simulations, these gradients were the hot spots themselves that were created by the turbulent flame brush. In this presentation, we summarize these simulations and discuss their implications with respect to the basic mechanism by which DDT occurs, the nature and persistence of the flame front, and the turbulence in the flame brush.

We conclude this discussion by describing the applicability of the concepts shown in these simulations to transition to detonation in granular energetic materials (See, for example, [5]). It is possible for small channels and fissures to either occur naturally or develop in such materials. These channels trap reactive gases, and as these gases are heated, more reactive material evaporates into the channel. As the gases in the channel become more inhomogeneous, locally perturbed regions develop that may have conditions appropriate for a transition to detonation.

References
1. Scarinci, T. and Thomas, G.O., "Some experiments on Shock-Flame Interaction," UCW/det 905, Department of Physics, University of Wales, Aberystwyth, Wales, U.K., 1990; Scarinci, T., Lee, J.H., Thomas, G.O., Bambrey, R., and Edwards, D.H., Prog. Astro. Aero. 152:3--24 (1993). Thomas G.O., Sands, C.J., Bambrey, R.J. and Jones, S.A., "Experimental observations of the onset of turbulent combustion following a shock-flame interaction," Proc. 16th International Colloquium on the Dynamics of Explosions and Reactive Systems, Wydawnictwo "Akapit", Cracow, 1997, pp. 2-5.

2. Khokhlov, A.M., Oran, E.S, Chtchelkanova, A.Yu., and Wheeler, J.C., "Interaction of a shock wave with a sinusoidally perturbed flame," Combustion and Flame, 117, 99—116 (1999).

3. Khokhlov, A.M., Oran, S.E., and Thomas, G.O., "Numerical simulation of deflagration-to detonation: The role of shock-flame interactions in turbulent flames in the shock-flame interaction experiments," Combustion and Flame, 117, 323—339 (1999). Khokhlov, A.M., and Oran, S.E., "Numerical simulation of deflagration-to-detonation transition in a flame brush," Combustion and Flame, 119, 400—416 (1999).

5. Zeldovich, Ya.B., Librovich, V.B., Makhviladze, G.M., and Sivashinsky, G.I., Astronautica Acta 15:313-321 (1970).

6. Asay, B.W., S.F. Son, and J.B. Bdzil, "The Role of Gas Permeation in Convective Burning," Int. J. Multiphase Flow, 23, 923—952 (1996).

Aerothermochemical Model for the Interior Ballistics of Solid Propellant Rocket Motors

R. Caro
Fabricas y Maestranzas del Ejercito de Chile
Send correspondence also to dcmfamae@chilesat.net

J. Pérez
Complejo Químico Industrial del Ejercito de Chile

J. de Dios Rivera
Departamento de Ingeniería Mecánica y Metalúrgica, Pontificia Universidad Católica de Chile
V. Mackenna 4860 – Macul, Santiago, Chile
Tel: (562) 686 5886
Fax: (562) 686 5828
E-mail: jrivera@ing.puc.cl

To simulate the interior ballistics of a solid propellant rocket motor, a one-dimensional model was formulated, taking into account the mass, momentum and energy conservation equations applied to a control volume. The model describes the transient ignition process, the following flame spreading on the propellant surface, and finally, the complete combustion of the grain. The suitable selection of the numerical method allowed an efficient solution of the model, resulting in a very low computational cost that permitted the use of a personal computer.

Three steps were considered for modelling the ignition transient: induction, flame spreading on the propellant surface, and combustion chamber filling. The igniter is modelled by an empirical mass flow rate function, with time as the independent variable. For flame spreading calculation, the conservation equations were combined with a heat transfer model, which considers convection from the gases produced by the igniter and conduction through the propellant grain. In this way, the grain surface temperature evolution is calculated using a one-dimensional solution to the transient heat conduction equation. The induction interval and flame spreading are evaluated through a critical temperature of the grain surface (Peretz et al. 1973). Each element of grain surface is assumed to start burning when its calculated temperature reaches the critical value (Summerfield et al. 1966).

An outstanding feature of this model is the changing boundary conditions downstream of the nozzle. Initially, at the start of the ignition process, the zero-flow boundary condition is set, simulating the nozzle plug. Later on, when the plug expulsion pressure is achieved, the boundary condition changes to a subsonic outflow. Finally, when the critical pressure is reached in the combustion chamber, this B.C. turns into a supersonic one. Stability problems associated with the initial low Mach number flow were solved using an artificial diffusion term.

Finally, a form function was developed to describe the variation of the gas flow and propellant burning areas as a function of time. Also included was the blowing effect of the gases generated on the propellant surface on the friction coefficient, and a burning rate correlation considering the erosive burning effect.

For the resolution of the theoretical model, which is represented by a non-homogeneous system of hyperbolic partial differential equations, a finite difference numerical model based on the implicit Euler method of Chang et al. (1988) was used. The resultant discretised equations constitute a tri-diagonal block matrix system, which was solved efficiently using a non-iterative UL computational algorithm. The model was validated simulating the burning of a rocket motor having a cylindrical interior geometry. The calculated time pressure trace shows good agreement with experimental data. Some results are shown in Figures 1 to 3.

References

Chang C.L., Kronzon Y., and Merkle C. L. (1988). Time-Iterative Solutions of Viscous Supersonic Nozzle Flows, AIAA Journal, Vol. 26, pp. 1208-1215.

Peretz A., Caveny L.H., Kuo K.K., and Summerfield M. (1973). Starting Transient of Solid-Propellant Rocket Motors with High Internal Gas Velocities, AIAA Journal, Vol. 11, pp. 1719-1727.

Summerfield M., Parker K.H., and Most W.J. (1966). The Ignition Transient in Solid Propellant Rocket Motors. Aerospace and Mechanical Sciences Report, 769, Princeton University.
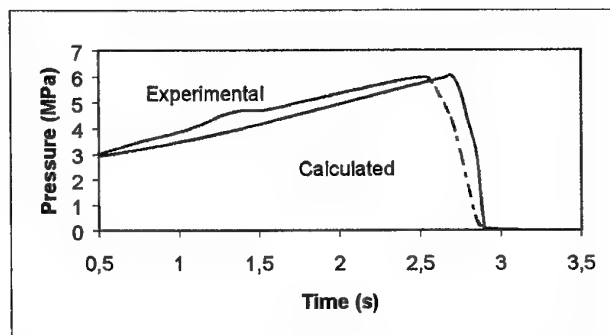
Fig.1. Comparison of measured and calculated axial pressure distributions
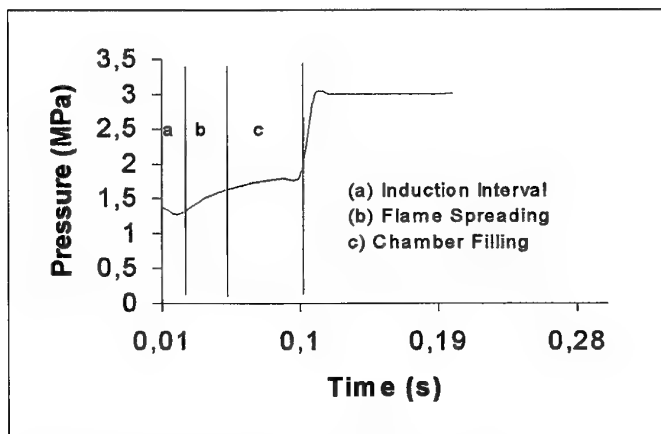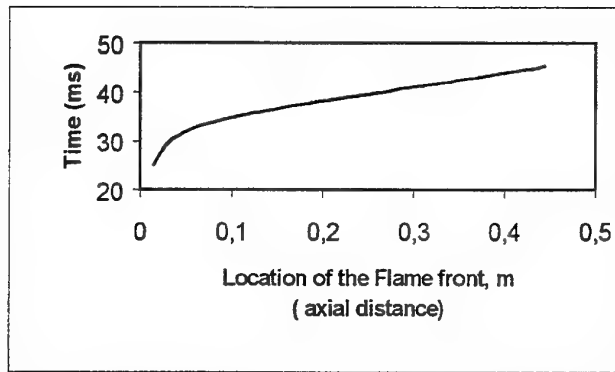

Fig.2. Calculated pressured transients

Fig. 3 Calculated flame spreading locations versus time

THIS PAGE HAS BEEN DELIBERATELY LEFT BLANK

Numerical Simulation of Combustion Processes in Rocket Motors

M. Yumusak
Research Engineer, Internal Ballistics Department
Roketsan Missiles Industries Inc., Ankara Samsun Karayolu 40. km
06780, Elmadag, Ankara, Turkey
Tel: 90-312-863 4200
Fax: 90-312-863 4208
E-mail: uarkun@rkts.com.tr

A.T. Uçer
Professor, Mechanical Engineering Department
Middle East Technical University, Ankara, Turkey

Present work is focused on the numerical simulation of flow and combustion processes in the combustion chambers and nozzles of rocket motors. An explicit Euler code with chemical source term treated implicitly is developed to evaluate reacting flow fields ranging from low subsonic to supersonic regimes for different propellants.

Results are demonstrated for two cases. The first test case is a small rocket thruster[4], containing a single swirl-coaxial injector with an outer fuel and inner swirling oxygen jet. The second test case is a simple test motor called as 6C4 Room & Haas motor[3], 19.0 inches long by 8.0 inches in diameter with axisymmetric grain configuration. Computational and experimental results are compared for these cases.

The first test case is a small rocket thruster[4], containing a single swirl-coaxial injector with an outer propellant and inner swirling oxygen jet. This rocket engine uses gaseous hydrogen/oxygen or methane/oxygen propellants. The combustion mechanisms are based on the detailed chemical reaction systems. The specific impulse Isp and C* efficiency are calculated for steady state condition. Results are compared with experimental data in Table 1. In Fig.1, computed concentration distribution at the head end is compared with the data obtained from one-dimensional premixed flame program[6]. The same test case is re-solved with chemically frozen flow assumption. Table 1 shows that simulation with finite rate chemistry model improves the performance prediction.

The computations for the second test case have been performed for three different geometries corresponding to three combustion time t=0.6, 1.1 and 1.4s. Mass injection boundary condition is implemented on the solid propellant surface whereas head-end is closed. The Mach number distributions of gas phase region of propellant with $H_2/O_2/CO_2$ species at t=0.6s is shown in Fig.2

The present solver gives promising results for the prediction of flow parameters and species concentrations of propellant for the rocket motor systems. It is a robust and efficient solver since combustion calculation achieves a residual reduction of over ten orders of magnitude only after over 3000 iterations. The solver is validated from low subsonic to supersonic velocities in combustion chamber and nozzle systems. Although the validation studies are done for premixed fuel-oxidizer systems, it can also be applied to non-premixed fuel-oxidizer

systems containing transversely injected fuel into main stream of oxidizer. However, the solver is still in a developmental state to examine viscous effects.

The full paper will discuss the test cases in details and include more flow and species prediction results inside rocket motors. The 2-Dimensional simulation of gas phase region of RDX solid propellant will be also included in the full paper. Detailed gas phase chemical reactions of RDX is used to find species concentrations near the flame zone. Mass injection boundary condition on RDX propellant surface is used for this test case to simulate flow and species distribution inside full rocket motor. Navier-Stokes solutions of the test cases will be also included in full paper.
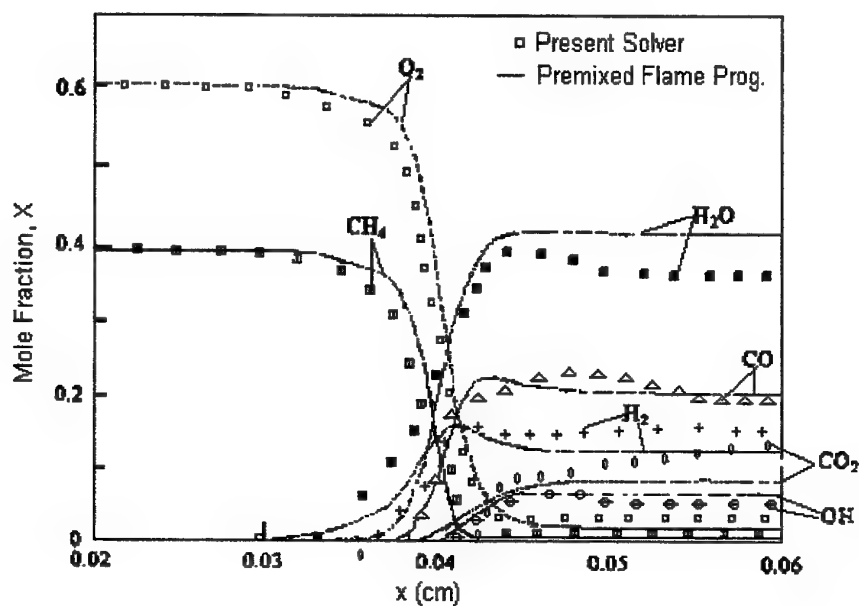
Figure 1. Concentration and temperature distributions in
Methane/oxygen premixed flames of test case

Propellant	Flow Type	Equivalence Ratio	C* Eff (comp.)	C* Eff (exp.)	Isp (sec) (comp.)	Isp (sec) (exp.)
Hydrogen	Reacting	1.95	0.73	0.75	201	215
Hydrogen	Non-reacting	1.95	0.69	-	188	-
Methane	Reacting	1.3	0.70	0.71	122	130
Methane	Non-Reacting	1.3	0.68	-	118	-

Table 1. Test Case 1 Results

Level   1   2   3   4   5   6   7   8   9   A
mach 0.009 0.015 0.029 0.398 0.789 1.174 1.566 1.957 2.298 2.740
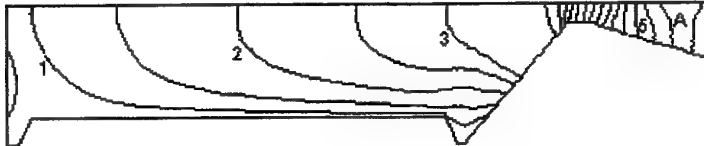
Figure 2. Iso-Mach Number of Test Case 2 at t=0.6s
for $H_2/O_2/CO_2$ Reaction Kinetics

157

REFERENCES:

1. Vuillot F., Yumusak M., Taskinoglu E., Tinaztepe T., " 2-D Internal Flow Applications for Solid Propellant Rocket Motors". Technical Report of RTO-AVT T-108 Support Project, December 1998.

2. Jameson A., Schmidt W., Turkel E., "Numerical Solutions of the Euler Equations by Finite Volume Methods Using Runga-Kutta Time-Stepping Schemes", AIAA Fluid and Plasma Dynamics Conference (14th), AIAA-81-1259, 1981

3. Arc Education Program Report, "Static firing Ballistic Analysis Program",1989

4. Kuo K., " Challenges in Propellants and Combustion", Begell House, pp.743-761,1997

5. Tinaztepe T., Çakiroglu M., Uhrig G., Ribereau D., "Performance Prediction of Solid Rocket Motors", Technical Report of NATO-AGARD PEP T71 Support Project, 1995.

6. Kee, R. J., Grcar, J. F., Smooke, M. D., et.al., "A Fortran Program for Modeling Steady Laminar One-Dimensional Premixed Flames", Sandia Report, SAND85-8240, 1985.

Numerical Simulation of the Vaporization/Combustion of a Single Aluminum Particle in Air

O. Orlandi, Y. Fabignon
Office National d'Etudes et de Recherches Aérospatiales (ONERA)
B.P. 72, 92322 Châtillon Cedex France
Tel: 33.1.69.93.60.18
Fax: 33.1.69.93.61.62
E-mail: orlandi@onera.fr

The purpose of this present study is to investigate the vaporization and the combustion of a single aluminum particle in air. A bidimensional model has been used to describe the effect of the convective stream over a 100 µm diameter particle. The aluminum combustion model in air includes nine reactions in vapor phase. Condensation of the aluminum oxide Al_2O_3 has not been taken into account.

In the literature, several models have been proposed for calculating the burning time and flame temperature of a single aluminum particle in air[1,2,3] but none predict the distributions of physical quantities and none analyze the effect of the convective stream.

Recently, very interesting results of a single aluminum particle combustion in air were published[4]. These numerical simulations concern the two dimensional combustion of a single aluminum particle free falling in air, including the physical processes of aluminum vaporization, finite gaseous reactions, surface reactions, aluminum oxide condensation, dissociation of liquid aluminum oxide and the formation of an aluminum oxide cap.

Even for an isolated aluminum particle, many uncertainties remain in the description of the processes involved in the combustion. The combustion behavior of aluminum particles is strongly dependent upon the nature of the gaseous oxidizing and inert species.

A numerical study was carried out to aid the interpretation of the experimental results in air[2,5,6] and to analyze the effect of the convective stream over the aluminum particle. We assumed that the aluminum particle burns as a vapor phase diffusion flame because of the lower boiling point for Al as compared to the final product Al_2O_3. The condensation process and growth of the final condensed-phase product, Al_2O_3, have currently not been included. Although surface reactions have been proposed by others[4], the present model assumed only vaporization of aluminum at the particle surface. Radiation heat transfer has not presently been considered.

Calculations were carried out by using ONERA MSD code. This code solves compressible, multiple species, Navier Stokes equations in body fitted coordinates. These equations can be represented in integral form as :

$$\frac{\partial}{\partial t}\int_v Q dv + \int_s (F - Fv)ds = \int_v S dv \qquad (1)$$

Q is the vector of conservative variables, F the inviscid flux, Fv the viscous flux and S the source term.

In order to check the accuracy of the computations, a first numerical simulation, at moderate Reynolds numbers for a inert particle, was performed. Results in terms of drag coefficient vs. Reynolds number are shown in Figure 1. A comparison with the standard law given by Schiller and Nauman[7] is presented. A second calculation was performed by introducing a vaporization of aluminum at the particle surface. A typical result is shown, in Figure 2, for the aluminum specie concentration over the particle. A third calculation was carried out taking into account a combustion mechanism. This vapor-phase mechanism contains nine reactions and seven species. It has been reduced from a more complex mechanism.

A more complete discussion of this numerical study will be presented in the full paper.

References

[1]Law, C. K., « A Simplified Theoretical Model for the Vapor Phase Combustion of Metal Particles », *Combustion Science and Technology*, vol 7, n^0 3 –4, 1973, pp. 197-212.

[2]Marion, M., « Etude de la combustion des particules d'aluminium sous pression », Ph. D dissertation, Université d'Orléans, Orléans, France, 1996

[3]Brooks, K. P ; Beckstead, M. W., « Dynamics of Aluminum Combustion », *Journal of Propulsion and Power*, vol 11, n^0 4, 1995, pp 769-780.

[4]Liang, Y., Beckstead, M. W., « Numerical Simulation of Unsteady, Single Aluminum Particle Combustion in Air », AIAA paper 98-3825, July 1998.

[5]Dreizin, E. L., « Experimental Study of Stages in Aluminum Particle Combustion in Air », *Combustion and Flame*, 105, 1996, pp 541-556.

[6]Bucher, P., Yetter, R. A., Dryer, F. L ., Parr, T. P., Hanson-Parr, D. M., Vicenzi, E. P.,« Flame Structure Measurement of Single, Isolated Aluminum Particles burning in Air »,Twenty-Sixth Symposium on Combustion Institute, 1996, pp 1899-1908.

[7]Schiller and Nauman from Clift, R., Grace, J. R., « Bubbles, Drops and Particles », Academic Press, New York, 1978.
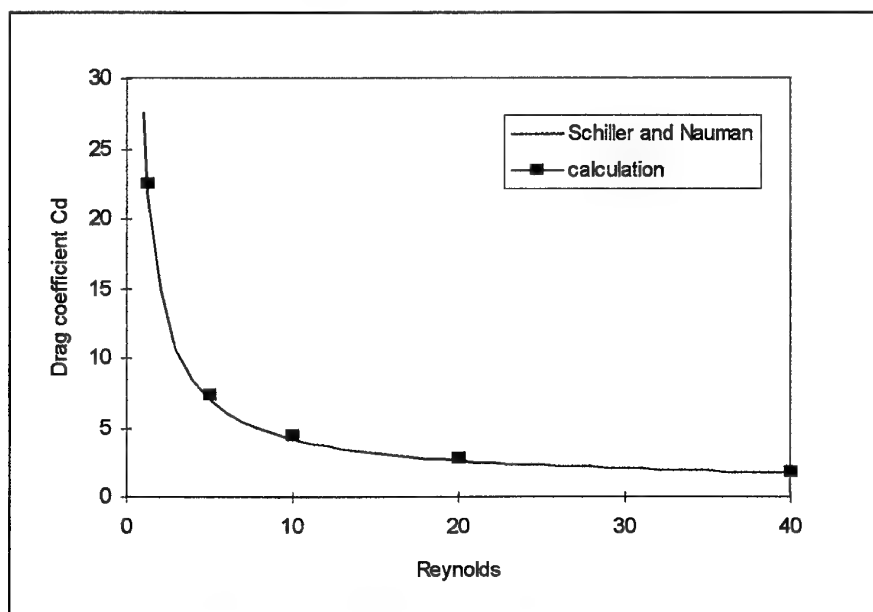
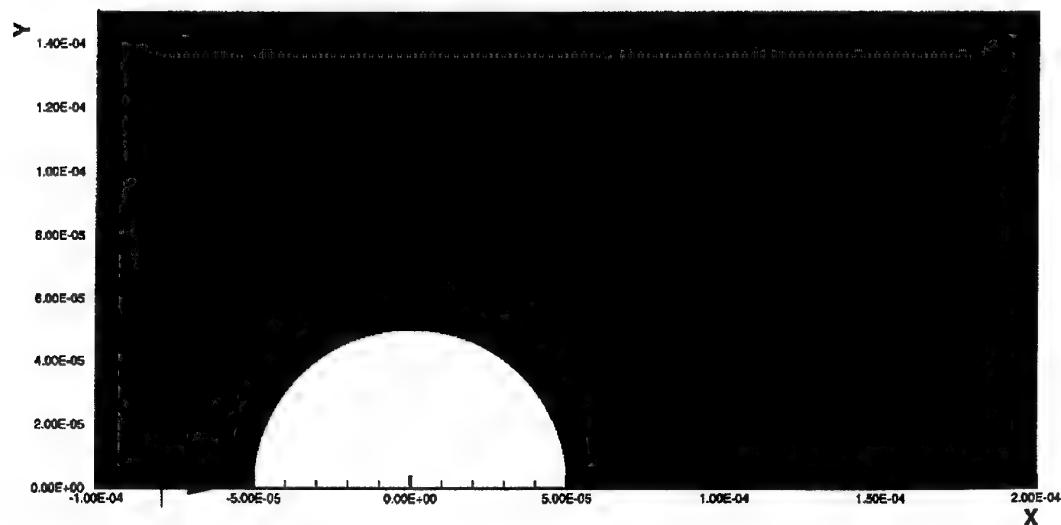Figure 1 -Cd (drag coefficient) calculations vs Reynolds number

Figure 2 -Contour of aluminum specie concentration (Re = 10)

161

THIS PAGE HAS BEEN DELIBERATELY LEFT BLANK

Numerical Analysis of Grain Burnback in Solid Propellants

G. Colasurdo, L. Casalino, and D. Pastrone
Dip. Energetica - Politecnico di Torino
C.so Duca degli Abruzzi 24, 10129 TORINO, ITALY
Tel (39) 011 5644426; Fax (39) 011 5644599;
E-mail: colax@polgc1.polito.it

Mashayek and Ashgriz, in their note "Solid-Propellant Grain Design by an Interface Reconstruction Scheme" (Journal of Spacecraft and Rockets, Vol. 31, No. 5, 1994, pp. 908-910), present an interesting technique for the calculation of the evolution of the solid-propellant grain geometry. The two-dimensional section of a cylindrical grain is discretized by imposing a rectangular grid on the grain. The propellant fraction in each grid cell is sufficient to reconstruct the geometry of the solid-gas interface and to follow its movement due to the combustion.

The authors have recently proposed a different approach which retains the capability of describing the geometry by means of just a single quantity for each cell. They introduce a sort of curvilinear coordinate "s" which runs clockwise along the cell perimeter. In order to define the grain geometry, it is sufficient to move clockwise and record the position of the transition from the solid to the gas phase. It is easily recognized that the gas-solid transition is automatically recorded in an adiacent cell. By recording the position of the interface instead of the fuel fraction, the reconstruction of the geometry is avoided and the discretized interface is implicitly continuous. The replacement of the rectangular frame with a polar grid is straightforward. On the contrary, Mashayek and Ashgriz's approach does not assure the interface continuity, while the extension to a polar frame is not immediate.

The accuracy of this kind of technique depends on the grid size, i.e., the number of cells used to cover the grain section. In the proposed paper, the authors describe an improved procedure which provides a more accurate tracking of the propellant regression and allows the use of coarser grids. Attention is moved from the cell perimeter to the grid lines connecting two adjacent nodes. The precision of the procedure is greatly increased by recording both the position and inclination of the solid-gas interface with respect to the grid lines, as the grain geometry is reconstructed using straight lines and circular arcs. Numerical results are presented in the paper. In particular, the procedure is applied to analyze the combustion of a multi-hole grain that requires the tracking of the merging combustion surfaces.

THIS PAGE HAS BEEN DELIBERATELY LEFT BLANK

Mass Transfer Effects on Sound Propagation in a Droplet-Gas Mixture

J. Dupays
Fundamental and Applied Energetics Department
Office National d'Etudes et de Recherches Aérospatiales (ONERA)
B.P. 72, 92322 Châtillon Cedex France
Tel: 33 1 69 93 60 30
Fax: 33 1 69 93 61 62
E-mail: dupays@onera.fr

The effect of mass transfer on the propagation of a plane acoustic wave in a stagnant two-phase medium is studied theoretically using a continuum formulation. This study extends previous work of Dupays and Vuillot,[1] who considered the vaporization of droplets in their vapor. With a mass transfer model based on a pure thermal conductivity-controlled process, these authors showed that vaporization could be a powerful driving mechanism for acoustic-related instabilities. However, the mass transfer model needs to be more realistic before it can be inferred that the vaporization process can be a major source of instability in a combustion chamber.

In the present work, the droplet cloud is assumed to vaporize in an inert gas so that the mass transfer is essentially controlled by the diffusion process. This problem has been studied in the past, for example, by Marble,[2] Cole and Dobbins[3] and Davidson,[4] who studied sound propagation in fogs. But the form of equations and two-phase exchange terms used in this study differ from that previously presented in the literature. The gas-droplet mixture is not at a saturated state and the gas temperature is higher than the droplet temperature. Therefore, the vaporization process produces by the wave is added to the steady contribution.

The other assumptions are the following:
- The planar wave has a small-amplitude and a monochromatic oscillatory motion,
- The droplet spacing is smaller than the acoustic wavelength so that the droplet cloud can be treated as a continuum,
- The suspension is dilute, that is to say the droplet volume fraction is small,
- The gas-to-droplet density ratio is small,
- The droplet-gas mixture is at rest,
- The vapor and the inert gas are calorically perfects and their properties are differents,
- The droplets are rigid, spherical and of uniform temperature and size,
- The liquid phase contains only one specie.

As the oscillatory motion has small amplitudes, Stokes' laws are used for the momentum and the heat transfer exchange terms. The impact of the vaporization rate on the exchange terms is taken into account via a correction factor term function of the Spalding number, whereas the effects of the oscillatory motion are neglected. Indeed, it can be shown that time-dependent terms in the expression of the force acting on an oscillating sphere and in the expression of the corresponding heat transfer rate can be neglected for very small gas-to-droplet density ratios. This simplification is relevant as far as the oscillation frequency remains relatively low. For the mass transfer exchange term, a classical d^2-law is retained although the use of a quasi-steady model is certainly less justified than for the others exchange terms.

The two-phase equations are linearized by considering small perturbations of the variables from their equilibrium values. Then, the system of linear differential equations is reduced to a system of linear algebraic equations by searching for a solution for the harmonic regime. In other words, it is assumed that all dependent variables of the problem are proportional to $exp[i(Kx - \omega t)]$, where $K = k_1 + ik_2$ is the complex wave number. After some rearrangements, this results in a system of six homogeneous equations, for which exists a non-trivial solution if and only if the determinant vanishes. The resulting complex equation is solved for K and, thus, for the non-dimensional spatial coefficients of attenuation and dispersion of acoustic energy, namely α^* and β^*, defined by

$$\alpha^* = \frac{a_0}{\omega}\alpha \quad \text{where} \quad \alpha = 2k_2$$

$$\beta^* = \frac{a_0^2}{\omega^2}\beta \quad \text{where} \quad \beta = k_1^2 - \left(\frac{\omega}{a_0}\right)^2$$

Typical attenuation and dispersion curves vs the Stokes number $\omega\tau_u$, where τ_u is the dynamic response time, are shown in Fig. 1. Results for vaporizing droplets are compared with the inert case, where there is no mass transfer.

With the adopted vaporization model, the propagation of the acoustic wave is strongly perturbed. The mass transfer amplifies the oscillation levels since the coefficient of attenuation becomes negative for some values of the Stokes number, whereas, without mass transfer, the coefficient is always positive. The impact on the velocity of the wave is also significant and depends strongly of the Stokes number. It is shown that the amplification results essentially from the temperature difference between the gas and the droplets. The first extremum of the « α^*-curve » becomes positive when the two phases are initially in thermal equilibrium (see Fig. 2). Incidentally, this theory gives an estimation of the critical frequency-diameter pairs (where the amplification is maximum) in a straightforward way.

A more complete discussion and a large parametric study will be presented in the full paper.
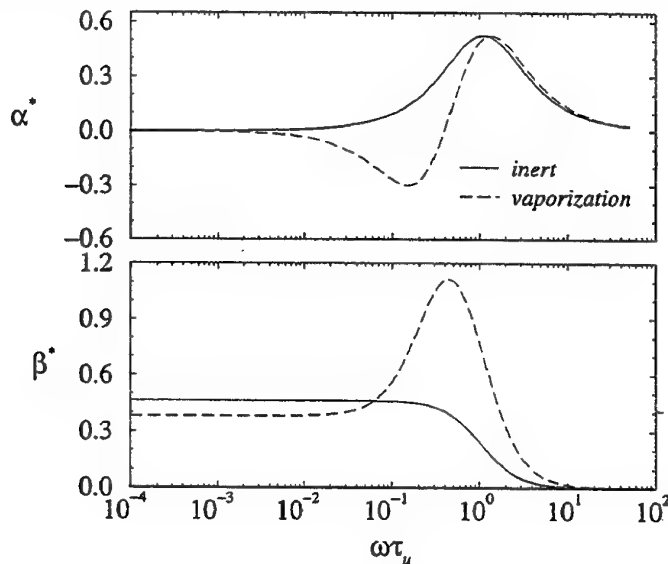

Fig. 1 Attenuation and dispersion vs the Stokes number when the initial temperature of the gas and the droplets is different.
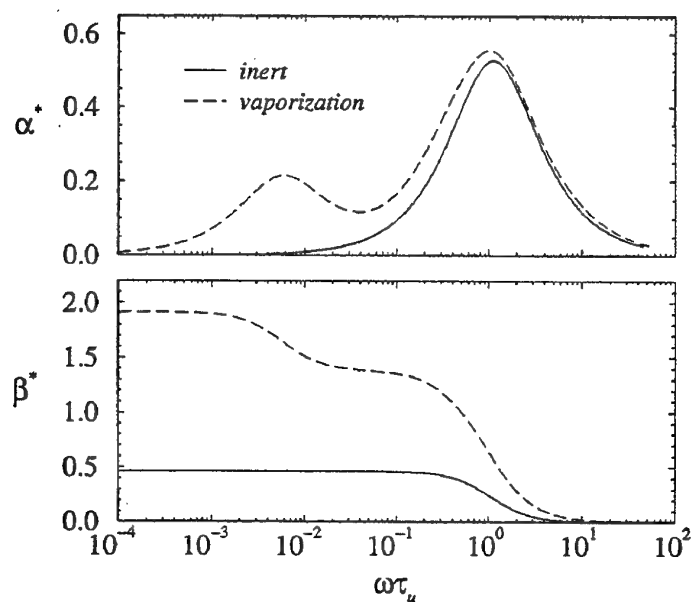
166

Fig. 2 Attenuation and dispersion vs the Stokes number when the gas and the droplets are initially in thermal equilibrium.

References

[1]Dupays, J., and Vuillot, F., "Propagation of an Acoustic Wave in a Two-Phase Reactive Medium," AIAA Paper 98-3696, July 1998.

[2]Marble, F. E., "Some Gasdynamic Problems in the Flow of Condensing Vapors," *Astronautica Acta*, Vol. 14, 1969, pp. 585-613.

[3]Cole, J.E., and Dobbins, R.A., "Propagation of Sound Through Atmospheric Fog," *Journal of the Atmospheric Sciences*, Vol. 27, 1970, pp. 426-434.

[4]Davidson, G.A., "Sound Propagation in Fogs," *Journal of the Atmospheric Sciences*, Vol. 32, 1975, pp. 2201-2205.

THIS PAGE HAS BEEN DELIBERATELY LEFT BLANK

A Numerical Simulation of the Pulse Detonation Engine with Hydrogen Fuels

H.B. Ebrahimi
Sverdrup Technology Inc.
Arnold AFB, TN 37389-6001
Tel: (931) 454-7491
E-mail: Houshang.Ebrahimi@arnold.af.mil

C.L. Merkle
University of Tennesee Space Institute, TN

The present computational study explores some issues concerning the operational performance of Pulse Detonation Engines (PDE) with hydrogen/oxygen propellants. One- and two-dimensional, transient CFD calculations are employed assuming finite-rate chemical kinetic approximations for hydrogen/oxygen combustion based upon eight chemical species and 16 reactions. Methods for ensuring detonation initiation in the computations by means of a specified high-pressure shock initiation region are also examined. To provide insight into the numerical detonation initiation process, the details of initiation at closed and open ends are contrasted. The open-end initiation results help to verify the computational methodology and to gain additional insight into the behavior of the opened/closed solution. The effects of reducing ambient pressure at the exit of the cylinder for multicycle operations are investigated. The results indicate that at sufficiently low ambient pressures, the flow conditions at the exit of the open-ended cylinder remain choked throughout the entire cycle. Two-dimensional calculations were performed to study potential pre-combustion effects due to cyclic refueling processes in the engine. Preliminary results indicate that elevated chamber wall temperatures (approximately 1500 K) simulating multiple cycle heating produce some reactions near the wall, but for the tube lengths studied, only a minimum amount of combustion occurs. Overall, one-dimensional and two-dimensional approximations are in close agreement. Thrust and specific impulse are computed for a variety of conditions to give an indication of potential performance of a PDE.

Figure 1 depicts a detonation chamber with a closed end on the left and an open end on the right. At the start of the computation, the entire chamber is filled with a mixture of unburned hydrogen and oxygen in stoichiometric proportions. For this particular example, the initial pressure of the propellant mixture for the first cycle is 1 atm, while the initial temperature is 300 K. For successive cycles in multicyclic operation, the incoming fuel is set to 300 K, while the pressure takes a level determined by the solution. The ambient pressure outside the detonation tube is taken as 1 atm for most of the computations, and as 0.1 atm for the remainder.

To initiate the detonation in the one-dimensional computations, we use a small 'spark' region like that shown in Fig. 1 adjacent to the closed end of the tube. The pressure and temperature in the spark region are initially raised to elevated levels, P_H and T_H so that a shock begins propagating to the right into the unburned propellant. To prevent combustion in the spark region, it is initially filled with gaseous H_2O.

A series of constant Mach number contours in the vicinity of the closed end are shown in Fig. 2 to illustrate the characteristics during the 'initiation' of the detonation process. At the interface between the spark region and the unburned gases, an expansion fan propagates

toward the closed-end wall and is reflected from it. Simultaneously, a shock wave moves to the right, compressing the unburned gases. The shock is followed by the familiar contact surface. Computational experiments show that an initial pressure of about 30 atm and an initial temperature of 3000 K is sufficient to provide repeatable detonations in the computational solution over multiple cycles for most conditions considered in the present study.

The multicycle operation sequence is summarized as follows:

1. The detonation wave is generated and propagates through the combustion cylinder at supersonic speed.
2. The detonation wave exits the engine, and the series of rarefaction waves generated by the detonation propagate upstream into the closed end of the chamber and push the burned gases toward the exit of the chamber.
3. At the closed end of the tube, the pressure eventually decays to ambient levels so that the impulse falls to zero (and can become negative), and velocity throughout the entire tube approaches zero. This is the terminal condition of the first cycle.
4. At this point, the valves on the closed end of the chamber are opened to allow the chamber to be recharged with fresh fuel and oxidizer.
5. As for the blowdown process, the time required for the refueling process is a function of the PDE length and the velocity at which the gaseous mixture is injected into the engine.

Two-dimensional calculations were performed to assess the effect of the initial starting profile on the detonation behavior. The first solution assumed uniform starting conditions, $P_H = 30$ atm and $T_H = 3000$ K, identical to the 1D case, except that a complete 2D solution procedure was applied. The second case assumed a circular profile in the spark initiation region to test the effects on non-one-dimensional spark initiation. These results (Fig.3) indicate that 1D and 2D solutions assuming uniform start conditions are very similar.
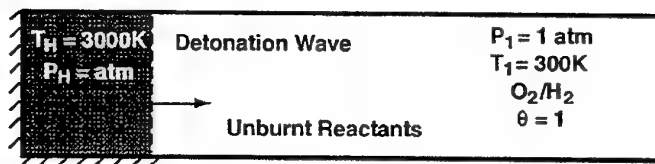

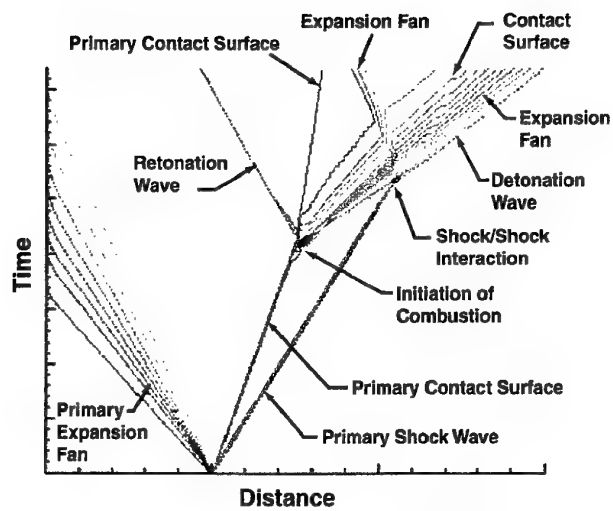Fig.1: Schematic of detonation from closed end cylinder
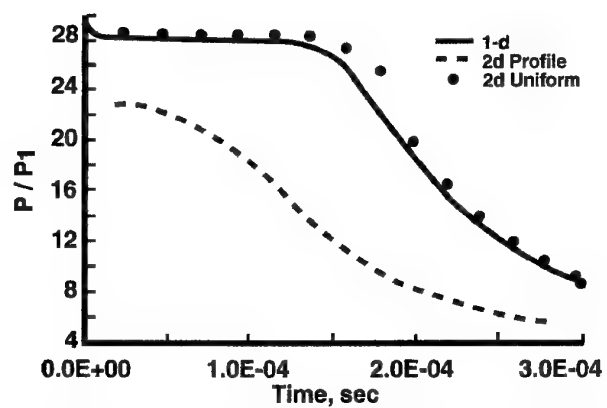
Fig.2: Detonation Shock wave behavior.

Fig. 3: Pressure Profile comparison at closed end.

THIS PAGE HAS BEEN DELIBERATELY LEFT BLANK

AREA 10:

PROPELLANT AND MOTOR STABILITY

SESSION CO-CHAIRS:

PROF. FRED CULICK
AND
PROF. SUBRAMANIAM KRISHNAN

Summary of Multi-Disciplinary University Research Initiative in Solid Propellant Combustion Instability

F.S. Blomshield
Naval Air Warfare Center
Code 4T4320D, Propulsion Research Branch
China Lake, CA 93555
Tel: (760) 939-3650
Fax: (760) 939-6569
E-mail: blomshieldf@navair.navy.mil

This paper presents an overview of a program to further the understanding of combustion instability in solid rocket motors. The multi-disciplinary program consists of 16 universities performing work in combustion of solid propellants and ingredients, metal combustion, chemical kinetics, steady and nonsteady combustion modeling, combustion response measurements and chamber gas dynamics. The overall objective of the program is to determine the mechanistic links between fundamental combustion processes and unsteady rocket motor chamber acoustics. The program is currently in the fifth and final year. This paper will provide a brief overview of the program and the various types of research taking place.

THIS PAGE HAS BEEN DELIBERATELY LEFT BLANK

Examples of Unsteady Combustion in Non-Metallized Propellants

M.W. Beckstead, K.V. Meredith
Brigham Young University, Provo, Utah
Tel: (801) 378-6239
Fax: (801) 378-6239
E-mail: mwb@byu.edu

F.S. Blomshield
NAWC, China Lake, CA

For over thirty years, the T-Burner has been the *de facto* standard for determining the unstable response of solid propellants. This paper reviews some of the different approaches that have been used, and briefly summarizes advantages and disadvantages of the different techniques. Data from a variety of sources has been reviewed and is summarized showing the effect of various test conditions and propellant formulation variations. Much of the data taken in the 60's and early 70's were with so-called research propellants, with relatively low solids loading and usually monomodal AP as the oxidizer. Later, data was obtained with propellants containing solids loading, more typical of practical propellants. Several distinct differences were observed in the data for the different types of propellants. First, the higher solids loading propellants typically had response values on the order of one, which was lower than the values measured for the lower solids loading research propellants. This trend was verified by systematically varying the solids loading in a series of propellants. The data indicated that the response does indeed decrease with increased solids loading.

Data varying AP particle size distributions indicate that either a greater amount of fine AP, or decreasing the size of the fine AP, usually increases the propellant response. A significant reduction in the response can be achieved by reducing the amount of fine AP or increasing the size of fine AP in a formulation, while holding burning rate constant either by adding a catalyst or by varying the overall AP size distribution.

A significant amount of T-burner data has been obtained for reduced smoke propellants incorporating stability additives. The most common additives used are ZrC, graphite flake, Al_2O_3, and various other solid particles. Definitive T-burner tests have been performed showing quantitative verification of the particle damping theory. The dependence of particle damping on concentration, particle size, and frequency, all appear to be consistent with the theory. The data indicates that additives can provide significant particle damping, and most often, also reduce the propellant response. Although the latter observation has not been explained on a quantitative basis, the general observation is significant, as it provides the propellant chemist with an additional degree of freedom in formulating propellants to avoid combustion instability. Data obtained from systematic motor testing verifies that additives can have a significant effect on motor stability, thus linking T-burner test results to motor application.

Data from double base propellants indicates a much broader response over a wide frequency range than is normally observed with composite propellants. This implies that double base propellants are more unstable than composite propellants at higher frequencies, which should

correlate with instability in tangential modes in motors. This trend seems to be consistent with observed motor data.

Active Damping of Combustion Instabilities With Oscillatory Liquid Fuel Sprays [P]

E. Lubarsky[1], Y. Neumeier[2], and B.T. Zinn[2]
School of Aerospace Engineering
Georgia Institute of Technology
Atlanta, Georgia 30332-0150
Tel: (404) 894-3033
Fax: (404) 894-2760
E-mail: ben.zinn@aerospace.gatech.edu

This paper describes results of recent studies of active control of combustion instabilities by periodic modulation of a fuel stream's injection rate into the combustor. The developed active control system (ACS) consists of a sensor that measures the combustor pressure, an observer that determines the amplitudes, frequencies and phases of the unstable combustor modes in real time, a controller that determines the phase and gain of the control signal and a fuel injector actuator that modulates the flow rate of fuel stream into the combustor. Apparently, this ACS controls the instability by either reducing the driving provided by the primary combustion process and/or generating secondary combustion process heat release oscillations within the combustor that are out of phase with respect to the unstable combustor oscillations and, thus, damp the instability (following Rayleigh's criterion). Earlier studies under this program have shown that this ACS can effectively damp combustion instabilities by modulating the injection rate of a gaseous fuel. This paper describes results of a follow on, ongoing, program that is investigating active control of combustion instabilities with liquid fuels. These studies characterized the oscillating liquid spray flames and investigated their application in adaptive, closed loop, control of combustion instabilities. The overall objective of this program is to determine whether liquid fuels can be used in active control of combustion instabilities and the conditions under which their damping is optimized.

In pursuit of the above stated objectives, initial studies under this program investigated:
1. The dependence of the characteristics of "controlled" (oscillatory) combustion processes upon the mode of operation of the liquid fuel injector actuator and spray properties and
2. Active control of combustion instabilities with liquid fuel sprays. Both studies were conducted in the experimental setup shown in Fig. 1, which was developed in the course of this study. It consists of liquid fuel and air injection systems, a liquid fuel injector actuator that can rapidly modulate the injection rate of a liquid fuel stream (using a magnetostrictive actuator), a quartz combustor and optical diagnostics that can measure the liquid sprays properties (e.g., droplet size and velocity distributions) and the characteristics of the combustion process. Initially, the dependence of the characteristics of oscillatory combustion processes and their sprays upon the frequency of oscillations and duty cycle (i.e., fraction of the cycle during which fuel is injected into the combustor) was investigated. These were

[1] Research Engineer and AIAA Member
[2] Senior Research Engineer and Adjunct Professor
[3] David S. Lewis Jr. Chair, Regents Professor, and AIAA Fellow

flames, high-speed combustion process visualizations and measurements of spray properties under cold flow conditions. These data were then analyzed to determine the conditions under which active damping of combustion instabilities by the investigated flame would be optimized. In the second study, closed loop control of combustion instabilities in the developed setup was investigated. First, conditions under which instabilities were spontaneously excited in the setup were detennined. Next, the ACS was used to modulate the fuel injection rate with the frequency of the most unstable mode and a phase the optimized the damping. The latter was determined adaptively (e.g., phase and gain of the control signal were initially assumed and then adjusted based on the system's response to the control action).

The results of these studies show that: 1. Modulation of a liquid fuel spray can be effectively employed in active control of combustion instabilities, 2. The effectiveness of the damping process strongly depends upon the mode of operation of fuel injector actuator, and 3. Adaptive approaches can be used in active control of combustion instabilities. In conclusion, these results clearly show that liquid fuels can be effectively employed in active control of combustion instabilities and that the active damping process can be optimized with judicious choice of the mode of operation of the liquid fuel actuator and phase of the control signal.

178
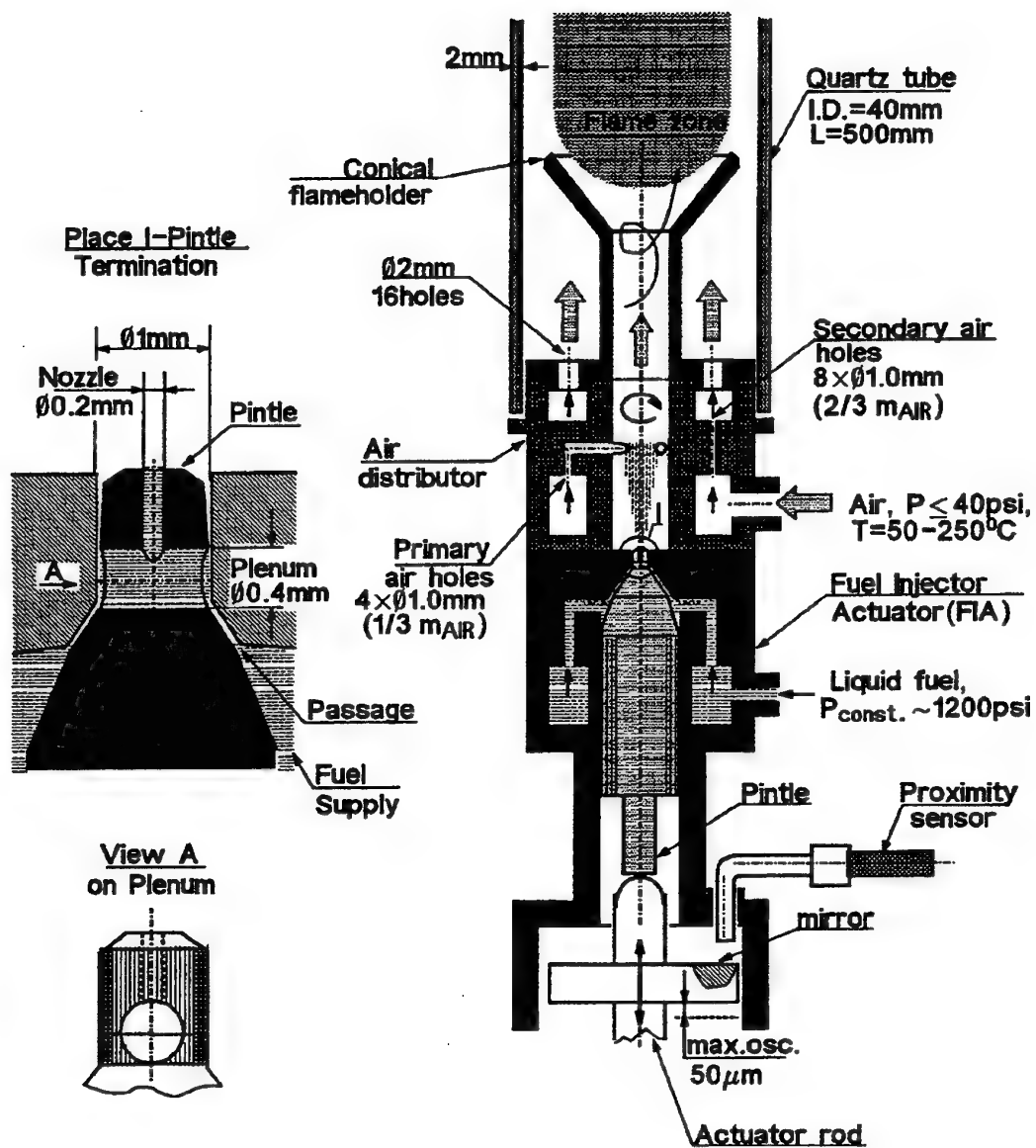
Figure 1. A schematic of the developed experimental setup.

THIS PAGE HAS BEEN DELIBERATELY LEFT BLANK

Limit Cycles for Solid Propellant Burning Rate at Constant Pressure

B.V. Novozhilov

Institute of Chemical Physics, Russian Academy of Science
4, Kosygina Street
Moscow, 117977 Russia
Tel: 007-095-432-8575
Fax: 007-095-137-6130
E-mail: boris@center.chph.ras.ru

F. Cozzi, L.T. DeLuca
Dipartimento di Energetica, Politecnico di Milano, Milan, Italy

Any burning propellant features an intrinsic combustion stability boundary. In the linear approximation of the problem, close to this boundary the propellant, during combustion at a constant pressure, is an oscillating system with some natural frequency and damping parameter. On one side of the stability boundary, the oscillating amplitude is observed to grow with time while on the other side it decreases. A propellant, however, is a nonlinear oscillating system. Both the heat conduction equation and non-steady burning laws, needed to consider any non-steady propellant burning processes, are nonlinear. Thus, one expects limit cycles at constant pressure to reveal the nonlinear nature of the underlying physical problem. Experimental data also report showing the existence of self-sustained oscillatory propellant burning at constant pressure, for a variety of operating conditions and diagnostic techniques.

The objective of this work is to analyze the limit cycle problem in the framework of the Zel'dovich-Novozhilov (ZN) theory. The first two oscillating modes are considered with the third order nonlinearity of the heat conduction equation and non-steady burning laws. Three principal nonlinear effects are involved in the analytical study:

a) the first mode self-interaction that gives second order corrections to the zeroth and second mode;
b) the zeroth and first modes' interaction to give third order corrections to the first mode;
c) the first and second modes' interaction to give third order corrections to the first mode.

Equations for the limit cycle amplitudes of all modes are obtained from which it is also possible to find a limit cycle frequency. Three propellant models with different steady state burning laws have been studied. The simplest one features linear non-steady burning laws, the second one contains only two parameters, and the third one - the most realistic - contains three parameters.

The results of the work may be formulated in terms of the derivatives of the steady state burning rate u^0 and the surface temperature T_s^0 with respect to the ambient temperature T_a:

$$k=(T_s^0 - T_a)[(dlnu^0)/(dT_a)], \qquad r=(dT_s^0)/(dT_a),$$

and the value of the frequency ω^* at the stability boundary

$$\omega^* = \sqrt{k} / r^*, \qquad\qquad\qquad r^* = (k-1)^2/(k+1).$$

There are two branches of the limit cycles close to the stability boundary.

The a-branch exists in the region where steady state combustion is linearly unstable, $r < r^*$. The amplitudes of the first and second modes grow with increasing value of r^*-r. At the stability boundary the amplitudes are equal to zero. The limit cycle frequencies at this branch are close to the natural frequency ω^*.

If the steady state burning regime is linearly stable, $r > r^*$, another branch, the b-branch, appears. The first mode amplitude increases from zero at the stability boundary with growing the difference $r-r^*$. The second mode amplitude, however, is approximately constant and has a nonzero value even at the stability boundary. The limit cycle frequencies at this branch, $\omega^*/2$, are close to one half of the natural frequency.

The zero mode (DC shift) in both cases is negative and proportional to the square of the first mode amplitude.

For physical reasons one may expect the limit cycles at the a-branch to be stable. The opposite is, probably, true for the b-branch.

Characteristic Features of Burning Rate
Response Functions of Solid Propellants: A Review

A.A. Zenin, S.V. Finjakov
Semenov Institute of Chemical Physics,
Russian Academy of Sciences
4 Kosygina Street
117977 Moscow, Russia
Tel: (007-095) 939-7355
Fax: (007-095) 938-2156
E-mail: anatoly@zenin.msk.ru

Burning rate response functions to acoustic pulses of solid propellants obtained by calculations in the framework of the Zel'dovich-Novozhilov approach are reviewed. The response functions are obtained by calculations on the base of experimentally received dependencies of burning rates and burning surface temperatures on pressure and initial temperature. Data for monopropellants HMX, ADN, and GAP, and for modern double-base propellants and propellant mixtures of nitramine-thermoplastic elastomers are used. Characteristic points of real and imaginary parts of the response functions and their dependencies on pressure and initial temperature are described and discussed. Results of resonance frequencies obtained at maximum values of the real parts of the response functions and at zero values of the imaginary parts of the that functions are analysed. A significant influence of the liquid layer at the burning surface on the response functions is pointed out. The effect of nitramine additions to propellants is noted and discussed. The work considers peculiarities of pulsating behaviour of burning rates of different substances at small perturbations. Future tasks are mentioned.

THIS PAGE HAS BEEN DELIBERATELY LEFT BLANK

HMX T-Burner Pressure Coupled Response at 200, 500, and 1000 psi

J.C. Finlinson, R. Stalnaker, F.S. Blomshield
Naval Air Warfare Center Weapons Division
Research and Technology Group, Code 4T4320D
China Lake, CA 93555
Tel: (619) 939-3814
Fax: (619) 939-6569
E-mail: FinlinsonJC@navair.navy.mil

This paper contains continuing pressure coupled combustion response T-burner measurements on pressed pellets of HMX. Pellets of pure oxidizer were pressed with a donut die to allow a 0.45 inch center hole required for pressure pulsing. The pellets were burned in T-burner pipes in lengths of 10, 15, 22, 36, and 50 inches at pressures of 200, 500, and 1000 psi. HMX oscillated spontaneously in the T-burner at 200 and 500 psi, but required pulsing at 1000 psi. As the lowest pressure of 200 psi, HMX oscillated spontaneously with growth rates of 2.4 to 11.8 s-1. At 500 psi, the growth rates ranged from -5 to 31 s-1; and at 1000 psi, the growth rates ranged from -12 to +4 sec-1. This data is of special interest to instability modelers, especially those doing transient monopropellant modeling, as there has not been any pure ingredient pressure coupled response data.

THIS PAGE HAS BEEN DELIBERATELY LEFT BLANK

The Stationary Modes of the Reaction Front and Their Stability for Solid Media with Regard to Chemically Induced Internal Stresses and Strains

A. G. Knyazeva
Institute of Strength Physics and Material Science
ISPMS, pr. Akademicheskii 2/1, Tomsk, Russia, 634021
Tel: 7-382-2-286876
Fax: 7-382-2-25-95-76
E-mail: anna@ispms.tsc.ru

It is well known, that some solid-phase chemical reactions may proceed in various modes, including slow and quick ones. On the one hand, it depends on the conditions of the reaction initiation, on the other hand, it is determined by the specific features of the solid-phase conversions. It is known also from the thermal combustion theory that the complex kinetic scheme of reactions and heat losses in the environment control the features of the combustion wave propagation. So, two or more conversion regimes are possible in this case (that connects immediately with the additional heat loss or heat release in the combustion wave), and we may talk about the nonuniqueness of the conversion mode. In this paper, it is shown that factors of other nature may also lead to the nonuniqueness of the modes of the front propagation. Mechanical stresses and deformations accompany practically any solid-phase chemical reaction and may have an effect on its course by different ways. The external mechanical action may be absent. Some particular problems on the stationary propagation of the front of the solid phase chemical reactions were analyzed, see for example [1-5]. So, in the coupling model, taking into consideration only thermal stresses, it has been shown that the existence of various modes may be connected with the possibility to initiate the reaction by different ways - due to the change of the internal energy and due to the work of mechanical forces under a chemically reacting system. Two ways of energy transfer lead also to principally different modes of the solid phase reaction. One of them is the thermal combustion regime. The second is "solid-phase detonation". It has been demonstrated also, that the fracture in the reaction zone leads to the appearance of new conversion modes. Similar models allow to explain the existence of quick solid phase stationary regimes for decomposition reactions of explosives, metallic-thermal reactions in the mixtures, some endothermic reactions, and low temperature radical reactions. The asymptotic analysis of some problems, investigations of the stability of different regimes with the help of the perturbation method, and some numerical solutions are carried out.

1. Timokhin A.M. and Knyazeva A.G., Modes of reaction front in a coupled thermal and mechanical model of solid phase combustion, Chemical Physics, 1996, No 8.
2. Knyazeva A.G., The front rate of the simplest solid phase chemical reaction and the internal mechanical stresses, Fizika Goreniya i Vzryva (translated in USA, Combustion, Explosion, and Shock Waves), 1994, No 1.
3. Knyazeva A.G. and Dyukarev E.A., Stationary wave of the chemical reaction in deformable medium with finite relaxation time, Fizika Goreniya i Vzryva, 1995, No 3.
4. Knyazeva A.G. and Dyukarev E.A., The thermomechanical model of self-similarly propagation of low temperature reactions with the fracture, Fizika Goreniya i Vzryva, 1998, No 4.

5. Knyazeva A.G., Kidin N.I., and Istratov A.G., On the thermal-elastic stability of samples at SHS-wave propagation, PAC RIM Meeting Program, Abstracts, November 7-10, 1993, Honolulu Hawaii 735 Ceramic Place Westerwille, Ohio 43081 SXVIII-53-93.

AREA 9:

COMBUSTION DIAGNOSTIC TECHNIQUES

SESSION CO-CHAIRS:

PROF. ALDO COGHE
AND
PROF. VLADIMIR. ZARKO

Critical Assessment of the Microwave Method for Measuring Steady-State and Transient Regression Rates of Solids

V.E. Zarko, V.V. Perov, and V.N. Simonenko
Institute of Chemical Kinetics and Combustion
Russian Academy of Sciences,
Novosibirsk 630090, Russia
Tel: 7-3832-332292
Fax: 7-3832-342350
E-mail: zarko@ns.kinetics.nsc.ru

It is known that for studying transient combustion of solids, the experimental technique needs to provide spatial resolution for displacement of the burning (regressing) surface on the order of several microns. At the present time, the only experimental technique that ensures such resolution is the microwave (MW) method which may have different design options. Unfortunately, despite several decades of development, there is nothing available in the open literature concerning the detailed analysis of technical possibilities or recommendations for correct use of the MW method. This paper is intended to discuss principal design solutions for measuring quasi-steady and transient regression rates, to analyze restrictions and sources of error, and to formulate recommendations for correct treatment and optimization of the measurement system.

Historically, this method started in the 1960s with use of 3-cm (Shelton, 1967), then 8-mm (Wood, 1970) and recently, 2-mm (Zarko et al., 1997) wavelength radiation. It follows from the experimental works that the shorter the wavelength, the better the spatial resolution of the method. However, there is attenuation due to absorption and scattering of the radiation signal that depends directly on the metal content in the solid propellant and on the properties of the components. This factor imposes restrictions on the applicability range of the MW method. Thus, for a typical metal content (ca. 16-20%) in solid propellants with a hydrocarbon binder, only 3-cm or 8-mm MW radiation can be used to efficiently measure the regression rate. The 2-mm MW radiation can be used most effectively for propellant formulations with metal content not exceeding 5%.

Another important point is the choice of the measurement principle. Usually, the radiation energy is introduced from the cold end of the propellant sample and reflects from the burning surface. The signal is then recorded for deducing the distance burned. The reflected wave can be mixed with a non-disturbed wave that gives amplitude modulation. The resulting sinusoidal signal allows the determination of the travel time corresponding to the quarter of the wavelength moved through by the combustion front of the propellant (up to ca. 250 microns when using MW wavelength of 2 mm). In the case of continuous recording of the phase of the reflected wave, one may measure the instantaneous regression rate. Two approaches for continuous measurement of the phase of the microwave signal are discussed. A spatial resolution of several microns can be achieved with a MW radiation of 2-8 mm wavelength.

In addition to the two common principles of regression rate measurement, some other possibilities of using the wave passing through the propellant sample, or reflected from the burning surface from the incident wave coming from the gas flame side, and other configurations of a measurement scheme are analyzed.

The potential sources of error due to non-planar (rough) burning surface, scatter of electromagnetic wave on metallic particles, attenuation of radiation in finite-length propellant samples, and reflection of radiation from the waveguide elements and high-pressure vessel walls are analyzed. Some methods for diminishing and eliminating the disturbing factors are suggested. Recommendations for optimization of parameters of the propellant samples and microwave measurement system are discussed.

Laser Recoil Experiments

F. Cozzi, L. Asa, S. Palozzo, R.O. Hessler
Laboratorio di Termofisica, Dipartimento di. Energetica
Politecnico di Milano, 20133 Milan, MI, Italy
Tel.: 39-02-2399.3872; Fax: 39-02-2399.3940;
cozzi@clausius.energ.polimi.it

Experimental characterization of propellant combustion response to small pressure oscillations is a key point in the design of a rocket motor. In this work, an alternative approach has been taken by evaluating the radiation driven frequency response of the recoil force, R_{fq}, instead of the pressure driven frequency response. The implemented radiant source is a CO_2 laser and its instantaneous flux is monitored through a fast infrared detector. The radiant laser flux has been time modulated using different waveform (chirp, sine and pseudorandom patterns), a 25% modulation depth, referenced to the mean flux level, has been usually enforced. Tests have been carried in a nitrogen flow at ambient pressure. The investigated frequency range spans from 5 Hz to about 700 Hz. A PCB piezoelectric force transducer is used to measure the unsteady recoil force, and care is addressed to minimize noise (electrical, acoustical and vibrational). The signals are pre-amplified, anti-aliasing analogue filtered, and simultaneously sampled by a 16 bit acquisition board. A software developed in LABView^{TM} framework is used for signal analysis.

For several tested material, both R_{fq} magnitude and phase were measured. The highest response is shown at low frequencies, corresponding to the condensed phase thermal relaxation time. The composite propellants tested have shown a peak in the response at about 100 Hz, which is probably related to the propellant condensed phase heterogeneity. To clarify its nature further experiments are currently in progress. All tested propellant have shown a further peak at about 500 Hz. The results collected till now suggested as a cause; a resonance in the pedestal-transducer assembly.

Higher background noise of recoil signal during combustion as compared to the pre-ignition period has been observed in modulated laser recoil test. Further tests conducted at constant heat flux have shown the same behavior. Propellant heterogeneity, irregular burning surface, and non ideal experimental conditions could be all responsible for this higher noise level.

THIS PAGE HAS BEEN DELIBERATELY LEFT BLANK

Determination of the Temperature of Condensed Particles Within the Flame by Their Radiation

I.S. Altman[*], Yu.L. Shoshin
Institute of Combustion & Advanced Technologies, Odessa State University
Dvoryanskaya 2, 65026, Odessa, Ukraine
Tel: (380-482) 441398, Fax: (380-482) 219981
E-mail: ialtman@tm.odessa.ua

D. Lee, J.D. Chung, M. Choi
National CRI Center for Nano Particle Control, School of Mechanical and
Aerospace Engineering, Seoul National University, Seoul 151-742, Korea

The knowledge of the combustion temperature is very important for understanding the processes occurring within flame. There exist many different methods of the determination of this temperature. These methods could be separated into two groups: 1) the gas temperature determination, and 2) the condensed particle (CP) temperature determination. Usually it is assumed that there is no the difference between the temperatures obtained by these methods, when the sizes of CP are small ($\leq 0.1 \mu m$), i.e. that the gas temperature and the condensed phase one are the same. However, according to the new result, it recently appeared [1,2] the difference between CP and gas temperatures could be essential. At least for the metal containing flames, where the oxide particles are formed, CP temperature can be above and below the gas temperature, depending on the stage of the oxide particle growth [2]. In this case, the local CP temperature concept loses its meaning as within each small volume of CP at the different stage of growth exists.

In this connection, let us dwell upon the methods of the temperature determination of CP within the flame. There is the two-color method or more advanced the multi-color method. These methods are based on the comparing of the flame luminosity $I(\lambda)$ (continuous spectrum) with the Planck function. The slope of $I\lambda^5$ upon $1/\lambda$ gives the inverse temperature. However, such experiments on the temperature determination are carried out, usually in the narrow spectral interval in the visible region. In case we measure the flame luminosity in ultraviolet and restore the flame emissivity $\varepsilon(\lambda)$ using the temperature obtained by the above mentioned method, we obtain that the emissivity abruptly increases in ultraviolet [3]. In our opinion, this increase is caused by the existence of CP with the temperatures above the mean temperature obtained from the flame spectrum.

The present work is devoted to the determination of the CP temperature distribution from the flame luminosity. The latter one could be written as $I(\lambda) = \int_0^\infty f(T) I_0(\lambda, T) dT$, where $I_0(\lambda, T)$ is the Planck function, and $f(T)$ is the function describing the CP temperature distribution. Of course, when the temperatures of all CP are equal, then $f(T) = \varepsilon \cdot \delta(T - T_p)$.

In this work the procedure of the function $f(T)$ restoration is developed. For the known luminosity of Al dust flame, the temperature distribution is obtained. This distribution corresponds to the temperature dependence of the oxide particle temperature upon the stage of

the particle growth predicted in [1]. The width of distribution is about *1000 K* for each small volume within the flame front.

Thus with the help of the flame luminosity in ultraviolet, it is possible to obtain the CP temperature distribution. The method of the temperature distribution restoration could be used for the hydrocarbon flame containing soot particles where the emissivity increase in ultraviolet also is observed [4].

1. I. S. Altman. On Condensation Growth of Oxide Particles during Gas-Phase Combustion of Metals. 17-th ICDERS, Heidelberg, Germany, July 25-30, 1999, CD, paper 107, submitted in *Combustion Science and Technology*
2. I. S. Altman. On Heat Transfer Between Nanoparticles and Gas at High Temperatures. *Journal of Aerosol Science*, 1999, 30, S1, p. S423-S424.
3. A. V. Florko, I. S. Altman, N. I. Poletaev. On Possibility of End Product of Aluminum and Magnesium Combustion Dispersivity Determination by the Radiation Spectrum. 10-th All-Union Symposium on Combustion and Explosion, Chernogolovka, Russia, September, 1992, p. 79-81 (in Russian).

4. B. Block, W. Hentschel, W. Ertmer. Pyrometric Determination of Temperature in Rich Flames and Wavelength Dependence of Their Emissivity. Combustion and Flame, 1998, 114, p.359-369

Comparison of PIV and Colour-Schlieren Measurements of the Combustion Process of Boron Particle Containing Solid Fuels Slabs in a Rearward Facing Step Combustor

A. Thumann and H.K.Ciezki
DLR Space Propulsion
Lampoldshausen, Langer Grund
D-74239 Hardthausen, Germany
Telephone: +49(6298)28-321, Fax: +49(6298)28-176, E-mail: Helmut.ciezki@dlr.de

The addition of metal and non-metal particles, like aluminum or boron, to the commonly used hydrocarbon type binders, as for example HTPB (hydroxyl terminated polybutadiene), is of interest for air breathing propulsion systems like ramjets and ducted rockets. They offer the possibility to build compact engines, or engines with better flight performances due to their theoretically high energy release per unit volume. Therefore boron is of special interest because it has the highest value. [i-iii].

In order to get a better insight into the governing processes in a ramjet combustor, a plane rearward facing step combustor has been chosen as test facility. The experiments have been conducted under ramjet relevant conditions concerning the air inlet temperature and velocity. Windows on three sides of the combustion chamber give (laser-)optical diagnostic tools a direct access to the combustion process. These windows are equipped with a N_2-protection flow to minimize window pollution. The solid fuel slabs consists of HTPB R 45 M, IPDI and 30% by weight of boron particles. These slabs of 200 mm length and 100 mm width are mounted flush to the combustor bottom immediately behind the rearward facing step of 20 mm height. Vitiated hot air is produced by heating the air flow with a H_2-O_2-burner. This flow is made homogeneous by two flow straighteners and sieves.

Various intrusive and non-intrusive diagnostic tools, e.g. sampling probes, LDA, CARS, Two-colour-pyrometry, have been used to investigate the multiphase combustion process in the step combustor. In order to get a characteristic of the flow-field and the combustion process, all these 0-d diagnostic techniques are very time-consuming. In our highly turbulent combustion process, only probability density function's are achieved. A visualization of the turbulent multiphase mixing and combustion process, however, can be realized with two-dimensional measurement techniques.

The colour coding of the Colour Schlieren technique, which is independent of the particle concentration in a first assumption [iv], shows the highly turbulent structure of the combustion process. The different colours present different refractive index gradients caused by density gradients, as well as changes of the species distribution of the gas phase due to the combustion process. A study of the particle movement in the flow or the ejection of particle assembles or bigger flakes from the burning fuel-slab is not possible with the Colour-Schlieren setup. A direct observation of the burning particles, however, is possible with the Mie-scattering technique. Here we used Particle Imaging Velocimetry (PIV) as a variation of these technique, also showing the movement of the reacting particle phase in the combusting flow.

The high time resolution of both measurement techniques (~13 µs for Schlieren and 10 ns for PIV) show a quasi frozen state of the flow. For the PIV measurements, the time between the two laser-pulses was set to 7 µs. The observation area for the PIV-measurement was 50x40 mm, whereas the Colour Schlieren setup visualized nearly the whole combustor at the same time. Both measurement techniques observed large scale vortical structures. In Fig. 1 a

195

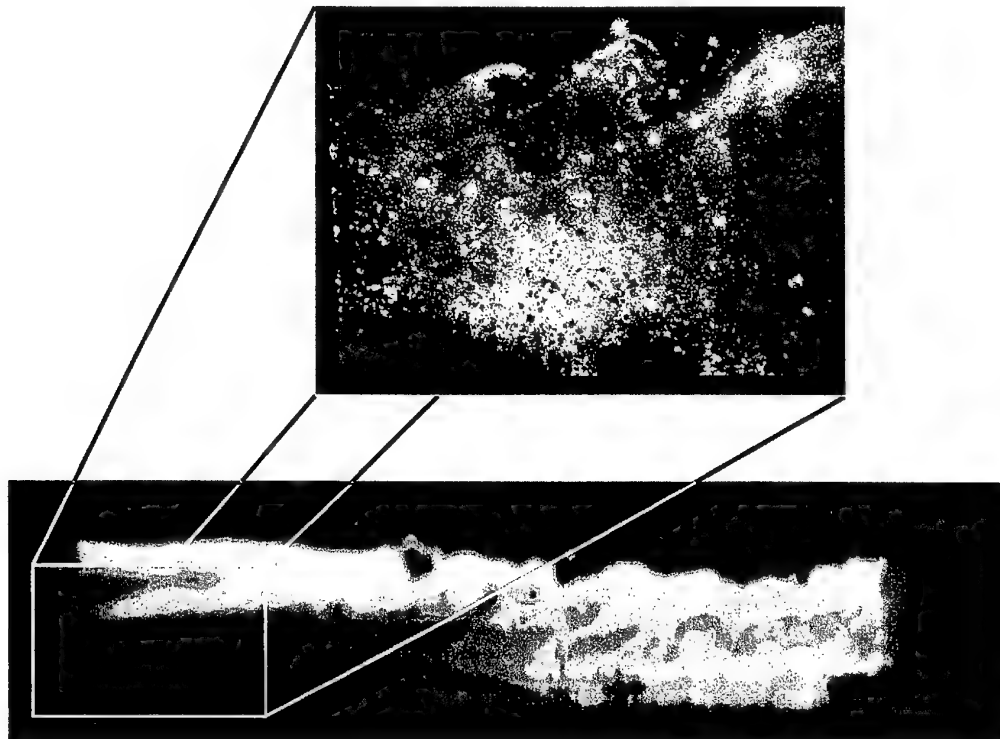Schlieren picture of the combustion process is shown together with a PIV measurement under same conditions.

Fig. 1: Schlieren-Image (bottom) of the combustion process and PIV-Measurement (top) under same conditions.

References
[i] Y.M. Timnat, Recent Developments in Ramjets, Ducted Rockets and Scramjets, Prog. Aerospace Sci., Vol. 27, 1990
[ii] A. Gany, Combustion of Boron-Containing Fuels in Solid Fuel Ramjets, in: Combustion of Boron-Based Solid Propellants and Solid Fuels (K.K. Kuo, R. Pein, Eds.), CRC Press, Boca Raton, 1993
[iii] M.K. King, A Review of Studies of Boron Ignition and Combustion Phenomena at Atlantic Research Corporation over the past Decade, in: Combustion of Boron-Based Solid Propellants and Solid Fuels (K. K. Kuo, R. Pein, Eds.), CRC Press, Boca Raton, 1993
[iv] H.K. Ciezki, Investigation of the Combustion Behaviour of Solid Fuel Slabs in a Planar Step Combustor with a Colour Schlieren Technique, AIAA-99-2813, 35th AIAA Joint

Quick Spectroscopic Diagnostics for the Flame Temperature

Wenhua Zhao, Shuguang Zhu, Kuo Tian, Di Liu
Department of Engineering Mechanics, Tsinghua University
Beijing, China (100084)
E-mail: zhaowh@mail.tsinghua.edu.cn

A quick spectroscopic diagnostic system (see Figure 1) for the flame temperature is set up in this paper. It consists of optic imaging system, scanning system, dispersive system, photoelectricity conversion cell, operational amplifier, a computer-based data collection system, and data processing. The temperature profile varying with the time can be quickly measured with this system. The intensity of up to four spectral lines can be simultaneously measured.

The satisfied results have been obtained in measuring the temperature of two kinds of flame (the transparent optics-thin flame and the flame with enough solid particles) by the system.

1. The flame of coal powder:

By analyzing the radiation characteristics of the flame of coal powder, a four-wavelength model is proposed in this paper to measure the flame temperature of coal powder. The model is that four equations are set up in four chosen wavelengths and the flame temperature can be obtained by solving the equation group. With the measurement system based on the model, in which the radiation of the combustion chamber surface and the scattering of the solid particles are consistently accounted for, the temperature of the flame can be quickly and accurately measured without a reference radiation source.(Table 1)

2. Thermal plasma:

The temperature profiles varying with time for the nonsteady arc and flashover arc near the surface of a polluted plate are derived by employing the relative intensity method and the absolute intensity method.(see Figure 2,3,4)

3. Solid propellants: (Figure 5, Figure 6)

The spectrum for the flame of the solid propellants is measured. A lot of spectral lines are found in the spectrum of the flame, which are important information for temperature diagnosis.

Key words: spectroscopic diagnostics, flame temperature , solid propellants
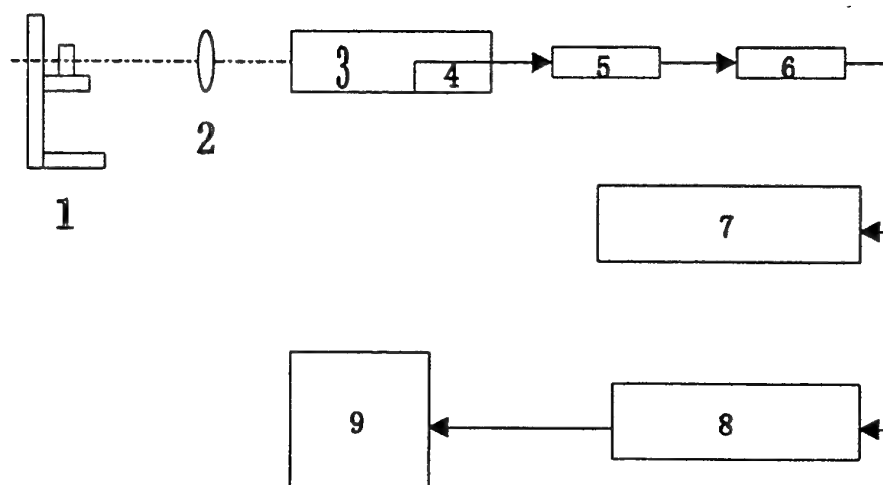
Figure 1: Sketch of the spectroscopic system [1] Workstation for measurement [2] Lenses [3][4] Dispersive system (Scanning system if necessary) [5] Photoelectricity conversion cell [6] operational amplifier [7] Monitor [8] a computer-based data collection system [9] Computer.

Number Code	Temp. By thermo-couple K	Temp. K	Voltage			
			Channel 1	Channel 2	Channel 3	Channel 4
1	1458	1450	0.011	0.030	0.109	0.259
2	1472	1461	0.021	0.039	0.199	0.468
3	1495	1482	0.034	0.038	0.255	0.545
4	1520	1493	0.036	0.044	0.315	0.626
5	1526	1502	0.038	0.057	0.389	0.720

Table 1: The results compared with the temperature by thermocouple
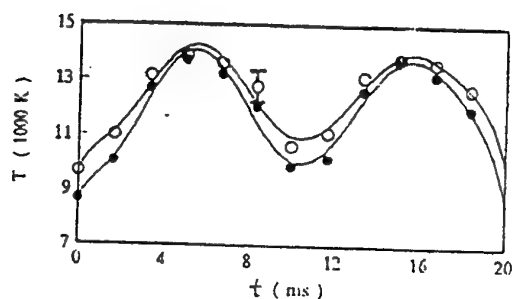
Figure 2: Axis temperature for a 170-A ac argon arc (50Hz)
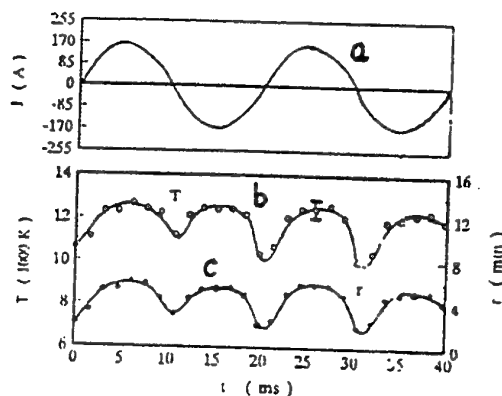
Figure 3: Current (a), temperature (b), and Radius of the ac argon arc(c) at power frequency
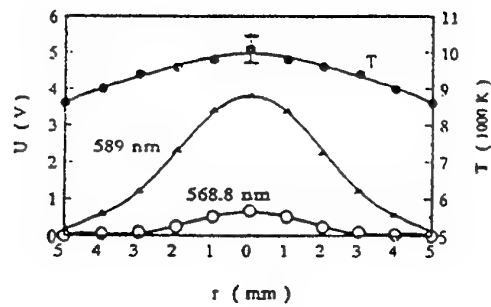
Figure 4: Typical output from the photomultipliers for two sodium spectral lines and the derivel radial temperature profile for the flashover arc by relative intensity method
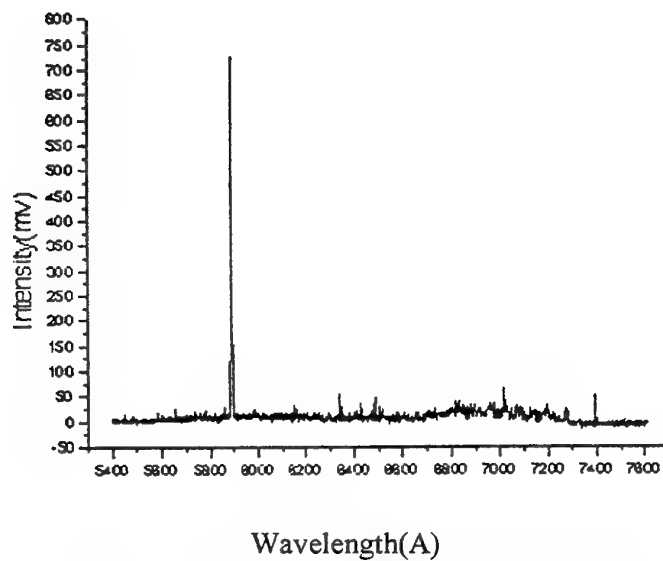
Wavelength(A)

Figure 5: Spectrum for composed propellants

199
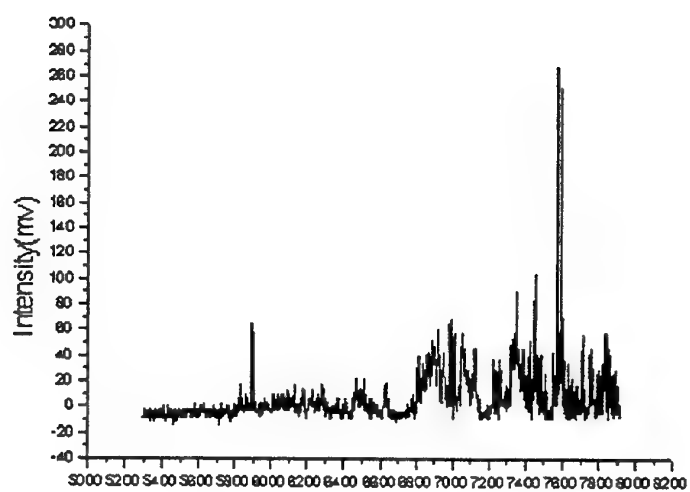
Figure 6: Spectrum for double-based propellants

Process Tomography (PT) as Diagnostic Tool for Combustion Phenomenon

T. Piotrowski, A. Plaskowski, B. Zygmunt
Institute of Organic Chemistry
6 Banopol Street
03-236 Warsaw, Poland
Tel: 0048-22-8111231
Fax: 0048-22-8110799
E-mail: bzygmunt@polbox.com

In the paper we would like to present some aspects of the process of tomography (PT) in application to combustion phenomenon diagnosis.

We present electrical methods, precisely electric capacitance tomography (ECT), based on generally known phenomenon that flames are rich in charged particles, ions and free electrons. This means that dynamic changes of electric parameters occur in permittivity and conductivity in the combustion volume.

These changes are different in different points of the combustion volume. They can be measured with electrodes put around combustion volume. Measurement circuits, to which electrodes are connected, take measurement of capacitance. The number and size of the electrodes used depends on the specific application. For example, a large number of electrodes allow higher resolution images to be obtained, but the measurement sensivity will be lowered compared with sensivity with fewer electrodes. Using longer electrodes can increase the system sensitivity, but this will lower the axial resolution of the system. In our experiments, we apply 12 electrodes placed around research volume, which gives us 66 measurements. These measurements are used to image reconstruction, which shows electrical permittivity $\Box$ distribution resulting from changes of ion quantity (density) and other combustion properties influencing these changes. This can be done in number of different ways. However, the simplest and fastest method currently used is the so-called linear back projection (LBP). For the image based on a 32 x 32 pixel grid, approximately 812 pixels will lie inside the circular cross-sections. The task, therefore, is to calculate the value of the permittivity of each of the 812 pixels from only 66 capacitance measurements. This can be not done directly because there is simply insufficient information, and so use is made of the second set of data known as the sensitivity map. Using actual techniques, we can get approximately 100 frames (images) per second. We believe that with electronics and reconstruction algorithms development 1000 frames per second could be obtained.

PT is implemented for the research of dynamic phenomena, such as steady and non-steady multiphase flow. The main advantage of PT, which should be underlined, is possibility of visualisation of the phenomena at chosen cross-section and time. The authors have focused their attention on following combustion processes: burning of fuel in torches, dust-air and gas – air mixture combustion, pyrotechnic mixtures and propellants. The pyrotechnics mixtures and propellants under normal (atmospheric) and decreased pressure can be easily observed using PT system. Some technical problems appear when we want to test combustion processes in real conditions (in rocket engine chambers) – the electrodes should be placed inside of the metal body of the chamber. An ring of electrodes appropriately located could be used to detect the presence of the flame, its size, location and stability. The measurement data

and reconstructed flame images can provide useful information on the dynamics, and help to design optimisation of the combustion process and theoretical models to be developed or verified.
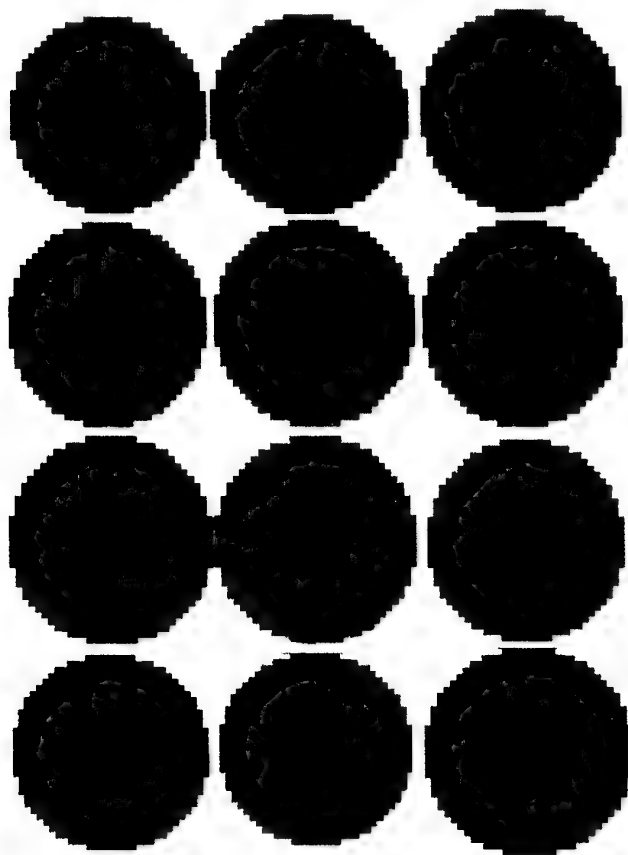

Fig. 1: Pictures obtained using the capacity tomograph after the ignition of sample of the calcium steariniane dust (with an increased mass) in the Hartmann's chamber.

AREA 10:

PROPELLANT AND MOTOR STABILITY

SESSION CO-CHAIRS:

DR. BENNY NATAN
AND
PROF. BEN ZINN

Some Influences of Noise on Combustion Instabilities and Combustor Dynamics

F.E.C. Culick[*] and C. Seywert[H]
California Institute of Technology
M/C 205-45
H. Pasadena, CA 91125
Tel: 1-626-395-4783
Fax: 1-626-395-8469
E-mail: fecfly@caltech.edu

The chief purpose of this paper is to investigate the influences of noise, more generally stochastic sources of any sort, on linear and nonlinear unsteady motions in combustion chambers. Our primary applications here relate to combustion instabilities in solid propellant rockets, particularly linear stability. Two aspects are especially relevant to practical applications: the direct effects of noise on stability; and extraction of information about stability margin from noisy pressure records taken for stable motors. However, the formulation and results are relevant to combustors generally. A fundamental issue is the distinction between, and relative importance of self-excited (linearly unstable) oscillations on the one hand, and forced oscillation on the other. This has been a controversial, and occasionally misunderstood topic for many years. The essential ideas can be clarified unambiguously within the context of global dynamics treated here. We are not so concerned with the details of data processing as with the physical interpretation of the results.

---

[*] Richard L. and Dorothy M. Hayman Professor of Mechanical Engineering and Professor of Jet Propulsion; Fellow AIAA.
[H] Graduate Student

THIS PAGE HAS BEEN DELIBERATELY LEFT BLANK

A Computational Study of the L* Instability with a Nonlinear Frequency Response

K.R. Anil Kumar and K.N. Lakshmisha[6]
Department of Aerospace Engineering, Indian Institute of Science,
Bangalore 560012, India.
Tel: 91-(80)- 3092755
Fax: 91-(80)- 360 0683
E-mail: knl@aero.iisc.ernet.in

Introduction

L* instability is the spontaneous, low-frequency (~300 Hz) pressure oscillations in the bulk of the chamber exhibited by solid propellant rocket motors with a small characteristic length, L* (Price, 1992). This is a result of coupling between the bulk flow of hot gases in the combustor, and the transient response of propellant burning to the combustor pressure oscillation. Early studies employed simplistic models of propellant burning with an unsteady, zero-dimensional model for the combustor gasdynamics. Subsequently Beckstead and Price (1967) assumed an isothermal combustor, but represented the propellant burning by a linear, QSHOD response function. Although it has been recognized that a nonlinear response function analysis is more appropriate because the L* instability involves large-amplitude oscillations and extinction (Beckstead, 1968), no solution has been proposed yet.

Recently, the present authors computed the pressure-driven response function including (1) gas-phase unsteadiness and (2) finite-amplitude pressure oscillations (Anil Kumar and Lakshmisha, 1999). When the amplitude of driving pressure is large, the burning rate oscillations develop considerable magnitudes of higher harmonics. Further, the response function was clearly modified by the mean pressure. Such features cannot be described within the framework of linear stability, QSHOD models. In this paper, a model for the L* instability is developed including (a) the nonlinear response function and (b) a zero-dimensional combustor model in which the pressure and temperature are determined by the instantaneous mass and energy balance.

The Model and Numerical Method

We consider an L* burner with end-burning propellant grain. The problem domain is divided into two regions, 1) a thin zone R_1 near the burning surface, and 2) the rest of the combustor free-volume, R_2 up to the nozzle entrance. Unsteady, 1-d conservation equations for the species and energy are solved over a doubly-infinite space in the region R_1 (see Anil Kumar and Lakshmisha, 1999). This yields the instantaneous burning rate ($\dot{r}$) and the temperature (T_∞) of the hot gases released into R_2. The region R_2 is considered as a homogeneous, adiabatic control volume, for which the unsteady conservation of overall mass and energy are solved to obtain the instantaneous chamber conditions (p_c, T_c, ρ_c). The resulting set of PDE's (of unsteady burning of propellant) and the ODE's (of unsteady flow of mass and energy in the chamber) are nonlinear and strongly coupled, and a numerical approach becomes necessary for solution. The two systems of equations are time-integrated using a fourth order Runge-Kutta method for the ODE's and an *Operator-Splitting* method for the PDE's.

---

[6] Corresponding Author, E-mail: knl@aero.iisc.ernet.in

Results and Discussion

As a representative case, we consider the A-35 propellant whose typical properties are listed in Table 1. The critical initial L^* for a given mean pressure was predicted with the following procedure: Suitable initial values are selected for the L^* and the area ratio K; the initial values for the burning rate $\dot{r}$ and the flame temperature T_∞ are obtained from the solution of region R_1 alone for the specified mean pressure. Then the regions R_1 and R_2 are integrated together. If the combustion were stable, this would lead to a new set of steady state pressure and mass burning rate. For sufficiently large values of initial L^*, *e.g.*, 200 *cm* in this case, the amplitude of pressure oscillations monotonically decreased from t=0, and attained steady values. With an initial L^*=150 *cm*, (see Figure 1) a small initial pressure perturbation is found to first increase the amplitude of the oscillations; however, as the L^* increases due to propellant surface regression, the amplitude started decreasing. A sufficiently small initial L^* results in extinction (e.g., 138 *cm* as shown in Figure 1). This behavior has been experimentally observed for different propellants (Beckstead and Price, 1967; Kumar and McNamara, 1973; Shöyer, 1986). Similar calculations were performed at different mean pressures (3–12 *atm*) and the initial L^* for stable (*i.e.*, initial pressure perturbations eventually decay and chamber pressure reaches a steady-state) and unstable (*i.e.*, initial pressure perturbations increase continuously leading to extinction) operation are shown in Figure 2. In the present case, the critical initial L^* decreases with mean pressure. This may not be true for all propellants. Calculations made for a different set of properties, which correspond to lower surface temperature, showed a minimum mean pressure below which extinction did not occur for realistic values of small initial L^*. This suggests a decrease in the critical initial L^* with mean pressure at low pressures.

The correlation of frequency with mean pressure predicted by the present model (Figure 3) compares fairly well with the experimental results of Beckstead and Price (1967). Figure 4 shows the lead-time of burning rate relative to pressure, as function of frequency. Experimental results are those obtained by Beckstead and Price (1967). The latter have calculated the response function and lead time of burning rate relative to pressure from the measured values of chamber pressure growth rate, frequency and instantaneous L^* using a linear stability, QSHOD model. The qualitative trend predicted by present model is in agreement with the experimental results extracted using simple model. However, when the experimental data used are those corresponding to large amplitudes, for example those leading to extinction, a nonlinear model has to be used to evaluate the response function and lead-time of the burning rate.

The present model could not predict *chuffing*, which has been observed in several experiments (*e.g.*, Beckstead and Price, 1967). Perhaps, a distributed chemical reaction in the condensed phase may have to be included in the description of propellant burning. Such a reaction in the condensed phase could also affect the response function. This aspect is presently under investigation.

References

Price, E.W. (1992), "L* Instability", Chapter 9 in Non-steady Burning and Combustion Stability of Solid Propellants, Eds. L.De Luca, E.W.Price and M. Summerfield, Vol.143, Progress in Astronautics and Aeronautics, AIAA, Washington, DC, pp.325-361.

Kumar, R.N. and McNamara, R.P. (1973), "Some Experiments Related to L* Instability in Rocket Motors", AIAA Paper No.73-1300.

Beckstead, M.W. and Price, E.W., (1967), "Non-acoustic Combustor Instability", AIAA Journal, Vol.5, No.11, pp.1989-1996.

Beckstead, M.W. (1968), "Low Frequency Instability: A Comparison of Theory and Experiment", Combustion and Flame, Vol.12, No.1, pp.417-426.

Schöyer, H.F.R. and de Bent, R.T.M. (1986), "Experimental Verification of Temperature Fluctuations During Combustion Instability", AIAA Journal, Vol.24, No.2, pp.340-341.

Anil Kumar, K.R. and Lakshmisha, K.N.(1999), "Nonlinear Intrinsic Instability of Solid Propellant Combustion including Gas-phase Thermal Inertia, Technical Report IISc/AE/Prop/99-01 of Dept. of Aerospace Engineering, Indian Institute of Science, Bangalore, India (to appear in Combust. Sci. Tech.).

T'ien, J.S., Sirignano, W.A. and Summerfield, M. (1970), "Theory of L* Combustion Instability with Temperature Oscillations", AIAA Journal, Vol. 8, No. 1, pp. 420-426.

Table 1: Typical Properties of A-35 propellant (T'ien et al., 1970)

Steady burn rate (cm/s), at 7 atm	0.338	k_c (W/m·K)	0.2563
Pressure index	0.5	k_g(W/m·K)	0.08372
Propellant density (kg/m^3)	1580	Molecular weight	22.0
Surface Temperature (K)	860	Flame temperature (K)	2161
$E_s = E_g$ (J/kg)	83720	Surface heat release (kJ/kg)	549.2
Ambient Temperature (K)	300	$c_g = c_c$ (J/kg·K)	1381.38
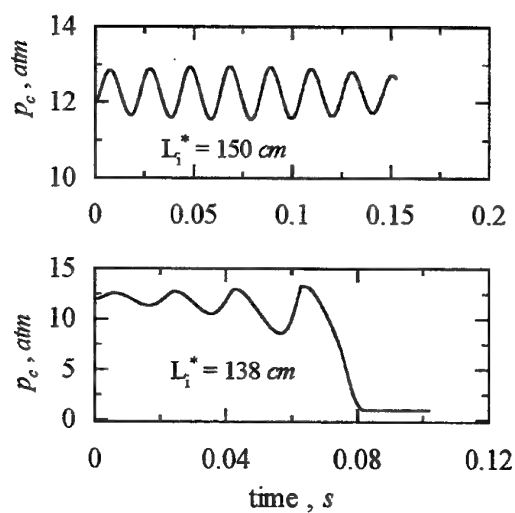
Figure 1. Variation of chamber pressure
with time (p_c = 12 *atm*)
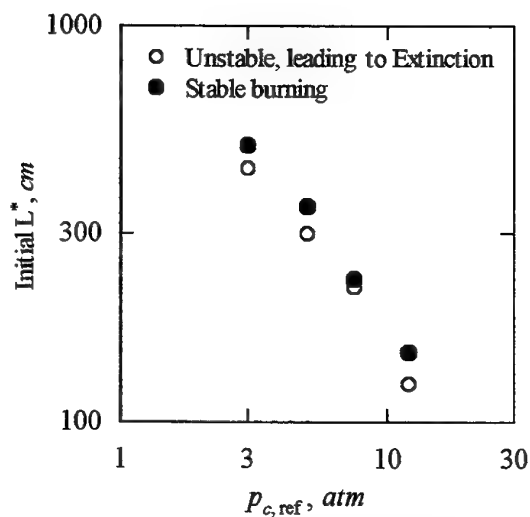
Figure 2. Stability diagram, showing
regions of stable and unstable operation.
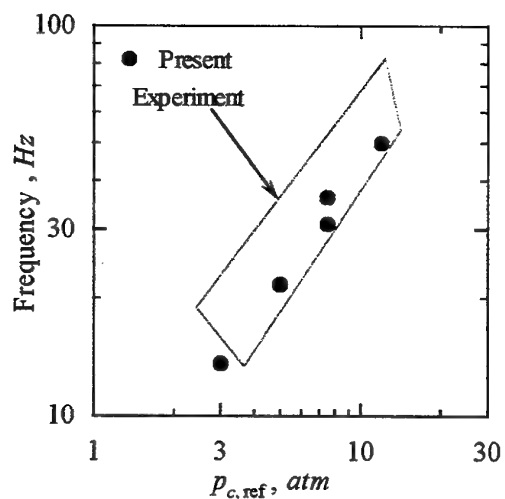
Figure 3. Frequency *vs.* mean
pressure for A-35 propellant.
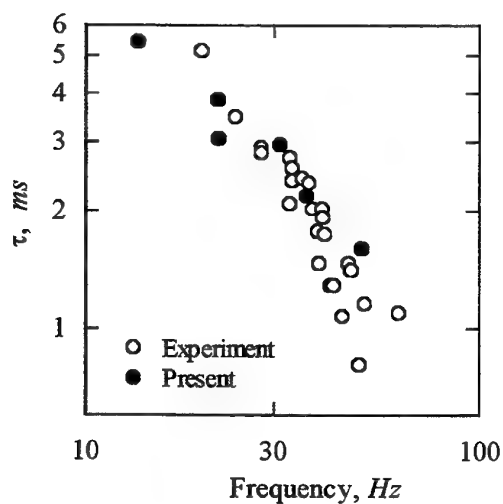
Figure 4. Lead time of burning rate
relative to pressure for A-35 propellant.

Low-Frequency Stability of Solid Propellant Combustion in Rocket Motors

O. Romanov
Baltic Academy of Technology, Economy and Culture
1, First Krasnoarmeyskaya Street, St. Petersburg, 198005 Russia
Tel: (7-812)-534-58-15
Fax: (7-812)-251-12-08
E-mail: petr1@home.ru

Phenomenological models of solid propellant (SP) nonsteady burning, or models with specific burning mechanism (i.e., flame structures), are commonly used in existing theories of low frequency SP combustion stability (LFS). In both cases, intrachamber processes were examined assuming zero-dimensional flow and possible effects connected with one-dimensional combustion products' flow were described using delay time (for example, entropy waves i.e. Mache effect). In general, detailed features of combustion chambers were not taken into consideration.

The LFS problem has been approached in this paper using automatic control theory methods. Response functions and frequency response functions have been applied to describe nonsteady SP burning rates. An attempt has been made to take into consideration most factors influencing LFS, including those defining detailed features of combustion chambers, in forms useful to the zero-dimensional approach. The necessary information has been acquired by analyzing the one-dimensional steady intrachamber processes.

The general system of equations describing the average physical parameters of combustion products in the volume of combustion chamber includes:
- ordinary differential equations for changes of mass, energy, and volume;
- the ideal gas state equation;
- the common equations for nonsteady burning rate and for nonsteady enthalpy of combustion products flow from burning surface; and
- nonsteady total temperature in the nozzle throat versus the average gas residence time in combustion chamber.

To describe detailed features of combustion chambers, definite coefficients have been included in the general system of equations and examined as functions of both variable pressure and nonsteady burning rate. These are:
- the coefficient determining the average nonsteady burning rate at the burning surface of a charge, taking into consideration the influence of both pressure decrease and erosive burning;
- the coefficient of combustion completeness near the burning surface and heat losses;
- the coefficient of total pressure restoration in the nozzle throat in comparison with the average volume combustion chamber pressure to take into consideration gasdynamic losses due to local resistances and friction;

At the beginning, an investigation was carried out for steady combustion stability in combustion chamber implementing a linear approach in dimensionless form. Response functions for burning rate-pressure connections and corresponding to them frequency response functions were used. It was possible to examine theoretical or experimental versions

of them as alternatives. The experimental ones published earlier have been used in this investigation.

It was convenient to analyze the influence of each factor separately under a linear approach since: first, that is advisable to proceed methodically; second, some combinations of factors are unrealistic for actual combustion chambers; and third, common activity of factors is additive and consequently easy to calculate. The case with isothermic process in the combustion chamber and with steady enthalpy of combustion products from burning surface has been taken as the basic one. Corresponding combustion chamber gain factor for pressure equals 1 (Novozhilov's variant in his book, 1973). Then the influence was examined of factors as such adiabaticity, dependence of combustion products enthalpy versus nonsteady burning rate, other factors related to the above enumerated coefficients, and entropy waves as well.

These factors influence at first upon combustion chamber gain factor and therefore upon the static stability reserve defined as the difference between this factor and exponent in burning rate-pressure dependence. On the other hand, this factor in common with apparatus constant (dimensionless value proportional to well known characteristic length) influence strongly upon dynamic stability boundary. That is explained with the equation defining the frequency of pressure oscillations on the boundary. Approximate solutions have been obtained.

Nonlinear stability of combustion chamber processes has been examined the for transient regimes to lower pressure levels. Nonlinear response functions determined experimentally earlier were used and harmonic linearizations of nonlinearities were carried out. Increasing the pressure levels' differences, the amplitudes of pressure oscillations increased as well but the decrement of attenuation on the contrary decreased and the stability boundary "in large" could be reached. The least pressure levels' differences leading to stability loss were determined. The influences of most of the above enumerated coefficients are discussed.

210

Intrinsic Burning Stability of Solid Propellants with Variable Thermal Properties

M. Verri*, L.T. DeLuca
Facoltà di Ingegneria, Politecnico di Milano
20133 Milan, MI, Italy
Tel: +39-02-2399-3912; Fax: +39-02-2399-3940
e-mail: fivbd@tin.it

Intrinsic burning stability of solid propellants has been studied under nonlinear conditions in the framework of QSHOD flame modeling, but connections with the classical Zeldovich-Novozhilov approach were also underlined. Both pressure- (Ref. 1) and radiation-driven (Ref. 2) burning were analyzed under the assumptions of chemically inert condensed phase and thermal properties being only pressure-dependent. However, in several instances the condensed-phase thermal properties have been observed to vary with temperature for both homogeneous and heterogeneous compositions. Although the actual importance of this effect has not been fully assessed, there is no doubt that under critical burning conditions (for example, near deflagration limits) it may have a decisive influence. Thus, the previous analyses have somewhat been extended to temperature-dependent thermal properties within the same nonlinear framework used in Refs. 1-2. In the limiting case of a common temperature-dependence for specific heat and thermal conductivity, an analytical solution has been obtained extending and recovering the previous results. In general, it is found that the two-parameter, a and b, formulation of the stability problem is kept for the surface-driven burning configuration (pressure-driven or radiation-driven in the limiting case of surface absorption). Likewise, the oscillating frequency just at the stability boundary, is found to keep the previous expression in terms of a and b parameters. The new, generalized parameters explicitly include the assumed temperature- dependence law for the thermal properties through its average values (over the entire condensed-phase thermal profile) and the burning surface value.

Other developments shedding further light on the matter of intrinsic stability will be discussed as well. These respectively deal with the importance of the starting assumptions concerning the existence and uniqueness of the fundamental time-invariant solution and the subtle connections of the intrinsic stability features with the denominator of the pressure- or radiation-driven frequency response function.

References

1. De Luca L.T, Di Silvestro R., and Cozzi F., "Intrinsic Combustion Instability of Solid Energetic Materials", Journal of Propulsion and Power, Vol. 11, No. 4, pp. 804-815, 1995.
2. De Luca L.T, Verri M., and Jalongo A., "Intrinsic Stability of Energetic Solids Burning under Thermal Radiation", Chapter 12, Volume 173 of AIAA Progress in Astronautics and Aeronautics, American Institute of Aeronautics and Astronautics, edited by Sirignano, W.A. and Merzhanov, A.G. and DeLuca, L.T., Reston, VA, USA, 1997, pp. 195-218.

THIS PAGE HAS BEEN DELIBERATELY LEFT BLANK

Frequency Response of a Model Subscale Rocket Motor

R.O. Hessler
93 Cryer Road
Somerville, AL 35670
Telephone: 1-256-778-8014; E-mail: ROHessler1@aol.com

R.L. Glick
1159 S 525 E
Rensselaer, IN 47978

R. Bertelé, D. Cedro, G. Fiorentino, and L.T. DeLuca
Laboratorio di Termofisica
32 Piazza Leonardo da Vinci
Politecnico di Milano
20133 Milano, Milan, Italy

Rocket motor development programs continue to encounter episodes of pressure oscillations that are potentially threatening to a successful mission accomplishment. When the oscillations are large, the condition is usually called "Combustion Instability," so named because the combustion process is responsive to pressure oscillations, and the combustion response may be large enough to cause a feedback-coupled instability of the acoustic modes.

FFT analysis of motor data with no large oscillations indicates the presence of small acoustic oscillations, distinguishable from electrical, combustion, or flow noise by appreciable amplification at the acoustic mode frequencies. The magnitudes of the acoustic oscillations range from a few kiloPascals down to fractional Pascals, and repeat at about the same levels from test to test of the same motor design.

These repeated observations are consistent with forced oscillations of the motor acoustics caused by noisy combustion or flow processes. Rederivation of motor instability theory including non-acoustic perturbations shows that the classical transient solution (exponential growth or decay of disturbances) is augmented by a forced solution if non-acoustic perturbations are present. The forced solution has the form of the frequency response of a series of linear oscillators, with each oscillator having the properties (frequency and stability margin) of one of the acoustic modes.

The forced solution can be exploited as either a predictive tool or a diagnostic tool. Given models of the combustion and flow noise, the forced solution can be used to make *a priori* predictions of pressure amplitude spectra of a candidate motor design at a fraction of the cost of full numerical Navier-Stokes solutions. Because of the linear form of the forced solution, commonly available linear system analysis tools can be used to make passive linear stability measurements in tested motors without the cost or risk of pulsing. Use of these tools in combination can potentially provide the motor designer or analyst industrial-strength tools to prevent or combat the presence of large oscillations in a motor design.

The full paper will present the current status of a research subtask to measure the frequency response of models of a subscale rocket motor. The paper will include, as available,

comparisons with results from motor tests and forced solution predictions. The subscale rocket motor is routinely used for burning rate measurements of production mixes of an aluminized AP propellant. Three motors of the same geometry are tested for each mix, with different nozzles used to achieve different mean chamber pressures. The propellant grain is of cylindrically perforated design with L/D ratio about two to produce relatively constant pressure during burn. A plastic 1/1 scale model of the motor has been fabricated. The model has been instrumented with microphones at 16 locations to measure chamber response to external acoustic stimulation. The model has interchangeable nozzles of the sizes used in the motors. The model also has interchangeable grains corresponding to nominal propellant grain geometry at 0, 20, 35, 50, 65, 80, and 100% of web thickness burned so model results can be compared directly with motor results as the motor geometry changes during burn.

Tests are conducted in an isolated chamber by applying acoustic pressures from an audio speaker to the exit of the model nozzle and recording the response of microphones embedded in the model walls. A pseudorandom sequence with constant spectral amplitude, uniformly distributed phase, and ½ s period is used as input and repeated several times for a test. Although the signal is tailored to constant magnitude to permit examination of frequency response details without input signal noise, the signal retains a Gaussian distribution in the time domain.
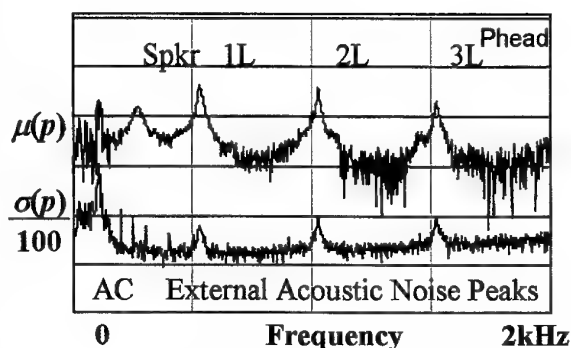
Fig. 1 Log Pressure Magnitude Mean and Standard Deviation.

The figure at right shows the averaged spectrogram of one microphone for nine pseudorandom periods. The first three longitudinal acoustic modes are clearly visible, with about 0.5 Pa peak magnitude at 1L. A speaker resonance peak at 270 Hz will be removed by calibration. The standard deviation (shifted down two gridlines) indicates signal-to-noise ratio near the acoustic mode peaks to be about 20/1 over the baseline electrical noise, but only about 5/1 over external acoustic noise (indicated by the peaks in the standard deviation).

214

Charge Design and Non-Acoustic Instability of Solid Rocket Motors

I.G. Assovskiy
Semenov Institute of Chemical Physics, RAS,
Kosygin St. 4, Moscow 117977 Russia
Tel: (7-095) 939-7267
Fax: (7-095) 939-7417
E-mail: assov@chph.ras.ru

S.A. Rashkovskiy
Moscow Heat Technique Institute, RSA
Moscow 127276 Russia

The purpose of this paper is a theoretical analysis of non-acoustic low-frequency instability (the L^*-instability) of combustion in a solid rocket motor (SRM). Emphasis is on correlation between the critical conditions of stable combustion and sizes of the charge and pre-nozzle volume of motor. The problem is considered in details for SRM having a tubular charge.

The L^*-instability of SRM manifests itself as "chuffing" or periodical pressure pulsations with frequency not more than 10 Hz. Despite of great importance of this problem for the motor design, there is not any commonly accepted quantitative theory of this phenomenon. Dependence of pressure pulsations on the charge geometry is typically considered as a sign of acoustic instability. Therefore the problem of the charge geometry influence on L^*-instability needs special consideration.

The critical conditions of stable combustion depend on characteristics of propellant as well as on motor cavity. That is why any advanced theory of L^*-instability needs appropriate understanding of the combustion process and gas-flow inside SRM. This paper is further development of the model of unsteady combustion in SRM that has been proposed in [1] for the end-burning charges. The model allows the flame temperature and temperature distribution in gas-flow to fluctuate with the chamber pressure (Mache-effect). A laminar one-dimensional gas-flow (without dissipation and mixing) is assumed. The propellant unsteady combustion is described using Zel'dovich phenomenological approach and taking into account variation of the propellant surface temperature (Novozhilov model) as variation of flame temperature (Gostintsev and Sukhanov model). The gas-pressure in combustion chamber is uniform and varies only with time; the distribution of gas-flow velocity is uniform in any cross-section of the chamber. A set of equations for dynamics of the entropy disturbances in the chamber uses the Lagrangian description of gas flow.

A free volume W of combustion chamber has two parts: a channel volume and a pre-nozzle volume. Therefore the "apparatus constant", determined as $\mathcal{X} = \tau_P/\tau_T$, contains two terms: $\mathcal{X}=\mathcal{X}_0+\beta$, where $\mathcal{X}_0$ and β are associated respectively with the pre-nozzle cavity and the channel volume; τ_T, is the time-scale of thermal inertia of combustion wave, $\tau_P \sim W$ is the time scale of pressure relaxation in the motor cavity. Influence of β, $\mathcal{X}_0$, and other parameters on the critical conditions of the L^*-instability has been tested. Figure 1 demonstrates dependence of the boundary of the instability region on parameters of the SRM and propellant (notation the same as in [1]).. The region of instability is on right side from the boundary. All

boundaries have vertical asymptotes. In the case of SRM with end-burning charge (7) the asymptote of boundary, $k=k^*$, corresponds to the criterion of combustion instability under constant pressure (intrinsic instability). Such a correlation does not take place if the propellant charge has a channel (see curves 1-6).

The stability region on the plane (χ, k) for the tubular charge is more narrow than that one for the end-burning charge. The pre-nozzle volume stabilizes the combustion process in SRM. The boundary of L^*-instability depends weakly on the channel volume but significantly on the pre-nozzle volume. In a limit case of SRM without pre-nozzle volume, $\chi_0=0$, the stability region is minimum.

1. I.G. Assovskiy, S.A. Rashkovskiy, "Mache Effect and Combustion Instability in Rocket Motor ", AIAA Journal of Propulsion and Power, Vol. 16, No. 1., Nov.-Dec., 1999.
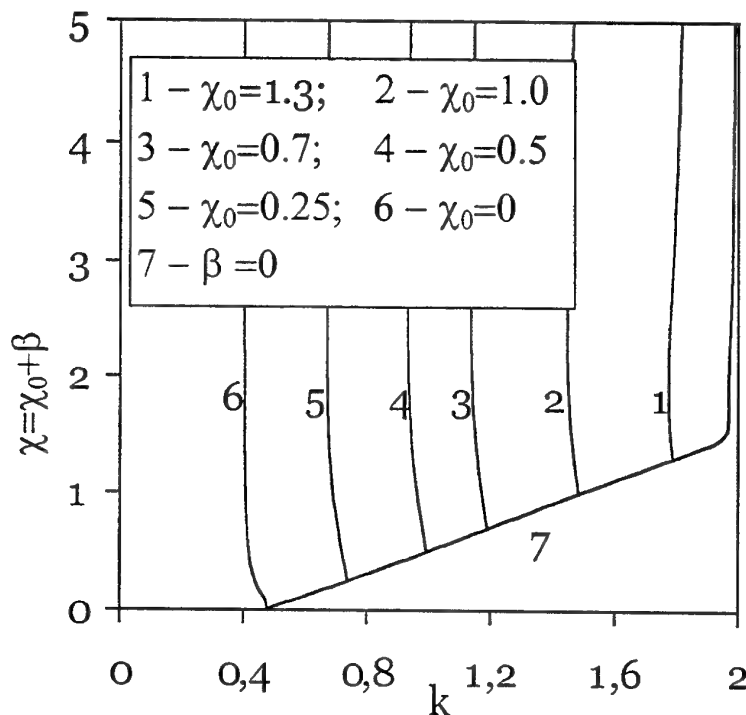
Fig.1. Boundaries of stability region for different values of pre-nozzle volume ($\mu = \varepsilon = 0$, $r = 1/3$, $v = 2/3$, $a = 0.25$, $n=1.2$).

Space Shuttle Booster Internal Flows and Slag Expulsion

R.H. Woodward Waesche
Editor-in-Chief, *Journal of Propulsion and Power*
Science Application International Corporation
4319 Banbury Drive
Gainesville, VA 20155-1122
Tel: (703) 754-7214
Fax: (703) 753-0217
E-mail: woodward.waesche@saic.com

A series of cold-flow tests, employing either air or water, was conducted in a 1/8-scale (18-inch-diameter) model of the aft sections of the Space Shuttle Booster, including simulation of transpiring propellant surfaces at different burning times. Measurements of pressure distribution were made for several internal geometries, as well as visual observations with dye. Particular attention was paid to the possibility of rotating flow in the joints between the four segments of the Booster, as well as in the aft dome as propellant burned out.

There was little evidence of circumferential flow in the joints; the pressure gradients observed could not drive any such flow. However, the pressure gradients that existed in the aft dome cavity, especially when the model nozzle was vectored to simulate thrust vector control, were sufficient to drive strong vortical flows in the dome. These flows led to periodic pumping of the aft dome and expulsion of dye from the cavity through the nozzle.

Shortly after the conclusion of these tests, pressure and thrust excursions were noted in several Booster flights. Since there was concern about the possible effects of such excursions on Shuttle integrity, and the pumping observed in cold flow was suggested as having a possible connection with excursions, a static test program was set up to evaluate such a connection. Real-time X-rays and radiometers were employed. At the same time, simulations of possible flows of slag through the nozzle were conducted.

These tests led to visual observation of the expulsion of molten aluminum oxide slag, with an increase in exhaust luminosity that directly correlated with the pressure excursions. Further, the X-rays showed flow patterns that were nearly identical with what had been observed in cold-flow tests.

A presentation will be made that includes a description of the test article and the techniques employed, as well as some videos of the flow field. In addition, data on the excursions observed and the other data taken will be presented, together with the slag flow rate that could explain the excursions. Comments will be made on the significance of these results on the Shuttle program and on other potential Space Launcher designs.

ABSTRACTS OF PAPERS
TO BE PRESENTED IN POSTER SESSIONS

POSTER SESSIONS:

AREAS 1-10

SESSION CO-CHAIRS:

PROF. LUCIANO GALFETTI
AND
MR. ERIC BOYER

AREA 1:

REACTION KINETICS OF ENERGETIC MATERIALS

Cyclodextrin Polymer Nitrate

B.M. Kosowski
MACH I Inc.
340 East Church Road
King of Prussia, PA 19406
Tel: (610) 279-2340; Fax: (610) 279-6605; E-mail: machi@machichemicals.com

The military and aerospace community has an on-going interest in, and need for energetic materials with high-energy performance, but with low sensitivity characteristics. MACH 1, Inc. has completed a Small Business Innovation Research program sponsored by the U. S. Air Force to evaluate nitrate polymers of cyclodextrin as possible components of insensitive, high-energy explosives. These materials will also be suitable for components in insensitive, minimum smoke-producing propellants.

This paper describes the four types of cyclodextrin polymers synthesized and evaluated by MACH I, and our assessment of the suitability of their nitrated forms as Insensitive Munition energetic candidates for future use and formulation development. They consisted of:

1. Nanotube polymer of α cyclodextrin

2. Linear polymer of β cyclodextrin

3. Isocyanate polymer of γ cyclodextrin

4. Epichlorohydrin polymer of γ cyclodextrin
    The epichlorohydrin polymer was selected for scale-up evaluation and characterization. Five pounds of nitrate were produced.

THIS PAGE HAS BEEN DELIBERATELY LEFT BLANK

Thermal Decomposition of 1,3,3-Trinitroazetidine in Gas and Liquid Phase

V.V. Nedelko, B.L. Korsounskii, N.V. Chukanov, T.S. Larikova
Institute of Chemical Physics Problems of Russian Academy of Sciences
(142432 Chernogolovka, Moscow Region, Russia)
Tel: 7(095) 7204959 call 3281
Fax: 7(096) 5153588
E-mail: nedelko@icp.ac.ru

N.N. Makhova, I.V. Ovchinnikov
Zelinsky Institute of Organic Chemistry of Russian Academy of Sciences
(117977 Moscow, Russia)

1,3,3-Trinitroazetidine (TNAZ) is the prospective high-energy explosive with some practically important properties (low sensitivity, high thermal stability, low melting point). The thermal decomposition kinetics of TNAZ has been investigated by the method of volumetry in gas and liquid phase. The gas-phase reaction (the temperature range was 170 to 220 C) followed the first order of kinetics and obeyed Arrhenius equation with activation energy 40500 cal/mol and logarithm of pre-exponential factor 15,6. According to IR-spectrophotometric data, the complete TNAZ decomposition at 220 C resulted in the formation of nitrogen, nitrogen dioxide, carbon dioxide, nitroacetaldehyde and the traces of CO and NO. The total quantity of the gaseous products, non-condensed at normal conditions, was about 4 moles per 1 mole of TNAZ. The more complex kinetics has been measured for TNAZ decomposition in m-dinitrobenzene solution (180 v 231 C). One could observe the small self-acceleration of the process at low reaction conversions (up to 25%) and gas-formation level increasing from 4 to 5 moles per 1 mole of TNAZ. Simultaneously, the nitrogen content in the gaseous decomposition products was reduced from 14% in the case of the gas-phase reaction to the traces. The possible decomposition routes are discussed.

THIS PAGE HAS BEEN DELIBERATELY LEFT BLANK

None Equilibrium Reactions in Combustion and Detonation Processes

F. Volk
Fraunhofer Institut
Chemische Technologie (ICT)
D-76327 Pfinztal-Berghausen
Tel: 0049-721-4640-164
Fax: 0049-721-4640-111
E-mail: vo@ict.fhg.de

For the calculation of the performance of combustion processes, in many cases equilibrium thermodynamic reactions are being taken into account. The reason is that the knowledge of the reaction kinetics of combustion is incomplete. On the other side, so-called none-equilibrium reactions occur in which metastabile products are being produced, especially in the low pressure range.

In another case, thermodynamic equilibria freezes out at a distinct temperature, so that the heat output and the product composition cannot agree with those values calculated with equilibrium codes.

In this paper, several examples of a none equilibrium combustion of propellants will be shown. It will be discussed under which conditions an equilibrium burning can be achieved, and how it will be possible to calculate as well the heat output as the reaction products of single base, double base and nitramine propellants. The products, analyzed by gas-chromatography and mass spectrometry, are compared with those calculated using the ICT-Thermodynamic Computer Code. It was found that NO is a none equilibrium product mostly formed from nitrate ester propellants, whereas N_2O, NO and HCN are products contained in the reaction gases of nitramine propellants.

The results lead to a better understanding of combustion and recycling processes of energetic materials.

With regard to detonation processes by analyzing the products, the reason for discrepancies between experimental and calculated detonation parameters could be explained.

THIS PAGE HAS BEEN DELIBERATELY LEFT BLANK

AREA 2:

ENVIRONMENTAL, COMMERCIAL, RECYCLING AND SAFETY OF ENERGETIC MATERIALS

FTIR Absorption Spectroscopy of Environmentally Friendly Airbag Gas Generant

H.R. Blomquist
TRW Automotive
4051 North Higley Road; Mesa, AZ 85215
Tel: (480) 807-7120, Fax: (480) 807-7312
E-mail: Harry.Blomquist@trw.com

S.T. Thynell and C.F. Mallery
Department of Mechanical Engineering
Pennsylvania State University
University Park, PA 16802

Gas generant formulations based on sodium azide have proven to be an excellent source of non-toxic, low temperature gas for automotive inflatable restraint systems. Nevertheless, non-azide compositions are desirable to minimize potential environmental releases of sodium azide mixtures. Critical characteristics of candidate non-azide compositions must be efficiently characterized, including high burning rate, breathable combustion products, low hazards, and wide temperature ballistic performance capability. Excellent results have been obtained using high pressure, windowed, strand burner coupled with species distribution measured in the flame using FTIR. Candidate formulation T-239 was characterized by these methods and found to have suitable burning rate properties and species distribution for use as an airbag gas generant. This is, in turn, used as critical input to inflator performance simulation wherein gas phase kinetics are also modeled.

Table 1 Species measurements during combustion of T239 propellant.

Time after ignition (sec)	$\chi CO/\chi CO_2$	$\chi H_2O/\chi CO_2$	$\chi CO_2/\chi CO_2$	Other species
0.5	0.083	1.151	1	CH_4
0.8	0.096	1.289	1	CH_4
1.1	0.077	1.078	1	CH_4
1.5	0.095	1.019	1	CH_4

THIS PAGE HAS BEEN DELIBERATELY LEFT BLANK

Nitramine Propellant Formulations for Airbag Inflators

C. M. Walsh
Explosives and Propellants Division
Naval Surface Warfare Center Indian Head Division
101 Strauss Avenue, Indian Head, MD 20640
Tel: 301-744-2554; Fax: 301-744-4683
E-mail: walshcm@ih.navy.mil

Several nitramine propellant formulations have been developed specifically for use in automobile airbag inflators. These formulations are used in place of sodium azide type propellants in hybrid inflator systems. They are clean burning propellants that are designed to have very safe and environmentally friendly combustion products and to produce no, or very low levels of solid reaction products. Two of the formulations are modified LOVA type propellants that are primarily RDX-filled cellulose acetate butyrate systems. One is used primarily as a heat source for the inert gas systems of hybrid inflators. The other is an oxidizer-modified propellant that acts as more of a gas generator and contributes to the effluent gases that inflate the airbag. The third propellant developed and patented at NSWC, Indian Head Division uses a novel polyacrylate elastomer binder, and has the unique property of being a high solids-loaded propellant that is manufactured without the use of any plasticizer. This new binder system gives the propellant superior mechanical properties and stability. The absence of a plasticizer also makes it very reliable in aging testing and allows it to perform in heat tests better than many of the propellants in use currently. All three of these propellants have been successfully tested in commercial airbag inflators.

THIS PAGE HAS BEEN DELIBERATELY LEFT BLANK

Combustion Properties Relevant to Cofiring of Solid Rocket Motor Washout Material

S.G. Buckley
University of Maryland Department of Mechanical Engineering
2181 Glenn L. Martin Hall
College Park, MD 20742
Tel: 301-405-8441; Fax: 301-314-9477
Email: buckley@eng.umd.edu

R. Moehrle, J. Lipkin L.L. Baxter
Sandia National Laboratories, Livermore, CA 94551

G. Mower
Thiokol Propulsion Division, Brigham City, UT 84302

High-pressure water washout of large solid rocket motors yields a residue which is primarily comprised of aluminum flake, polybutadiene rubber, ammonium perchlorate, and asbestos entrained from the liner. Treatment following washout recovers most of the ammonium perchlorate from the residue for reuse, desensitizing the washout residue. Often this material is then disposed of through open burning/open detonation (OB/OD) or in landfills.

Cofiring combustion is a compelling alternative disposal option for desensitized EM that would capture the energy value in the fuel and also would mitigate many environmental hazards associated with other options through the use of boiler pollution controls. We have previously shown that issues surrounding the fate of the asbestos and the potential production of unwanted chlorinated byproducts are not an item for concern in a properly operating combustor. However, the presence of aluminum powder in the residue results in a measured combustion temperature of over 2000 °C for particles of approximately 1 mm in size. Concern over potential damage to boiler equipment from the high temperature material is therefore an issue. In addition, the effect of the residue on the ash stream from the boiler must be determined, if the ash has value in a particular application (e.g. cement additive, asphalt, fertilizer, etc.).

This paper presents results from a small bed combustor (Figure 1) designed to examine materials issues and ash chemistry in a configuration similar to a grate-fired industrial combustion system. Desensitized EM has been mixed with various traditional fuels and burned in the bed combustor under a variety of combustion conditions. Temperature measurements (Figure 2) in the bed and inspection following the combustion event were used to assess the potential for materials damage in a full-scale system. FTIR analysis (Figure 3) was used to determine the fate of gas-phase chlorine and potential chlorinated emissions, including dioxin / furan precursors. Residual ash samples were analyzed to determine the amount of chlorine retained in the ash (Figure 4), as well as to inspect for asbestos fibers persisting through the combustion event (Table 1). We discuss the significance of these results with respect to the plans for a full-scale commercial cofiring test.
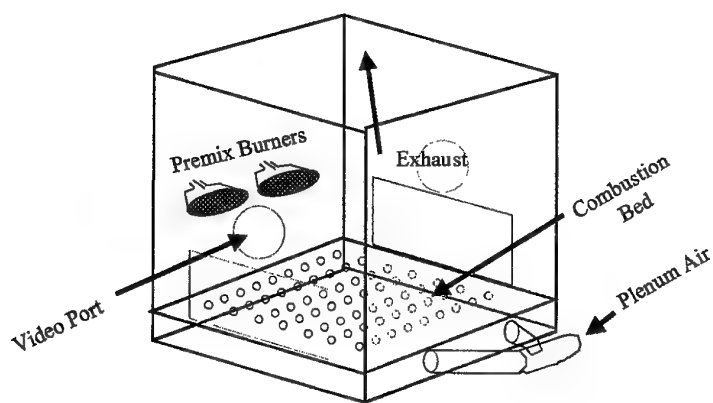
Figure 1: Experimental Schematic for Bed Combustion.
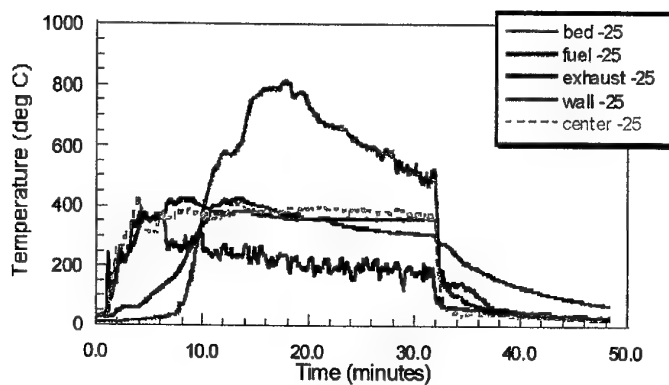
Figure 2: Temperature / time profiles for 75% biomass / 25% EM blend.
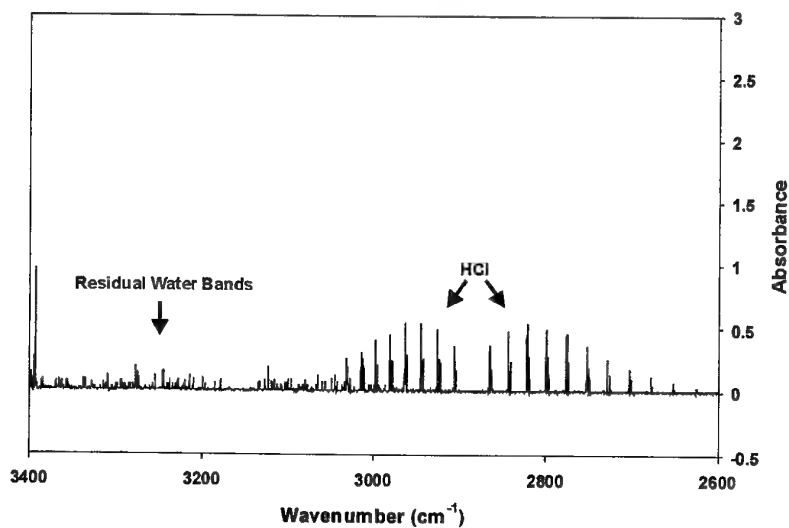
Figure 3: FTIR Spectroscopy shows 99.9+% of the gas-phase chlorine is emitted as HCl, which can be easily scrubbed – no gas-phase toxic byproducts detected.
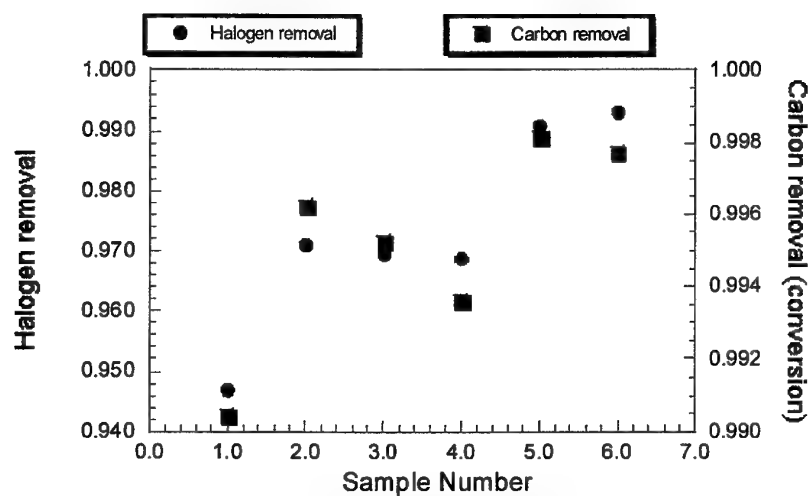
Figure 4: Halogen removal from the solid fuel (determined from ash analysis) correlates well with carbon removal.

Experimental Result	REACTOR WALL TEMPERATURE						
	600 °C	700 °C	800 °C	900 °C	1000 °C	1100 °C	1200 °C
Asbestos found in unburned rubber particles in ash	YES	YES	YES	YES	NO	NO	NO
Free-floating asbestos in ash	NO	NO	NO	NO	NO	NO	NO
Heat-conversion of asbestos occurred	NO	NO	NO	NO	YES	YES	YES
Carbon Content of Ash (percent)	8.6	1.55	1.44	0.85	1.42	0.49	

Table 1: Experimental results showing asbestos conversion (to aluminum/magnesium silicates) at combustor temperatures of 1000 °C and above.

THIS PAGE HAS BEEN DELIBERATELY LEFT BLANK

Aerosol Emission Measurements of Rocket Motors
From Contained Open Burn Events

J.R. Stephens
Los Alamos National Laboratory
PO Box 1663, MS J-565
Los Alamos, NM 87545, USA
Tel: (505) 667-7363
Fax: (505) 665-4631
E-mail: jrs@lanl.gov

NIKE and HAWK rocket motors were burned in an underground chamber as part of the Joint Demilitarization Technology (JDT) Program between the Departments of Defense and Energy. The program is designed to measure the gas and particulate emissions from munitions and rocket motors under conditions similar in scale to open detonation (OD) and open burn (OB) events used in demilitarization activities. Performing the rocket motor burns in a large (4644 m3), sealed chamber allows quantitative determination of emissions that is not possible for burns that are performed in the open atmosphere.

Reported here are measurements of particulate size distribution, mass concentration and elemental aerosol content as a function of time for three rocket motor tests; 2 and 4 NIKE motors, and 2 improved HAWK motors. Each NIKE rocket motor contains 750 pounds of double base type propellant. Each Improved HAWK motor contains 605 pounds of composite type propellant.

The aerosol samples were collected after each burn by drawing aerosol-laden gas through the chamber barrier into two parallel sampling systems. One system (impactor) collects aerosol samples from 0.1 to 10 μm in aerodynamic diameter (respirable fraction) and measures the mass concentration (mg/m^3) in each of 7 size bins in real time. The other system (streaker) collects three size fractions, > 10 μm, 2.5 - 10 μm, and < 2.5 μm. The latter two size fractions are collected on rotating substrates, thereby providing a time history of the aerosols present in the test chamber. The streaker samples are analyzed using Proton-Induced X-ray Emission (PIXE) Spectroscopy to determine the aerosol elemental composition for elements of atomic number greater then sodium (Z=11). The elemental composition of chamber materials, including shotcrete, concrete, aggregate, and tuff, were measured to provide background measurements for comparison with the aerosols produced in the burn.

For the NIKE burns, the respirable aerosol concentration reached about 200 mg/m^3 10 minutes after the burn (our first sample) and fell to half this value in 90 minutes. Aerosols were predominately in the low micron and submicron range, with the mass concentration peaking at 1 μm aerodynamic diameter. The elemental composition was dominated by elements from the chamber materials, including calcium, aluminum, silicon, potassium, titanium, chromium, manganese, and iron.

The HAWK rocket motors contained aluminum, which resulted in a large concentration of aluminum oxide in the collected particulate. Respirable particulate concentrations were 120 mg/m^3 for our first sample 10 minutes after the burn. Particle mass size was highest between 1 and 2 μm diameter for the first sample, with the size peak shifting to below 0.5 μm by 20

minutes after the burn as the large particles settled out. The elemental composition of the aerosols was dominated by aluminum, which accounted for greater than 80% of the particle metal mass, followed by magnesium, iron, copper and lead.

Implications of the results for emissions from open burn demilitarization activities will be discussed.

Combustion Experiments on TNT and Tritonal in Closed Chambers with Either an Air or Nitrogen Atmosphere

J.W. Forbes, J. Chandler, B. Cunningham, L. Green, J. Reaugh , A. Kuhl, J.D. Molitoris
Lawrence Livermore National Laboratory
P. O. Box 808, L-282
Livermore, CA 94550
Tel: (925) 423-3496
Fax: (925) 424-3281
E-mail: molitoris1@llnl.gov

Approximately 800 g explosive charges were detonated in the center of a 16.6 K-liter cylindrical chamber. Five blast wave transducers were placed around the chamber to record the pressure-time history from the initial air-blast and continued to record much later in time to measure the quasi-static pressurization. Gas sampling of the atmosphere following the experiment was also conducted. Six 800 g pressed TNT charges were detonated in one-bar air atmosphere and four in a one-bar nitrogen (99.94% pure) atmosphere. Five 720 g pressed Tritonal charges (TNT/Al 80/20 weight %) were detonated in air and five in nitrogen. All charges used an additional 50 g, LX-10 (HMX/Viton 95/5 weight %) booster. The Tritonal charge has a total combustion energy equal to that of the TNT charge in air.

The blast wave records had many pressure oscillations from multiple wave reflections off the chamber walls making interpretation difficult, but the late-time (40 ms after detonation) pressure rise is more amenable to interpretation. The TNT charges produced an average late-time increase of 0.9 bar in nitrogen and 2.8 bar in air (see figure). The corresponding Tritonal charges produced 1.1 bar in nitrogen and 2.8 bar in air. Chemical analysis of the gases after the nitrogen atmosphere experiments, in conjunction with results from an equilibrium

thermochemical code, provides an assessment of the fuel available for late-time combustion in the air experiments. A numerical simulation[1] using a turbulent mixing code demonstrates that late-time combustion kinetics is dominated by turbulent mixing.
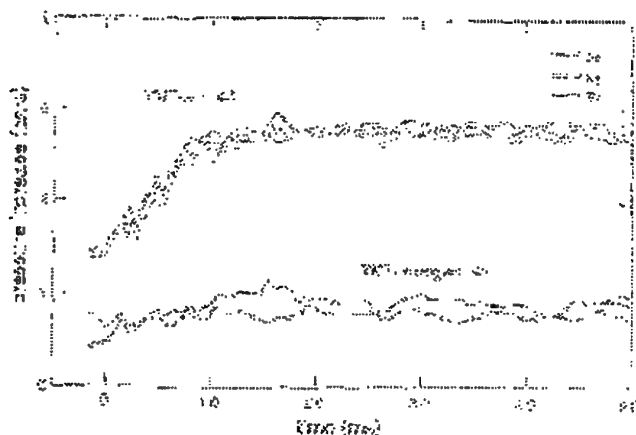
In two smaller scale experiments, 25 g of TNT was detonated inside a 5.3 liter calorimeter bomb. In the first experiment the bomb was charged with 3 bars of nitrogen and in the second with 2.6 bars of oxygen. Two pressure transducers recorded multiple pressure wave reflections from the walls. The detonation product concentrations in these experiments differ from those found in the large-chamber experiments. We explain this difference as metastable product concentrations obtained during the temperature drop of the small-chamber experiments.

[1]A.L. Kuhl, J. Forbes, J. Chandler, A.K. Oppenheim, R. Spektor, and R.E. Ferguson, "Confined Combustion of TNT Explosion Products in Air," UCLRL-131748, and the

Methods for Recovery of Ingredients from Solid-Propellant Rocket Motors

A. Vorozhtsov, A Salko, S. Bondarchuk
Tomsk State University
36, Lenin Ave, Tomsk, 634050, Russia
Fax: 7-3822-553836
E-mail: tnk@post.tomica.ru

In connection with the removal of the ground and marine based strategic solid rockets from battle duty, the problem of destruction and utilization of large solid-propellant (SP) rocket motors becomes very urgent. In addition to economic expedience, this problem must be solved in order to minimize harm to the environment. At present, both in Russia and the USA, rockets are being destroyed by means of explosion and incineration. This method is not optimal as it causes pollution of the environment locally as well as globally, and the possible further use of the solid-propellant rocket components is eliminated. This paper analyzes the calculated atmosphere pollution as a result of rocket motor destruction on an open stand by means of incineration. The equilibrium compositions of combustion products containing ecologically harmful products (HCl, Cl, CO, etc.) are calculated, with change of the equilibrium composition depending on the temperature of the combustion products. The interaction of the combustion products with air depends on their composition. One of the suggested methods of solution is the injection of alkaline solutions into the exhaust stream of the rocket motor in order to sterilize ecologically harmful products.

The following two methods are considered attractive possible solutions of rocket motor destruction due to the fact that they produce useful products without polluting the environment.

1) Incineration of the solid-propellant rocket motor in a special set-up which would allow limiting of loads on the environment and also organizing the collection of aluminium oxide.

2) Processing of solid-propellant charges by means of preliminary destruction and further chemical destruction of the polymeric binder.

In this investigation, the possible solutions to the technical problem are considered, the results of the technical schemes are given, and the various refinements on the computational basis of the setups are offered. These schemes could be utilized to increase the output of useful products. Cited are data of laboratory experiments which are indicative of the efficiency of offered methods. Each engineering solution is accompanied by a mathematical simulation of the process. It is shown that with implementation of the first method, for combustion of a solid-propellant charge in a water solution used as an oxidizer, the output of aluminum and its oxide (which can be used a second time) exceeds 90 percent of the initial amount of aluminum content in the propellant charge. The implementation of the second method enables the extraction of more than 90 percent of ammonium perchlorate, HMX, and aluminum ingredients from their respective initial weights in the solid-propellant charge.

THIS PAGE HAS BEEN DELIBERATELY LEFT BLANK

Chemical Conversion of 2,4,6-Trinitrotoluene (TNT) to New High Performance Polymers[†]

A.L. Rusanov*, L.G. Komarova and M.P. Prigozhina
A.N.Nesmeyanov Institute of Organo-Element Compounds
Russian Academy of Sciences, 117813, 28 Vavilov St., Moscow, Russia
Telephone: +7(095) 135 6166
Fax: +7(095) 135 5085
E-mail: komarova@ineos.ac.ru

V.A. Tartakovsky, S.A. Shevelev, M.D. Dutov
N.D. Zelinsky Institute of Organic Chemistry
Russian Academy of Sciences

2,4,6-Trinitrotoluene (TNT) is a well-known military explosive. For chemists, however, TNT represents a polyfunctional molecule that could serve as a source for various higher value products. We have systematically investigated numerous chemical transformations of TNT with the goal of producing useful materials for civilian applications. We have developed techniques for the selective conversion of the nitro and methyl groups in TNT, which has allowed the subsequent production of new high performance polymers.

We initially converted TNT to 1,3,5-trinitrobenzene (TNB). TNB was then transformed into a variety of dinitro- and diaminoarenes containing phenoxy, thiophenoxy, phenylsulfoxide and phenylsulfone substituents. The substituted dinitroarenes were used for the preparation of aromatic polyethers. The substituted diaminoarenes were used for the preparation of aromatic polyamides and polyimides having improved processibilities combined with good thermal and mechanical properties.

THIS PAGE HAS BEEN DELIBERATELY LEFT BLANK

Development of Passivated Pyrophoric Metal Powders
(Hafnium and Zirconium) With Reduced Electrostatic Discharge (ESD) Sensitivity

B.M. Kosowski
MACH I Inc.
340 East Church Road
King of Prussia, PA 19406
Tel: (610) 279-2340; Fax: (610) 279-6605; E-mail: machi@machichemicals.com

High-density metals such as hafnium and zirconium are of interest to the propellant, explosive, and pyrotechnic industry due to their high oxidation enthalpies; however, these metal fuels suffer from electrostatic discharge (ESD) complications, creating safety concerns. Previous attempts to passivate these powders have failed due to abrasion of the protective coatings. Two novel methods for desensitizing hafnium powder based on technology developed by MACH 1, Inc. were successfully demonstrated in a Phase I SBIR project: both approaches negate abrasion complications. First, *Reactive-Milling (RM)* of hafnium. powder with NH_4OH to 800° C in a N_2 atmosphere produces a thin protective coating of HfN on hafnium. The olive-gold material exhibited elevated ESD thresholds. The second method, *RM* of hafnium and aluminum powders in an Ar atmosphere to 700° C followed by nitridation at 610° C, generated a protective intermetallic coating (Al_2Hf) on hafnium, which also exhibited excellent passivation levels. These materials were fully characterized by optical, SEM, and XRD analyses.

THIS PAGE HAS BEEN DELIBERATELY LEFT BLANK

Deflagration Regimes and Safety Areas of Nitrobenzene and Proparhyl Alcohol

G.D. Kozak and B.N. Kondrikov
Mendeleev University of Chemical Technology
Moscow, 125047, RF, Russia
Tel: (095)496-6818
Fax: (095)200-4204
E-mail: bkondr@orc.ru

The line dividing explosive and non-explosive substances in the danger-and-safety area is a very relative line due to strong dependence of the form of explosive transformation on the conditions of initiation and propagation of deflagration or detonation waves. The systems having weak explosive characteristics are of interest, in this respect, from both theoretical and practical points of view. Some organic nitrocompounds having one nitro-group and three or more carbon atoms, as well as some acetylene derivatives, fall into this intermediate area. This work deals with the explosion safety of two organic liquids, nitrobenzene ($C_6H_5NO_2$) and proparhyl alcohol (propynol, C_3H_4O). These are not usually considered liquid propellants, and moreover are regarded as safe chemical reagents; however, they appeared to be substances disposed to deflagration and perhaps to detonation. It should be noted that sometimes it is difficult to distinguish between deflagration and detonation in these very indefinite cases.

Results of investigation of explosive transformation conditions in these substances are described. The calculated heat of explosion of nitrobenzene, at zero porosity, is Q = 4, and of propynol is Q=4.3 MJ/kg. These are just slightly less than Q of Dinitrotoluene (4.5 MJ/kg). The detonation ability of melted Dinitrotoluene has been shown to rise drastically with increasing porosity. Accordingly, the influence of porosity on detonation ability of both nitrobenzene and propynol should be investigated.

Experiments were carried out in steel tubes (diameter d = 10, wall thickness h = 13, and length l= 250 mm). The radial holes (d=2 mm at a space of 25 mm from one another) were drilled in a wall of the tube to register luminosity of the process by means of a streak camera (GFR-3). As a booster, a small pellet of RDX was used. To reduce the charge density of nitrobenzene, it was gelled by the addition of colloxylin (5%) and intensively mixed at T≈500C after the addition of a small amount of a surfactant. For the preparation of porous charges from propynol, the tube was filled in by porous polystyrene spheres (diameter 2.5 - 3.5 mm) and the top of the channel was closed by a fine mesh wire gauze to prevent flotation of the porous spheres.

Experimentally measured velocity of deflagration or detonation in nitrobenzene at a density of 0.5-0.7 g/cm3 was in the range of 0.8-1.1 km/s. In the case of propynol (at ?=0.43-0.44 g/cm3) it was 2.2-2.3 km/s. The velocity for nitrobenzene is about two times slower than the ideal detonation velocity calculated by means of our thermodynamic computer code.

Mechanisms of the explosive transformation of the liquids consists in auto-ignition of the porous media under influence of the compression wave. A part of the liquid that has a temperature close to the initial temperature of the substance and does not undergo the auto-ignition process, but burns in the usual conductive regime. The critical porosity values for

both substances were calculated theoretically. The results of the calculations correlate very well with our experimental findings.

Combustion Synthesis of SiO$_2$ in Premixed Flames

C.L. Yeh
Department of Mechanical Engineering, Da-Yeh University
Chang-Hwa, Taiwan
Telephone: 886-4-8528469 ext. 2118; Fax: 886-4-8528767;
E-mail: clyeh@aries.dyu.edu.tw

E. Cho and H.K. Ma
Department of Mechanical Engineering, National Taiwan University
Taipei, Taiwan

Fused silica (SiO$_2$) has been widely used as a precursor material in the semiconductor, fiber-optic, and ceramic industries. Deposition of SiO$_2$ vapor to form insulating films by combustion of silane (SiH$_4$) is the major approach currently. However, due to the toxic and hypergolic nature of silane, safety considerations of the chemical vapor deposition (CVD) motivate the study of alternative methods to produce SiO$_2$.

This study is to develop a novel technique to produce SiO$_2$ particles in the post-flame region of a premixed flame burner. Formation of SiO$_2$ particles in gas phase has been achieved by the addition of small amount of hexamethyldisiloxane (HMDS), (CH$_3$)$_3$-Si-O-Si-(CH$_3$)$_3$, vapor into the flame zone of premixed C$_3$H$_8$/air flames. The schematic diagram of experimental setup is shown in Fig. 1. The wash-bottle method is used to carry the HMDS vapor to the premixed gas stream. The carrying gas (air) was sent through a feeding tube into the liquid HMDS, resulting in the bubbling liquid surface of HMDS. Due to the high volatility of HMDS, the HMDS vapor was easily entrained into the air stream. In the post-flame region, the HMDS was proposed to react with the OH and O$_2$ to form high-purity and fine-sized SiO$_2$ particles, which was then quenched on a stainless-steel plate.

The objective of this research is to investigate the effects of flame temperature and HMDS concentration on the size and purity of SiO$_2$. The quenched samples were observed under a scanning electron microscope (SEM) to determine the size. The chemical composition of collected powders was analyzed by an energy dispersive spectrometer to examine any impurity. In addition, qualitative observations of the flame color and structure were performed. Results showed the appearance of orange-yellow color in the post-flame zone when the HMDS vapor was added. The detailed results and discussion will be given in the full paper.

THIS PAGE HAS BEEN DELIBERATELY LEFT BLANK

AREA 3:

COMBUSTION PERFORMANCE OF HYBRID AND SOLID ROCKET MOTORS

Bomb Testing and Similarity of Propulsion Systems

I.G. Assovskiy
Semenov Institute of Chemical Physics RAS
Kosygin St. 4, Moscow 117977 Russia
Tel: (7-095) 939-7267
Fax: (7-095) 939-7417
E-mail: assov@chph.ras.ru

Bomb testing of propellant performances plays an important role in the quality control of propellant production and in experimental investigations. Starting from the pioneering works of Vieille and Muraour, bomb testing is considered as a simulation of combustion in real propulsion systems. Different types of closed and vented bombs are widely used to obtain information on ignition, combustion, and other ballistic characteristics of propellant to predict the ballistic performances or to understand anomalous phenomena. However, the problem of prediction based on bomb testing is still far from being solved. For example, the rate of combustion in real propulsion system is typically determined by full-scale fire testing, despite the bomb testing gives this information. That is why the goal of this paper is to analyze the sensitivity of the solid propellant performance to combustion conditions in rocket motors, guns, and in bomb testing. Influence of ignition conditions, erosive burning, thermal radiation and heat losses is analyzed. The emphasis is on similarity of high-pressure propulsion systems (large-caliber guns and small rockets) having propellant charges consisting of longitudinal tubular elements. The analysis uses an advanced thermodynamic model of the interior ballistics process based on the theory of unsteady combustion in high-pressure chambers [1].

The modern tendency in propulsion systems design is to increase the loading density (i.e., propellant weight divided by the volume of combustion chamber). For such systems the charge ignition (initiation and flame spread over the charge surface) is a relatively long process taking a large part of the ballistic cycle. In addition, instabilities and abnormal phenomena (known as "travelling waves", "negative temperature gradient of the pressure peak", and so on) may occur as result of improper ignition or other property of the charge. Investigation of ignition and flame spread phenomena is sometimes difficult and expensive to perform in real guns or rocket systems (large-caliber guns, in particular). Therefore, some special bombs (closed and vented) are used as laboratory simulators of real systems to perform this interior ballistic research. In some cases the simulator is a gun chamber without a barrel. Depending on the purpose of the experiment, the projectile is replaced by a nozzle with membrane, shear disc, or other device to simulate the pressure-time curve of real chambers. Such full-scale simulators are useful tools since ignition and subsequent combustion processes can be sensitive to even small deviations of the controlling parameters. On the other hand, it reflects disability of the interior ballistics theory to predict the actual charge performances in a full-scale system using fire tests in small-scale simulators. This paper analyzes differences and similarities of ignition and combustion conditions in rocket motors, guns, and typical simulators that influence the pressure-time curve of the process.

The analysis carried out in this paper shows that ignition is responsible for the effect of accelerated combustion [1] of the surface layers of the charge elements and influences significantly the pressure peak in a rocket motor, gun, and vented bomb. This influence increases with the loading density. That is why the rate of combustion in the traditional

closed-bomb testing (where the loading density is not more than 0.25 g/cm^3) cannot reproduce the combustion rate observed in full-scale system (with loading density 0.7- 0.8 g/ cm^3). However, similar conditions can be realized in vented bombs. Also the standard processing of experimental data obtained in closed bomb testing uses only that part of the pressure-time curve between 25 and 75 percent of the maximum pressure. This makes quite reasonable to derive the law of steady-state combustion, but unsteady combustion data are ignored. Fire tests in vented bombs with high loading density can compensate the lack of such information.

1. I.G. Assovskii, "A Phenomenological Theory of Propellants' Ignition and Subsequent Unsteady Combustion in High Pressure Chambers", in "Challenges in Propellants and Combustion.100 Years After Nobel", Ed. by K.K. Kuo, Begell House Inc., NY - Wallingford (UK), 1997, pp. 1035-1045.

Burning Rate Data Reduction of Ariane Boosters Small-Scale Test Motors

L.T. DeLuca, A. DeNigris, C. Morandi, F. Pace, A. Ratti, M. Servieri
Laboratorio di Termofisica, Dipartimento di Energetica
Politecnico di Milano, 20133 Milan, MI, Italy
Tel: +39-02-2399-3912
Fax: +39-02-2399-3940
E-mail: fivbd@tin.it

A. Annovazzi, E. Tosti
Fiat Avio - Comprensorio BPD
Colleferro, RM, Italy

R.O. Hessler, R.L. Glick
Consultants
Somerville, AL, and Rensselaer, IN, USA

Small-scale solid rocket tests are routinely carried out by propulsion industries to measure propellant steady burning rate both for propellant batch control and for research and development. A Working Group, initially started as AGARD PEP (Propulsion and Energetics) Panel and later continued as NATO AVT (Advanced Vehicle Technology) Panel, has recently completed a 3-year study in this area. The purpose was to analyze and possibly standardize the procedures employed in many countries, and sometimes within the same country, of steady burning rate data reduction from pressure traces collected in small-scale test motors. The activities of this Working Group, however, have concentrated on ideal (i.e., computer generated) pressure traces and less on real world pressure traces (i.e., obscured by imperfect measurements including variations in motor manufacture, variations in motor operation, instrumentation noise, etc.). In this paper, 54 pressure traces obtained in the so-called Baria motor (a small-scale test motor implemented for Ariane-5 solid propellant boosters) and 24 pressure traces obtained in a standard 2 inches motor (a small-scale test motor implemented for Ariane-4 solid propellant boosters) are examined. Several data reduction methods based on the thickness-over-time definition, used by leading European companies and also by the new RHG technique, have been applied. Moreover, a mass balance method used at NSWC, Indian Head in USA has also been implemented. Since the actual steady burning rates are unknown, results can be compared based only on the statistical quality of the deduced ballistic data (typically, percent standard deviation of relevant parameters). In addition, easiness of application and capability of automatic handling are of interest especially for industrial propellant production facilities. Within this framework, specific features and general trends of the tested methods are discussed.

THIS PAGE HAS BEEN DELIBERATELY LEFT BLANK

Motor Variability Effects on Burning Rates Measured in Subscale Rocket Motors

R.O. Hessler, R.L. Glick
Consultants
Somerville, AL, and Rensselaer, IN, USA
Tel: 1-256-778-8014
Fax: 1-256-778-8014
E-mail: ROHessler1@aol.com

C. Morandi, L.T. DeLuca
32 Piazza Leonardo da Vinci
Politecnico di Milano
20133 Milan, MI, Italy

A. Annovazzi, E. Tosti
Fiat Avio - Comprensorio BPD
Colleferro, RM, Italy

The burning rate of a solid propellant is a primary ballistic property, needed for design of end-item motors and for quality control of production mixes. The burning rate of a propellant varies with pressure, and the rate-pressure relationship for a mix is usually determined by testing a series of strands or subscale motors at different relatively constant pressures.

Burning rate is fundamentally defined as the velocity of a combustion wave through the propellant. Although instantaneous measurements are under development, most motor measurements rely on an average, which requires definition of a burning time. However, burning times are not easily determinable from motor pressure-time histories, because beginning and ending transients tend to obscure the actual starting and stopping of burning. Consequently, different facilities have defined a considerable variety of burning time endpoints, resulting in a range of differences in burning rate data in the industry.

Data scatter is the only available indicator of the "goodness" of procedures or measured rates, because the true rate of a propellant mix is unknown. A number of industrial burning rate measurement procedures have recently been compared in a data analysis round robin, using sets of simulated motor data for which the true input burning rate equations are known. Except for one procedure requiring human interaction at several points, none of the procedures appeared to intrinsically contribute to data scatter. This indicates that observed data scatter must be caused by variability of the propellant itself or by variability of the subscale motor operational behavior not accounted for in the analysis procedures.

The full paper will present current status of research to develop useful measures of motor variability, to determine sensitivity of existing analysis procedures to motor variability, and to develop procedural steps and/or motor remedies to reduce data scatter.

A commonly used measure of burning rate data scatter is the standard deviation $\sigma(r_b(p))$ of rate data about the least-squares $r_b=ap^n$ line for a mix. Taken one mix at a time, $\sigma(r_b(p))$ averages about 0.44% for the mixes shown in Fig. 1. However, the offsets of the three pressure groups from the mean (dotted line) indicate that a constant exponent n assumption is

inadequate and/or that motor operation varies systematically with pressure other than by the rate equation. Taking one pressure group at a time indicates that $\sigma(r_b|p)$=0.22% may be a closer estimate of propellant variability, and that the range of $\sigma(r_b|p)$ and the difference from $\sigma(r_b(p))$ provide estimates of motor variability and inability of the analysis procedure to account for motor variability.

A sensitive technique for detection of motor

Fig. 1: Deviations of Motors from Mix Rate-Pressure Lines.

variability is to suitably normalize the pressure-time history to define the "trace shape." The trace shape of a motor reflects all the processes and many conditions affecting motor operation, so deviations in trace shape between motors or groups of motors indicate differences in the motor operating processes. In Fig. 2, which shows mean trace shapes for the pressure groups of Fig. 1, all three groups show the s-shaped region from 40% to 70% time (a deviation typical of motors manufactured by plunge-casting) and a trend of deviations after 70% consistent with the trend of nozzle erosion differences. The trace shapes before 50% do not show a trend complementary to the later nozzle erosion trend, indicating motor variability in this region is likely responsible for the offsets of the pressure groups. Standard deviations within each group indicate that motors in the middle pressure group are significantly more variable before 20% time, which may account for the larger $\sigma(r_b|p)$ of the middle group.

Fig. 2: Variation of Normalized Pressure-Time History with Mean Motor Pressure.

Ballistic and Combustion Properties of High-Pressure Exponent Hydrocarbon-Based Fuel-Rich Propellants

G.J. van Zyl

Somchem, a Division of Denel

P O Box 187 Somerset West, 7130, South Africa

Tel: + 27 21 8502511, Fax: + 27 21 8502433

e-mail: deonvzyl@somchem.denel.co.za

To satisfy the requirements for a variable fuel-flow gas generator of a ducted rocket, in terms of ballistic and energetic properties, the propellant formulator finds himself in a precarious situation. These requirements must be met by using two conflicting formulating techniques. In the case of end-burning gas generator configurations, a propellant with a high burn rate and high pressure exponent is required. This can easily be achieved if the propellant contains a high oxidiser content. However, a propellant with high oxidiser content has a very low heating value, which makes it unsuitable for a gas generator of a ducted rocket. Both requirements must therefor be achieved by incorporating enough oxidiser to achieve the desired ballistic properties, while having enough fuel left to produce the desired heating value.

In this paper some of the results of an extensive investigation to formulate a suitable fuel-rich gas generator propellant for a variable fuel-flow ducted rocket is discussed. The required ballistic properties, especially the pressure exponent, needed for a variable fuel-flow gas generator are unique when compared to conventional solid propellants. A high-pressure exponent of 0.5 - 0.6 is required with a pressure coefficient of 4 - 6 mm/s. The effect various formulation changes have on the ballistic properties of a polystyrene HTPB-based propellant was studied. Some of the aspects investigated include (a) the effect of AP concentration, particle size and particle size distribution (b) partial replacement of AP by RDX and $KClO_4$ (c) the effect of different burn rate catalysts and modifiers such as Fe_2O_3, Cr_2O_3, Al_2O_3, Butacene and carbon fibre and combinations of these compounds. The effect of including a small amount of Al and Mg on the ignitability of the secondary combustion products was also studied. Processing and mechanical properties of the various propellant formulations are reported.

A few formulations were also studied on the optical bomb of the ICT with the objective of determining the nature of the combustion zone. The ballistic properties were also determined during these studies and compared with the results obtained with a Crawford bomb and small-scale ballistic assessment motors. The temperature of the combustion zone was also determined at the ICT with visible spectroscopy by making use of Planck's Law for grey body radiation. These results were compared with the theoretical flame temperatures determined with two different thermodynamic codes.

THIS PAGE HAS BEEN DELIBERATELY LEFT BLANK

Rocket Testing at EMRTC

J.L.M. Cortez, J. Forster, A. Perryman
Energetic Materials Research and Test Center
New Mexico Institute of Mining and Technology
801 Leroy Pl., Socorro, New Mexico 87801
Tel: (505) 835-5701
Fax: (505) 835-5630
E-mail: jcortez@emrtc.nmt.edu

J. Rusek
School of Aeronautics and Astronautics, Purdue University

The Energetic Materials Research and Test Center (EMRTC) of the New Mexico Institute of Mining and Technology, Socorro, NM 87801 is engaged in testing of rockets, employing a number of technologies and concepts that offer the potential to reduce launch vehicle costs dramatically.

These concepts that utilize pressure fed rocket engine technology are being applied in programs supported by the U.S. Government. In particular, the EMRTC is currently assisting in the testing of the rocket motors under development for two programs known as the SCORPIUS and EXCALIBUR Programs.

In addition, EMRTC is in the process of adding to its LOX-Kerosene fuel lines, liquid Hydrogen and Hydrogen Peroxide capability in order to conduct small rocket motor testing in the 5-100K thrust level using these fuels. Cooperation with Purdue University in the area of catalysis and stabilization of Hydrogen Peroxide in engine testing will also be discussed.

THIS PAGE HAS BEEN DELIBERATELY LEFT BLANK

Study of Multi-Perforated Combustion Paste Propellant Rocket Motor

B. Gao, D.Y. Ye, S.X. Jia
Shaan Xi Power Machinery Institute
PO Box 169
Xi'an 710025 China
E-mail: yan.x2@163.net

Multi-start pulse rocket motor can act as attitude control motor and terminal velocity adjustment motor in mid-stage guidance for strategic missile warhead, propulsion system for anti-missile and anti-satellite weapon, terminal velocity adjustment motor for re-entry vehicles of intercontinental ballistic missile and motor for the warhead of kinetic weapon etc. It is of great importance in enhancing the mobility of strategic and tactical missiles and realizing miniaturization of warhead. The paste propellant pulse rocket motor studied in this report synthesizes the advantages of both solid propellant rocket motor and liquid propellant rocket motor with the functions of multi-start and random adjustment of motor thrust, so it has attracted much attention from related research units and experts both at home and abroad. The report presents a new paste propellant pulse rocket motor design through analysis of flow, ignition, combustion and extinction of paste propellant, a non-Newtonian fluid of oxidizer and fuel uniform-mixture, in a cylindrical tube of large length-diameter ratio. With no need of extra energy for multi-ignition, the new-designed paste propellant rocket motor utilizes the residue heat of chamber itself as the multi-ignition energy. The critical technique of it is the design of re-ignition device and the realization of re-ignition, which can guarantee the reliable ignition and reliable extinction with no occurrence of uninvited combustion.

1. Study on flow properties of paste propellant in multi-perforated re-ignition device
The rheological properties of several paste propellants are measured with Haake viscometer and their rheological curve, flow index and viscosity coefficient are determined. By using single-perforated re-ignition test system, many tests are carried out and the relations between paste propellant flow rate and squeezing pressure gradients are obtained. Based on experiments, a flow model of paste propellant in re-ignition device is established. Through solving the flow equation of non-Newtonian fluid, the flow properties of paste propellant are obtained. The relations of propellant squeezing pressure in multi-perforated re-ignition device and the length and diameter of cylindrical tube of re-ignition device with paste propellant flow rate and flow speed are determined.

2. Study on ignition and extinction of paste propellant in multi-perforated re-ignition device
By use of laser ignition test system and high-speed movement analysis system, the ignition delay time of paste propellant is comprehensively and systematically studied through experiments. The relation curve of the ignition delay time of the paste propellant versus ignition energy and surface heat-flow density is obtained. The whole ignition and extinction process of paste propellant is recorded. Based on the experiments, an ignition model on the basis of comprehensive ignition theory of solid propellant is built, which considers all the influence factors. Through numerically solving the governing equation sets of ignition process, the relation curve of extrinsic heat flux versus the ignition delay time of paste propellant is obtained and the calculation values are well fit to the experiment results. The analysis of the relations between flow and heat transfer of paste propellant in re-ignition device is performed. The criterion of ignition and extinction of paste propellant is determined

and an axially symmetrical coupling heat transfer model for paste propellant and multi-perforated ignition device is established. Through numerically solving the governing equation sets, the temperature change of paste propellant in the flow process within re-ignition device and the temperature change of re-ignition device during motor ignition are obtained. Combined with the ignition criterion, the correlation between temperature, length, channel diameter and squeezing pressure gradients of re-ignition device for the reliable ignition of the motor and the conditions for motor extinction are got. In order to determine the maximum allowable interval time between pulses of motor, simple analysis for temperature change of extinct motor chamber are done.

3. Study on steady combustion law of paste propellant

By use of infrared thermal imaging system, the experimental study on steady combustion characteristics of paste propellant is carried out, so as to obtain the flame temperature distribution and combustion surface temperature of the paste propellant. Based on experiment and combined with BDP steady combustion model of solid propellant, a model for analyzing steady combustion characteristics of paste propellant is developed. The model takes these factors like the effect of propellant ingredient, particle size of oxidizer and propellant state (dilute slurry or the cured) etc. on propellant burning rate into consideration. Both computation and experiment indicate that the burning rate and pressure exponent of slurry (paste) are higher than that of cured slurry (solid). So the model can be used in development of paste propellant formulation and study of combustion characteristics of solid propellant slurry.

4. Design and test of paste propellant pulse motor

By synthesizing all the factors like chamber operating pressure, squeezing pressure, propellant flow rate and burning rate etc., the design and fabrication of conceptual paste propellant pulse motor is finished. Through static firing test, not less than seven good pulses are gotten, each of which works about 2s. The interval between pulses is not less than 2s. According to the measured pressure profile, the thrust curve of paste propellant pulse motor is derived. So the feasibility of the motor design is demonstrated.

The following conclusions are drawn from this study:

a. The design program of a new paste propellant pulse motor presented in this study is feasible and can realize thrust adjustment and multi-start.

b. The flow properties, ignition characteristics, steady burning rate, combustion temperature and squeezing pressure of paste propellant are the main factors that influence the work performance of paste propellant pulse rocket motor and also are the main design parameters of paste propellant pulse rocket motor.

c. The multi-perforated re-ignition device is the key part of paste propellant pulse rocket motor and is the guarantee of reliable ignition and extinction of motor.

d. The experimental method adopted in the study is feasible. The experimental data obtained are credible and the theoretical model established is accurate. So the study results provide theoretical and experimental basis for design and study of paste propellant pulse rocket motor.

Under the sponsor of National Natural Scientific Funds, this research job is the first to systematically study paste propellant pulse rocket motor in China and some important conclusions are drawn. In the world, only some news reports on this field have been found out. No open study report has been seen.

Through this study, a doctoral student has been fostered. Another two doctoral students participated in some important works. Two Master degree students took part in the first phase research and had graduated.

THIS PAGE HAS BEEN DELIBERATELY LEFT BLANK

Parametric Investigation on Similarity and Scale Effects in Hybrid Motors

R.D. Swami and A.Gany
Faculty of Aerospace Engineering, Technion-Israel Institute of Technology
Haifa 32000, ISRAEL
Tel. 972-4-8292544, Fax 972-4-8230956
E-mail: <gany@techunix.technion.ac.il>

The objective of the present investigation is to provide experimental data on scale effects in hybrid motors operating under similarity conditions. It is mainly intended to examine the validity of a proposed theoretical analysis characterizing the similarity conditions under which lab-scale tests should be conducted in order to simulate firings of full-scale hybrid rocket motors. Such analysis provides a twofold advantage: 1) it gives better understanding of the fundamental phenomena in hybrid rockets; and 2) it saves enormous time and expense in the development of propulsion systems.

The hybrid motor comprises unique features which differ fundamentally from those of other rocket engines. Typically it consists of a cylindrical polymeric solid fuel grain having a single- or multi-port shape, placed in the combustor and burned with an oxidizer flowing through its ports. As a result, a gas phase diffusion flame is established between the fuel gasification products and the oxidizer within the port flow.

The fundamentals of hybrid combustion were studied by many investigators. While giving quite good insight, those investigations revealed complex phenomena affected by geometry, as well as flow and operating conditions demonstrating non-uniformity along the fuel grain. Nevertheless, the development of hybrid rockets and the prediction of their characteristics have generally been based on simplified empirical methods and cerrelations. Consequently, different aspects have been disregarded and the predictions have often been unsatisfactory, particularly for scaling purposes. Moreover, the use of empirical correlations with numerous parameters and constants might involve misinterpretation of the true physical processes, and hence inaccurate predictions when extrapolating to unstudied ranges.

Modeling the dominant, controlling combustion processes, it has been shown in the analysis that in order to correctly interpret experimental results and extrapolate them to a different-scale system, the following main operating conditions should be preserved: 1) geometric similarity; 2) the same oxidizer and fuel combination; and 3) scaling the oxidizer flow rate in proportion to the length scale. Thus the experimental data obtained from a laboratory-size apparatus can be applied to a full-scale system. The study includes test data obtained from different-size hybrid motors scaled according to the similarity analysis. Polymethylmethacrytlate and gaseous oxygen is used as fuel and oxidizer respectively in the tests.

THIS PAGE HAS BEEN DELIBERATELY LEFT BLANK

AREA 4:

ENERGETIC MATERIALS COMBUSTION FOR ROCKET PROPULSION

Active Electric-Discharge Control of Slow-Combustion-to-Detonation Transition

V.V. Afanasyev, S.V. Ilyin, N.I. Kidin, N.A. Tarasov, A.V. Lapin, A.K. Kuzmin
Department of Physics of Heat, Chuvash State University Moskovsky pr.15
Cheboksary 428015, Russia
Telephone: (7-8352) 498352, Fax: (7-8352) 428090
E-mail: ilyin@cuvsu.ru

To control slow-combustion-to-detonation transition, passive means such as turbulizers, walls exhibiting varying acoustic resistance, fuel mixtures additives, electric fields applied to the flame zone, etc. are generally used. The present authors have been the first to propose and demonstrate the possibility of actively controlling slow-combustion-to-detonation transition in half-closed pipes by exposing the flame zone to diffuse electric discharges from a special-purpose power supply unit. The physical mechanism of the influence exerted by discharges is as follows: It is well known, that flame front turbulization is the stage playing a dominant role in the transition of slow combustion to detonation. The more vigorous the flame front turbulization process, the higher the mixture burning velocity is, and consequently, the sooner the transition to detonation will occur. The turbulization process is associated with the variation in the flame zone electrical resistance. This being so, when a current-stabilized electric discharge is applied to the flame zone, the variable Joulean heat release will occur in anti-phase with the heat release fluctuations as the result of the turbulent combustion. This, in turn, will inhibit the increase in the variable pressure component, thus interfering with the flame front turbulization process. The process of slow-combustion-to-detonation transition will then be retarded. Alternatively, when a voltage-stabilized electric discharge is applied to the flame zone, the variable Joulean heat will be released in phase with the heat release fluctuations. This will enhance the turbulent combustion process, thus fostering the development of detonation.

The report deals with an experimental investigation into the phenomena under discussion occurring in half-closed and closed bodies.

Experiments to study pre-detonation flame acceleration were conducted in a rectangular-section pipe, two opposite walls of which were made of steel (these serving as electrodes), and the two remaining walls made of polymethyl methacrylate. The fuel mixture was ignited by a spark, either at the closed or the open end of the pipe. The pressure and flame propagation velocity were recorded during the experiments, and the combustion wave structure was visualized.

As the experimental findings suggested, the influence of electric discharges on the flame propagation velocity essentially depends on the fuel mixture composition, the spark initiation location, and the electric discharge stabilization technique used. Specifically, the flame propagation velocity in lean and rich propane-air mixtures will increase whatever electric discharge stabilization technique is utilized, whereas in stoichiometric mixtures, current-stabilized discharges will lead to the decrease in the flame propagation velocity. The process will become more vigorous when the air is enriched with oxygen.

The manner in which the pressure oscillation amplitude varies depends on the discharge stabilization technique employed and is essentially unaffected by the fuel mixture

composition and the spark initiation location. As far as the pressure oscillation amplitude is concerned, it will always decrease when current-stabilized discharges are applied, and will invariably increase when voltage-stabilized discharges are applied to the flame zone.

To gain a better insight into the potential of active electric-discharge control of burning velocity, experiments were also run in a constant-volume bomb. Resulting combustion wave toeplerograms and pressure oscillograms revealed that it is possible to actively control the pressure build-up and burning velocities by electric discharges. It was found that in the case of lean propane-air mixtures, voltage-stabilized electric discharges will allow a pressure build-up to be produced in a bomb similar to that in near-stoichiometric mixtures. This phenomenon carries the promise of being used in engines to reduce the fuel consumption and the discharge of harmful combustion products into the environment.

This paper also discusses plausible mechanisms to account for the results obtained.

Combustion of Propellant Grain, Forcing by Heat-Conducting Elements with Memory Effect

V.A. Arkchipov

Lenin Ave. 36 Tomsk, GSP-14, Russia

Tel: (007-3822) 410-556

Fax: (007-3822) 410-347

E-mail: mishura@niipmm.tsu.tomsk.su

Modem condition and nearest prospects of development in rocket-cosmic technology bring forth a requirement of making the reliable motor installation with the deep regulation thrust - for use as management bodies during flight (orientation, maneuvering, link-up in cosmos, soft landing etc.).

One of the classical ways of governing combustion velocity of solid propellant in simple controlled solid propellant rocket motors is by using the grains, forced by heat-conducting elements. Essence of given way consists in the realignment of combustion surface to the account of local increasing a velocity of propellant combustion along heat-conducting element and corresponding increasing gas flow.

Greatly raise a depth of regulation allows an use heat-conducting elements with the memory effect. When using such elements alongside with the heat influence on soled propellant grain is connected a mechanism of destruction propellant in consequence of destroying adjoining to element layer to the account of heat-conducting element deformation, warmed in the wave of combustion before the temperature of martensite transition. Mechanism of influence usual elements on the soled propellants burning rate was shown by the subject of sufficiently intensive studies, as a result which received algorithm of efficient burning rate calculation, in particular, Bakhman-Lobanov formula. In ditto time to the combustion heat-conducting elements with the memory effect are denoted only single publications.

In this reporting presented results of studies on the clarification of soled propellant with memory effect heat-conducting elements burning mechanism. Offered combustion model of such grains for spiral form elements from titanium nickelide. Adequacy proposed models is experienced data confirmed by processing, conducted by means of deciding an internal ballistics inverse problem (IBDP).

At the building models was considered cigarette burning simple, forced by heat-conducting element in the form spirals by the diameter D, made from delays by the diameter d. with memory effect (fig. 1). Grain a change in the combustion chamber of diameter D_k with the critical section diameter d_{cr} of nozzle block. In models is taken increasing a value of into account free volume of camera V in the process of grain burning.

Experiences were conducted on installation, scheme which brought on the fig. 1. Data processing an experiment was internal ballistics conducted by the method of deciding an inverse problem of. Problem was decided within the framework of following admissions: 1. parameters of gas average on the whole volume of combustion chamber; 2. are not taken into account heat lasses on walls of combustion chamber; 3. counting out a time is realized with

the beginning of influence on the process of combustion; 4. before the influences beginning the combustion chamber bases in the stationary condition, i.e. consumption of gas is its receipts from the area of combustion; 5. combustion chamber works in the supersonic mode of gas outflow. Experienced given on dependencies p(t) were interpolated cubic spline.

Fig. 1. Experimental rocket motor grain:
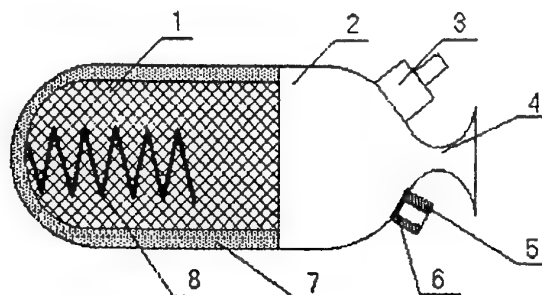
1 - propellant grain;
2 - combustion chamber;
3 - pressure gauge;
4 - main nozzle;
5 - safety valve;
6 - protecting membrane;
7 - protecting coat;
8 - heat-conducting element.

On the fig. 2 brought IBIP-calculation for the typical element. Seen that has a significant increasing an area of burning surface. When using heat-conducting elements of the different form a degree of increasing a burning surface different. So, for element in the manner of twisted plates an area of burning surface increases nearly in 4 times. This shows efficiency and advance using heat-conducting elements, possessing memory effect for gas receipts controlled.
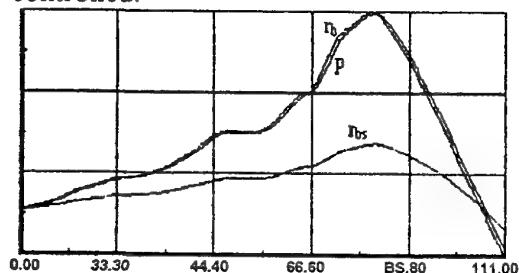
Fig. 2. Results of deciding an inverse problem of internal ballistics IBIP (in non-dimensional coordinates):
p - pressure;
rb - burning rate;
rbs - burning rate, calculated by power-mode law;
Sb - burning surface;
t - time.
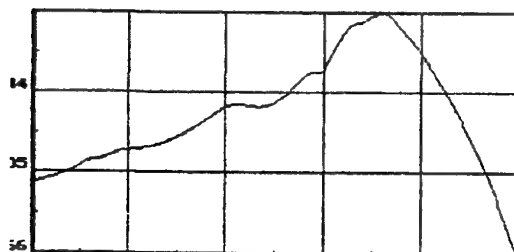
With using the tinning results, within the framework of the thermodynamic approach offered physicist-mathematical model and algorithm of working processes in rocket motors with the grain, forced by heat-conducting elements calculation (as usual, so and with the effect of memory of the form).

On base developed models are conducted parametric calculations, received controlled feature and determined times of transient processes.

THIS PAGE HAS BEEN DELIBERATELY LEFT BLANK

Acoustic Emission of Underwater Burning Solid Rocket Propellants

S. Rampichini, D. Ruspa, and L.T. DeLuca
Laboratorio di Termofisica, Dipartimento di Energetica
Politecnico di Milano, 20133 Milan, MI, Italy
Tel: +39-02-2399-3912
Fax: +39-02-2399-3940
E-mail: fivbd@tin.it

Samples of ammonium perchlorate (AP) - based composite solid propellant were ignited and burned in a combustion chamber filled with water and pressurized by gas (air or nitrogen). The acoustic signal of the combustion process, picked up by a submerged microphone, can be analysed in the time domain to obtain information about steady burning rates. Notches purposely cut on the propellant strand can usually be identified. The combustion sound can also be studied in the frequency domain, and its dependence on mass burning rate deduced. By a spectrogram analysis, it is possible to study important features of the whole combustion process, including ignition delays, burnouts, and local extinctions.

The testing apparatus is a stainless steel cylindrical chamber of 25 cm radius and 50 cm height, partially filled with water and pressurized up to 20 atm by nitrogen. Cylindrical propellant samples, 3 cm tall and 0.5×0.5 cm^2 square cross-section, were employed. A thin copper wire used to ignite the propellant sample is drowned in one end; the opposite end is glued to a support in the middle of the chamber. The sample is ignited upside-down, and during combustion the burning surface moves upward from the lower surface. Two "V" shaped notches, 1 cm spaced, are cut on the lateral surface. A standard electric microphone, modified to be resistant to water and pressure, is submerged in the water and placed close to the sample. An optical window allows direct observation of the combustion phenomena by a video camera. During the test, the chamber pressure remains virtually constant due to the large pressurization gas volume above the water level. The audio signal is digitalized by a PC soundcard and then processed by special software packages. For each test, steady burning rates are measured by three different methods: by a standard video recording technique, by a microphone used to determine the entire combustion duration; and by a microphone used to determine the time delay between the two notches.

The acoustic signal, collected during combustion, is first analysed in the time domain. The instantaneous sound power level is computed and plotted versus time. In this plot (Fig. 1), one can recognize the ignition and burnout times. The t_{start} and t_{end} instants are determined by comparing combustion sound power with noise sound power. The length used to determine mean steady burning rates is the distance between the hot wire igniter and sample top end. Steady burning rates measured by the ratio of this distance to the overall combustion duration provide the first data set. Filtering with a low pass filter, the acoustic power vs time plot, reveals the occurrence of two minima corresponding to the two notches (Fig. 2). Between notches, combustion appears essentially steady. Steady burning rates between the two notches, measured with the acoustic technique as illustrated in Fig. 2, provide the second data set. Finally, steady burning rates between notches can also be measured by a standard optical technique (superimposing a timer on a common video recording). This provides the third data set. Several interesting results were obtained by contrasting these three data sets. Yet

comparison of the best curve fittings shows that no appreciable differences exist between mike and video measurements.

The acoustic emission signal was also analysed in the frequency domain by FFT with 20 ms time step. The spectra so obtained are visualized in a spectrogram (Fig. 3). In this way it is possible to find combustion regions where spectra remain almost constant in time. Video recordings testify that these regions are steady burning zones. Thus, steady combustion processes seem to produce an invariant spectral shape. Moreover, a peak frequency exists whose position is very sensitive to the enforced set of testing parameters, in particular pressure and water level. An "I" shaped propellant sample, having three different cross-section areas, tested under constant pressure, pointed out that the peak frequency depends on the burning area, and therefore mass burn rate. Slight oscillations in the peak frequency position during steady burning are probably due to fluctuations of the burning surface normal position.

Figure 1

270
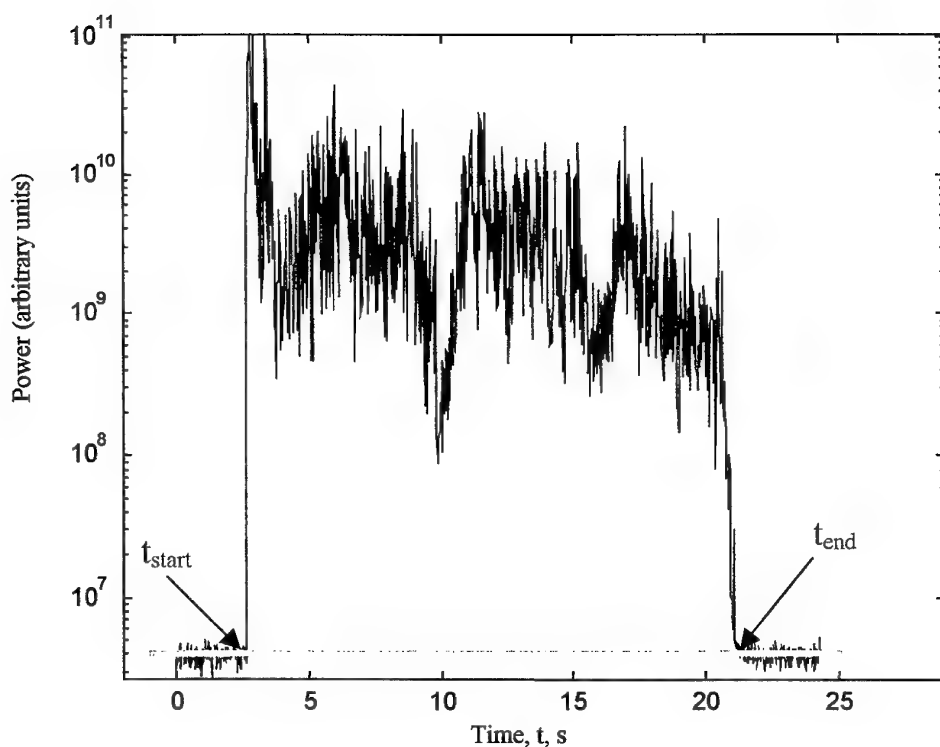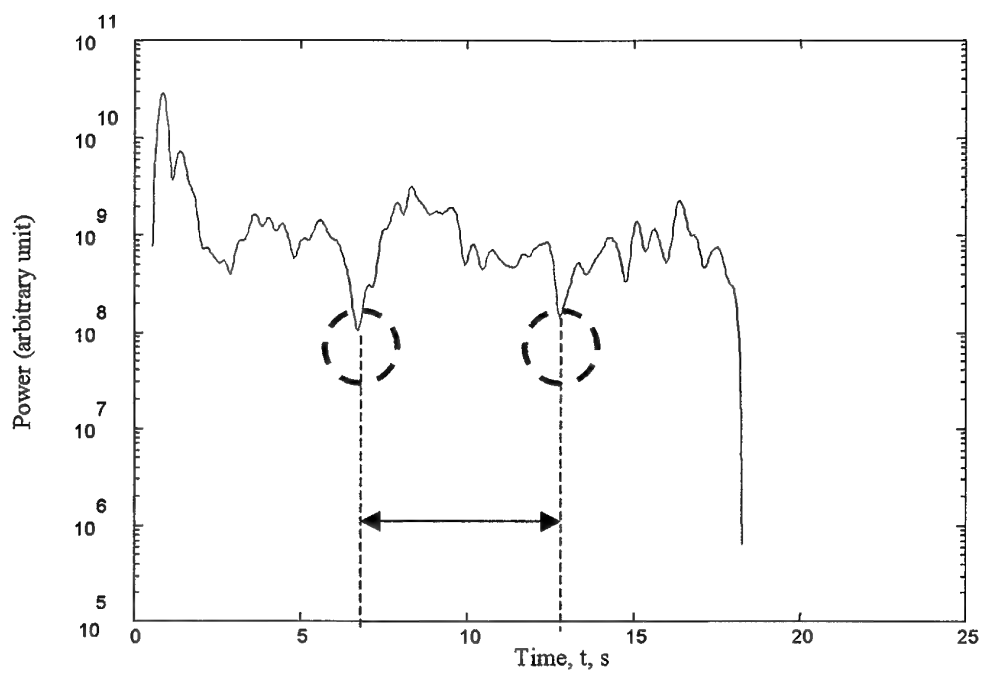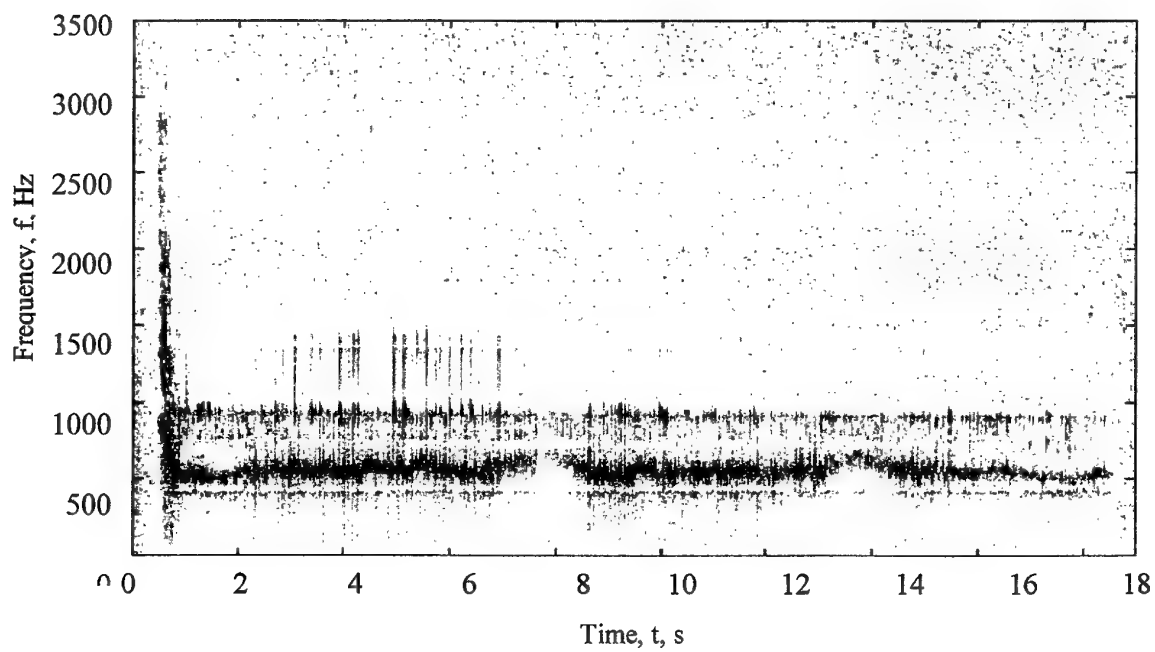
Figure 2

Figure 3

THIS PAGE HAS BEEN DELIBERATELY LEFT BLANK

Solid Propellant Ignition by CO_2 Laser Radiation

B.N. Kondrikov
Mendeleev University of Chemical Technology
Moscow 125047, Russia
Telephone: +007-095-496-6818, Fax: +007-095-200-4204, E-mail: bkondr@orc.ru

L.T. DeLuca
Laboratorio di Termofisica, Dipartimento di Energetica
Politecnico di Milano, 20133 Milan, Italy

CO_2 laser is a very convenient tool to investigate energetic materials ignition, and has been used in burning and ignition experiments for at least three decades. The fundamental investigations carried out by the authors at Princeton University Solid Propellant Laboratory, at the end of 60's and beginning of 70's with several double-base propellants, demonstrated the outstanding possibilities of the installation and resulted in discovery of several unusual peculiarities of the process (increasing ignition time for big values of radiant flux, transition from ignition to steady state gasification for very big values of radiant flux, extinction of burning and gasification under abrupt interruption of radiation, etc.). Further laser ignition results and trends were offered in the international literature for a variety of compositions and operating conditions. The aim of this presentation is to present some recent measurements concerning the laser ignition of a metalized Ammonium Nitrate (AN) – based composite solid propellant and compare these results with past data.

Ignition peculiarities of the tested AN propellant are centered around three main groups of facts:
1. The ignition time, t_i, under the investigated experimental conditions is unusually big compared to other propellants.
2. The pressure influence on t_i, in the interval from 1 to 5 atm, is also abnormally strong while the dependence t_i on q is very close to that of double-base propellants.
3. When pressure increases to 10 atm, the $\log(t_i)$ vs $\log(q)$ line slope suddenly becomes about half compared to that observed at 1 and 5 atm.

In particular the N-5 catalyzed double-base, extensively studied by the authors, under laser beam radiation is characterized by n=1.7 slope of the $\log(t_i)$ vs $\log(q)$ line, about the same as demonstrated by the tested AN propellant. Yet the t_i values are at least 50 to 100 times smaller than those for the AN propellant in the comparable range of radiant flux. For pressure increasing from 2 to 21 atm, in the region of no burning instability effects, the N-5 ignition delay changes within about 20%, whereas the AN propellant discloses at least twice as big difference in the t_i values for pressure increasing from 1 to 5 atm.

The unusually big ignition time of the tested AN propellant does not seem to be connected with the excessive radiant flux effect, in the sense of the Librovich interpretation of ignition theory experimentally proven in our previous work. All of the data measured in the course of ignition experiments at 1 and 5 atm are located along straight lines in the $\log(t_i)$ vs $\log(q)$ coordinates. This would hardly be possible if the excessive radiant flux effect were an essential factor in the conducted experiments.

What actually occurs in the tested AN propellant under radiation, which specific mechanisms of interaction between laser beam and the irradiated material take place in this particular case, what connections exist between the AN composition and other solid propellant ignition mechanisms will be elucidated in detail in the paper.

Laser Ignition Characterization of N-5 Double-Base Solid Propellant

G.A. Risha[§], K.K. Kuo[¶], and D.E. Koch[†]
High Pressure Combustion Lab
The Pennsylvania State University
University Park, PA 16802
Tel: (814) 863-2264
Fax: (814) 863-3203
E-mail: gar108@psu.edu

J.R. Harvel[‡]
Eagle Picher Technologies, LLC
C & Porter Street
Joplin, Missouri 64801

An experimental investigation of the ignitability of various material lots of N-5 double-base solid propellant has been conducted. In order to investigate an observable variance in the ignition stages of the N-5 solid propellant lots (EP-A, EP-B, and EP-C), the ignition behavior (including the onset of initial gas evolution, first light emission, and self-sustained ignition) was determined. Original ring-shaped N-5 propellant samples were cut into eight equal samples, inserted into the sample holder, and ignited using the radiant heat flux of a high-powered CO_2 laser, which produces an infrared laser beam at a wavelength of 10.6 μm. For each test run, the sample was carefully placed in a specially designed carbon-carbon (graphite) sample holder (as shown in Fig. 1). The laser output power was varied from 70 to 150 Watts. This laser power input delivered to the propellant surface corresponds to the radiative heat flux ranging from 29 to 61 W/cm^2. The CO_2 laser shutter was set to the pulsed mode having a one-second-pulse length. This ensures that the external heat flux duration is consistent for all tests. The major results of the experiments was to determine the time duration for each individual stage of ignition including initial gas evolution (t_{GE}), first light emission (t_{LE}), and the onset of self-sustained ignition (t_{IGN}). The required energy delivered to the propellant surface to achieve each stage of ignition was calculated for both raw material lots of N-5. The energy required to ignite the propellant sample was calculated for the two raw material lots of N-5 (EP-A and EP-B). The materials lots manufactured in 1984 (EP-B) were found to have more reproducible experimental results. After each test, a small amount of residue remained in the sample holder. For the 1990 material lots (EP-A), there was less condensed-phase residue after the test run. The energies supplied from the laser to initiate gas evolution and first light emission from the propellant surface agreed well between both older and newer raw material propellant lots. However, the ignition delay time (t_{IGN}) for the newer N-5 lot is much longer than that of the older N-5 lot. This implies that the thermal pyrolysis induced fragmented species from these two lots are much different. Also, the dependency of t_{IGN} on heat flux had opposite trends. The recovered N-5 propellant sample (EP-C) from a failed gas generator test run showed a prolonged ignition delay period. The data obtained from six equal segments of a single ring exhibited severe scattering in the measured t_{IGN}. This

---

[§] Ph.D. Student, PSU
[¶] Distinguished Professor of Mechanical Engineering, PSU
[4†] Research Staff, PSU
[‡] Program Manager, Eagle Picher Technologies, LLC

implies that the material is non-uniform due to exposure to the hot product gases and condensed-phase particles from the Triple Six booster charge.
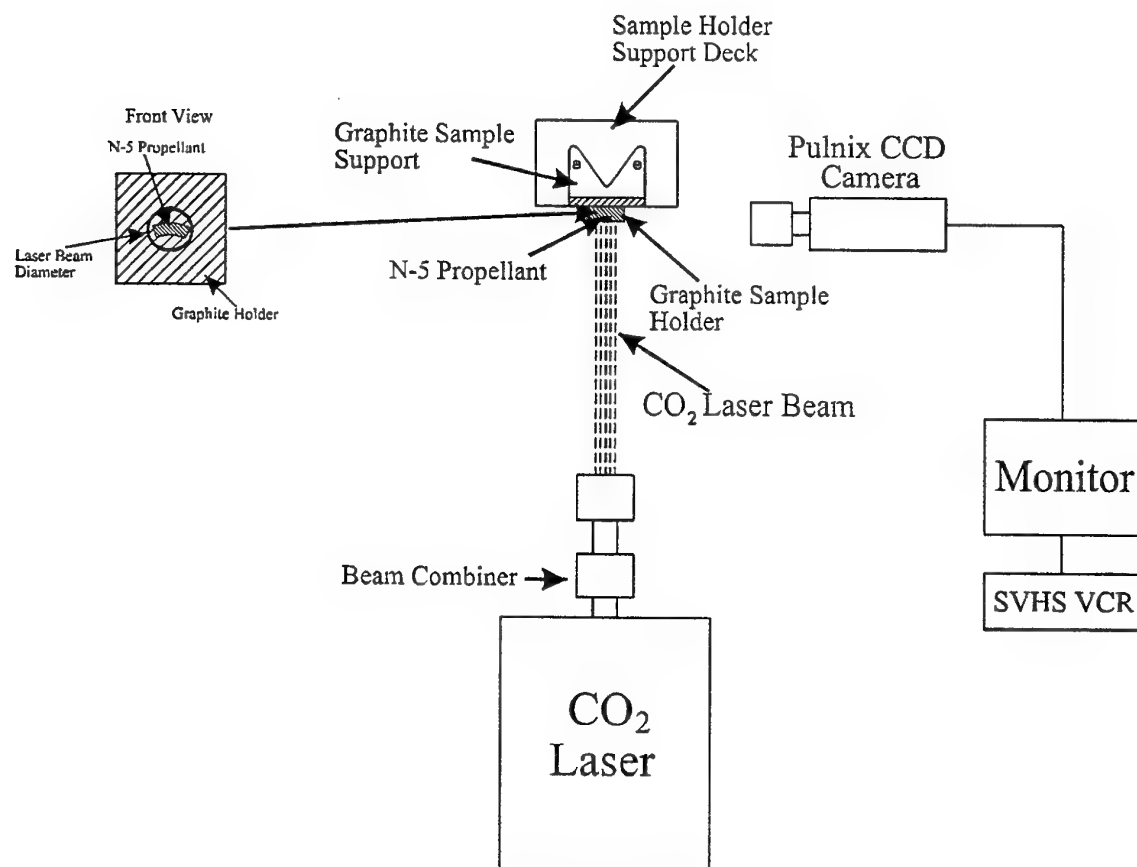
Fig. 1. Schematic-diagram of the ignition characterization experimental setup

The Nimic Energetic Materials Compendium (EMC)

M. Fisher and M. Sharp
NIMIC, NATO HQ, B-1110 Brussels, Belgium
Tel: (32-2)707.54.16, Fax: (32-2)707.53.63
E-mail: nimic@hq.nato.int

Building on an earlier document published in hard copy form by the NATO Insensitive Munitions Information Centre (NIMIC) in 1994, the NIMIC staff is continuing work on a database of energetic ingredients and formulations that have application in munition systems. This compendium contains descriptive information, performance data, mechanical properties, and results of hazard assessment and insensitive munitions (IM) testing. The new edition of the Energetic Materials Compendium (EMC), produced in electronic format, is currently available to NIMIC member nations and contains information on ingredients and high explosives. Currently, details on over 200 high explosive formulations that exhibit reduced vulnerability are included, along with information on more commonly used formulations provided for comparison.

The process of expanding and updating the information that has already been compiled will be an on going task in order to keep this tool current. Updates will be provided at regular intervals on the latest ingredients, in the form of data sheets, and formulations. A new section concerning solid rocket propellant formulations is also being developed. Due to the sensitivity of information on rocket propellants, some of the information included is generic in nature and relates in some cases to propellant "families" rather than individual formulations.

We envision the use of the EMC as a tool particularly for weapons system developers and formulators to aid in the selection of insensitive energetic material to meet their specific needs. It is hoped that the EMC will become a valuable reference tool for anyone looking for information on international energetic material formulations.

1. **Background**

1.1   The Need For The EMC

One objective of the NIMIC is to stay abreast of, and maintain the international munitions community's awareness of new developments in IM technology. One aspect that receives particular attention is the energetic material, this being the source of the hazard. With this in mind, the NIMIC issued, in 1994, three compendia concerning new energetic ingredients and formulations for high explosives and gun propellants. A fourth document dealing with rocket propellants was planned but never issued due to limitations in the release of such data from the participating nations.

1.2   The Original Compendia

The scope of the original compendia was limited to those formulations deemed to be potential candidates for IM. This seemed like a reasonable restriction since the documents were to include the full range of uses for energetic materials, including solid and liquid gun

propellants, solid rocket propellants, and high explosives for various applications. The compendia included not only qualified formulations, but also many formulations still under investigation or development. Several declared failures were also included since failures also offer useful information for researchers.

The stated purpose of the original compendia was to provide scientists and engineers in the NIMIC member nations with a research tool. Each compendium consisted of a general discussion of the subject area, e.g., "Solid Gun Propellants," followed by individual data sheets containing information on the specific formulations in that category. Data sheets contained the formulation's name, use or purpose, composition, performance characteristics, sensitivity data, and specific references from which the data were extracted. So, this tool could be used to compare various formulations using the data sheets, while the included references could be consulted for more complete research of formulations of interest.

2. The New Compendium

2.1 Electronic Format

The original documents produced by the NIMIC in 1994 were intended as the first editions of compendia that would incorporate periodic updates, with new formulations and additional data and references added to the existing documents. In keeping with this vision, and in order to make the EMC a more useful tool, in 1998 the NIMIC staff began a process of reviewing and updating the original documents for input into a database application. This application, written in Delphi™ 4, runs on a personal computer in the Microsoft Windows® environment (95/98/NT). The new Energetic Materials Compendium takes advantage of the power and flexibility of this database format, providing ease of maintenance, data sorting and searching capability, thus becoming a more accessible, efficient and useful tool. Throughout the coming year, the NIMIC staff will be demonstrating the software at various symposia and during staff visits to NIMIC customers. A short tutorial of the application, including screen captures showing the various data windows, is also available from the NIMIC.

2.2 Status of The New EMC

A review copy of the new EMC was released by NIMIC in July 1999, through the NIMIC National Focal Point Officers (NFPOs), to each of the NIMIC member nations. With the approval of the NFPOs, interested individuals or organisations can receive a review copy. The NIMIC staff appreciates input on the format and utility of the EMC, as well as contributions of data for inclusion in the database. Subsequent editions of the EMC will include input from the reviewers, as well as additional data gathered by the NIMIC staff, including information on solid rocket and gun propellants as mentioned above.

2.3 Adding Solid Propellant Data

Toward this end, a solid rocket propellant questionnaire has been generated, along with guidelines for completing it. These documents are available from NIMIC. Those individuals from NIMIC member nations who work in the solid rocket propellant field are encouraged to submit data, limited to that which is releasable, for propellant formulations or "families" of formulations that have been developed with IM requirements in mind. Data are requested not only for developed, qualified formulations, but also for those still under development, those

that are in the early stages of investigation but show promise, and even those that never achieved their goals and were abandoned, as they are still sources of important information.

2.4   Putting The Data to Use

As mentioned in section 2.1, the use of the electronic format offers many advantages. One interesting application is use of the data to investigate trends. Bar graphs, based on the data contained in the compendium, showing shock sensitivity with velocity of detonation and binder content are given in Appendix A, Graphs 1 and 2 respectively. Although detonation velocity is just one of the parameters which determines the overall performance of an energetic material, it is interesting to note that high velocity of detonation does not necessarily mean high shock sensitivity. The complexity of the relationship between shock sensitivity and formulation composition is demonstrated by Graph 2. The NIMIC hopes to be able to report some interesting trends and relationships in the future as the content of the database expands.

2.5   EMC Data Fields

Listed below are the various data windows used by the EMC software to organise the data, along with comments regarding the type of data included in each field. The Appendix B gives examples of the actual screen displays for the data fields listed below.

1. **Components**: Each of the energetic material ingredients is listed here, along with weight percents, if available. Each ingredient is linked to the ingredient database, which provides information on the individual propellant constituents. The density of the material is also given if known.

2. **Performance**: Various performance parameters, such as velocity of detonation, Gurney energy, burn rate, specific impulse, density-impulse are listed here; these parameters are linked to a parameter database which will include notes on the particular test or method used to determine the values reported. Performance parameters are also linked to the reference document from which they were extracted.

3. **General**: This field contains information regarding the formulation (processing) method, the manufacturer and/or developer of the formulation, and information on its application(s), e.g., general purpose explosive, metal accelerating explosive, tactical rocket motor, booster, gas generator, etc.

4. **Generic Test Data**: The Generic Test Data field is a key section of the EMC, since it is here that we record test results for Insensitive Munitions testing, including Bullet and Fragment Impact, Fast and Slow Cookoff, Sympathetic Detonation (Reaction of Adjacent Munitions), and Shaped Charge Jet Impact.

5. **Sensitivity Data**: All available data on the energetic material's sensitivity testing are listed here, including shock, impact, electrostatic and friction.

6. **Notes**: This area provides a text field for inclusion of general information on the formulation. Data input in this field may include notes on processing, information concerning hazard classification or propellant signature, or any comments regarding

information listed in the other fields, or the reference documents from which the data were obtained.

7. **Mechanical Properties**: Typical stress and strain data and modulus values can be included in this field. NIMIC's plans for future functionalities of the software include linking to PDF files. This will allow us to input stress-strain curves, master curves and the like in whatever form is provided by the contributor of the data.

8. **References**: All of the data listed in the other fields are linked to the specific reference documents from which they were extracted. This field lists the ID numbers for all references related to the chosen formulation on the left-hand side. By clicking on an individual reference number, the user can call up on the right-hand side of the screen a window listing the details of the reference, including title, author, date of publication, the journal or proceedings in which the reference was included (if applicable), and the volume number and page numbers if appropriate.

3.   Plans for the Future

The NIMIC will continue to research data on ingredients and appropriate energetic material formulations for inclusion in the EMC. Copies of this document will be forwarded to organisations and individuals within the NIMIC member nations along with a request to submit data on formulations that they wish to include in the database. Modifications to the software will be made to include new functionalities and in response to input from the NIMIC customers. As previously stated, the NIMIC staff appreciates greatly any input regarding the format and utility of this tool, as well as contributions of data, or appropriate references. The EMC will be as successful and as useful as the members of the NIMIC nations make it, through their critique and their contributions of data.

Plot Indicating Shock Sensitivity and Velocity of Detonation for Various Formulations

GPa
V of D

High Shock Sensitivity

Low Shock Sensitivity

Comp B

High Explosive Formulations

Graph 1

Plot Indicating Shock Sensitivity and Binder Content for Various Formulations

High Shock Sensitivity

Low Shock Sensitivity

GPa
% Binder

Comp B

High Explosive Formulations
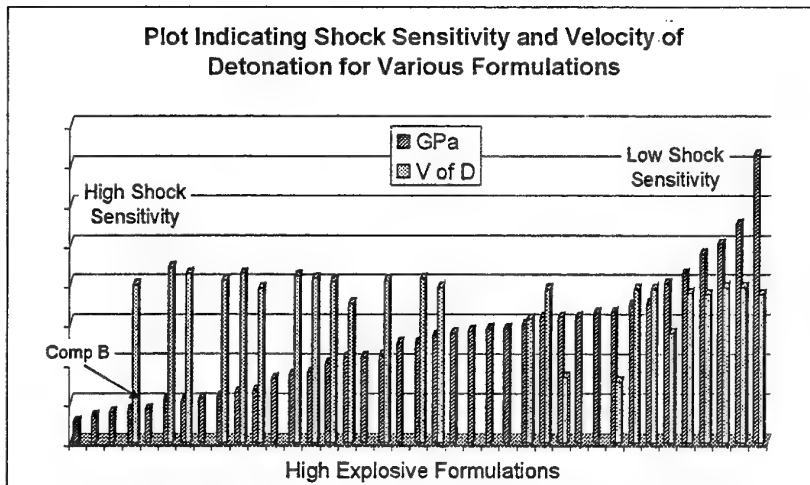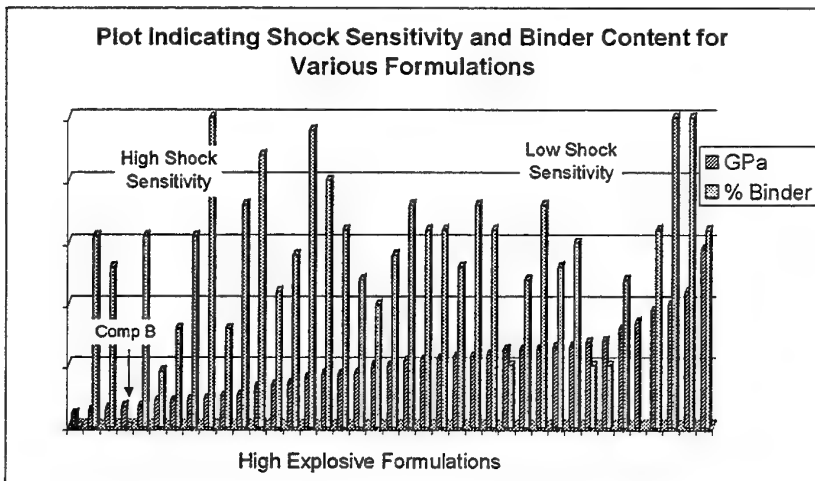
Graph 2

APPENDIX B - EMC Screen Examples

Formulation   Search   Help   Lookup Formulation

Name 1000   Aliases N/A
Name 1001   Aliases N/A
Name 1002   Aliases N/A

[Components] | Performance | General | Generic Test Data | Sensitivity Data | Notes | Mechanical Properties | References |

Attached Components

Component Name	Percent
HMX	95
PU	5

All Components

Name ADDF

Aliases 1,4,4,10,10,13-hexafluoro-1,1,7,7,13,13-hexanitro-3,5,9,11- tetraoxotridecane

Show Data Sheet

Lookup Component

Formulation Density [   ]   Units [   ]

INFORMATION RESERVED FOR NIMIC NATIONS ONLY

Components

Formulation   Search   Help   Lookup Formulation

Name 1000   Aliases N/A
Name 1001   Aliases N/A
Name 1002   Aliases N/A

Components Performance | General | Generic Test Data | Sensitivity Data | Notes | Mechanical Properties | References |

Attached Performance Parameters

Name   Detonation Pressure
Reference 59
Value 30   GPa
Notes For This Test Result
N/A

Name   Detonation Velocity
Reference 59
Value 8600   m/s
Notes For This Test Result
N/A

All Performance Parameters

Name Burn Rate (strand)   Units in/s
Notes On This Test

All References

UIN 59   N/A
Title No Reference Available

Authors N/A

Performance

282

General

Generic Test Data

Sensitivity Data

Notes

References

285

THIS PAGE HAS BEEN DELIBERATELY LEFT BLANK

CO$_2$ Laser Applications in the Combustion of Energetic Materials

C. Zanotti, P. Giuliani
TEMPE-C.N.R.
Via Cozzi, 53
20125 Milano, Italy
Telephone: ++39-02-66173.310, Fax: ++39-02-66173.307
E-mail: Zanotti@tempe.mi.cnr.it

CO2 laser systems, used as an external energy source, are useful tools for the study of the processes associated with the combustion or degradation of solid materials. This technique permits us to test different kinds of solid materials and to study peculiar phenomena as presented in the following:

Solid Rocket Propellants:
Heating and ignition processes, by radiant energy, are well described by the temperature histories of the irradiated propellant surface. The general trend of this curve indicates that the temperature increases enough to reach the ignition value where an abrupt change of the curve slope occurs. Ignition boundaries, go-nogo boundaries and ignition temperatures can be estimated from these data.

Radiation energy influence on the steady burning rate can be determined very easily by the means of a standard technique, The common feature is that, for any propellant, the steady burning rate increases with the radiant energy augmentation and a linear dependence on the incident flux. Steady burning becomes a self-sustained oscillatory when the operating pressure is close to the Pressure Deflagration Limit (PDL). Below its value, the oscillatory regime can be maintained if radiant energy is supplied to the propellant. Oscillatory combustion can also be driven by means of CO2 lasers when the power has a sinusoidal modulation (and the results obtained in this way indicate that) for any operating condition existing, and a frequency which induces the maximum burning propellant response. The burning propellant can be extinguished by a CO2 laser pulse, and the results obtained at fixed pressure define the curve separating the regions where the burning propellant has a different response to the external stimulus (extinction or combustion).

Thermal Protections:
Penetration depth of the interface between the transformed material and the virgin one, as a function of the laser power and exposure time, can be measured. Data obtained by testing different thermal protections permit us to compare the ablation capability of these materials. Temperature, on the irradiated surface or inside the material and at any fixed position, can be recorded by microthermocouples.

Graphite:
A CO$_2$ laser system has been used to heat and sustain the combustion process of graphite spheres to determine the ignition temperature. Simultaneous measurement of the regression rate and the combustion temperature allow us to evaluate the surface activation energy (Arrhenius law) from data collected in a single test.

Combustion Synthesis of Powder Mixtures:
In the field of combustion synthesis, the possibility to obtain the self-propagating combustion mode, instead of the explosion mode, depends on the temperature distribution in the pellet before the ignition, thus, the capability of controlling the heating transient features is the necessary condition to guarantee a consistent comparison among the obtained results. Radiant energy was used to ignite different powder mixtures (Ni-Al, Ni-Ti and Zr-B2), and the ignition transient is described by the temperature history of the irradiated pellet surface. Results show that the presence of the liquid phase of one reactant plays a major role during the ignition process.

288

AREA 5:

COMBUSTION ANOMALIES OF ENERGETIC MATERIALS

Influence of Microcracking on Pressure-Dependent Energetic Crystal Combustion+

R.W. Armstrong*, C.F. Clark** and W.L. Elban***
*Department of Mechanical Engineering, University of Maryland, College Park, MD 20742;
Explosives and Propellants Division, Naval Surface Warfare Center, Indian Head, MD 20640; * Department of Electrical Engineering and Engineering Science, Loyola College, Baltimore, MD 21210.
E-mail: rona@eng.umd.edu, clarkcf@ih.navy.mil, welban@loyola.edu

The suggestion has been put forward that unstable growth of microcracks that are thermomechanically-produced below the melt surface of burning crystals could produce a sudden increase in the pressure-dependent burn rate and hence transition to unstable combustion behavior.[1] Here, such behavior is proposed to occur at relatively low pressures for two reasons: (1) the presence of a melt layer over the crystal surface lowers the required crack surface energy to the liquid-solid interfacial value; and, (2) the presence of the micrometer-sized cracks appreciably reduces the pressure needed for unstable crack growth in accordance with fracture mechanics predictions. Evidence is produced for microcracking below a liquid surface layer observed at grazing laser-heated hot spots on the surface of RDX (cyclotrimethylenetrinitramine) crystals and a comparison is given of reported surface energy lowering values tabulated for several materials.[2] Then, fracturing pressures are estimated from modified indentation fracture mechanics measurements made on RDX and PETN (pentaerythritoltetranitrate) crystals.[3] The indication is that smaller sized crystals should require greater pressures for unstable cracking.

References

1. R.W. Armstrong, W.L. Elban, A.L. Ramaswamy and C.Cm. Wu, "Thermomechanical Aspects of Energetic Crystal Combustion", in Challenges in Propellants and Combustion: 100 Years after Nobel, K.K. Kuo, (Ed.), Begell House, Inc., NY, 1997, 313.

2. W.L. Elban, R.W. Armstrong and T.P. Russell, "Plasticity/Interfacial Energy Influences on Combustion-Driven Cracking of RDX Energetic Crystals", Philosophical Magazine A, 78 (1998) 907.

3. R.W. Armstrong and W.L. Elban. "Cracking at Hardness Impressions in RDX Explosive and MgO Single Crystals", Materials Science and Engineering, A111 (1989) 35.

THIS PAGE HAS BEEN DELIBERATELY LEFT BLANK

Experimental Research of Typical Defects Propagation Process in Solid Rocket Motor

He Guoqiang, Cai Timin, Liu Peijin
College of Astronautics, Northwestern Polytechnical University
127 Youyi Rd. W. Xi'an, 710072, P.R. China
Tel: 086-29-8493646; Fax: 086-29-8491000
E-mail: gqhe@nwpu.edu.cn

Chamber pressurization rate and combustion induced debond, weak-bond, and gas cavity propagations in solid grain are of practical concern to many rocket motor designers, as the propagation of these defects are the main reason of combustion transition to detonation, and of anomalous internal ballistic property during the motor firing. This paper presents the experimental investigation results from some recent test motor firings. A real-time X-ray radiography (RTR) system was used in this study. RTR allows to obtain debond, weak-bond and gas cavity propagation process pictures of a solid propellant sample in the test motor during a static firing. In this study, some main factors affecting debond propagation were researched at first; such as boundary constraint of solid grain, the pressurization rate of ignition, maximum chamber pressure and its duration, geometry and size of debond cavity, combustion characteristics of propellant, and bonding intensity of propellant/insulation. The second study aspect was an analysis of anomalous combustion and structural destruction of propellant sample with gas cavities. Many samples with varies gas cavity scale were fired in the quadrate test motor to analyze the factors of gas cavity propagation. The third research aspect was an analysis of for dynamic tearing between HTPB propellant and restrictor. The relationship between the tearing speed and the ignition pressurization rate was discussed.

It is the aim of this research to determine the factors affecting the propagations of these defects, and modes of propagation for HTPB propellant under the operation of various motor conditions. In order to generate images of propagation processes, the real-time X-ray radiography system and quadrate test chamber were used to incept many instantaneous images of the solid propellant sample as it burns in a high-pressure chamber. A schematic diagram of the X-ray system is shown in Figure 1.

The two-dimensional sample containing a triangular cavity is installed in the main chamber and held in position between the top and bottom walls. An igniter bag is composed of propellant shavings and black powder. The pressurization rate can be adjusted by the igniter strength, and by the free volume of the test chamber (see Fig.2). When the igniter is initiated, the high pressure, high temperature product gases and condensed phase particles ignited the propellant, and at same time caused mechanical deformation and debond propagation in the test sample. The peak chamber pressure and depressurization rate are controlled by the strength of bursting diaphragm. The date acquisition system consists of an amplifier, transducers mounted on the chamber wall and date processing equipment.
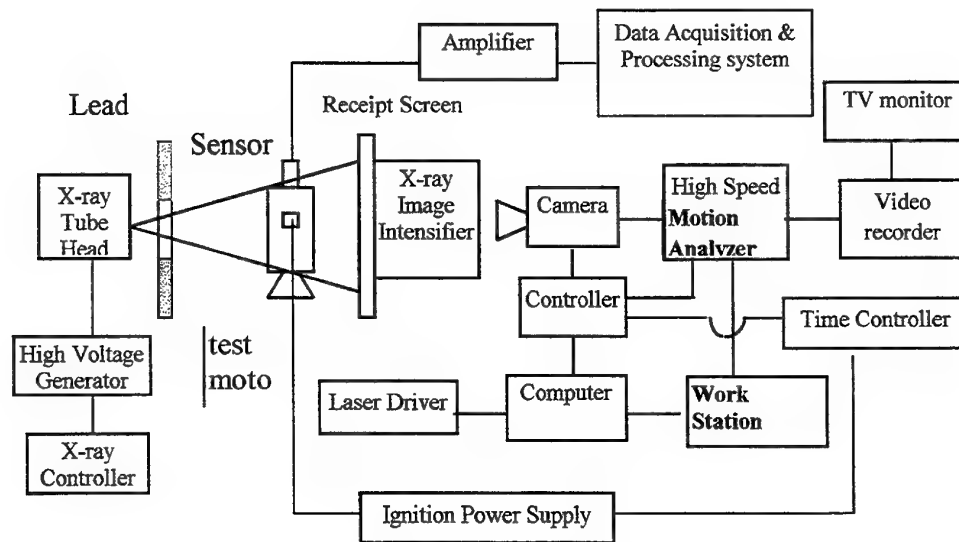
Fig. 1: Layout of the Real-Time X-Ray Radiography System
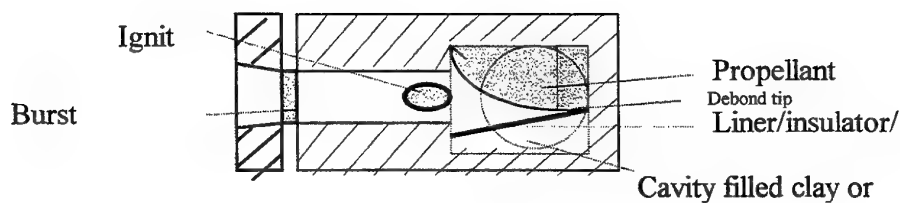
Fig.2: Schematic diagram of the test sample and debond propagation chamber

In the experimental work, the effects of pressurization rate and boundary condition on the development of debond propagation under various operating conditions were studied. Chamber pressurization rates were varied from 0.5 to 15.0 GPa/s. Two different kinds of boundary condition, with the void region underneath the case filled with or without the clay, were investigated. Typical debond propagation processing images are shown in Fig. 3.
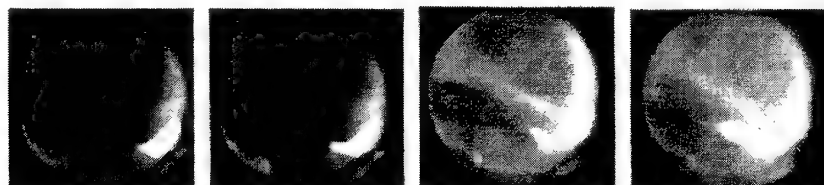
Fig.3: Pictures of a debond propagation with a restricted case

Weak-bond between propellant and restrictor are one kind of typical defect during the production
of a solid rocket motor. The defect may cause a catastrophic failure during the motor firing. The experimental study of dynamic tearing between HTPB propellant and restrictor was accomplished in a quadrate test motor (see Fig.4).
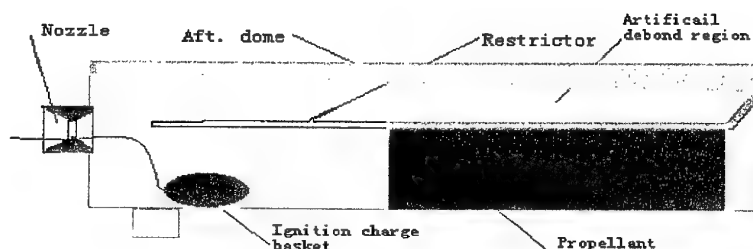
Fig.4: The sketch of test motor

It was discovered that the interface of propellant/restrictor was slit by the load of ignition impact for weak-bond sample. The main affecting factors are the load of ignition impact, the length of redundant restrictor and the gap of artificial debond region. The series pictures of slitting process are shown in Fig. 5.

Fig.5 The images of interface structural destruction with the defect of weak bond

The gas cavity in solid grain is also one of the typical defects, and may also cause anomalous internal ballistic property and motor explosion. The test motor and the typical pressure-time trace are shown in Fig.6~Fig.7. The series pictures of grain slitting process are shown in Fig.8.
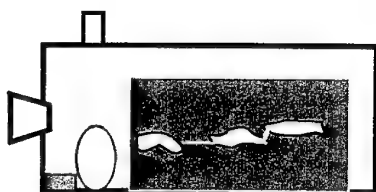
Fig. 6: The sketch of gas cavity propagation cavity test motor
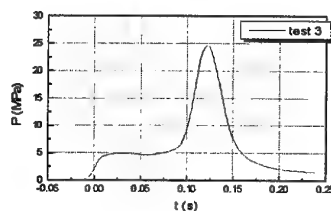
Fig. 7: Pressure-time trace of gas propagation process
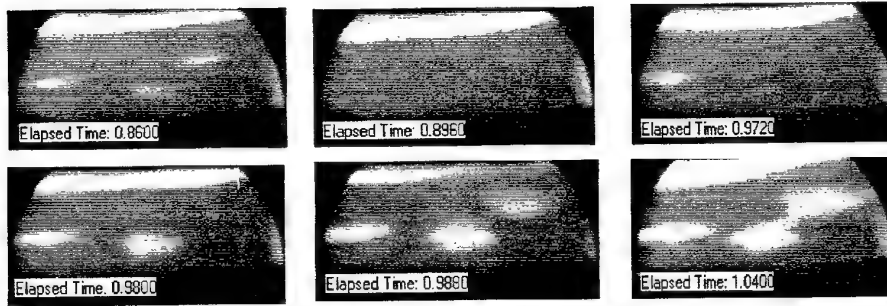
Fig. 8: The images of structural destruction with multi-perforated sample

Some major findings from this research are listed as follows: The first is that single gas cavity near the grain surface cannot be propagated under the ignition shock, but can be closed by chamber pressure. The second is that insular multi-perforated cannot be propagated in a general way, but its combustion may alter the chamber pressure of motor. The third is that connective multi-perforation may cause the grain structural destruction, and abnormal internal ballistic property when the ratio of burning surface to port area is greater than critical value under certain boundary constraints of the sample (see Fig.7).

Subject terms: Solid Propellant rocket motor , Grain defect, Propagation, Combustion

Aerodynamics and Combustion in the Countercurrent Type Vortex Combustion Chamber

V.A. Arkchipov
Tomsk State University Research Institute of Applied Mathematics and Mechanics
634050, Tomsk, GSP-14, Russia

O.V. Matvienko
Department of Theoretical Mechanics
Tomsk State University of Civil Engineering and Architecture
Solyanaya sq 2, Tomsk, Russia
Tverskaya Str. 117, Apt. 6, 634041, Tomsk, Russia
Tel: (007-3822) 553-532
Fax: (007-3822) 410-347
E-mail: mishura@niipmm.tsu.tomsk.su

In this paper some results of numerical and experimental investigation of aerodynamics and combustion in the countercurrent type vortex chamber are presented.

The experimental investigation of aerodynamics of a countercurrent vortex chamber was carried out by an air blown-down of a model under isothermal and flame conditions. The airflow rate, as well as the distribution of the velocity vector and the static pressure, were determined in the experiments. For this aim the method of a cylindrical pneumatic-metric gauge has been used.

The 2D Reynolds equations were used for description of the flow field. The turbulence characteristics were calculated on the basis of two-equation $k - \varepsilon$ model with a Richardson number correction the dissipation equation due to the strong swirling of the flow.

The set of the equations was solved with the use of an algorithm suggested by Patankar, where the finite difference equations where obtained by integrating the differential equations over scheduled volumes which incorporated points of a staggered finite-difference grids. The continuity equation was satisfied indirectly using an iterative method named *SIMPLE*.

The value of the tangential velocity w sharpness increases from a zero on axis of a chamber to w_{max}, after which there occurs the decrease w. Some increasing w in the vicinity of the wall is due to blown-in of the swirling flow through a swirler. The radial distribution on the axial velocity u has more complicated character. This distribution is characterized by the presence of an axial zone of return flows. The presence of a reverse flow is due to inflow of free air into the volume of a vortex chamber caused by decrease in a static pressure due to a strong swirling of the flow.

The combustion in the chamber with no swirl occurs in an induction regime with zones of preparing reagent, however, in the presence of a swirl the conduction regime is mainly realized. The flow swirl leading to the displacement of the circulating vortex contributes to the flow to be penetrated deep into the chamber.

Unburned gas mainly flows near the wall of the nozzle. The swirl preventing the flow turn, reduced the amount of unburned gas, issuing in the nozzle, and favors to increase the completeness of combustion; in this case the fuel fraction of unburned gas disposed from a chamber nearly linearly decreases with a swirl intensity. A high completeness of combustion can be achieved with a swirl strong enough. The analysis of gas flow in a nozzle shows the possibility of forming there recirculating zone at high w, which favours the completeness of combustion at insignificant distance from the entrance into it.

Parametric Investigation of Supersonic Combustion of Solid Fuels

I. Feldman, A. Gany
Faculty of Aerospace Engineering Technion - Israel Institute of Technology
Haifa 32000, ISRAEL
Tel.972-4-8292554, Fax 972-4-8230956
e-mail: gany@techunix.technion.ac.il

Supersonic combustion of solid fuels may be of interest for a simple version of a scramjet engine, whose thermodynamic cycle may be superior to that of the conventional, subsonic combustion solid fuel ramjet (SFRJ) at hypersonic flights (say, above Mach number of 5). However, the combustion of solid fuels under supersonic airflow is not straightforward. Ignition, flameholding, mixing of fuel gasification products and air, as well as reasonable combustion efficiency have to be accomplished under unfavorable conditions characterized by very high flow speeds and very short residence times.

The objective of the present experimental investigation was to investigate supersonic combustion behavior of different fuel types: a pure polymeric fuel (polymethylmethacrylate, PMMA) and a fuel-rich propellant (consisting of 60% hydroxyl-terminated-polybutadiene, HTPB, with 40% ammonium-perchlorate, AP) .

The static test facility simulated the conditions existing within a scramjet combustor flying at Mach number of up to 5.5. Vitiated air heater consisting of hydrogen combustion, with oxygen replenishment to keep the oxygen molar concentration at 21%, provided hot inlet air with stagnation temperature and pressure as high as 1500 K and 50 atm, respectively. Air Mach number at the combustor inlet was deigned to 1.5.

Dependence of flameholding capability, fuel regression rate, and combustion efficiency on operating parameters (air mass flow rate, total air temperature and grain geometry) was studied experimentally. Both of the fuel types were tested under similar supersonic flow characteristics within the combustor. The fuel surface pattern after combustion indicates the existence of oblique shock waves in the combustor cavity during the supersonic combustion. Data on flameholding limits of PMMA solid fuel grains have been obtained during this study and were added to experimental results that were gathered previously in our laboratory. In addition, results on flameholding characteristics of the fuel-rich propellant have been obtained as well. The parameters investigated in the present research were flameholding section geometry, total air temperature, and air mass flow rate. The results reveal a critical flamehlding section diameter of 25 mm and a critical air mass flow rate of 200 g/s, below which no sustained combustion could be obtained. Dependence of fuel regression rate on fuel type and flow parameters has been studied as well. Experiments showed a similar qualitative influence of flow parameters on fuel regression rate for both fuels: fuel regression rate increased with increasing the airflow rate. However, the fuel-rich propellant produced higher regression rates than the PMMA fuel, as well as somewhat higher combustion efficiencies.

THIS PAGE HAS BEEN DELIBERATELY LEFT BLANK

Supersonic Combustion Phenomena Under Different Combustion Chamber Design

Jir-Ming Char
The Chinese Air Force Aeronautical Technology School
P.O. Box 90395, Kang-Shan, Taiwan
Tel: (0) 07-6254189
Fax: (0) 06-2358894
Email: char@cc.cafa.edu.tw

Wen-Jay Liou
Institute of Aeronautics and Astronatuics
National Cheng Kung University
Tainan, Taiwan 70101

Evident technological, economical, and operational advantages exist when liquid hydrocarbon fuels , such as JP-8, RJ-5 are used in comparison with hydrogen-based system for the development of the small hypersonic vehicles. Throughout the continuing development of the scramjet concept, the mixing of fuel and air in the combustor has been one of many important and persistent problems. The length of the combustor must be limited to a few feet due to the impact that the size of the combustor can have on the overall performance of a highly integrated hypersonic flight vehicles. Therefore, the sufficient entrailment and subsequent micromixing followed by significant heat release must all occur in the short residence time of a fuel-air mixture, which is $<10^{-3}$ sec. The parametric analysis of fuel droplets ignition and combustion phenomenon plays an important role in the design of scramjet. Shock tube is a basic equipment to simulate the flowfield of scramjet combustor. In this research, experiment results are presented. The mutual relation between ignition delay time of JP-8 fuel sprays and the affecting parameters, especially, the factor of wedges features this paper.

The schematic diagram of the experimental apparatus is illustrated in fig.1. A helium driven shock tube is used to produce uniform strength shock wave. The driven section of the shock tube is filled with air. The glass windows exist in the test section to observe the ignition process. Pressure is detected by piezoeletric pressure transducer($PT_1 \sim PT_5$). One photo-detector device is installed on the end plate of the test chamber through the window to sense the luminescence from the ignition of fuel sprays. The output data are recorded by the data acquisition system. Fig.2 is the typical test curve. The pressure gauges are used in the test and are shown as PT_1, PT_2, PT_3 line respectively. The abrupt increase of light intensity curve as Tig indicates the ignition occurred. The period between the incident shock passing by the droplets (SG, shown in fig.1) and their ignition is what we call ignition delay time.

Three types of wedges, (i.e., 5-deg, 7-deg, and 9.5-deg) are used in this test. The diagram of the experimental configurations is illustrated in fig.3. In this study, three different shock wave Mach number are adopted, i.e., Ms=3.5,Ms=4.0,Ms=5.0. The pressure of driver gas is 7atm to 10atm, and the driven gas ranges between 13torr to 170torr. Table.1 shows the relation of Mach number (Ms) and wedges with ignition delay time. It can be seen that in the case of high Mach number (Ms>4), wedges will shorten the ignition delay time to 50 % as compared with no wedges case. The wedge angle seems not affect the ignition delay time. The mechanisms of this flowfield are analyzed and the difference between them will be discussed in detail in the full paper.

Also, the ignition process is pictured as shown in fig.4. The explanation of its phenomena will be coupled with pressure-time traces in full paper.
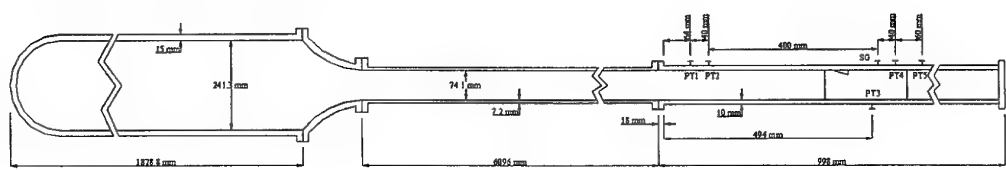
Fig1. The schematic diagram of the test section
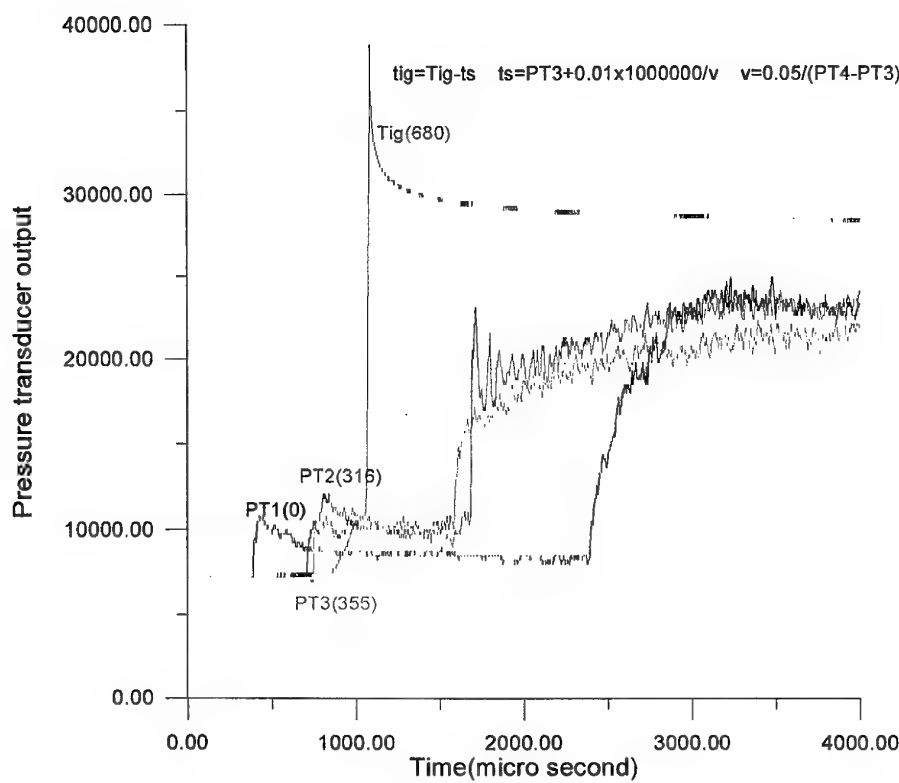
Fig.2 The test curve
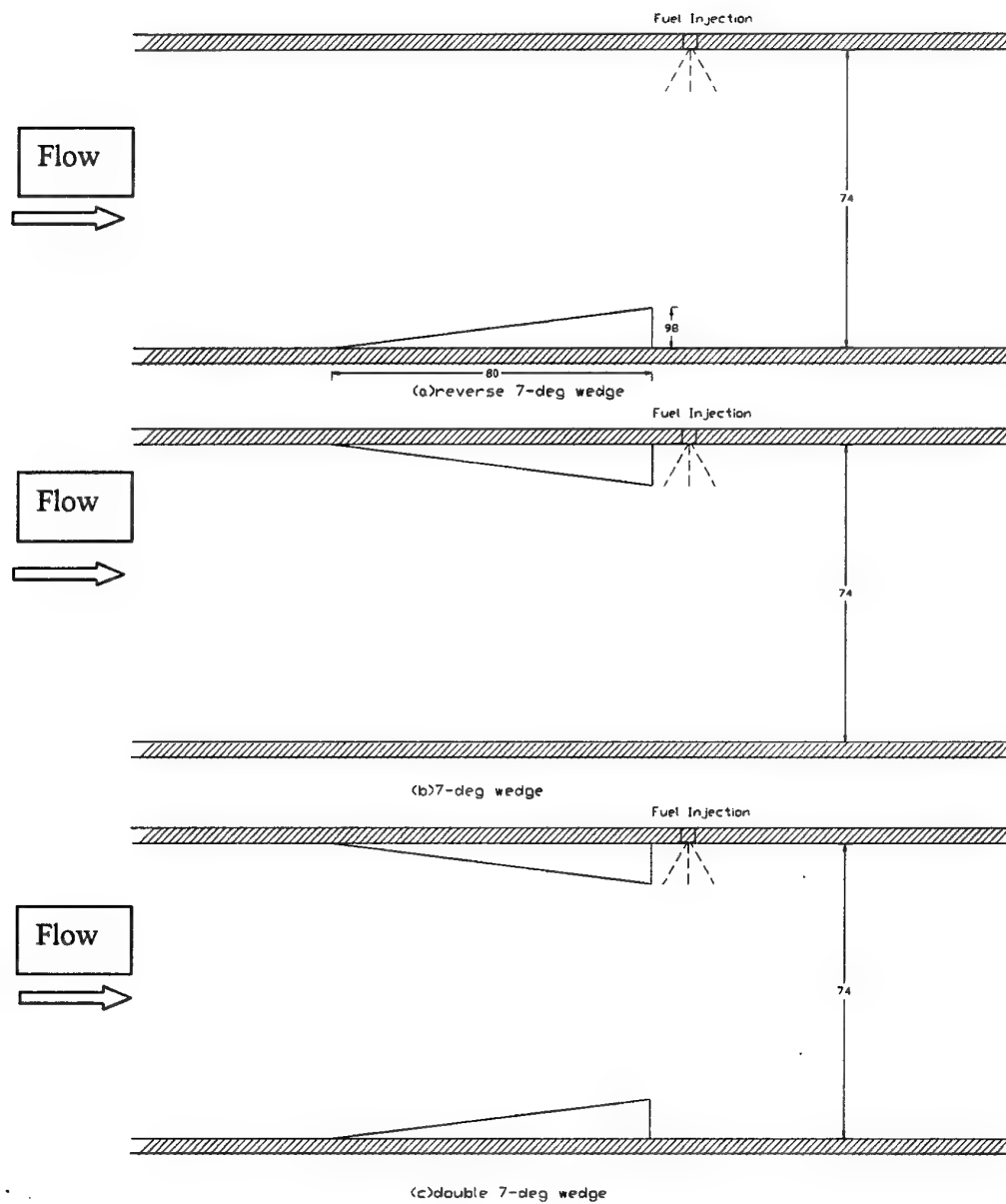
Fig.3 Test-chamber experiment configurations
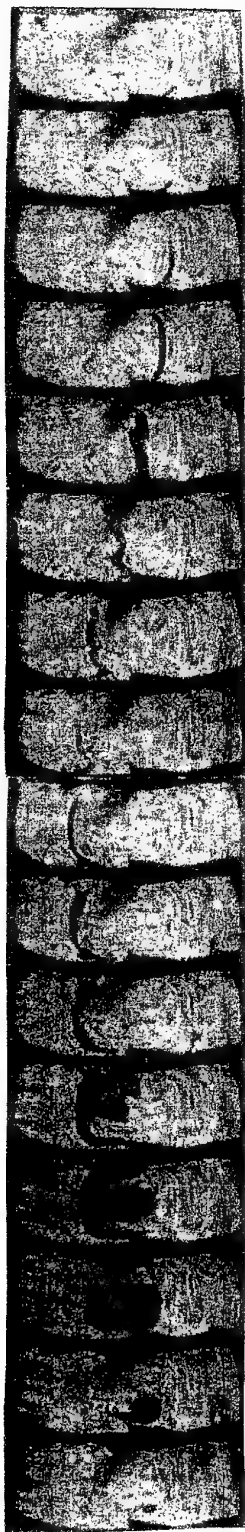
Fig.4 The ignition process

Table.1 The ignition delay time

P4/P1 Mach No.	No wedge (Tig;micro sec)	7-deg wedge	Reverse 7-deg	Double 7-deg
7atm/61torr Ms= 3.5	431	444	442	447
10atm/87torr Ms=3.5	421	461	438	466
7atm/34torr Ms=4.0	368	330	223	431
10atm/48torr Ms=4.0	340	201	180	358
10atm/13torr Ms=5.0	144	60	35	41

THIS PAGE HAS BEEN DELIBERATELY LEFT BLANK

AREA 6:

METAL COMBUSTION

Combustion and Flame Spreading of Aluminum Tubing in High Pressure Oxygen

M.M. Mench, K.K. Kuo
15 Research Building East
The Pennsylvania State University
University Park, PA, 16802
Tel: (814) 863-2264, Fax: (814) 863-3203
E-mail: mmm124@psu.edu

J. Haas
Allied Signal Aerospace
NASA White Sands Test Facility
Las Cruces, NM 88004

Aluminum has been utilized in many propulsion devices. It can serve as an energetic fuel when burning with oxygen. This research is motivated by the need for an improved understanding of aluminum combustion in an oxygen-rich environment in order to reduce hazards associated with metal combustion.

The promoted ignition, flame spreading, and combustion phenomena of aluminum alloy 3003 tubing in gaseous oxygen (GOX) were studied. The motivation for this study is to compare the high pressure burning phenomena of aluminum in GOX to that in liquid oxygen (LOX) at lower pressures. The violent burning of aluminum in a LOX environment has been termed a violent energy release, or VER reaction. This reaction has been observed to result in extremely rapid combustion of aluminum at rates many times greater than that of aluminum in a GOX environment at similar pressures. The density of GOX at 69 MPa is nearly equivalent to the density of LOX at 3.9 MPa. Therefore, high pressure burn rates for aluminum tubing in a GOX environment were obtained for comparison to promoted combustion tests of similar tubing in a LOX environment at lower pressures. Other parameters investigated or discussed include the effects of pressure, aluminum tube wall thickness, ambient gas impurity concentration, and sample tube diameter on observed burning rates.

The test chamber utilized in this study, located at the NASA White Sands Test Facility, is capable of testing in static pressures of 69 MPa. The 12.4-liter chamber is equipped with a 5 cm diameter sapphire window through which video data were recorded. An array of up to seven resistive breakwires was used at known locations along the test sample to measure the flame-spreading rate of the upward burning sample. For some tests, an ultrasonic burn rate transducer was used. Figure 1 shows a distance versus time plot deduced from breakwire data for determining the flame-spreading rate. Figure 2 is a typical pressure versus time plot. The small oscillations in the pressurization rate are a result of molten particle droplet formation and ejection from the burning tube, and provide insight into instantaneous burning phenomena. At regular intervals, droplets of accumulated molten mass are ejected from the burning surface. The time interval between consecutive ejections can be shown to be a function of burning rate or pressure. The molten mass accumulation and ejection is believed to be a key parameter in the transition to VER in a LOX environment. The aluminum tube samples used were 30.48 cm long and either 3.175 or 6.35 mm in outer diameter. Two different wall thickness of the aluminum tube samples (0.254 and 0.356 mm) were used for

comparison testing. High-speed video of the burning event was also recorded, showing the periodic dripping of molten satellite particles. The results of a metallurgical analysis of some recovered slag particles from the chamber are also discussed in this paper. Additionally, a computer code based upon a control volume analysis of the test chamber was developed and used to analyze the data, allowing deduction of parameters such as instantaneous heat release rate.
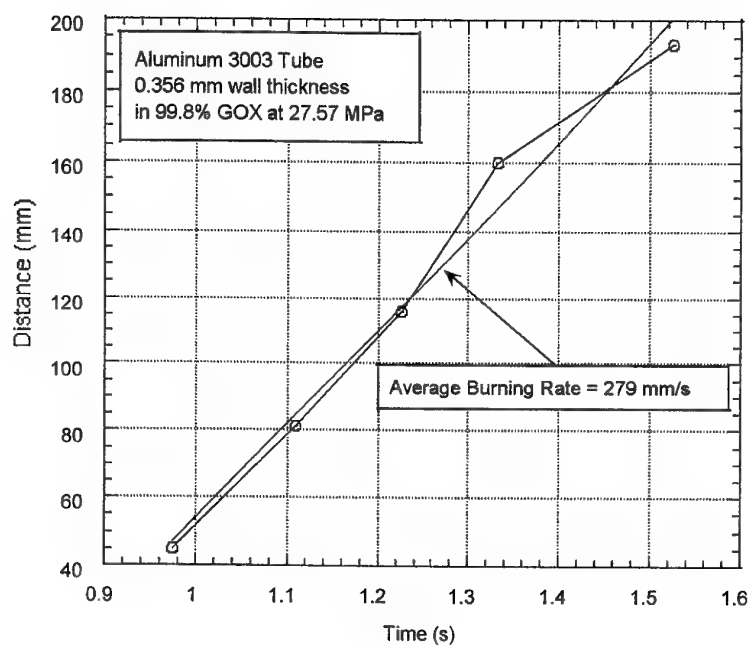
Fig. 1 A distance versus time plot deduced from breakwire data for determining the flame-spreading rate
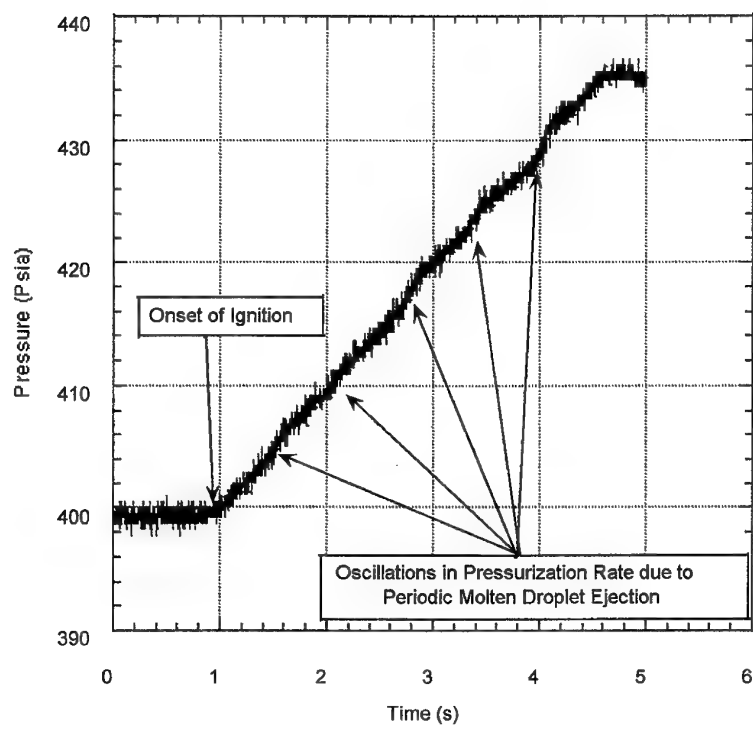
Fig. 2 Pressure versus Time Plot Showing Oscillations in Pressurization Rate Due to Molten Droplet
Formation and Ejection from the Burning Region

THIS PAGE HAS BEEN DELIBERATELY LEFT BLANK

Ignition and Combustion of Boron Particles in Fluorinated Environments: Experiment and Theory

A. Ulas, K.K. Kuo
Department of Mechanical Engineering
The Pennsylvania State University
15 Research Building East
University Park, PA 16801 USA
Tel: 814-863-2264, Fax: 814-863-5985
E-mail: axu102@psu.edu

C. Gotzmer
Naval Surface Warfare Center, IH

The ignition and combustion of isolated boron particles in fluorine-containing environments were investigated both experimentally and theoretically. Boron particles (1-μm amorphous and 3-μm crystalline) were ignited and burned completely in the post-flame region of a multi-diffusion flat-flame burner, which provided a uniform zone of combustion products of $CH_4/NF_3/O_2/N_2$ mixtures at atmospheric pressure. As shown by the characteristic difference between Fig. 1b and Fig. 1a, no clear distinction was observed in fluorinated environments to define a two-stage combustion process, which is characteristic of boron oxidation without fluorine. The burning trajectories of boron particles in fluorinated environments showed pronounced jetting and spinning phenomena (Fig. 1b). At low ambient gas temperatures (around 1,780 K), boron particle ignition required a higher oxidizer concentration in non-fluorinated environments than in fluorinated environments. The atomic fluorine was found to significantly reduce the total burning times (t_b) of boron particles, while the HF species tend to slightly increase t_b.

Based upon the experimental data from the current study and the other data available in the literature, a theoretical model was developed for simulating the combustion of an isolated boron particle in fluorine-containing environments. The boron oxide layer removal process was modeled using a reaction mechanism, which considers the vaporization process and four global surface reactions of oxide layer with O_2, H_2O, F, and HF. The major products during the oxide removal process were found to be OBF, FBOH, HBO_2, and BO_2. The "clean" boron combustion model includes four global surface reactions of O_2, H_2O, F, and HF with boron. BF_3, OBF, HBO_2, and B_2O_2 are the major products during the "clean" boron combustion stage. Predicted t_b are in good agreement with the measured data in the current study (Fig. 2) and other published experimental data in the literature. The model results show that both oxide layer removal and "clean" boron burning rates dramatically increase in the presence of atomic fluorine, as much as 4 times when the combustion is kinetically limited. HF is found to decrease the oxide layer removal times (t_1); however, it increases the "clean" boron burning times (t_2). In accord with the previous data, the burning times of boron particles decrease with increasing ambient temperature and/or pressure.

(a)   (b)
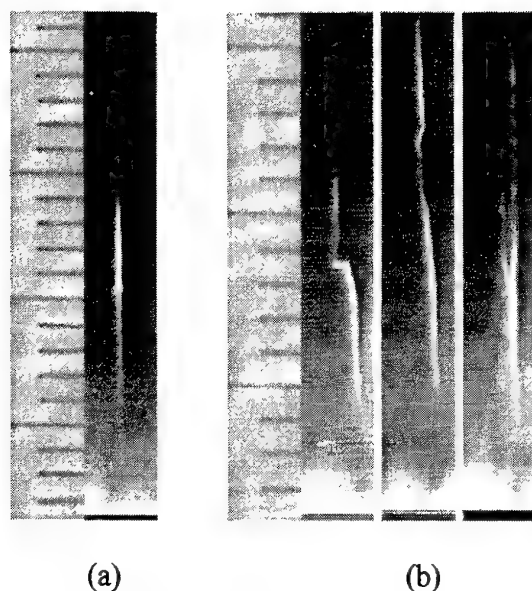
Figure 1   Typical Burning Trajectories of 1-μm Amorphous Boron Particles in; (a) $CH_4/O_2/N_2$ Flames and (b) $CH_4/NF_3/O_2/N_2$ Flames (T_{amb} = 2,020 K, Each Graduation on the Scale is 1 mm)
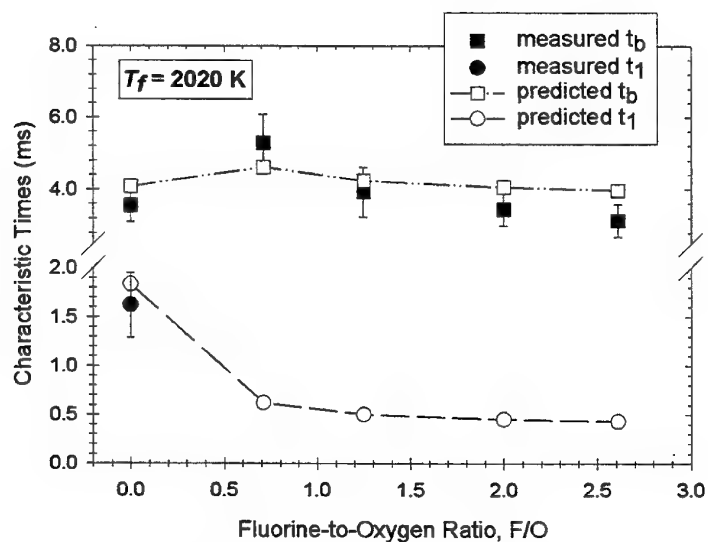
Figure 2   Comparison of Predicted and Measured First-Stage Combustion and Total Burning Times of 3-μm Crystalline Boron Particles at an Ambient Temperature of 2,020 K and a Pressure of 1 atm

AREA 7

PYROLYSIS AND COMBUSTION PROCESSES OF NEW INGREDIENTS AND APPLICATIONS

Reforming and Pyrolysis of Liquid Hydrocarbons and Partially Oxidized Fuels For Hypersonic Propulsion

C. Bruno, M. Filippi

University of Rome "La Sapienza" - Mechanics and Aeronautics Department

Via Eudossiana, 18

000184 – Roma (Italy)

Tel: 39-06-4458-5280

Fax: 39-06-4881759

E-mail: c.bruno@dma.ing.uniroma1.it

Chemical reforming and pyrolysis of liquid hydrocarbons (LHCs) and partially oxidised fuels (POFs) on board hypersonic vehicles are analysed as an alternative to carrying liquid hydrogen fuel. The purpose is to check the (gaseous) hydrogen yield obtainable, the cooling effects due to the endothermic nature of both processes, and the potential for fuel tank volume reduction. Moreover, an analysis of performance and fuel consumption is made for an AJAX-type vehicle.

The hydrocarbons used to simulate reforming are methane and n-dodecane, as a synthetic representative of kerosene. Some partially oxidised fuels have been used simulating cracking and reforming. Their use is particularly interesting because soot formation and heavy dehydrogenated species may be drastically reduced.

The software package used to simulate reforming and pyrolysis of LHCs is a non-commercial code called D.S.M.O.K.E. This software has been validated comparing its results with those obtained with the NASA C.E.C.-86 program.

Other simulations have been made involving different POFs (Methanol, Methyl Glycol, Ethyline Glycol) as real fuels (not ignition improvers) using the CEA400 code and CHEMKIN III. A broad range of initial conditions has been investigated by varying initial pressure, temperature mixture composition and also residence times in the reformer. The stagnation temperatures, reached in correspondence of the wing leading edge or nose of the aircraft at high Mach numbers, have been used as initial reforming/pyrolysis temperatures. This may be considered as a limiting case obtained, considering the Prandtl number of the air $P_r=1$ (recovery factor $r = \sqrt{P_r} = 1$) and assuming that heat transfer between the external surface and the reformer internal wall is realized without losses. Constant enthalpy and pressure reactions have been simulated in order to evaluate the temperature drop due to the endothermic nature of the processes. Figure 1 shows the temperature drop obtained by cracking of HCs (n-dodecane and C_3H_8) and POFs (CH_3OH) for P=5atm., T_i=1500K.

The results obtained show that high cooling capability and high H2 fractions are obtained. Figure 2 shows the main products of n-dodecane pyrolysis at P=5atm., T_i=3000K and t=0.1s. Results for temperature drops (reformed/pyrolysed gas composition and soot production) are presented as a function of the initial parameters. They indicate that large GH_2 fraction may be obtained from methane-rich or n-dodecane-rich mixtures reforming/pyrolysis performed at low pressure and high initial temperatures with residence times between 0.1 s and 1 s. From POFs cracking/reforming, GH_2, CO and other gaseous HCs (GHCs) are obtained, reducing

practically to zero the amount of soot. Temperature drops are also presented showing the cooling properties of the processes.

The gaseous products of reforming/pyrolysis of LHCs and/or POFs can be used as fuels for a scramjet combustor. Performances are calculated by varying flight Mach number and considering a constant dynamic pressure trajectory. A complete conceptual scheme of an integrated system for a future hypersonic airbreathing vehicle is shown in Figure 3. Reforming/pyrolysis process refers to the blue boxes; performance calculation refers to the pink boxes. In Figure 4, the Specific Impulse (I_{SP}) obtained burning the products od POFs pyrolysis is shown as a function of flight Mach number (expansion ratio is 50, equivalence ratio is 1). Assuming equilibrium at the exit of the combustion chamber, performance of an AJAX-type vehicle are calculated in terms of specific impulse and fuel consumption. An analysis of fuel tank volume has been carried on showing the advantage of carrying LHCs or POFs on board instead of LH_2.

DSMOKE simulation - HC and POF PYROLYSIS : Adiabatic/Isobaric, Ti=1500K, P=5.0Atm
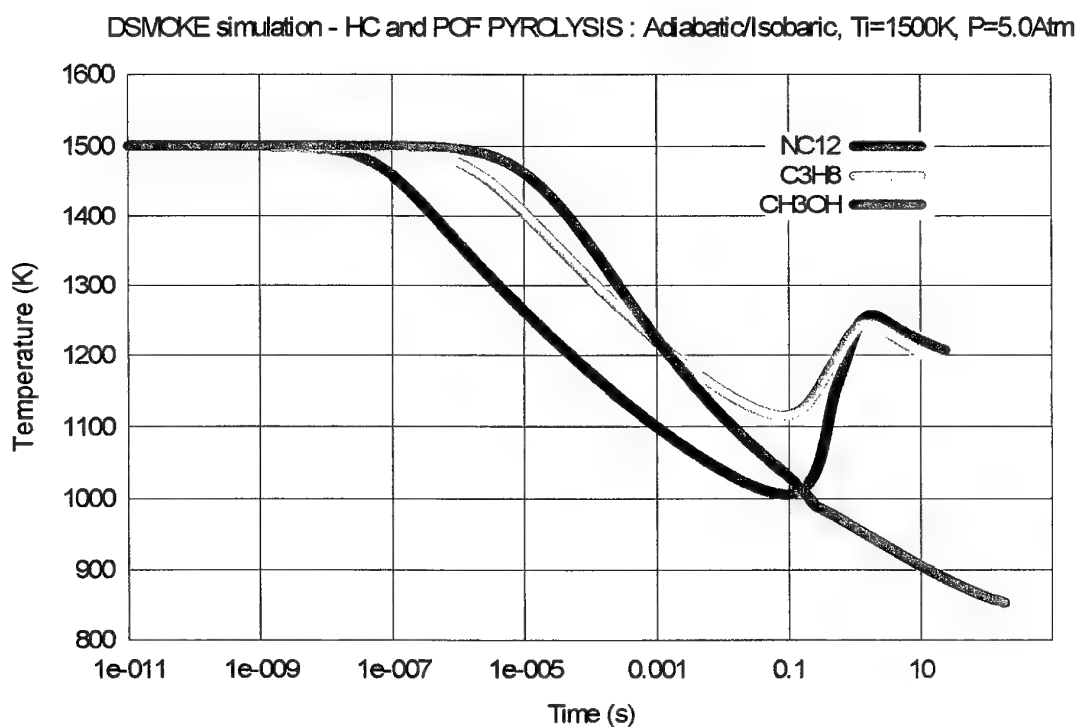
Fig. 1
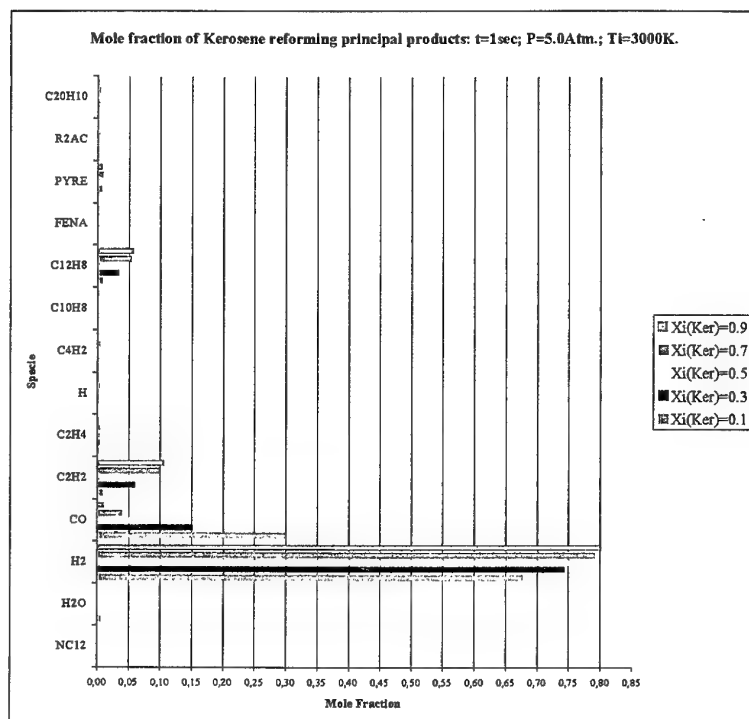
Fig.2

NC12=N-dodecane
$C_{12}H_8$=CycloPhentaNaphtalene
$C_{10}H_8$=Naphtalene
R2AC=EthinylAcenaphtalene
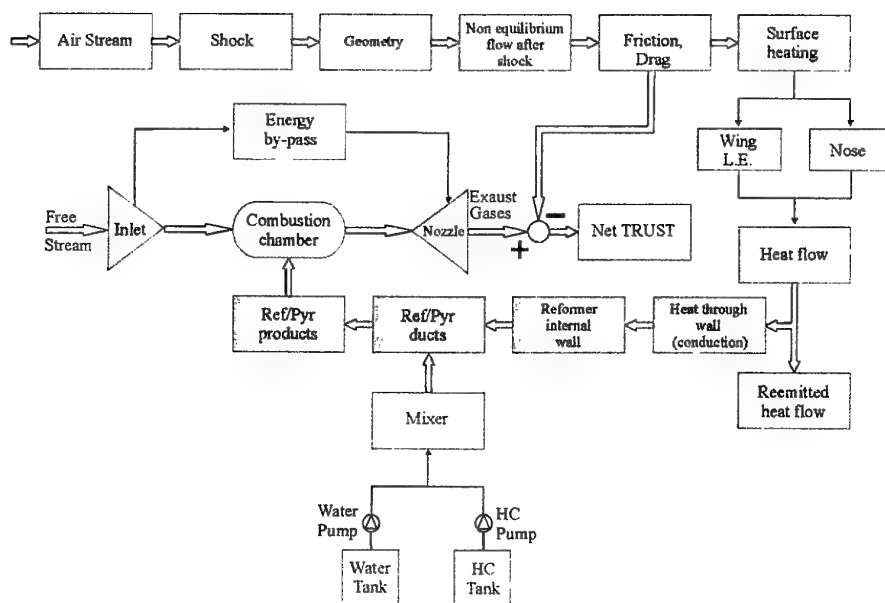
Fig. 3

313
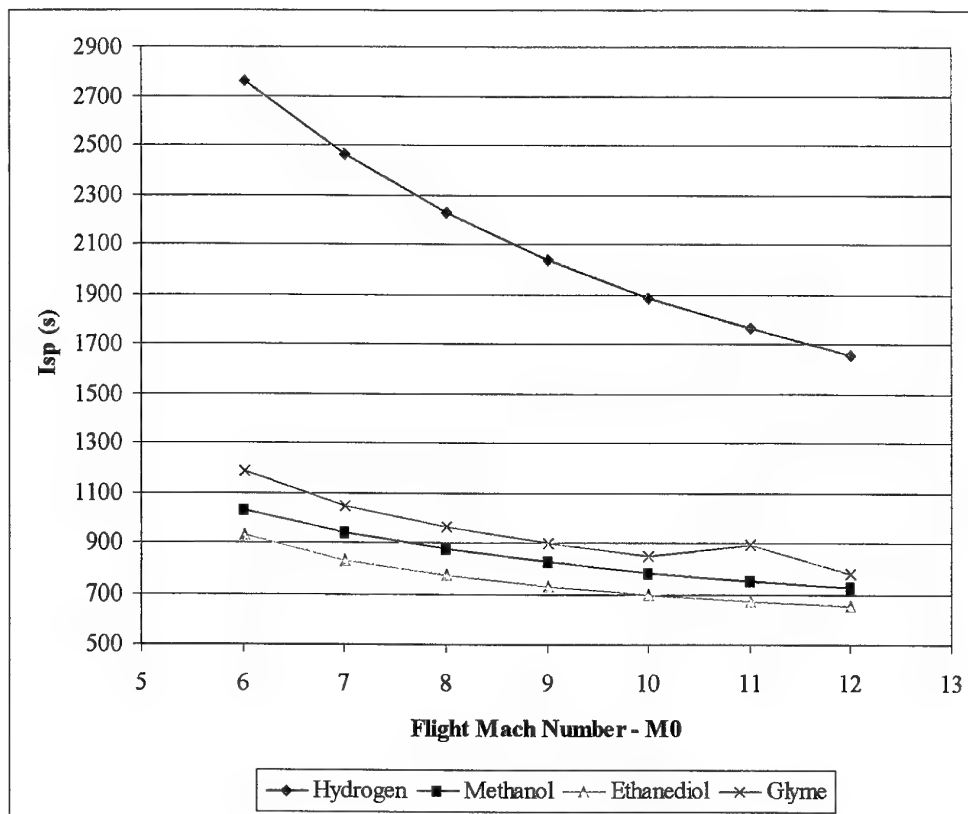
Fig. 4

Burning Rate Characterization of OXSOL Liquid Oxidizer

G.C. Harting, J.W. Mordosky, B.Q. Zhang, T.T. Cook, K.K. Kuo
140 Research Building East
The Pennsylvania State University
University Park, PA 16802
Tel: (814) 863-2264
Fax: (814) 863-3203
E-mail: gch104@psu.edu

Characterization of the burning behavior of OXSOL liquid oxidizer (70% HAN, 15% AN, and 15% H_2O by weight) was performed in transparent test tubes in a windowed liquid propellant strand burner. The burn rate of OXSOL was deduced from the regression history of the liquid surface. The burn rate was found to be a function of test tube diameter and ranged from 40 to 550 mm/s for the pressure range of 2.5 to 20 MPa. OXSOL exhibited two slope breaks with a pressure exponent near 3 from 2.5 to 5 MPa, 0.4 from 5 to 9 MPa, and – 0.8 above 9 MPa. The effect of the tube diameter on the burning rate of OXSOL is believed to be due to hydrodynamic instability of the burning surface, based upon the simulation of surface ripples with a vibrating membrane model. Additionally, the combustion product gas temperatures were measured to range from 500-650 K as a function of pressure. The burning rate slope break at 5 MPa was found to be very close to the slope break at 5.5 MPa in the plot of the ratio of heat of vaporization to the boiling point of water versus pressure. This demonstrates the importance of the water vaporization process in the low-pressure combustion of OXSOL. According to Levich's analysis, the influence of liquid viscosity and gravity is stabilizing. Burning rate measurements of OXSOL gelled with fumed silica as well as OXSOL chilled to very low temperatures (~ 220 K) were conducted to determine the effects of increased viscosity and reduced temperatures on the burning rate of OXSOL with respect to the tube diameter. Analysis of the influence of gelling agent content and temperature was performed in order to determine the intrinsic burning rate of OXSOL at room temperature without a gelling agent. The burning rate of the gelled formulations was found to be significantly lower than the apparent burning rate of OXSOL observed in the room temperature tests. These results provide further evidence that the planar burning of liquids is intrinsically unstable without the stabilizing effects of liquid viscosity.
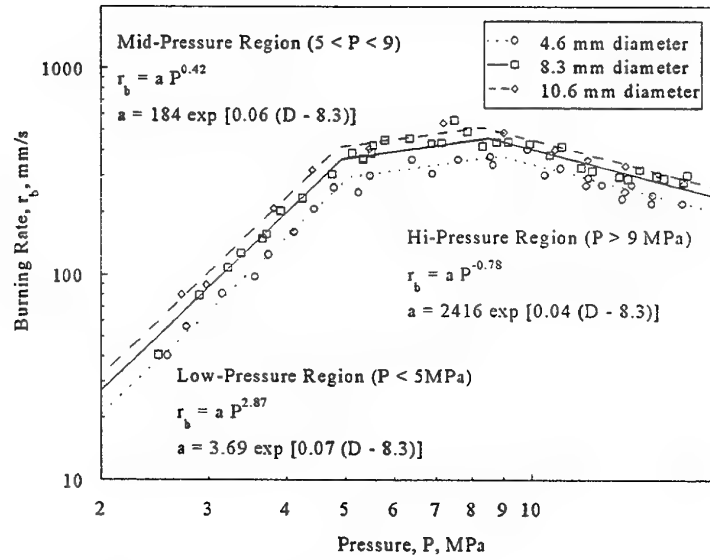
Measured burning rate of OXSOL demonstrating tube diameter effect

Mechanism of Modifying the Burning Rate of Compositions Containing Nitro- and Nitrato Groups by High-Energy Polynitrogen Compounds

V.P. Sinditskii, V.Y. Egorshev, V.I. Kolesov, M.V. Berezin, A.E. Fogelzang
Mendeleev University of Chemical Technology
9 Miusskaya Square, 125047, Moscow, Russia
Tel: (095)-496-6027
FAX: (095)-496-6027
E-mail: vaslav@muctr.edu.ru

High-energy polynitrogen compounds, such as azides and tetrazoles, are currently under investigation because they are of particular interest as energetic binders and plasticizers for solid rocket propellants and gunpowders. These compounds have the advantage of not only high energetic performance, but also are often capable of affecting the burning rate of the propellants. However, the general principle of the modifier action remains to be solved. It may include either a physical contribution by the high burning rate of the modifier and prompt heat release in the combustion zone, or a chemical one at the cost of increasing the rate of the leading reaction in the flame. High-reactive intermediate nitrenes are known to be the initial products in the decomposition of azides and tetrazoles in which reactions with nitrogen oxides can be expected to proceed very fast. The main nitrene decomposition products are compounds containing the nitryl group. Subsequent oxidation reactions of these substances also occur with high speed and generate a lot of heat.

The goal of the present paper is to study flame structure of double-base propellant formulations containing high-energy polynitrogen compounds and to reveal the mechanism of modifying the burning rate. Glycidyl Azide Polymer (GAP) with molecular weight of 500 and low-melting 2-Methyl-5-Nitrotetrazole (MNT) were used as plasticizers for Nitrocellulose (NC). Two NC-based propellant formulations, NC/GAP/process additives (49/49/2) and NC/Nitroglycerine (NG)/Dinitrotoluene (DN)/MNT/process additives (24.4/49.6/9.6/13/3.4), were prepared through the ballistite technology.

A comparison of burning rates between the GAP/NC formulation and NC, on the one hand, and between NG/NC/DNT/MNT and NG/NC/DNT formulations, on the other hand, reveals an increase in the burning rate in both cases over all pressure ranges studied on addition of the polynitrogen compounds. Thermocouple-aided measurements in the combustion wave of the GAP/NC formulation indicate that both the fizz zone and the final flame zone temperatures are 200 K and 700 K less, respectively, than those of NC. In contrast, MNT having much better oxygen balance proves to increase both of the temperatures as compared to the base NG/NC/DNT composition.

The temperature gradient above the burning surface has been measured to increase substantially for both propellants, suggesting an increase in the heat release reaction rate in the fizz zone. In the case of the MTN-containing propellant, there is a decrease in the reaction time in the dark zone as compared to the formulation without MNT additive. Correlation between NG/NC/DNT/MNT and NG/NC/DNT propellant formulations as to the time delay in ignition of their secondary flames shows that acceleration of the reaction in the dark zone by the addition of MNT is caused by the increased temperature in the zone as it was proposed previously for a NG/NC/GAP propellant.

Contrary to aromatic azide nitro compounds, which flame structure is characterized by a spatial separation of heat release zones resulted from the azide group decomposition and nitro group reduction, combustion of formulations composed of nitroesters like NC or NG and high-energy polynitrogen compounds, suggests a merged zone for the azide/tetrazole decomposition and NO_2 reduction in the flame. In this case, the increased burning rate is assumed to arise mostly from high rate of exothermic decomposition reactions of the polynitrogen compounds and, to a lesser degree, chemical interaction of their decomposition products with nitrogen oxides.

Flame Structure of Hydrazinium Nitroformate

V.P. Sinditskii, V.V. Serushkin, S.A. Filatov
Mendeleev University of Chemical Technology
9 Miusskaya Square, 125047, Moscow, Russia
Tel: (095)-496-6027
FAX: (095)-496-6027
E-mail: vvs@rctu.ru

Hydrazinium nitroformate (HNF), an energetic salt of hydrazine, N_2H_4, and organic acid, $HN(NO_2)_3$, called nitroform, is of considerable interest as a potential oxidizing component of propellant formulations [i, ii, iii]. In order to model and predict burning characteristics of formulations containing HNF, it is essential to know the combustion mechanism of HNF. This paper presents results on investigation of HNF flame structure by fine tungsten-rhenium thermocouples.

Hydrazinium nitroformate studied under investigation had the burning rate and physicochemical characteristics close to ones described in the literature [ii, iii]. Thermocouple measurements carried out at 0.04, 0.1, 0.5, 1 and 2 MPa have shown the following peculiarities of HNF flame:

In the condensed phase, the temperature rises monotonically from the initial temperatures to the melting point temperature (T_{melt} = 396 K). This region is followed by the melt/foam layer. At low pressures, this layer may be divided into two zones: in the first one, the temperature increases slowly (for example, at 0.1 MPa from 400 to ~425 K over the distance of 0.1-0.15 mm) and the zone of exothermic reaction in which temperature rises more quickly (for example, at 0.1 MPa from 425 K to the surface temperature (T_s ~ 615 K) on the length of 0.15 mm).

The temperature profiles in the gas phase show two distinct flames. In the first flame, the temperature rises from the surface temperature to 1320-1540 K, depending on pressure. It is followed by a dark zone, which is most often observed on profiles at pressure 0.4 MPa and practically disappears at 2 MPa. After this zone, the temperature again begins to rise sharply to values of 2300-2720 K, which is 170-390 K less than the adiabatic flame temperature for HNF.

Probably due to the other technique of thermocouple and strand preparation, surface temperatures measured in the present work are higher than previously reported [i, ii]. The data on T_s plotted in the coordinates pressure *vs.* reciprocal temperature fall satisfactorily on a straight line. The slope of the line yields the enthalpy of salt sublimation of 37.4 kcal/mole.

Formation of ammonium nitroformate (ANF), along with H_2O, N_2O and N_2 was observed in the first stage of decomposition by several research groups [iv, v]. Thus, it is possible to assume that the surface temperature of HNF is controlled by dissociation of one of nitroform salts. Enthalpy of dissociation of HNF is equal 40.9 kcal/mole, it is a little bit larger then that of ANF (36.1 kcal/mole). The ability of HNF to sustain its burning at low pressures in the absence of the gas flame, on the one hand, and high reactivity of hydrazine on the other hand allows us to assume that hydrazine reacts practically completely in the condensed phase and

that it is ANF dissociation which determines the surface temperature at HNF combustion. Heat calculated for this reaction is enough for warming up the condensed phase and following dissociation of ammonium salt at the surface at low pressures. In contrast, according to the temperature profiles, heat feed back from the gas phase to the surface is insignificant.

The appearance of the second flame zone in the gas phase at low pressures indicates that chemical processes proceeding at combustion of HNF differ considerably from those proceeding at burning of nitroesters, aromatic nitrocompounds and double-base powders whose second flame zone occurs only at pressures above 2-3 MPa. Based on possible decomposition pathways of nitroform, a suggestion can be made that, in the first gas flame zone, decomposition of nitroform and oxidation of NH_3 and carbon-containing products (supposedly, nitrile N-oxide, CNO, or its isomer isocyanate, NCO radicals) take place. The second flame zone temperature rise is due to exothermic decomposition of N_2O and NO. The measured flame temperature of HNF agrees with the temperature calculated under the assumption that 1.46 moles of NO (per mole of HNF) remain unreacted in the flame. The amount of NO assumed to be unreacted is also coincident with NO content experimentally found in the HNF flame by means UV spectroscopy [**Errore. Il segnalibro non è definito.**].

References

i. McHale, E.T., and von Elbe, G. "The Deflagration of Solid Propellant Oxidizers", *Combustion Science Technology*, 1970, vol. 2, pp. 227-237.

ii. Louwers, J., Gadiot, G.M.H.J.L., Versluis, M., Landman, A.J., van der Meer, Th.H., and Roekaerts, D. "Combustion of Hydrazinium Nitroformate Based Compositions", AIAA Paper 98-3385, Cleveland, OH, July 13-15, 1998.

iii. Louwers, J., Parr, T., and, Hanson-Parr, D. "Decomposition and Flame Structure of Hydrazinium Nitroformate", AIAA Paper 99-1091, Reno, NV, January 11-14, 1999.

iv. Koroban V.A., Smirnova T.I., Bashirova T.N., and Svetlov B.S. "Kinetics and Mechanism of the Thermal Decomposition of Hydrazin Trinitromethane", *Trudy MKhTI im. D.I. Mendeleeva (Proc. Moscow Mendeleev Institute of Chemical Technology)*, 1979, vol. 104, pp. 38-44.

v. Williams G.K., and Brill T.B., "Thermal Decomposition of Energetic Materials 67. Hydrazinium Nitroformate (HNF) Rates and Pathways under Combustionlike Conditions", *Combustion and Flame*, 1995, vol. 102, pp. 418-426.

HNF/HTPB Based Composite Propellants

A.E.D.M. van der Heijden, H.L.J. Keizers
TNO - Prins Maurits Laboratory
P.O. Box 45
2280 AA RIJSWIJK, The Netherlands
Tel: +31 15 284 3774; Fax: +31 15 284 3974
E-mail: heijdena@pml.tno.nl

W.H.M. Veltmans
Aerospace Propulsion Products b.v.
P.O. Box 697
4600 AR BERGEN OP ZOOM, The Netherlands
Tel: +31 164 245950; Fax: +31 164 245960
E-mail: app@tip.nl

In a search for new storable high performance propellants for the European Space Agency (ESA), the solid oxidiser Hydrazinium Nitroformate (HNF) was identified as a very promising ingredient for a new storable composite propellant. Two distinct advantages of HNF based propellants over presently used Ammonium Perchlorate (AP) based propellants were the basis of this promise: a very high specific impulse which dramatically increases the performance of the solid propellant and chlorine free exhaust products which prevent the formation of hydrochloric acid in the environment.

Modern solid rocket motors are generally based on AP in a hydroxy-terminated polybutadiene (HTPB) binder system. Replacement of the AP with HNF will, as indicated above, result in significant performance gains, chlorine free exhaust products, and a reduced smoke trail; whereas it represents a relatively small change in composite propellant production (all existing knowledge and production infrastructure for HTPB based systems can be kept in place). Early investigations in the USA, during the sixties, seemed to indicate that HNF could not be combined with HTPB. However, recent studies performed at TNO Prins Maurits Laboratory show that acceptable propellants can be produced using this combination. A summary of the results obtained with HNF/HTPB formulations will be presented.
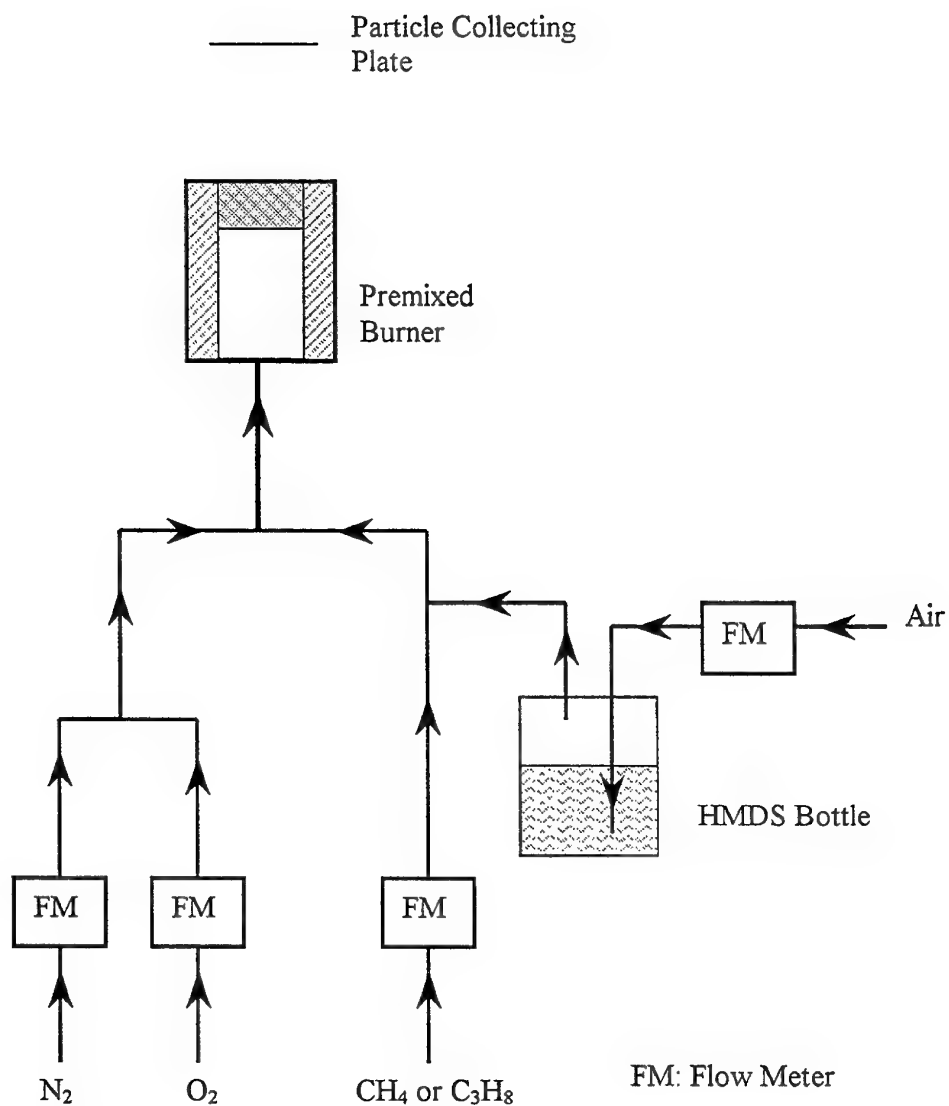
Figure 1 Schematic diagram of Experimental Setup of
Combustion Synthesis of SiO$_2$ Particles

AREA 8:

THEORETICAL MODELING AND NUMERICAL
SIMULATION OF COMBUSTION PROCESSES

Application of a Eulerian-Lagrangian Two-Phase Flow Solver on a LPP Reactive Flow

O. Boisneau, R. Lecourt
Onera Dmae Centre Du Fauga-Mauzac
F-31410 Noe
Tel: 5-61-56-63-84, Fax: 5-61-56-63-87
E-mail: lecourt@onera.fr

Lean Premixer Prevaporizer (LPP) has been developed during the last few years to reduce NO_x emission into turbo-engines in order to respect environmental specifications. Positioned just before the main chamber, they allow better gas mixing and drop vaporization for a better combustion efficiency and a lower flame temperature. This decrease in temperature reduces NO_x emissions, which are produced at high temperatures. Flow in LPP is normally non-reacting but undesirable combustion can occur when hot gas from the main chamber comes back (flash back phenomenon) or because of auto-ignition.

As LPP is a key-device in turbo-engines, its operating conditions have to be known accurately both to predict vaporizing efficiency and flash back and auto-ignition. Moreover, as all two-phase flow phenomena are involved in LPP, it is a good benchmark to validate physical models. So, at ONERA-TOULOUSE we performed flow computations at each step of our two-phase flow research on a simplified LPP geometry. The two-phase flow is computed by coupling a gas-phase Navier-Stokes solver (MSD) and a condensed phase flow solver (LSD).

For the gas phase, Navier-Stokes equations are solving with a K-L model for the turbulence. Interaction with drops in an inert flow is expressed by source terms in momentum, in species and in energy equations.

A Lagrangian description is used for the droplets. The influence of turbulence is taken into account by a correlation in space and time. For drop vaporization, the code uses an Abramzon-Sirignano model with convection around the drop, temperature increase and conduction inside. Finally the solver computes the source terms needed by the gas-phase solver.

For every droplet, auto-ignition is tested using local gas properties to calculate a Damköhler's number defined by Makino's models for a purely oxidant medium and to compare it with a critical Damköhler's value. Location of the auto-ignition points is saved to be used by the gas phase computation step.

For reactive flow, combustion takes place in the gas phase solver with the CRAMER model which is an Eddy-Break-Up one reaction model with poor and rich boundaries. When auto-ignition is detected by the criterion, the CRAMER model is triggered. An iterative process is necessary between liquid phase and gas phase computations to take into account the flow modification brought by combustion.

In the simplified LPP geometry, air is injected at 900K and kerosene (JP8) at 288K with the $0.729Kg.s^{-1}$ and $0.07Kg.s^{-1}$ respective mass flow rates. Jet atomization is modeled by injection of drops in five points. Five computations have been done to study single size drop

vaporization in a reactive flow. Another one with five drop sizes altogether has been made to study differences between a reactive flow and a non-reactive one.

It results from this study that complex two-phase reactive flows can be analyzed using simple models altogether. Drop vaporization is increased by the presence of hot gases from the combustion especially for little drops which have a strong influence on combustion.
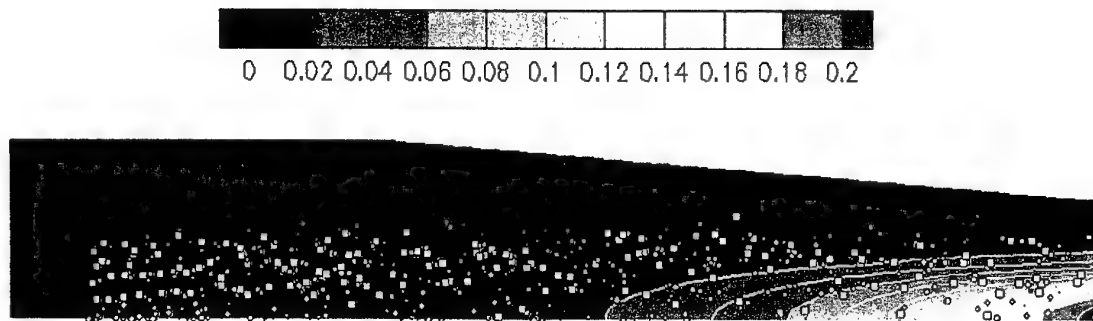
Two-phase flow computation in a simplified LPP – burned gas mass fraction and fuel drop locations

Numerical Simulation of Solid Motor Ignition Transient

M. Di Giacinto
Dipartimento di Meccanica e Aeronautica
Facoltà di Ingegneria
Università La Sapienza
Via Eudossiana 18, 00184 Roma, Italy
Tel: +39-06-4458-5895, Fax: +39-06-488-1759
E-mail: digiacinto@dma.ing.uniroma1.it

A simulation model has been developed in order to reproduce the behaviour of large solid motors during the ignition transient.

The sudden pressure rise during the transient requires an accurate time discretization and, at the same time, the large dimensions of the combustion chamber involve a heavy spatial discretization. For these reasons, the adoption of multidimensional flow models is not suitable for practical pourposes, even if the more affordable 1D models, at least in principle, have no possibility of simulating the very complex phenomena occurring at the combustion surface. Therefore, an unsteady quasi-1D Euler flow model has been adopted coupled with suitable semi-empirical models that take into account the main phenomena influencing the ignition transient. To this extent, special attention has been devoted to develop reliable models that simulate the effects of the following phenomena:

- The impingement of the igniter flux on the combustion surface and the ignition and combustion velocity in the impingement region.
- The heat exchange between the gas and the propellant surface in order to predict the ignition and the flame propagation along the grain surface.
- The combustion velocity along the grain surface after ignition.
- The breakdown of the internal diaphragm of the motor.
- The nozzle behaviour during the initial transient, until the chocking condition is attained.
- The possible presence of grain slots with lateral combustion and sudden enlargement of the port area.

Obviously, the basic flow model includes suitable terms that take into account the mass addition due to both the igniter flow and the grain regression, and the time evolution of the port area of the combustion chamber.

The numerical results have been extensively compared with both existing literature and experimental results for different solid motor configurations.

THIS PAGE HAS BEEN DELIBERATELY LEFT BLANK

Zero-Dimensional Unsteady Internal Ballistic Modeling

A. Annovazzi
Fiat Avio – Comprensorio BPD
Colleferro, RM, Italy
Tel: +39-06-9728-5518
Fax: +39-06-9728-5316
E-mail: p.rossi@mclink.it

A. Tamburini, F. Gori
Università degli Studi di Roma – Tor Vergata
Rome, RM, Italy

Design of solid rocket motors requires theoretical models for prediction/test analysis having particular characteristics of effectiveness and short computer time, specially when these models are used for statistical calculations as dispersion analysis or thrust imbalance evaluation between two coupled flight boosters. To this purpose, a specific internal ballistic model was developed at Fiat Avio-BPD with the following requirements: 1) the flow field solution in the propellant grain channel is obtained considering mass adduction, port area change, erosive burning, and different burn rate for each segment; 2) the motor ignition transient is described under unsteady conditions in the simplest way taking into account igniter mass flow rate, flame spreading, and chamber filling. These two requirements were properly combined through: 1) a steady-state solution of the propellant grain flow channel with a convenient linear combination of simple one dimensional flow in integral form (thus allowing Mach number, pressure, propellant mass flow rate, burn rate, etc. along the motor axis to be calculated); 2) unsteady internal ballistic model based on zero-dimensional operating conditions. Pressure, temperature, burn rates, and chamber volume are integrated in time taking into account the effective pressure and temperature values obtained from the previous point 1. A good match was obtained during ignition transient and steady-state phase comparing the obtained results with more sophisticated models, and also with experimental measurements.

THIS PAGE HAS BEEN DELIBERATELY LEFT BLANK

Numerical Modeling of Solid Rocket Motors

L. Galfetti
Laboratorio di Termofisica, Dipartimento di Energetica
Politecnico di Milano - Campus Bovisa, 20158 Milan, Italy
Tel: +39-02-2399-8526
Fax: +39-02-2399-8566
E-mail: galfetti@clausius.energ.polimi.it

This paper presents the first step of a research program on the numerical modeling of combustion processes involved in solid propellant rocket motors.

A two-dimensional model to simulate the combustion chamber of a solid rocket motor is presented. The model includes the unsteady fluid-dynamic field of the chamber coupled with the unsteady behavior of the propellant grain. A moving boundary approach has to be considered in the model because of the regression of the propellant combustion surface; consequently a remesh problem is faced up, connected with the progressive increase of the fluid domain and the corresponding decrease of the condensed phase domain. To solve this problem, the same approach followed in the KIVA code from Los Alamos National Laboratories is taken: spatial differences are formed with respect to a generalized mesh of arbitrary cells whose corner locations are specified functions of time. This feature allows a lagrangian, eulerian, or mixed description which is useful in order to describe curved or moving boundaries.

For the grain treatment, a one-dimensional unsteady approach is followed. This implies a uniform regression rate of the grain because of the propellant surface temperature, which is assumed to be uniformly distributed. In this first step of the modelling, the combustion surface temperature is assumed to be the average of the temperature distribution along the grain. Such a constraint will be removed according to the implementation of a combustion deformable surface, not yet introduced at this moment.

The geometry of a small solid rocket motor, designed to measure the burning rate, is assumed for numerical experiments. Numerical results are shown, and a comparison with the experimental pressure trend is discussed, in order to show capabilities and limits of the numerical approach. In addition, developments currently in progress are noted, and finally the plan for future developments is presented.

THIS PAGE HAS BEEN DELIBERATELY LEFT BLANK

The Features of the Reaction Initiation for the Singular Crystals in the Thermomechanical Ignition Models

A.G. Knyazeva
Institute of Strength Physics and Material Science
ISPMS, pr. Akademicheskii 2/1, Tomsk, Russia, 634021
Tel: 7-382-2-286876
Fax: 7-382-2-25-95-76
E-mail: anna@ispms.tsc.ru

In this report, simple models of ignition of the single crystals are discussed taking into account the internal mechanical processes. This work is an extension of previous investigations devoted to the ignition with the internal stresses and strains, see for example [1]. The simple models for the crystals are based on the medium models offered in [2] and extended for anisotropic materials. The tensors of the coefficients of the concentration and structure expansion, which are analogous to the tensors of thermal expansion coefficients, are introduced in this model. That allows to construct the thermal conduction equation for corresponding materials. The derivation of the kinetic equation for the additional parameter (relative damage volume or damages) is a separate problem. We may introduce a different additional parameter - the specific square of the internal surfaces, that is more suitable for some practical problems. The balance equations derivative will be the same.

It is demonstrated that the ignition model for some crystals may be analyzed in the one dimensional formulation. In this case, the coupling coefficient may take negative values which lead to new qualitative effects. The problem was solved analytically for parameters interval where the ignition regime exists. In the general case, the problem was solved numerically. The time dependencies of the reaction excitation on various parameters are found.

The results of analysis of the problem on the ignition of body with finite size are interested for the single crystals [3]. For example, it was shown that the character of the body surfaces fixation effect is essential for the body temperature. So, if the surfaces are free, the temperature in the center of the body drops in the initial moment, and then it grows up due to external heating and chemical release.

Of course, the discovered features may be "smoothed" in polycrystals due to collective effects, or in single crystals due to phase transitions. This question could be discussed specially.

1. Knyazeva A.G. and Zarko V.E., Modeling of Combustion of Energetic Materials with Chemically Induced Mechanical Processes, Journal of Propulsion and Powder, 1995, No 4.
2. Knyazeva A.G., Introduction to the local equilibrium thermodynamics of the physical-chemical conversions in the deformable media, Tomsk, 1996, 148 pp.
3. Knyazeva A.G., Do effect the condition of the specimen fixation on its heating rate?, Fizika Goreniya i Vzryva (translated in USA, Combustion, Explosion, and Shock Waves), in press.

THIS PAGE HAS BEEN DELIBERATELY LEFT BLANK

Navier-Stokes Solution for Solid Fuel Regression Rate in 2-D Hybrid Rocket Motor

L. N. Serin, Y. Gögüs
Department of Aeronautical Engineering, Middle East Technical University,
Inonu Bulvari, 06531Ankara, Turkey
Tel.: +90 312 210 24 32; Fax: +90 312 210 12 72
E-mail: nserin@sage.tubitak.gov.tr

Hybrid rocket motors offer substantial advantages over the solid and liquid rocket motors, such as higher safety, better reliability and low cost. On the other hand, the level of technical maturity of the hybrid rocket technology is questionable. The primary objection comes from the fact that accurate calculation of the regression rate for the design of hybrid rocket motors still needs more effort.

A commercial Navier-Stokes CFD code, CFD-ACE, was employed for computing the solid fuel regression rate in a hybrid rocket motor analog. The computational domain has a 2-D planar geometry, identical with a hybrid test set-up of a High Pressure Combustion Laboratory in Pennsylvania State University (PSU). Investigating the regression rate variations, both in time and space, by means of thermal analysis and chemical kinetics associated with flow dynamics is the main purpose of this paper. The computational results will be compared with the real time x-ray radiography and ultrasonic pulse-echo measurements.

CFD-ACE was validated by solving a conjugate heat transfer problem over a flat plate and comparing the results with analytical solution. As a second problem for validation, flame speeds of methane/air flame under different stoichiometric ratios and inlet velocities were investigated, and the results were compared with the theoretical and experimental results.

A structured grid was generated for the computational domain identical to a 2-D hybrid rocket motor of PSU. Some cold flow results for gaseous oxygen flow were obtained by solving 1st order upwind scheme Navier-Stokes equations together with RNG k-ε turbulence model. More results were obtained for the cold oxygen flow with gaseous nitrogen injection from the fuel surface, which is originally a mass addition and mixing problem. Finally, the problem was solved with an equilibrium combustion model, including chemical dissociation.

The program has three combustion models: instantaneous, multi-step finite rate and equilibrium. These three models were separately applied to a hybrid rocket problem and their advantages and the disadvantages have been investigated. According to the results of these calculations, equilibrium combustion models was found to be the best model that can simulate the combustion. Details will be given in the paper.

Regression rate in time and space will be solved interactively. The regression of fuel, and corresponding change in mass flux on the fuel surface, will be modelled by changing local grid spacing such that the grids on the surface move at the same rate with the regression rate.

THIS PAGE HAS BEEN DELIBERATELY LEFT BLANK

Prediction of Hybrid Fuel Regression Rates in Turbulent Boundary Layer Combustion

H.Y. Wang, J.M. Most
Laboratoire de Combustion et de Détonique
C.N.R.S. UPR 9028 -E.N.S.M.A., Université de Poitiers
BP 109 - Site du Futuroscope
86960, Futuroscope Cedex, France
Tel: (33) 05 49 49 82 95
Fax: (33) 05 49 49 82 91
wang@lcd.ensma.fr

G. Lengellé
ONERA
DEFA
Centre de Palaiseau
Chemin de la Hunière
91761 Palaiseau Cedex

An efficient parabolized numerical procedure is developed for calculating the reacting flow field and the performance of hybrid rocket motors. The fuel vapors, evolved by the decomposition and evaporation of the solid due to heat transferred from the flame, diffuse from the solid fuel surface, while the oxidizer diffuses from the core parallel flow both towards the reaction zone. The combustion takes place in a thin turbulent boundary layer region where the oxidizer-fuel ratio is close to stoichiometric.

The coupling of the heat and mass transfers at the interface between the burning wall and oxidizer parallel flow is simulated using k - ε model. Turbulent combustion is modeled by the Eddy-Break-Up and the Eddy-Dissipation Concept both with fast chemistry. The main innovations of the present investigation are:

1) Modified wall functions using a two-layer approach to evaluate local variations of turbulent quantities, and extention of the two-layer treatments to the enthalpy equation.

2) Effect of the longitudinal pressure gradient, with the presence of the strong mass flow rate at the burning surface, along a confined duct is taken into account.

3) Strong coupling of heat and mass transfers at the solid burning surface in a confined, chemically reacting flow is rigorously modeled.

The calculation of the regression rate is based on the usual assumption, that its value is proportional to the heat transferred from the flame to the wall. This heat is transferred mainly by convection and radiation. The convective heating can be calculated from the coupling of heat and mass transfers. A two-dimensional adaptation of the Discrete Ordinates Method is used for estimating the flame radiation energy to the burning wall. Therefore, for a successful prediction of hybrid fuel regression rates in such turbulent reacting flow, the following models are used: 1) a model for the turbulent fluid flow, 2) a model for the interaction

between turbulence and combustion, 3) models for chemistry and thermodynamics, 4) a model to predict the radiation field in combustion systems; 5) specific treatment of the coupling between heat and mass transfers at the solid burning surface 6) an efficient numerical procedure capable of taking into account the streamwise pressure gradient. The selected fluid dynamic results are compared with the available experimental data.

The Analysis of Gun Pressure Instability

A.K. Macpherson
Department of Mechanical Engineering and Mechanics
Lehigh University #19
Bethlehem PA 18015
Tel: (610) 758-4105; Fax: (610) 758-6224
E-mail: Macpherson@lehigh.edu

A.J. Bracuti and D.S. Chu
ARDEC US Army
Picatinny Arsenal
NJ 07806 5000

P.A. Macpherson
Department of Mathematics and Computer Science
1200 E Colton Ave
Redlands University
Redlands CA 92373

The stability of the pressure in a gun has traditionally been analyzed by Fourier transforms that seek the frequencies which carry the maximum energy. The usual method of analysis is to use Fourier transforms of the signal from a time domain to a frequency domain in order to determine the predominate frequencies. In a steady state situation this can often lead to finding the location of the source of the wave. If the events are time dependent the regular Fourier analysis, where the signal is integrated over all time, may not provide a useful result. Our auditory senses respond to signals both in time and frequency and an integrated signal is difficult to interpret. This is overcome by using windowed Fourier transforms. In the windowed transform a short time window is chosen and the transform performed over that time. The length of the time window is chosen to show the desired features of the signal. If the time window is long then it can represent long wave length frequencies, although the time is not accurately known. On the other hand, if the window is narrow the time is known accurately, but the long wavelengths are poorly represented. The result is that a small window will not detect low frequencies and a large window will not recognize high frequencies. This is similar to the uncertainty principle in quantum physics. It has been found that for accuracy, the relation between the window size and the frequency range Δf is $\Delta t \Delta f \geq 1 / 4\pi$.

Many cases were studied and representative examples are shown. For example, a typical pressure trace is shown in figure 1. This was generated in a two step chamber with step sizes 0.172 inches and 0.156 inches. The regular transform is shown in figure 2. The frequency ν of the initial wave can be measured and in a steady state situation it would be used in a relation such as $c = \lambda \nu$ to calculate the wave speed c, where the wavelength, λ would be determined from the geometry. In the present case the wavelength varies as the projectile moves down the barrel and the time averaged frequency cannot be used for such a calculation. It can be seen that the dominant frequency at all measurement points is approximately $0.5 \times 10^4 \text{sec}^{-1}$. The transformed pressure becomes significantly smaller in magnitude once the projectile starts moving.

A windowed transform with a window size of 0.2 msec was used to analyze the shot shown in figure 1. The first significant windowed results occurred in a window covering the time 0.4-0.6 msec (Figure 3). This does not quite satisfy the uncertainty criterion but it was found that it allowed the calculation of the principle wave velocity. It can be seen that the wave has developed in the booster with a dominant frequency of 2.5×10^4 sec^{-1}. An examination of the effect of the shape of the igniter booster shape and some wavelet results are also presented.

Several test shots using different configurations were studied and the maximum transformed pressure plotted against distance from the breech.

Time, msec
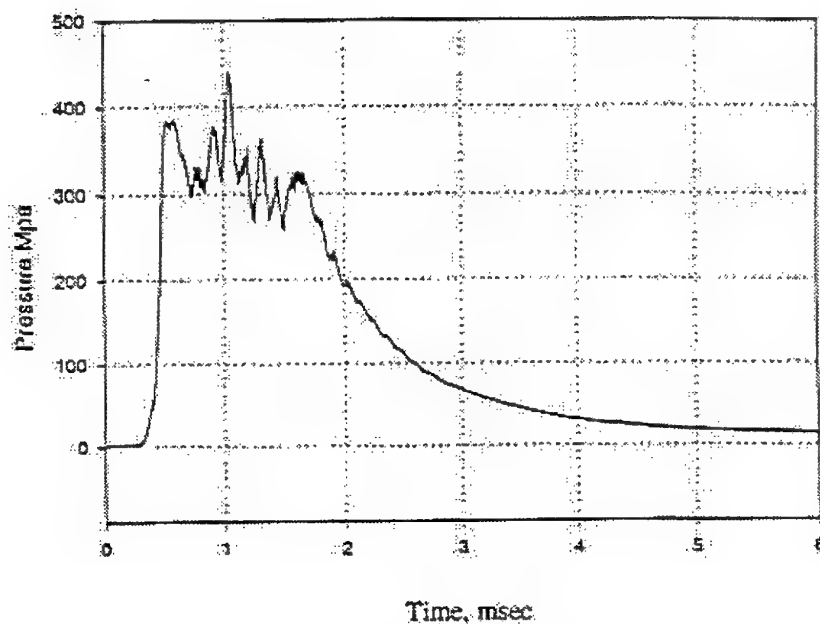
Fig.1 Pressure v Time in the Booster

338

Frequency, 5×10^4 sec^{-1}
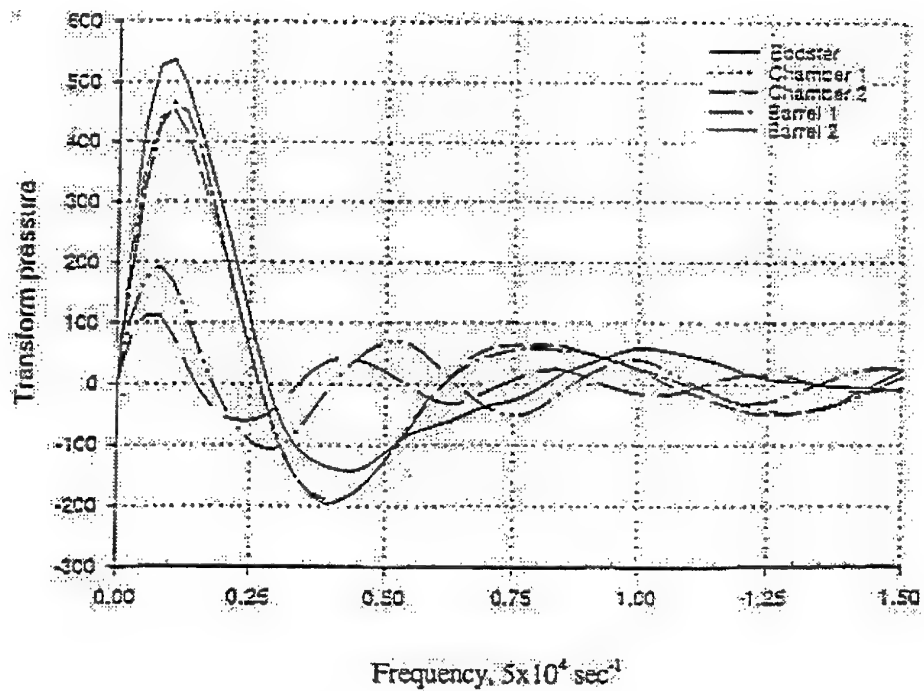
Fig. 2. Fourier sine transform v frequency

Frequency, 10^4 sec^{-1}
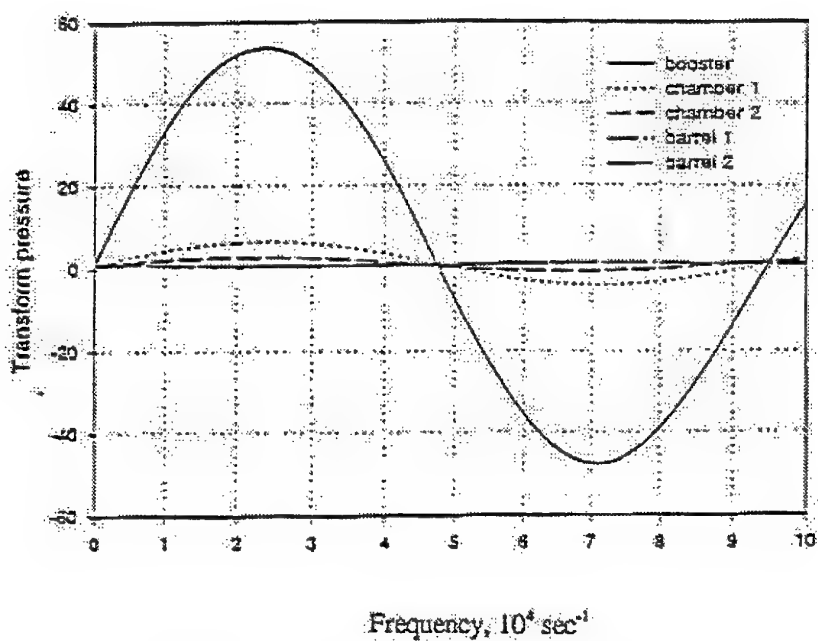
Fig. 3. Fourier window transform 0.4-0.6 msec

THIS PAGE HAS BEEN DELIBERATELY LEFT BLANK

Shock-Wave Calculation Model for Detonation of Multicomponent Energy Carrier Containing Combustible Phase

V.N. Okhitin, V.V. Selivanov, A.V. Zibarov
Bauman Moscow State Technical University
5, 2nd Baumanskaya St, 107005, Moscow, Russia
Tel: (095) 261-8970
Fax: (095) 261-8970
E-mail: astua@cityline.ru

Within the frames of single-velocity two-phase medium (gas with solid reactive aluminum particles), a form of the function describing energy release from aluminum particle combustion has been specified. Terms of mass and energy exchange in equation systems of considered process mathematical model have been defined. A generalized kinetics of aluminum ignition and combustion including the growth of aluminum cover, the combustion transfer into vapor-phase regime, and aluminum burning-out have been set. A calculation algorithm of thermodynamic and kinematic parameters at a front and in a medium after a front including energy released at aluminum particle combustion is presented.

A procedure of calculating an initial concentration of oxidizing elements, maximum fraction of reacting aluminum and specific heat of its combustion in detonation products of non-saturated and saturated multi-component mixtures is considered. Coefficients for determination of relations for the model of aluminum particle combustion in detonation products have been chosen and substantiated.

A computer code with a developed interface for the numerical modeling two-dimension shock-wave processes resulted from a detonation of multi-component energy carriers containing solid phase combusting in detonation products after a detonation wave front has been developed. Results of test problems are presented.

THIS PAGE HAS BEEN DELIBERATELY LEFT BLANK

Basic Scheme for Computer Simulation
of Decomposition Reactions for Energetic Compounds

T.S. Pivina

N.D. Zelinsky Institute of Organic Chemistry, Russian Academy of Sciences
Leninsky Prospect 47, Moscow 117913, Russia
Tel: 7 (095) 938 3645; Fax: 7 (095) 135 5328
E-mail: tsp@cacr.ioc.ac.ru

A.A. Porollo, T.V. Petukhova, V.P. Ivshin
Mari State University, Lenin Square 1, Yoshkar-Ola 424001
Mari El Republic, Russia

In general, a theoretical problem of computer modeling of energetic materials decomposition has two aspects: formulation of possible schemes of chemical transformations (i.e. advancement of the hypothesis about mechanism) and investigation of thermodynamic and kinetic characteristics of reactions that form this mechanism.

The second point of the problem is comparatively well-studied: there are developed methodologies and their computer implementation that allow to calculate kinetic and thermodynamic characteristics of the combustion and detonation processes. As for the first point of the problem, before our studies, there was no methodology for *ab initio* modeling and no methods to obtain the full list of thermal decomposition reactions for different compounds.

Therefore on the reaction network base, we developed the methodology, algorithms and computer program for computer generation of possible homolysis pathways for compounds with a correction of pathways using some empirical formal rules (generators of reactions), which are specified in accordance with the experimental data of combustion and detonation processes.

Mechanisms of chemical reactions we presented as a topologic structure, which is a function of source substances, intermediate and final products. It can be invariant for any concrete chemical system. To define a mechanism structure we used a graph theory, namely bipartite oriented graphs which have vertexes of two types: first type means molecular structures and the second one means reactions. Oriented edges define the role of reaction participants (reactants and products).

As a result of our study, we have formulated a novel general approach to the computer-assisted modeling of the mechanism of homolytical reactions for C-, N-, O-nitrocompounds. The effective mathematical apparatus and algorithms, as well as the program code CASB have been developed for the reaction network generation.

A set of chemical transformations generators based on experimental data has been formulated to follow up the more probable decomposition reactions for compounds of different chemical classes. Screening of the most advantageous pathways from the energy standpoint was carried out by traditional methods of quantum chemistry.

A high prediction capability for possible channels of thermolysis reactions was reached and a correct correlation of prediction pathways with the experimental data was observed.

AREA 9:

COMBUSTION DIAGNOSTIC TECHNIQUES

Diagnostic Methods for the Combustion of Energetic Materials

Y.M. Timnat
Faculty of Aerospace Engineering
Technion - Israel Institute of Technology
Haifa 32000, Israel
Tel: 972-4-829-2653
Fax: 972-4-823-1848
E-mail: aerbeny@aerodyne.technion.ac.il

The principal techniques for testing the performance of combustors are flow visualization, photography and cinematography (including the use of high speed cameras, schlieren, tomography, X-ray flash photography), velocity, pressure, temperature, density and concentration measurements, using probes and optical methods, sampling, regression rate measurements of solids and cold flow simulations of complex flows. I shall limit the discussion on a few of these methods, dealing mostly with those to which our laboratory contributed.

In the late sixties we developed a special chromel-alumel thermocouple with a millisecond response time, that can withstand the erosive action of the hot gases in the perforation of a propellant grain and succeeded in obtaining the axial temperature distribution within it. To reach higher temperatures (above 2000K), remote sensing methods are preferred, including spontaneous Raman scattering, Rayleigh thermometry and CARS. Before the advent of the laser, on which the above mentioned techniques and additional ones are based, one of the popular methods was line reversal. In our laboratory we adopted this technique to measurements performed in the range of 1800-3500K in a two-dimensional hybrid motor.

Using three wavelengths, we measured temperatures with an estimated accuracy of between 1 and 296. An example of the results is shown in Fig.1. Experimental data on fuel injection patterns during combustion and mixing processes are required to validate numerical models and to understand combustion efficiency and stability. These involve multiphase processes, in which liquid particles and gas participate in the case of turbojets and liquid fuelled ramjets, while in the case of solid fuel ramjets (SFRJ) there are also solid particles. Two of the important parameters required are particle and gas velocity and particle size, including their distributions. The two main techniques used to obtain such information are laser Doppler velocimetry (LDV) and phase Doppler anemometry (PDA). An experimental system using LDV is shown in Fig.2, while the optical package employed the pedestal amplitude, from which the particle size can be obtained, is presented in Fig.3. A detailed discussion of the system will be given. The PDA technique is based on the fact that when two coherent, monochromatic laser beams impinge on a liquid droplet, interference fringe patterns appear at different locations in space. From their spacing, one can determine the droplet diameter. The two methods will be critically compared, indicating the conditions for which each is more suitable. An important parameter for SFRJs is the regression rate of the fuel. This can be followed by photographic methods, in particular for transparent fuels like polymethylmetacrylate, as was done in our laboratory. Another method, which can be used also inside a motor, is based on the ultrasonic technique, which I used in the '90s. A further possibility is to exploit the change in the reflection coefficient of microwaves at the fuel; flame interface. The different techniques will be critically compared.
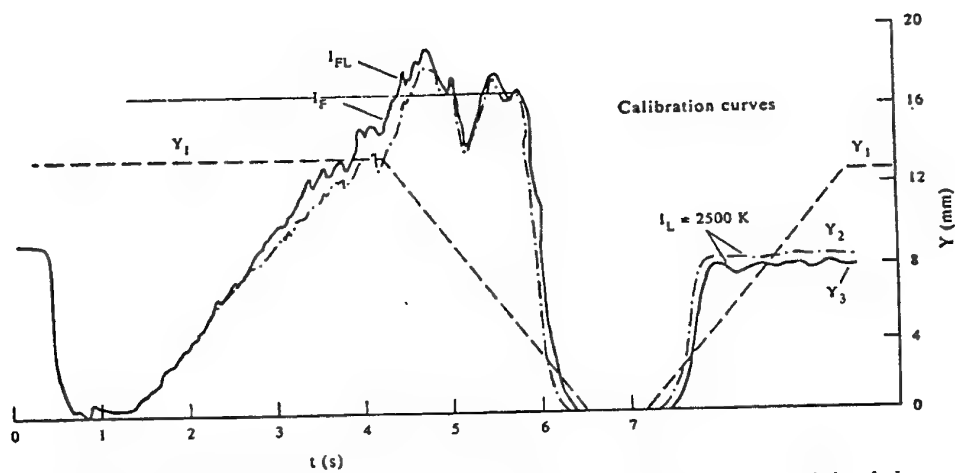
Fig. 1 Experimental radiation curve for polyester–oxygen system, utilizing the line reversal technique
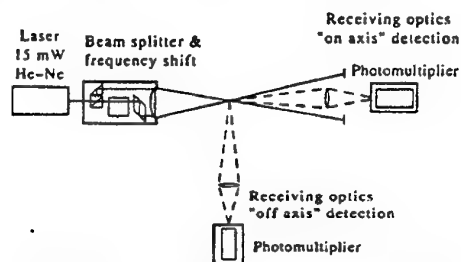
Fig. 2 LDA system for simultaneous measurement of velocity and particle size
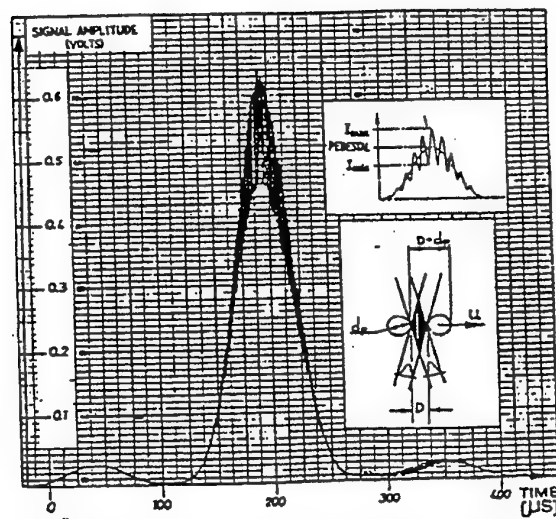
Fig. 3 The burst generated by a droplet crossing the control volume.

346

Interferometric Techniques and Automatic Data Processing in Propellants Combustion Research

V.S. Abrukov, I.V. Andreev, I.G. Kocsheev
The Chuvash State University, Moskovsky Prosp., 15, Cheboksary 428000, Russia
Fax: 7-8352-42-80-90
E-mail: victor@ chuvsu.ru

In [1,2] are shown wide and often unique possibilities of interferometry for investigation of the burning of propellants including the burning of transparent propellant models, which are to be studied by means of holographic interferometry in condensed and gas phases simultaneously. Interferometric methods can be used now for the measurement of very various characteristics: flame temperature and density field, burning rate and heat release power during ignition of propellant, heat release rate for explosion of the products of propellant gasification by laser radiation, heat release rate profile in the burning wave of propellant, the characteristic times of the individual stages of the initial period of ignition and of the period of response on laser radiation interruption, the thickness of the various zones of the burning wave of propellant both in gas and in condense phases, and other parameters.

Practical realization of the broad possibilities of interferometric methods require to automation of the process of measurement, first of all, for a stage of interferogram decryption (getting data about phases difference distribution in interferogram plane, eikonal value, etc).

Authors of this work have created some automation procedures, which permits to realize practically all possibilities of interferometric techniques discussed in [1,2]. This work generalizes some previous results of authors and presents principle new not known earlier procedure to automations of the interferogram decryption. This procedure processes an interferogram. as an ensemble of black and white pixels and allows defining of:

- the coordinates of interference bands borders and medium,
- the discrete kit of values of the function of phases difference distribution on interferogram (about 2000-3000 values),
- the eikonal (the double integral of the function of phases difference distribution on interferogram),
- the volume and surface of the object (if it possesses a cylindrical symmetry), as well as length of image border of object.

Authors believe that using of this procedure and TV-registration can make interferometric tools increasingly viable for use in the combustion research.

Authors suppose also that this procedure can be used for many other optical methods of combustion diagnostics. Its algorithm is sufficiently simple and quick. Theoretically, it can be used to develop real-time diagnostic and control systems for combustion processes.
At present this approach is used for monochrome images of interferogram. In the future we are planning to use it for analysis of the images with 256 gradation of gray, as well as for analysis of color images.

The automatic system "Interferometry" (user-friendly software complex as a whole) and the results of the experimental investigation of the burning of various propellants during some non-stationary and stationary regimes will be presented in this paper also.

The following experimental results were received by means of new automatic procedure:

-non-stationary flame temperature fields for the initial period of ignition and the period of response on laser radiation interruption with the time resolution 1 msec.,
-non-stationary mass burning rate and heat release power during ignition process with the same time resolution,
-heat release rate profiles in the gaseous phase of burning wave of varied propellants with the resolution about 0.01 mm,
 -convective heat flux profiles in the gaseous phase during ignition with the same resolution
-*computer animation of flame temperature fields and heat release rate profile in the burning wave during laser ignition of propellant,
 -some other experimental results concerning the mechanism of propellant combustion.

As a whole, this paper generalizes recent results and work in progress in the area of the using of interferometry in the study of propellants combustion in the Department of Thermophysics of the Chuvash State University, which is a leader in this area of science in Russia.

References.
1. Abrukov V. S., Ilyin S. V., Maltsev V. M. "Ignition of Propellants. Shaping and Development of the Burning Wave and Its Characteristics." - In: Proceedings of the Fourth Int. Symposium on Special Topics in Chemical Propulsion: "Challenges in Combustion and Propellants. 100 Years After Nobel" (Industrihuset, Stockholm, Sweden, May 2731,1996), Pennsylvania State Univ., USA, 1996, pp. 269-272.

2. Abrukov V.S., Ilyin S.V., Maltsev V.M., Andreev I.V., "Interferometric Technique in Combustion, Gas Dynamic and Heat Transfer Research. New Results and Technologies", CD-ROM Proc. Of VSJ-SPEE98 Int. Conference on Optical Technologies and Image Processing in Fluid, Thermal, and Combustion Flow, AB076, Yokohama, JAPAN, 1998 (http://www.vsj.or.jp/vsjspie/)

Imaging of Mixing and Combustion Processes in a Supersonic Combustion Ramjet Chamber

U. Brummund and F. Scheel
DLR Lampoldshausen - German Aerospace Center
74239 Hardthausen Germany
Tel: 49-6298-28-532
Fax: 49-6298-28-175
E-mail: uwe.brummund@dlr.de

Mixing and combustion processes within a high speed flow in a rectangular duct with a centrally mounted injector have been investigated. A supersonic air stream is generated inside this duct using the high speed flow developed by a vitiated air heater. Hydrogen fuel is injected into this flow, with the resultant mixing and combustion investigated using Schlieren imaging, together with temporally and spatially highly resolved planar Rayleigh scattering and laser induced OH fluorescence imaging.

For the mixing studies, non-reacting experiments have been performed in order to investigate both the compressibility effect on a supersonic mixing layer and a possible shock-induced mixing enhancement. Many experimental investigations have shown a reduction in growth rate of compressible mixing layers when compared with their incompressible counterparts of the same free-stream velocity and density ratios. For supersonic combustion ramjet (scramjet) propulsion, rapid and efficient mixing is required. A parameter characteristic of the compressibility is the isentropic convective Mach number, M_c, defined, in the case of equal specific heat ratios ($\gamma_1 = \gamma_2$), as: $M_c = \dfrac{U_1 - U_2}{a_1 + a_2}$, where U_1 (U_2) is the free-stream velocity and a_1 (resp. a_2) is the speed of sound of the faster (or slower) stream. Hydrogen was injected parallel to the center line of a supersonic model combustion chamber at the base of an injector plate into a Mach 2 air stream (see fig. 1). The convective Mach number of the resulting co-flowing mixing layer varied in the range of 0.8 - 1.1. We applied a method for enhancing the mixing between the air and the hydrogen by perturbation of the mixing layer with a shock wave. This oblique shock wave was generated by a wedge located at the upper plate of the chamber to impinge on the mixing layer at a fixed location. The shock/mixing layer interaction has been analyzed with shock angles of 36° and 45° with the shock position located at 40 mm downstream the injector.

Results concerning the normalized layer growth rate from planar Rayleigh scattering measurements are reported, compared with results from Schlieren photographs. We first analyzed the experiments without shock impingement to isolate the compressibility effect on the mixing layer. The evolution of the normalized growth rate is represented as a function of the convective Mach number in figure 2. As can be seen, the data fall in agreement with other experimental results showing a reduction in the normalized growth rate with increasing M_c (i.e. with increasing compressibility).

Furthermore, the results show that the normalized growth rate is generally higher with shock/mixing layer interaction than without, and that a stronger shock induces higher growth rates. Globally we can observe a decreasing growth rate with an increasing convective Mach number. It can be stated that the shock/mixing layer interaction reduces the mixing layer

normalized growth rates with increasing compressibility levels. The shock/mixing layer interaction appears as an efficient means to enhance mixing in compressible mixing layers.

The combustion process has been studied by applying planar laser induced OH fluorescence as well as spontaneous OH imaging. With these optical diagnostic techniques it was possible to detect the evolution of the flame zone along the combustion chamber and to characterize the supersonic flame into an ignition zone, a transition zone and fully turbulent zone. The effect of compressibility on organized large-scale structures in the fully turbulent zone of the supersonic mixing layer has been analyzed. Planar imaging techniques afford tremendous improvements in the spatial resolution of large-scale inviscid structures. From the results it can be concluded that application of planar OH fluorescence imaging provides evidence of the existence of these large-scale structures in the compressible mixing layer.

Figures:
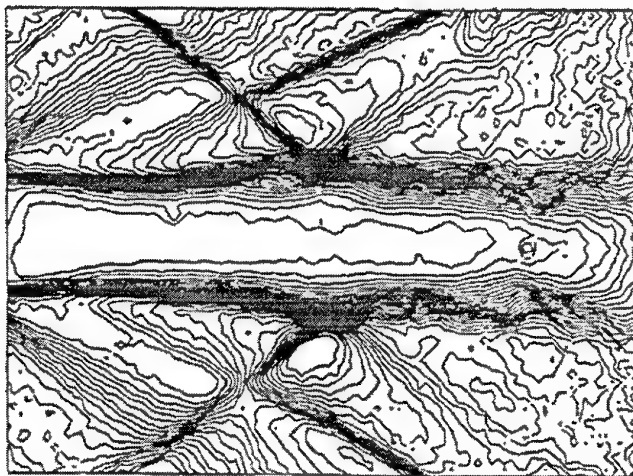
Figure 1:   Total density isoline plot of the mixing layer detected by planar Rayleigh scattering.
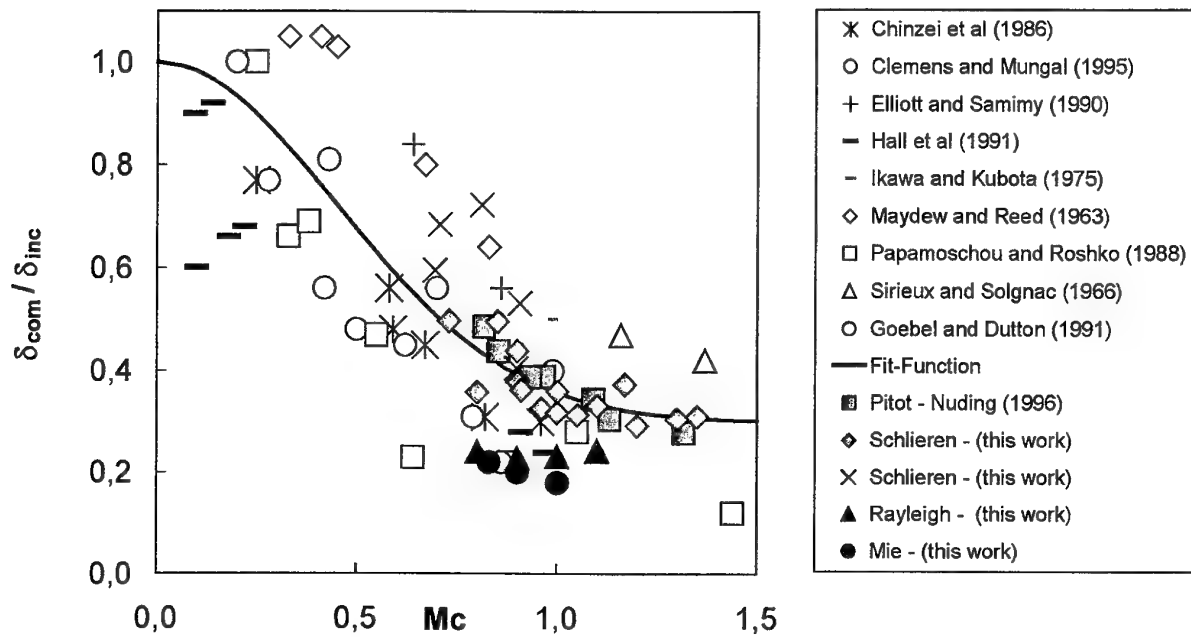
Figure 2: Normalized mixing layer growth rate in dependence of the convective Mach number M_c. Comparison of data from this work with data from literature.

THIS PAGE HAS BEEN DELIBERATELY LEFT BLANK

Spectroscopic Flame Diagnostics by Analyzing NIR Water Bands

W. Eckl, V. Weiser, N. Eisenreich
Fraunhofer-Institut für Chemische Technologie
Joseph-von-Fraunhoferstr. 7
76327 Pfinztal 1 (Berghausen), F.R.G.
Tel: 49 (0)721 4640-156
Fax: 49 (0)721 4640-111
E-mail: vw@ict.fhg.de

Near infrared water bands seem to be ideal for optical flame diagnostics. Nearly every combustion process is producing water. The absorption coefficient in the near infrared is in a range where, on the one side hot emission (e.g. in flames) shows a strong signal, and on the other side cold absorption (e.g. in air) can be neglected in the data analysis.

In the presented work, we investigated the wavelength resolved NIR water band emission of various energetic material flames to test this diagnostic method and to see the application limits.

Working in the near infrared allows the use of simple diode-array-spectrometer systems. We worked with a Zeiss MCS 511, a grating spectrometer with a 256 element InGaAs diode array as detector (spectral range 0.9 to 1.7 micron). The spectral resolution is about 15 nm at a scan rate of 300 spectra per second. The system is equipped with fiber optics.

We applied this system at a premixed hydrocarbon flame, at methane air deflagrations and at the combustion of HMX and CL20 propellant strands. The deflagration and propellant experiments were performed in an optical bomb, a high pressure vessel equipped with two opposite windows (maximum pressure 20 MPa) allowing a non-intrusive process monitoring applying optical flame diagnostics.

The modeling code of the near infrared water band spectra is based on the data published in the 'Handbook of Infrared Radiation from Combustion Gases'. It allows the calculation of the emission and transmission spectra of H_2O in a temperature range from 600 to 3000 K taking into account self absorption, pressure broadening and soot. The calculated intensity distributions are compared to experimental spectra by a least-squares fit routine with the parameter temperature and concentration length. An example for the data analysis is shown in figure 1.
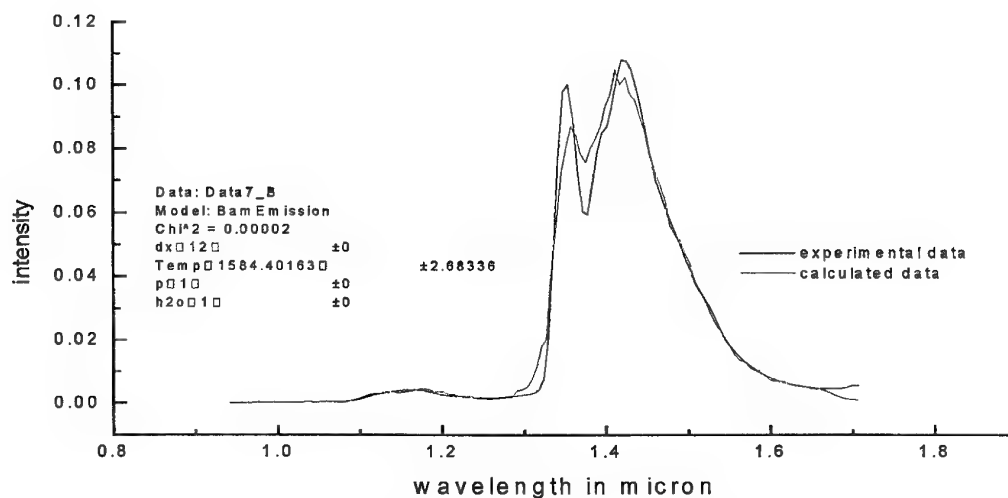
Fig.1: Comparison of an experimental and calculated NIR spectrum of a methane air deflagration

The data analysis showed that this method is suitable for monitoring of energetic material flames. Advantages are the simple experimental setup and the fast data analysis (possible online monitoring of gas temperatures), besides the vibrational temperature and the concentration of water, particle temperatures and concentrations are obtained, which is very useful in the investigation of composite propellants. The determined temperatures were all in the expected range (1500 K for hydrocarbon flames, 2500 for propellant formulations).

Quantitative Measurement of Flame Generated Particulate Oxide by Interferometry Technique

Yu.L. Shoshin, I.S. Altman
Institute of Combustion & Advanced Technologies, Odessa State University, Dvoryanskaya
2, Odessa 65026, Ukraine
E-mail: vov@ictg.intes.odessa.ua

The knowledge of combustion generated particulate matter is of broad practical importance. Ultra-fine particles formed within the flame region can be pollutants, products of combustion synthesis, or the mean source of radiance from flames. The existing non-intrusive methods of particle concentration determination are based on the measurement of particle radiation or on light extinction by particles. However, the radiation based methods are applicable only for optically thin flames. The light extinction methods require the knowledge of the particle size distribution, as light scattering strongly depends on particle size.

In the present work the alternative method of the ultra-fine particle concentration determination is proposed. This method is based on the measurement of the local refractivity within the flame region by interferometry. The contribution of ultra-fine particles into the local refractive index is proportional to their volume fraction. Therefore, this volume fraction can be restored by the measured refractivity.

The specially adjusted Mach-Zehnder interferometer was elaborated for the obtaining of the interferograms of high-emitting and high-scattering flame. Using this interferometer the interferograms of a flame of 1-2.5 mm magnesium particles burning in air were obtained. The 3-D distributions of the oxide volume fraction were calculated by the local refractive indexes restored by the inverse Abel transform. It was determined that ultra-fine oxide in the lower part of the flame is localized within the layer, which is about 50 μm thick. This layer is a distance of twice the initial particle radius from the center of the burning particle. The character value of oxide volume fraction within this layer is about $2.5 \cdot 10^{-3}$. In the upper part of the flame, the oxide smoke first appears on the spherical surface of the same radius.

The mean velocity of natural convection near the burning particle was calculated by the measured ultra-fine oxide volume fraction, initial particle mass and particle burning time. Calculations showed that the mean natural convection velocity is nearly proportional to the initial Mg particle size and changes from 0.16 m/sec for 1 mm Mg particle to 0.40 m/sec for 2.5 mm Mg particle.

As it is known[1], the emissivity of an ultra-fine particle is proportional to its diameter, unlike the constant emissivity of a large particle. Therefore, the basic characteristic of an ultra-fine oxide emitting property is the ratio of the particle emissivity to the particle diameter. This ratio was estimated by the interferometric measurements of ultra-fine oxide volume fraction in the flame region and by the measurements[2] in integral radiation fluxes. It was obtained that this ratio is not less than $2 \cdot 10^{5}$ m^{-1}. From this value, the imaginary part of the dielectric function of ultra-fine magnesia is restored. The obtained value is more than two orders greater than the equilibrium one at the flame temperature. This fact corresponds to the significant excess of electron concentration in a conductive band of magnesia above the

equilibrium concentration. The possible reason of this excess is the excitement of electrons during the condensation process[3].

1. L.D.Landau, E.M.Lifshits. *Electrodynamics of continuous media*. Nauka Moscow, 1982.
2. Yu.L.Shoshin, I.S.Altman. Experimental Study of Radiation Heat Loses During Single Magnesium Particle Combustion, Twenty-Seventh Symposium on Combustion (International), Boulder, USA, August 2-7, 1998. Book of Abstracts, p 256.
3. I.S.Altman. On Heat Transfer During Condensation of the Products of Metal Gas-Phase Combustion. *Fizika Gorenia i Vzryva*, 1998, 34, No. 4, p. 49-51 (in Russian) - translated in *Combustion, Explosion and Shock Waves*.

Spontaneous Radiation Heat Feedback Measurements in Radial Burning Propellant Samples

F. Cozzi, G.S. Tussiwand
Laboratorio di Termofisica, Dipartimento di Energetica
Politecnico di Milano, Milan, MI, Italy
Tel: 39-02-2399.3872
Fax: 39-02-2399.3940
cozzi@clausius.energ.polimi.it

A.L. Ramaswamy
Dept. of Elec. Engineering
University of Maryland, College Park, MD, U.S.A.

The thermal radiation emitted by the solid propellant combustion products is one of the major contributive factors affecting the burning rate scale factor. This is due to the fact that the radiation produced by the combustion products in the strand burners or small-scale motor tests is minimal as compared to that of the large full-scale motors. The objective of the present study is to investigate the effect of the thermal radiation on AP-based composite solid propellants, generated spontaneously from the flame combustion products and/or externally from a laser radiation source.

An experimental technique was developed utilizing micro-calorimeters as thermal radiation sensors, to measure the spontaneous radiant heat feedback flux emitted from the combustion products of small, cylindrical propellant samples. The micro-calorimeters designed are of low cost and easy manufacture. Calibration of the micro-calorimeters was performed to ensure measurement accuracy, since each sensor differs in weight, geometry, and optical interface. Each sensor is calibrated in the experimental set-up test frame, by irradiating it with a known laser power step input from a Nd-Yag laser. The two parameters required to characterize the mathematical response function of the micro-calorimeter are optimally fitted to the calibration data.

During the test, the micro-calorimeter and a video-technique allow the simultaneous measurement of the radiation feedback and burning rate. A closed-loop control system maintains the pressure constant during the combustion. Composite solid propellants were studied over pressure ranges varying from atmospheric to 15 atm. Propellant samples are cylindrical, with an axial hole and a radial burning surface. An ignition charge placed at the bottom of the central axial hole is ignited with a laser beam directed along the axis of the hole. The thermal radiation is measured through a 4 mm diameter lateral hole. The calorimeter's signal is also used to estimate a wavelength averaged optical extinction coefficient in the condensed phase of the tested propellant. The experimental data will also be compared with that obtained using a commercially available thermal radiation sensor.

THIS PAGE HAS BEEN DELIBERATELY LEFT BLANK

Propellant Characterization & Evaluation Using
Low and High Energy Laser Diagnostics

K.J. Fleming, W.J. Andrzejewski, V.M. Loyola, T.A. Broyles
Sandia National Laboratories[7], MS 1454
Explosives Components Facilities
1515 Eubank SE
Albuquerque, New Mexico, 87123
Tel: 505-845-8763
Fax: 505-844-5924
E-mail: kjflemi@sandia.gov

Aged or damaged propellant may hinder the performance, reliability, and safety of rocket motors in the US nuclear stockpile. Diagnosing and identifying suspect propellant, as well as characterizing energetic materials for age-related degradation, is of high importance for stockpile surveillance and lifetime assessments of rocket motors in the stockpile. Sandia National Laboratories' Explosive Components Facility has extensive diagnostic capabilities for analyzing both propellants and explosives.

Propellant ignition using a known, controllable heat source, is a good technique for evaluating the effects of age on a propellant's ignition surface. Unfortunately, heat sources such as hot particle and/or hot gas producers are very difficult to model and to control in a manner consistent with ignition threshold determinations. A new technique currently under development uses material/photonic interactions to accurately evaluate subtle differences in propellants that are aged, or suspected to have changed ignition thresholds. The first series of studies use a frequency doubled Nd:YLF laser operating at up to 6.5 Watts at 532 nanometer wavelength. Also used is a multi-kW Nd:YAG laser capable of delivering multi-Joule energies in less than a millisecond. Properly characterized, the laser is a good thermal source that is much easier to model than electrical igniters. The first propellant under investigation is used in the B61 Spin Rocket Motor. In the experimental evaluation, the attenuated laser beam is directed onto the propellant and reflectance/absorption measurements are taken for Joule delivery calculations. Then, the full power of the laser is allowed to interact with the propellant material until there is a sustained ignition in an unconfined condition. Several diagnostic/calibration measurements are recorded both before, during, and after ignition has occurred which is important in calibrating true energy delivery. Understanding the true absorption coefficients of the material for a given laser wavelength, as well as several other factors is important for accurate evaluation of the subtle differences in propellants. The propellant is characterized in both confined and unconfined configurations. The presentation will cover photonic/propellant interactions, absorption characteristics, diagnostic and modeling data, as well as ignition thresholds for the B61 propellant. This presentation will be Unclassified, Unlimited Distribution.

THIS PAGE HAS BEEN DELIBERATELY LEFT BLANK

On a Method for Measuring Non-Stationary Burning Velocity in Condensed Systems Based on Interferometric Measurements

S.V. Ilyin, O.S. Danilov
Department of Physics of Heat, Chuvash State University Moskovsky pr. 15
Cheboksary 428015, Russia
Telephone: (78352) 498352, Fax: (7-8352) 428090, E-mail: S.V. Ilyin

Condensed-system combustion is described in terms of gas-dynamic parameters, such as mass burning velocity, specific impulse, and specific thrust. Their determination presents an experimental challenge, especially in non-stationary combustion.

The authors of [1] came up with a method for the determination of those parameters using the results of a quantitative study of the dynamics of variations in interference patterns obtained from interference motion pictures taken using standard techniques. It was revealed that the method could be successfully applied to the investigation into the initial ignition stage by allowing the mass burning velocity, the reactive impulse, and the reactive thrust produced by the burnt gases to be determined. The subsequent development of the data processing technique for interferometric measurements revealed that a similar technique could be proposed to quantitatively investigate, with a sufficiently great time resolution, the response of the mass burning velocity to external disturbances produced by a steadily burning condensed system. In brief, the principle of the approach is as follows: The mass variation rate and the impulse of a non-stationary burnt gases flow section bounded by two planes are determined by the methods proposed in [1] based on interferometric measurements. The data allow, with certain commonly accepted assumptions (flow quasi-homogeneity, isobaric nature of the exhaust jet), the mass burning velocity to be calculated. The method in question offers obvious advantages over existing ones such as high time resolution and substantial immunity to external disturbances. Limitations of the method include those typical of interferometric methods.

The present paper presents both the findings of experimental research, using those methods, into the initial ignition stage for certain model condensed systems by laser radiation, and those of research into the response of the mass burning velocity to laser radiation shut-down. It also presents a description of the experimental findings as compared to those obtained by other research teams.

1. Abrukov, V.S., Ilyin, S.V. 1991 Analysis of the dynamics of non-stationary gas streams using interferometric techniques. Proceedings of Int. Symposium of Optical Applied and Engineering/ U.S.A., San Diego, pp. 540-543.

THIS PAGE HAS BEEN DELIBERATELY LEFT BLANK

Nonsteady Solid Propellant Regression Rate
Measurements by a Plane Capacitor Method

U. Carretta, R. Dondé, C. Guarnieri
Consiglio Nazionale delle Ricerche
Istituto per la Tecnologia dei Materiali e dei Processi Energetici
20125 Milan, Italy
Tel: (39 02) 66173-334; Fax: (39 02) 66173-334 or 321
E-mail: caretta@tempe.mi.cnr.it

A simple electrostatic method and a few representative experimental results obtained during the steady combustion below or at atmospheric pressure of composite propellants have been discussed in a previous work [1]. The conclusions arising from this first investigation were:

a) for non-metallized propellants, the method seems to achieve the goal, although a large amount of experimental work is required to definitely assess its reliability at higher pressures, especially under unsteady regimes;

b) for metallized propellants, the capacitor method is unable to detect the regression of the burning surface due to the exceedingly high conductivity of the flame with respect to the working frequency; the method is for use only as a very sensitive detector in go/no-go experiments or for monitoring the onset of gross instabilities inside the gaseous portion of the flame.

The present work presents and discusses some experimental results concerned with non-metallized composite propellants burning under: a) steady operations above atmospheric pressure; b) fast-depressurization transient regimes;

The guidelines for the present investigation are the following:

1. The higher the pressure, the lower the contribution should be of the flame conductivity affecting the measured real part ReC of the total capacitance. In fact, in a very simple theoretical model, a Lorentzian shape for the ionization space profile along the flame (see Fig. 1) (where ω_{pm} is the maximum value of the total plasma frequency, i.e. the value

$$\omega_p^2(x,t) = \frac{\omega_{pm}^2(t)}{1+\left(\dfrac{x-a(t)-s(t)}{\gamma(t)}\right)^2} \tag{1}$$

corresponding to the maximum of the volume density of the charge-carrier populations) suggests that in collisional regimes the flame contribution to ReC is proportional to the conductivity parameter $\dfrac{\omega_{pm}^2}{\omega_M \bar{v}_c}$, were ω_M is the working frequency (rad s^{-1}) and $\bar{v}_c$ (s^{-1}) is an average collision frequency.

F Fig. 1
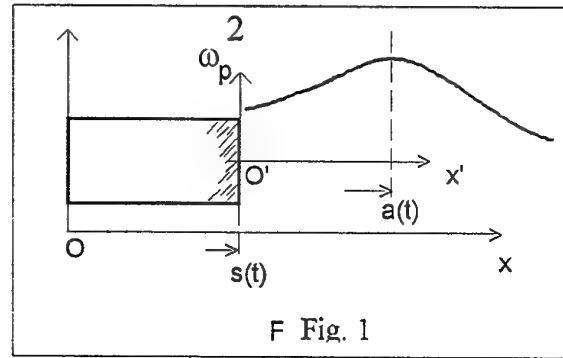
According to this model, the effects of the flame on ReC for $\dfrac{\omega_{pm}^2}{\omega_M \overline{v}_c} = 10$ are sketched in Fig. 2, where $C_2 = \text{Im}C$ is also shown. This run is related to p = 90 mbar and $v_M = 9\,\text{MHz}$.
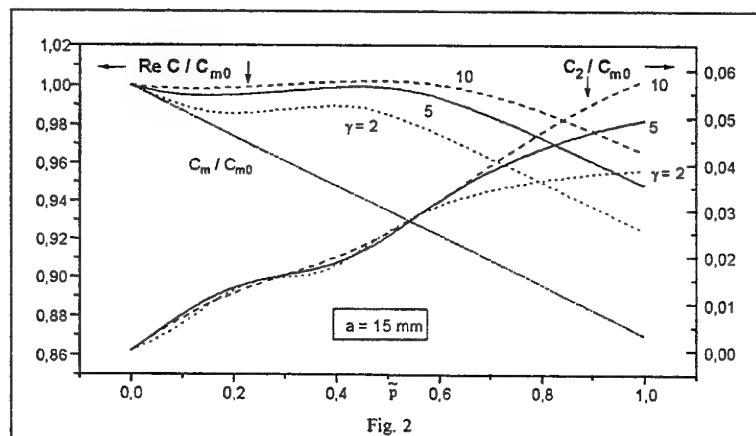
Fig. 2

In Fig. 2, C_{m0} is the starting value of the capacitance (i.e. in the 'ready to go' situation); C_m is the capacitance value of the residual solid strand of initial length L; $\tilde{p}$ is the penetration of the burning surface into the capacitor: $\tilde{p} = 1 - s/L$, a=15 mm and γ = 2, 5 and 10 (mm) are time-independent quantities. According to the expression of the conductivity parameter, an increase of the working frequency quenches the flame contribution to ReC, as demonstrated by the data collected at p ≤ 1 bar by the existing prototype (which now operates at $v_M = 14.5\,\text{MHz}$). Thus, the same should happen at higher pressures when $\overline{v}_c$ increases, but if things are so, it is also clear that fast depressurization transients could affect the response of the measuring system according to the flame behavior.

2. The regression rate r influences the precision of the measurement (see Fig. 3) where $\left|\Delta t\right|_M$ is the time interval between two successive measurements. This figure characterizes the measuring system and shows that, for a given $\left|\Delta t\right|_M$, an increase of r

results in a better precision. Thus, high-pressure regimes should be more favorable for this technique.

For comparison, the relative mean square error $\frac{\sigma_r}{r}$ from usual video camera recordings is $\approx 5\,\%$ in steady regimes.
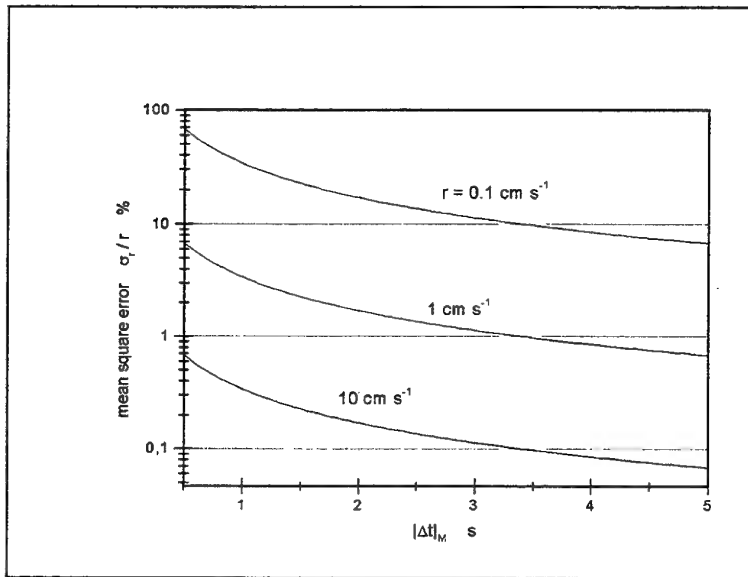
Fig. 3

It must be pointed out that, according to the achieved capacitance resolving-power of the system, there exists a minimum value $\left|\Delta t\right|_{min}$ for $\left|\Delta t\right|_{M}$, i. e., it must be $\left|\Delta t\right|_{M} \geq \left|\Delta t\right|_{min}$ in order to obtain meaningful measurements. This behavior corresponds to a minimum detectable length $\left|\Delta h\right|_{min} \approx 340\,\mu m$.

References
[1] Carretta, U., Dondè, R., Guarnieri, C., "Scope of Capacitive Methods in Solid Propellant Diagnostics", under press on AIAA-JPP, Vol. 15, No. 6, pp. 849-855, Nov - Dec 1999.

THIS PAGE HAS BEEN DELIBERATELY LEFT BLANK

AREA 10:

PROPELLANT AND MOTOR STABILITY
-
ABLATION

T-Burner Response Analysis Using the SPP/SSP Code

F.S. Blomshield
Naval Air Warfare Center
Code 4T4320D, Propulsion Research Branch
China Lake, CA 93555
Tel: (760) 939-3650
Fax: (760) 939-6569
E-mail: blomshieldf@navair.navy.mil

D.E. Coats, S.S. Dunn and J.C. French
Software and Engineering Associates
1802 North Carson Street, Suite 200
Carson City, NV 89701

This paper presents the results of a study to compare the stability results of the SPP/SSP code to actual T-Burner experimental data. The SPP/SSP code is the standard solid rocket motor performance program coupled to the Standard Stability Program. Four unique propellants were compared. Two were reduced smoke and two were metallized propellants. Pressure coupled response data was already available for these propellants. This experimental data was evaluated by the T-burner. For the metallized propellants, aluminum oxide particle analysis was also previously performed on the combustion products. The stability analysis was performed using the three-dimensional grain design and ballistic modules and the one dimensional stability module. Types of driving and damping mechanisms included in the analysis included pressure coupling, wall damping and for the metallized propellants, particle damping. The total predicted stability was then compared against the decay and/or growth measured in the T-Burner during a test. The results were surprising in that both the magnitude and trends in the analysis were verified by the data.

THIS PAGE HAS BEEN DELIBERATELY LEFT BLANK

Some Effects of Pressure Coupling and Velocity Coupling on the Global Dynamics of Combustion Chambers

F.E.C. Culick and G. Isella
Mechanical Engineering and Jet Propulsion
California Institute of Technology
Pasadena, CA 91125
Tel: (626) 395-4783
Fax: 1-626-395-8469
E-mail: fecfly@caltech.edu

Considerable data exists suggesting that the response functions for many solid propellants tend to have higher values, in some ranges of frequencies, than predicted by the conventional QSHOD theory. Recent theoretical work and simulations, including also a model for the surface dynamics, show that a combustion response function based on simple pressure coupling is not enough to explain the characteristics of the instability observed experimentally. Namely, differences in the shape of the response function fail to reproduce the differences observed experimentally in the characteristics of the limit cycle reached by propellants of different chemical (or physical) composition. On the other hand, velocity coupling in the combustion response seems a promising mechanism able to predict the changes in the unstable modes observed experimentally and to produce considerable effect on the shape of the resulting limit cycle. The Baum and Levine model is used as a starting point in the investigation of velocity coupling. Other models, in which the mass burning rate is modified by some function of the velocity, are also investigated through direct time-simulation and by the use of a continuation method. Response functions are shown for realistic ranges of the chief parameters characterizing the dynamics of the propellant. The results are also incorporated in the dynamical analysis of a small rocket motor to illustrate the consequences of the combustion dynamics for the stability and nonlinear behavior of unsteady motions in a motor.

THIS PAGE HAS BEEN DELIBERATELY LEFT BLANK

Radiation-Driven Burning of Energetic Solid Materials
With Phase Transition

F. Cozzi, L.T. DeLuca
Laboratorio di Termofisica, Dipartimento di Energetica
Politecnico di Milano, 20133 Milan, Italy
Telephone: +39-02-2399-3872; Fax: +39-02-2399-3940; E-mail:
cozzi@clausius.energ.polimi.it

B. V. Novozhilov
Institute of Chemical Physics, Russian Academy of Science, Moscow, Russia

Solid-propellant burning assisted by external radiation is an area of interest for both practical applications and fundamental knowledge. An extension of the Zeldovich - Novozhilov (ZN) approach to burning of energetic solid materials subjected to a concentrated phase transition is presented. The objective of this paper is to determine the frequency response function, including in-depth phase transition effects, for the linear approximation of radiation-driven burning. The corresponding problem for pressure-driven burning within the ZN framework was recently published [1]. For both problems, connections with the equivalent Flame Modeling (FM) formulation are discussed. Both approaches, ZN and FM, share the basic assumptions of Quasi-Steady gas phase, Homogeneous condensed phase, and One-Dimensional burning strand (QSHOD framework). The steady burning sensitivity parameters depending on initial temperature, r and k, are deduced by assuming a surface pyrolysis law. With respect to pressure-driven burning, two more parameters come into play. Both ZN and FM (distributed flames) formulations were deduced and shown to be fully equivalent in terms of the classical A and B parameters. Some typical results, with and without radiation penetration, are presented. The corresponding previous results for no-phase transition are recovered as a particular case. To validate these theoretical expectations, accurate error estimates of experimental data are needed.

References
[1] Cozzi F., DeLuca L.T., Novozhilov B.V., "Linear Stability and Pressure-Driven Response Function of Solid Propellants with Phase Transition", under press on AIAA-JPP, Vol. 15, No. 6, pp. 806-815, Nov – Dec 1999.

THIS PAGE HAS BEEN DELIBERATELY LEFT BLANK

On Stability of the Combustion of Ammonium Perchlorate

V.N. Marshakov, G.V. Melik-Gaykazov, A.G. Istratov
Semenov Institute of Chemical Physics, Russian Academy of Sciences
Kosygin St. 4, Moscow, Russia, 117977
Tel: (095) 137-4529
Fax: (095) 938-2156
E-mail: marsh@center.chph.ras.ru

The multidimensional front of combustion of the ammonium percolate (PA) as a representative of the class of unitary homogeneous explosive compounds is investigated. The experiments were performed under the pressure of 25-100 atm when the combustion of PA is conventionally considered to be stable. The combustion surface of the samples extinguished by 3 different methods is analysed. The first method is fast decreasing of the pressure, the second is via injection of the cooler onto the surface of combustion and the third is extinguishing of the samples near critical diameter of combustion at different pressures. It is demonstrated that the combustion surface consists of a set of separated "hot spots", and their size is not related to the dispersity of initial fraction of PA and varies approximately from 1mm till some saturated value depending on the pressure. For example, when the pressure is 30 atm then the maximum diameter of a hot spot is about 7mm, for 60 atm it is 5mm, and for 80 atm it is 4mm. The depth of the hot spots varies from tenth to hundredth parts of millimeter. The critical diameter of combustion is measured, it is defined as a critical (minimal) width of a rectangle sample. It varies from 16 to 7 mm in the scope of pressures from 30 till 80 atm. The registration of electric conductivity of the surface fibre and local luminosity shows existence of three different types of pulsations which characteristic times 180, 80 and 25 msec at 30 atm, and 100, 40 and 15 msec at 80 atm respectively.

The registered multidimensional structures in the burning wave demonstrate thermal instability of the burning wave.

The theoretical model of condensed compounds, taking into account the "hot spot" structure of the front of combustion is proposed and analysed. It is based on already existing in conventional theory of combustion ideas about instability of the flat structure of the front of combustion and possibility of arising of the waves of fast combustion (hot spots), propagating along the heated fibre in the direction transversal to the main direction of combustion. As a result, the model describes the sequence of transversal waves giving rise to the front of combustion of the form of several "steps." The parameters of these steps, dependence of their values on the physical background and macroscopic speed of the combustion are determined. The comparison of the theoretical results with the experimental measurements demonstrates that the geometrical parameters of inhomogeneties on the surface of combustion, their relations to each other, periods of fluctuations of electric conductivity and temperatures inside the combustion wave can be described from unique point of view within the proposed theoretical model, i.e. the model is satisfactory.

THIS PAGE HAS BEEN DELIBERATELY LEFT BLANK

Surface Spin Combustion in Gas-Solid System

I.A. Filimonov
Institute of Structural Macrokinetics and Materials Science RAS
Chernogolovka 142432, Russia
Tel: (7-09652) 48564; Fax: (7-095) 9628025;
E-mail: fil@ism.ac.ru

N.I. Kidin
Institute for Problems in Mechanics RAS
Vernadsky pr.101, Moscow, 117526, Russia

A.S. Mukasyan
Department of Chemical Engineering, University of Notre Dame
Notre Dame, IN 46556, USA

Mathematical model of surface spin combustion in a binary non-catalytic gas-solid system under approximation of the quasi-homogeneity of reactant porous media (i.e. low Semenov number, $Se \ll 1$) has been developed. The model takes into account the gas infiltration, kinetics of heterogeneous chemical reaction between condensed and gas phases, as well as difference in their temperatures.

The effects of infiltration parameters and reactant gas pressure on characteristics of spin combustion mode have been studied. It was shown that, depending on value of the infiltration Peclet number, two different regimes of the spin propagation can be realized: thermal $(Pe \gg 1)$ and infiltration $(Pe \propto 1)$.

In the early theoretical models, as well as in phenomenological theory, spin combustion is considered as a manifestation of two-dimensional *thermal instability* of the plane combustion front. This understanding of spin nature has determined methods for its further investigations. In a variety of studies related to combustion, wave stability, by using different approaches of the linear analysis or the bifurcation theory spin, was considered as a specific *small perturbation* (so-called *weak* spin) of plane steady-state combustion front. The obtained results describe well some qualitative features of observed phenomena, which are mainly related to the process of spin formation and forms of its manifestation. However, these models cannot explain some important experimental observations, for example, why hot spot (which, is treated as small perturbation) moves much faster (more than 10 times) along the front (in circumferential direction), as compared to front propagation in longitudinal direction.

Recently, a new approach has been proposed in which spin is considered as the *strongly developed* nonlinear phenomenon, which occurs far from the stability limit of steady-state mode. Further, this model was enhanced by taking into account more accurate thermal fluxes from the head of the spin and temperature distribution in the system. Also, stability of the obtained solutions was investigated. Although this approach does not allow us to study the process of spin formation, the obtained results on relations between combustion velocities in spin mode and the limits of its existence are in good agreements with experimental results.

On the other hand, the most experimental data on spin combustion available in literature are related to *gas-solid systems*, such as Ti-N, Hf-N, Zr-N. It was shown that the reactant gas pressure and porosity of a reaction media influence the characteristics of spin mode and define the regions of its existence. However, neither of the approaches based on evolution of spin as small perturbations of planar combustion front, nor strongly developed spin model, reflect any features related to the *infiltration* character of these processes. It is believed that spin has essentially thermal nature and appears when the heat of reaction is insufficient to support stable planar motion.

The goal of our present work is, by using general approach of strongly developed spin theory, to take into account and study the effects of gas pressure and its infiltration in the porous reaction media on characteristics of spin combustion in gas-solid system.

Degradation of a Thermal Insulator Under Vibration and Acceleration

A. Eythrib, F. Cauty
ONERA - Centre de Palaiseau
Chemin de la Hunière , F 91761 Palaiseau Cedex, France
Tel: 33-1-69-93-60-37
Fax: 33-1-69-93-61-62
E-mail: cauty@onera.fr

G. Colombo, A. Menalli, L. Galfetti
Laboratorio di Termofisica, Dipartimento di Energetica
Politecnico di Milano - Campus Bovisa, 20158 Milan, Italy
Tel: +39-02-2399-8526
Fax: +39-02-2399-8566
E-mail: galfetti@clausius.energ.polimi.it

The external and internal thermal insulators have been widely studied for decades. The knowledge of their degradation process is of a high interest for their sizing and thus for the safety margins. Here, the purpose is to have a first approach of the flight condition effect on the char behavior. Flight condition means the vibration and the acceleration. This work has been done in cooperation between the Politecnico di Milano (Italian University Lab) and ONERA (French National Organization).

Usually the charring material degradation can be split into three different phases depending upon the mechanical load level. The first phase is the pure pyrolysis phase: the char remains on the material surface (regime 1). This is a non-stationary regime, thermally speaking. Then, increasing the mechanical load, i.e. the wall shear stress due to the core flow, the char is ejected layer by layer (regime 2). This is a periodical thermal regime. Finally, at a high flow rate, the char is ejected as soon as created on the surface (regime 3). In that case, a stationary thermal regime is established very quickly.

The basic hypothesis is that the vibration frequency and the acceleration have the same effect as the wall shear stress. Depending on the heat flux level, by modifying the vibration frequency, the ejection will start, then the char ejection regime will move through the regime 2 up to the regime 3. At a low heat flux, only the regime 2 could be reached.

The tests have been performed at the Dipartimento di Energetica, Politecnico di Milano. The setup is composed of a closed vessel purged by nitrogen gas avoiding extra burning of the degradation gases at atmospheric pressure (Figure 1). The charring material is degraded by the heat flux coming from a CO_2 laser. The sample holder is screwed on the bar of a vibrator which is mounted outside on the head end of the vessel. The frequency of vibration is monitored and the acceleration is deduced from the weight of the sample and the sample holder via the calibration diagram of the vibrator.

The closed bomb is equipped with three windows: one for the 10.6 µm laser beam (ZnSe), one for a video camera and the third window for a photodiode. This photodiode is aiming at measuring the char ejection. The result is correlated with the video images.

The recorded video images show the ejection of the residue and permit to estimate the size of the ejected char. The photodiode trace corresponds to the light variation on the sample surface seen by the photodiode. The analysis of the photodiode trace is based on the frequency of the char ejection. Using a classical FFT code, frequency peaks appear but the main difficulty is to separate the basic frequency and the harmonic values which correspond to the parts of the same broken char layer ejected at delayed times (Figure 2).

Under vibration, the char ejection process is related to the size of the char confirming the hypothesis. One obtains three regimes with frequency: the frontiers depend on the heat flux value. Taking into account the pyrolysis rate, the results seem to indicate that there is a thickness value for the char layer, as well for the entire char layer as for the broken parts. As expected, the vibration acts by breaking the char layer. By changing the heat flux, the transition frequencies are shifted, the ejection frequencies move a little bit but the estimated thickness of the residue layer seems to be quasi constant regarding the accuracy of the measurements.

Acknowledgments
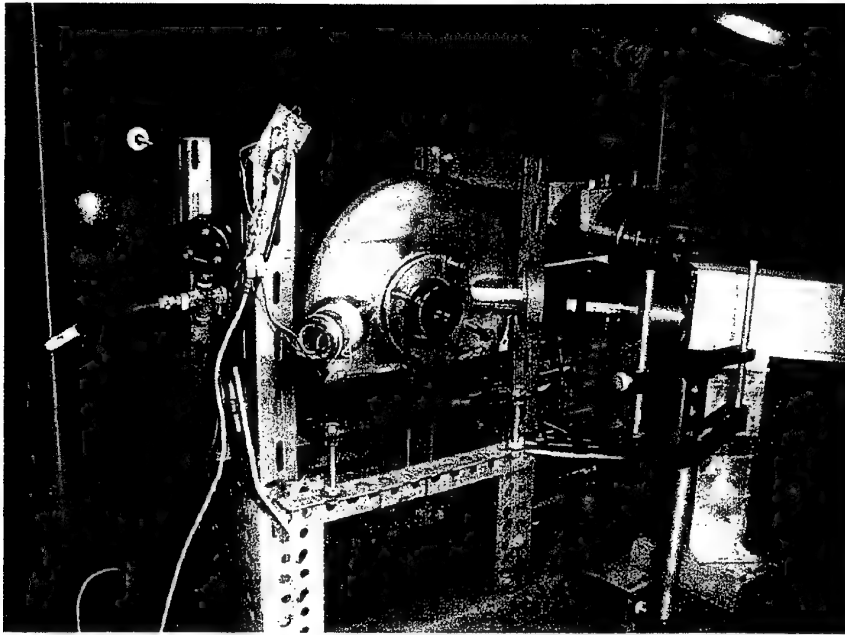
Front View of the vessel with windows
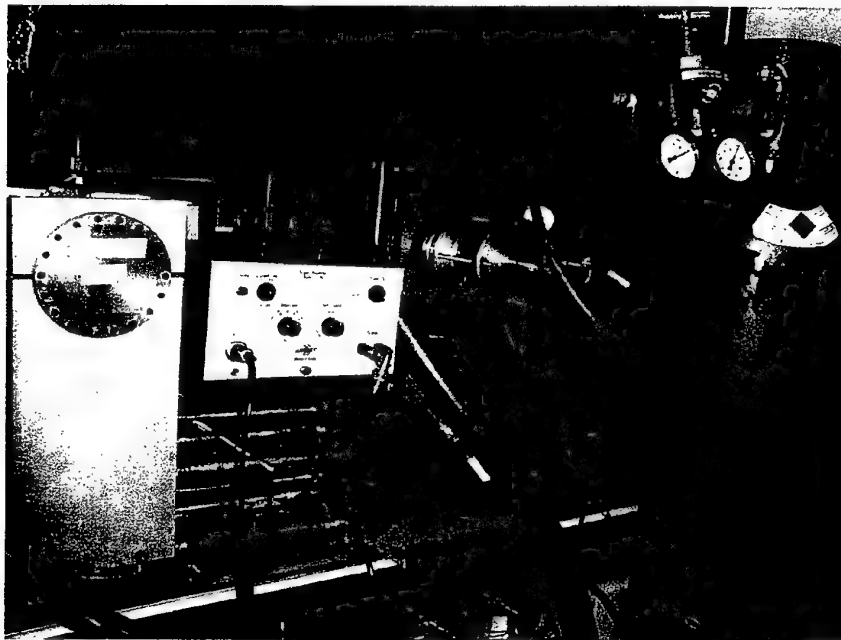
Backside with vibrator

Figure 1 – Experimental setup

Photodiode signal (zoom)
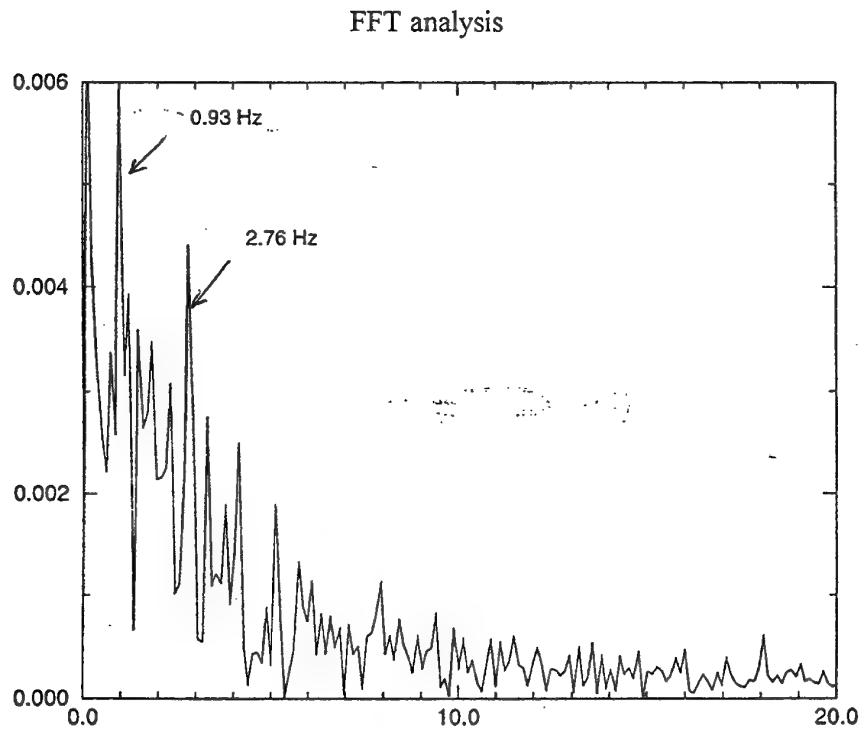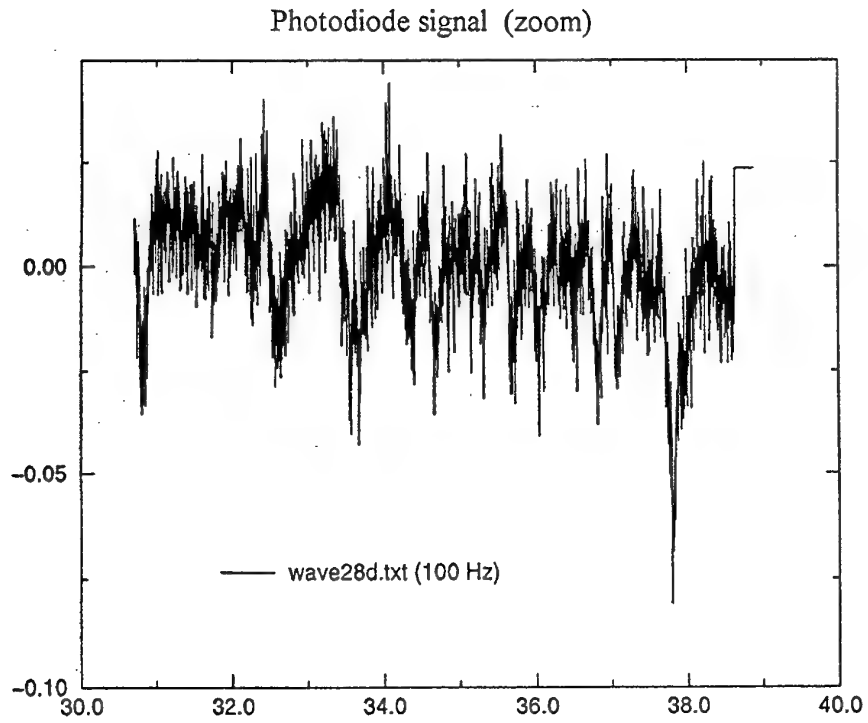
FFT analysis

Figure 2 - Example of ejection frequency analysis.

Thermal Protection Wall-Effect on the
Combustion of Solid Propellant at Subatmospheric Pressure

C. Zanotti, P. Giuliani, M.Turco
TEMPE-C.N.R
via Cozzi 53
20125 Milano (Italy)
Telephone: ++39-02-66173.310, Fax: ++39-02-66173.307
E-mail: Zanotti@tempe.mi.cnr.it

M. Kohno
Institute of Space and Astronautical Science
Sagamihara (Japan)

The solid rocket motors for high altitude applications operate under external vacuum conditions. During their life, the inner motor pressure can reach values which are lower than the measured Pressure Deflagration Limit (PDL) in laboratory tests. Although this condition should not allow any combustion process to have unexpected amounts of gas generated inside the motor, a small residual thrust is still active. The motor's operating time becomes longer than the estimated time, and therefore this occurrence cannot be neglected in the motor design. The thermal insulator degradation, coupled to the propellant combustion or high temperature decomposition at pressures below the PDL, can be the main causes of this unpredicted motor performance. For those reasons, an experimental study aimed to analyze the wall-effect due to the thermal protection presence in contact with the burning propellant, has been carried out in order to find out which parameters are more sensible to this operating configuration.

Results have demonstrated that the average propellant temperature increases when the burning surface approaches the thermal insulator because of the large value of the thermal wave thickness, especially when metallized propellants are used. Moreover, the radiant energy scattered by the inner part of the nozzle, or by the exposed thermal protection, is another possible cause that yields the propellant to burn, or gasify, below PDL. To verify this possibility, the degradation behavior of the thermal protections and the combustion of graphite have been considered. Results indicate that the energy amount emitted by these hot materials is enough to modify the propellant combustion process below PDL.

On the basis of these considerations, data has been collected using a non-metallized composite propellant to define the influence of the radiant energy on the combustion process above and below the PDL. The obtained results have pointed out that the tested propellant can be ignited, and the combustion process sustained at pressures much lower than the PDL value, if the operating conditions are properly chosen. Experimental tests have been carried out, using a metallized composite propellant for pressure lower than 30 kPa, to evaluate the PDL dependence on the operating conditions, and the effect of the thermal insulator presence on the combustion process. Simultaneous measurements of the burning surface position, and temperature history at the interface propellant/thermal insulator, have permitted us to estimate the propellant burning rate dependence on time.

Results pointed out that if the operating conditions are close to the PDL, the burning rate value increases with the diminution of the propellant burning surface distance from the interface propellant/thermal insulator. The data of this work has been collected, having recourse to a CO_2 laser system used as external energy source, and the following diagnostic techniques have been implemented:

- micro-thermocouples to measure the surface and internal temperatures;
- micro-load cell to measure the propellant weight changes;
- laser doppler anemometry to evaluate the gas velocity;
- TV camera systems to observe the phenomena under study, and to evaluate the steady burning rate.

Macrokinetic Characterization of Ablative Materials

A.A. Zenin
Institute of Chemical Physics, Russian Academy of Sciences, Moscow, Russia

L. Galfetti, A. Menalli
Laboratorio di Termofisica, Dipartimento di Energetica
Politecnico di Milano - Campus Bovisa, 20158 Milan, Italy
Tel: +39-02-2399-8526
Fax: +39-02-2399-8566
E-mail: galfetti@clausius.energ.polimi.it

Ablative thermal protection systems (TPS) are usually employed to protect hypersonic vehicles during atmospheric re-entry (heat shields) and in rocket motors to control the intensity of the aerothermal heat load. A knowledge of the characteristics of the ablation materials and of the degradation properties is of primary interest for the design and the sizing of ablating TPS. The complex decomposition mechanisms to be used in order to formulate exact analytical expressions are not generally known; therefore empirical kinetics has to be used. Kinetic constants for thermal decomposition are usually derived from thermogravimetric analysis, where the heating rate is in the range 273 - 300 K/min, while under real ablative conditions, the heating rate is in the range 5000 - 50000 K/min. For these reasons, a new diagnostic technique has been implemented.

Thermal response and degradation processes occurring in different polymer composite materials are investigated in order to measure the steady ablation rate and to determine the macrokinetic constants (activation energy, pre-exponential factor), which characterize the overall degradation. Experimental data are obtained measuring temperature profiles by means of microthermocouples put inside the material and at the heated surface. To heat the sample, a CO_2 laser beam, normally impinging on the cross section of the sample, is used. The trend of the surface temperature allows to check the pyrolysis initiation, while the in-depth temperature profiles allow to measure the steady ablation rate. The knowledge of these parameters allows a procedure to determine the macrokinetic constants.

To validate the technique, the ablation of polytetrafluoroethylene is studied, because of the fact that the physical properties of this material are fairly well known. Results are compared with those available in the literature and a critical discussion is offered.

THIS PAGE HAS BEEN DELIBERATELY LEFT BLANK

Analysis of Vorticity Effects in Oscillatory Flow Fields of Simulated Solid Propellant Rocket Motors

R. S. Brown
486 Birch Way
Santa Clara, CA 95051
Tel: (408) 248-8522
E-mail: bbbluefoot@aol.com

A number of experimental studies have been conducted to simulate the steady state and oscillatory flow fields in solid propellant rocket motors[1,2,3]. Using nitrogen flowing through porous walls to simulate the gas flow from the burning solid propellant surface, these studies have clearly established the rotational inviscid characteristics of these flows in cylindrical port geometries. For the steady state, analytical and finite element models predict much of the observed velocity profile behavior with reasonable accuracy[4,5,6]. Current limitations in these predictive methods include the failure to predict swirl and body force(buoyancy) effects within the first three diameters of the head-end of the combustion chamber.

For the oscillatory flows associated with combustion instability, current analytical and numerical models have been less successful and continue to be studied and developed[7,8,9]. A major focus of these studies has been predicting the contributions of both the oscillatory and steady state vorticity to the overall acoustic energy balance and the associated acoustic stability of the chamber. These contributions are substantial compared to other acoustic energy gains and losses and therefore reliable engineering models of these contributions are still needed to improve the accuracy of motor combustion stability prediction.

This paper will describe an effort to model these oscillatory flow fields using an expanded power series approach. It is believed this approach, which is currently under development, will eliminate some of the current limitations and apparent inconsistencies which are manifested in other modeling approaches. The specific objectives of the current study are to compare predicted and observed oscillatory velocity profiles, to predict the impact of vorticity on the acoustic stability (i.e., flow turning), and to show how oscillatory flows can influence the pressure-coupled combustion response function. The paper will describe an improved formulation of the multi-dimensional stability model, describe the oscillatory flow field model, compare predicted and observed oscillatory velocity profiles, describe a connection between the oscillatory flow and the pressure coupled combustion response, and discuss the limitations and difficulties with other modeling efforts.

REFERENCES

[1] Dunlap, R., et. al., "Internal Flow field Studies in a Simulated Cylindrical Port Rocket Chamber", J. Propulsion & Power, Vol. 6, No. 6, pp. 690-704, (1990).

[2] Brown, R.S., et. al., "Coupling Between Acoustic Velocity Oscillations and Solid-Propellant Combustion", J. Propulsion & Power, Vol. 2, No. 4, pp. 345-353, (1986).

[3] Brown, R.S., "Coupling Between Velocity Oscillations and Solid Propellant Combustion", AIAA Preprint No. 86-0531, (1986).

[4] Culick, F.E.C., "Rotational Axisymetric Mean Flow and Damping of Acoustic Waves in a Solid-Propellant Rocket", AIAA Journal, Vol. 4, No. 8, pp. 1462-1463, (1966).

[5] Beddini, R.A., "Aerothermochemistry Analysis of Erosive Burning in a Laboratory Solid-Rocket Motor", AIAA Journal, Vol. 18, No. 11, pp. 1346-1353, (1980).

[6]   Sabnis, J.S., et. al., "Navier-Stokes Analysis of Solid-Propellant Rocket Motor Internal Flows", J. Propulsion & Power, Vol. 5, No. 6, pp. 657-664, (1989).

[7]   Flandro, G.A., "Effect of Vorticity on Rocket Combustion Stability", J. Propulsion & Power, Vol. 11, No. 4, p. 607-625, (1995).

[8]   Majdalani, J., et. al., "Improved Time-Dependent Flowfield Solution for Solid Rocket Motors", AIAA Journal, Vol. 36, No. 2, pp. 241-248, (1998).

[9]   Majdalani, J., et. al., "Implications of Unsteady Analytical Flowfields on Rocket Combustion Stability", AIAA Preprint 98-3698, (1998).

AUTHOR INDEX

C

Egorshev, V.Y.	Azalea / 7a-oral	133
	Azalea / 7-poster	317
Eisenreich, N.	Azalea / 7c-oral	143
	Azalea / 9-poster	353
Elban, W.L.	Azalea / 5-poster	289
Ellison, D.	Azzurra / 1-oral	35
Engelen, K.	Azzurra / 2b-oral	51
Eythrib, A.	Azalea / 10-poster	377

F

Fabignon, Y.	Azalea / 8-oral	159
Fabrizi, A.	Plenary Paper	15
Fedotova, T.D.	Azzurra / 6-oral	97
Feldman, I.	Azalea / 5-poster	297
Filatov, S.A.	Azalea / 7-poster	319
Filimonov, I.A.	Azalea / 10-poster	375
Filippi, M.	Azalea / 7-poster	311
Finjakov, S.V.	Azalea / 10a-oral	183
Finlinson, J.C.	Azalea / 10a-oral	185
Fiorentino, G.	Azalea / 10b-oral	213
Fisher, M.	Azalea / 4-poster	277
Fischer, T.	Azalea / 7c-oral	143
Fleming, K.J.	Azalea / 9-poster	359
Fogelzang, A.E.	Azalea / 7a-oral	133
	Azalea / 7-poster	317
Forbes, J.W.	Azzurra / 2-poster	235
Forster, J.	Azalea / 3-poster	255
French, J.C.	Azalea / 10-poster	367
Fuimori, T.	Azzurra / 5b-oral	117

G

Gadiot, G.M.H.J.L.	Azalea / 7b-oral	137
Galfetti, L.	Azzurra / 5b-oral	121
	Azalea / 8-poster	329
	Azalea / 10-poster	377
	Azalea / 10-poster	383
Gany, A.	Azzurra / 6-oral	91
	Azzurra / 5b-oral	119
	Azalea / 3-poster	261
	Azalea / 5-poster	297
Gao, B.	Azalea / 3-poster	257
Gieras, M.	Azzurra / 2b-oral	49
Giuliani, P.	Azalea / 4-poster	287
	Azalea / 10-poster	381
Glick, R.L.	Azalea / 10b-oral	213
	Azalea / 3-poster	249
	Azalea / 3-poster	251
Glotov, O.G.	Azzurra / 6-oral	97
Godon, J.C.	Azzurra / 3-oral	53

Gögüs, Y.	Azalea / 8-poster	333
Gori, F.	Azalea / 8-poster	327
Gotzmer, C.	Azalea / 6-poster	309
Gray, W.	Azzurra / 1-oral	37
Green, L.	Azzurra / 2-poster	235
Grune, D.	Azzurra / 4a-oral	81
Guarnieri, C.	Azalea / 9-poster	363

H

Haas, J.	Azalea / 6-poster	305
Hansel, J.G.	Azzurra / 6-oral	93
Harting, G.C.	Azzurra / 3-oral	57
	Azzurra / 4a-oral	79
	Azalea / 7-poster	315
Harvel, J.R.	Azalea / 4-poster	275
Hasegawa, S.	Azzurra / 5b-oral	117
He, G.	Azzurra / 5a-oral	105, 109
	Azalea / 5-poster	291
Heiser, R.	Azalea / 7c-oral	145
Henson, B.F.	Azzurra / 1-oral	31
Hessler, R.O.	Azalea / 9-oral	191
	Azalea / 10b-oral	213
	Azalea / 3-poster	249
	Azalea / 3-poster	251
Hiskey, M.A.	Azalea / 7a-oral	125
Hori, K.	Azalea / 7b-oral	135
Houghton, P.	Azzurra / 6-oral	93

I

Iliyn, S.V.	Azalea / 4-poster	263
	Azalea / 9-poster	361
Isella, G.	Azalea / 10-poster	369
Istratov, A.G.	Azalea / 10-poster	373
Ivshin, V.P.	Azalea / 8-poster	343
Iwama, A.	Azzurra / 2b-oral	45

J

Jia, S.X.	Azalea / 3-poster	257
Jones, H.S.	Azzurra / 3-oral	57

K

Kaledin, L.A.	Azzurra / 4a-oral	77, 79
Kalontarov, L.	Azzurra / 6-oral	95
Karasev, V.V.	Azzurra / 6-oral	97
Karir, J.S.	Azalea / 7b-oral	139
Kato, K.	Azalea / 7a-oral	127
	Azalea / 7b-oral	135

L

	Azalea / 7-poster	317
	Azalea / 7-poster	319
Singh, H.	Azalea / 7b-oral	139
Son, S.F.	Azzurra / 1-oral	31
	Azalea / 5a-oral	103
	Azalea / 7a-oral	125
Stalnaker, R.	Azalea / 10a-oral	185
Stephens, J.R.	Azzurra / 1-oral	37
	Azzurra / 2-poster	233
Stoffels, G.G.M.	Azalea / 7b-oral	137
Sturges, J.H.	Azzurra / 6-oral	93
Swami, R.D.	Azalea / 3-poster	261
Szatan, B.	Azzurra / 2b-oral	49

T

	Azzurra / 2a-oral	39
Tallent, K.	Azzurra / 2a-oral	39
Tamburini, A.	Azalea / 8-poster	327
Tamura, T.	Azzurra / 2b-oral	45
Tarasov, N.A.	Azalea / 4-poster	263
Tartakovsky, V.A.	Azzurra / 2a-oral	43
	Azzurra / 2-poster	239
Tepper, F.	Azzurra / 4a-oral	77, 79
Tereschenko, A.G.	Azalea / 7a-oral	129
Thumann, A.	Azalea / 9-oral	195
Thynell, S.T.	Azzurra / 2-poster	225
Tian, K.	Azalea / 9-oral	197
Timnat, Y.M.	Azalea / 9-poster	345
Torella, G.	Azzurra / 3-oral	55
Tosti, E.	Azalea / 3-poster	249
	Azalea / 3-poster	251
Turco, M.	Azalea / 10-poster	381
Turner, A.	Azalea / 7a-oral	131
Tussiwand, G.S.	Azalea / 9-poster	357

U

Uçer, A.T.	Azalea / 8-oral	155
Ulas, A.	Azalea / 6-poster	309

V

van der Heijden, A.E.D.M.	Azalea / 7-poster	321
van Zyl, G.J.	Azalea / 3-poster	253
Vasilyev, V.A.	Azzurra / 6-oral	101
Velsko, C.	Azzurra / 1-oral	37
Veltmans, W.H.M.	Azalea / 7-poster	321
Verri, M.	Azalea / 10b-oral	211
Volk, F.	Azzurra / 1-poster	223
Volpi, A.	Azalea / 7b-oral	135
Vorozhtsov, A.	Azzurra / 2-poster	237

W

Waesche W.R.H.	Azalea / 10b-oral	217
Walsh, C.M.	Azzurra / 2-poster	227
Wang, H.Y.	Azalea / 8-poster	335
Wang, L.	Azzurra / 4b-oral	89
	Azzurra / 6-oral	99
Wang, N.F.	Azzurra / 4b-oral	89
	Azzurra / 6-oral	99
Watkins, B.	Azzurra / 1-oral	37
Weiser, V.	Azalea / 7c-oral	143
	Azalea / 9-poster	353
Williams, S.	Azzurra / 1-oral	37
Wilson, J.A.	Azzurra / 1-oral	35
Wolanski, P.	Azzurra / 2b-oral	49
Wood, J.	Plenary Paper	13

Y

Ye, D.Y.	Azalea / 3-poster	257
Yeh, C.L.	Azzurra / 2-poster	245
Yeh, J.H.	Azzurra / 3-oral	73
Yu, D.	Azzurra / 2b-oral	45
Yumusak, M.	Azalea / 8-oral	155

Z

Zanotti, C.	Azalea / 7b-oral	135
	Azalea / 4-poster	287
	Azalea / 10-poster	381
Zarko, V.E.	Azzurra / 6-oral	97
	Azalea / 9-oral	189
Zenin, A.A.	Azalea / 10a-oral	183
	Azalea / 10-poster	383
Zhang, B.Q.	Azzurra / 4a-oral	79
	Azalea / 7-poster	315
Zhang, P.	Azzurra / 3-oral	65
Zhang, W.P.	Azzurra / 5a-oral	105
Zhao, W.	Azalea / 9-oral	197
Zhu, S.	Azalea / 9-oral	197
Zibarov, A.V.	Azalea / 8-poster	341
Zinn, B.T.	Azalea / 10a-oral	177
Zygmunt, B.	Azalea / 9-oral	201